INFORMATION TO USERS

This manuscript has been reproduced from the microfilm master. UMI films the

text directly from the original or copy submitted. Thus, some thesis and

dissertation copies are in typewriter face, while others may be from any type of

computer printer.

The quality of this reproduction is dependent upon the quality of the copy

submitted. Broken or indistinct print, colored or poor quality illustrations and

photographs, print bleedthrough, substandard margins, and improper alignment

can adversely affect reproduction.

In the unlikely event that the author did not send UMI a complete manuscript and

there are missing pages, these will be noted. Also, if unauthorized copyright

material had to be removed, a note will indicate the deletion.

Oversize materials (e.g., maps, drawings, charts) are reproduced by sectioning

the original, beginning at the upper left-hand comer and continuing from left to

right in equal sections with small overlaps.

Photographs included in the original manuscript have been reproduced

xerographically in this copy. Higher quality 6" x 9" black and white photographic

prints are available for any photographs or illustrations appearing in this copy for

an additional charge. Contact UMI directly to order.

Bell & Howell Information and Learning

300 North Zeeb Road, Ann Arbor, MI 48106-1346 USA

800-521-0600

The Synthesis of Fluorescent Chemosensors Responsive to cAMP and Other Nucleotides

by Petra Turkewitsch

Meakins-Christie Laboratories and the
Seymour Heisler Cystic Fibrosis Research Laboratories
Department of Medicine, Division of Experimental Medicine
McGill University
Montreal, Quebec

September, 1998

A thesis submitted to
the Faculty of Graduate Studies and Research
in partial fulfillment of the requirements for the degree of
Doctor of Philosophy

© Petra Turkewitsch, 1998



National Library of Canada

Acquisitions and Bibliographic Services

395 Wellington Street Ottawa ON K1A 0N4 Canada Bibliothèque nationale du Canada

Acquisitions et services bibliographiques

395, rue Wellington Ottawa ON K1A 0N4 Canada

Your file Votre référence

Our file Notre reférence

The author has granted a nonexclusive licence allowing the National Library of Canada to reproduce, loan, distribute or sell copies of this thesis in microform, paper or electronic formats.

The author retains ownership of the copyright in this thesis. Neither the thesis nor substantial extracts from it may be printed or otherwise reproduced without the author's permission.

L'auteur a accordé une licence non exclusive permettant à la Bibliothèque nationale du Canada de reproduire, prêter, distribuer ou vendre des copies de cette thèse sous la forme de microfiche/film, de reproduction sur papier ou sur format électronique.

L'auteur conserve la propriété du droit d'auteur qui protège cette thèse. Ni la thèse ni des extraits substantiels de celle-ci ne doivent être imprimés ou autrement reproduits sans son autorisation.

0-612-44611-5



To my Opa, the late Dr. Wilhelm Turkewitsch, who inspired me to reach for the highest.

Acknowledgments

I would like to first extend a very warm thanks to my supervisor, Dr. William Powell. I am forever grateful that he agreed to take me on as his student after the untimely death of Dr. Seymour Heisler, my original thesis supervisor. His excellent guidance, advice, support and understanding throughout my studies has been invaluable. My journey began here at McGill with the late Dr. Seymour Heisler, and for this I express my profound thanks. I am also very grateful to Dr. Graham Darling for his advice and support, for his time, and for giving me bench space and a hood in his lab to conduct the syntheses presented in this thesis. I, and the other members of his lab, enjoyed many delicious lunches together, at his expense, to celebrate various occasions.

I also acknowledge Dr. F. Sauriol for her assistance with NMR measurements, Dr. J. Sylvius for his help with equations, and Dr. B. Lennox and Dr. W. Galley for stimulating and helpful discussions concerning the polymer data.

A special thank-you goes to Dr. B. Wandelt for her advice, encouragement and friendship, and for an absolutely fabulous summer in Poland. I have developed a wonderful friendship with my colleagues at the Meakins-Christie labs and at Otto Maass Chemistry. Betty, Barbara, Mary, Flo, Lise, Phil, Rik and Brent, you have always been there for me. Thank you!

My list would certainly not be complete without thanking my physicians, Dr. J. Gruber and Dr. M. Desrosiers for their excellent care, and for always making themselves available to attend to my numerous health care needs. I have put my trust and my life in their hands more than once and they have never let me down. I am forever grateful. In this regard, I also wish to express my gratitude to Sylvie, Claude, Nancy, Sylvie, Barbara and Tao for their time and their excellent physiotherapy skills.

My dream of earning a Ph.D. would never have come true without the unconditional love and absolute support of my entire family, Mom, Dad, Sam, Nena, Oma, Opa, Mr. Ev, Mrs. Elaine, Karen, Kevin, and my dear friends, Sara, Jen, Dawna and Linda. And finally, I am eternally thankful to the person who gives me strength, who is always there, who believes in me and stands by me, my fiancé, Bobby. I thank God for these treasures everyday.

Preface

List of Publications Comprising this Thesis

According to the Guidelines for Thesis Preparation of the McGill Faculty of Graduate Studies, candidates have the option of presenting a manuscript-based dissertation which consists of a collection of one or more published papers, or papers submitted, or to be submitted, for publication. I have chosen to present such a manuscript-based dissertation. The following four manuscripts comprise chapters 2, 3, 4 and 5 of this thesis:

Chapter 2. "Effect of Nucleotides on the Charge Transfer Fluorescence of trans-4-(p-N,N-Dimethylaminostyryl)-N-vinylbenzylpyridinium Chloride" by Petra Turkewitsch, Barbara Wandelt, Rik R. Ganju, Graham D. Darling, William S. Powell has been published in Chemical Physics Letters 1996, 260, 142-146.

Chapter 3. "Nucleotides Enhance the Fluorescence of trans-4-(p-N,N-Dimethylamino-styryl)-N-vinylbenzylpyridinium Chloride" by Petra Turkewitsch, Barbara Wandelt, Graham D. Darling, William S. Powell is in press in the Journal of Photochemistry and Photobiology, Section A: Chemistry.

Chapter 4. "Enhanced Fluorescence of 4-(p-Dimethylaminostyryl)pyridinium Salts in the Presence of Biological Macromolecules" by Petra Turkewitsch, Graham D. Darling, William S. Powell is in press in the *Journal of the Chemical Society, Faraday Transactions*.

Chapter 5. "Fluorescent Functional Recognition Sites Through Molecular Imprinting. A Polymer-Based Fluorescent Chemosensor for Aqueous cAMP" by Petra Turkewitsch, Barbara Wandelt, Graham D. Darling and William S. Powell has been published as an accelerated publication in *Analytical Chemistry* 1998, 70, 2025-2030.

Please note that some revisions have been made to the papers in the final copy of the thesis.

Contributions of Authors

The contributions of the co-authors to the manuscripts listed in the previous section are gratefully acknowledged. I obtained all of the data presented in this thesis. Rik R. Ganju (Chapter 2) performed some preliminary studies with dye 1 in the presence of cAMP during his employment as a summer student at McGill University by Dr. Darling. However, the results of these experiments do not comprise any part of Chapter 2, since they used different concentrations of dye 1 and cAMP. Dr. Barbara Wandelt's contributions were intellectual in the area of fluorescence spectroscopy. Dr. Graham D. Darling contributed his intellectual expertise in chemistry. He also provided financial support for the project, and the use of his laboratory facility in the Otto Maass Chemistry building while he was an assistant professor at McGill University. My supervisor, Dr. William S. Powell, contributed both intellectually and financially to these manuscripts. Drs. Wandelt, Darling and Powell all provided helpful feedback during the preparation of the manuscripts.

Table of Contents

| Acknowledgments | | i |
|-----------------|--|-------|
| Preface | | ii |
| List of pu | iblications comprising this thesis | ii |
| Contribut | tions of Authors | iii |
| Table of | Contents | iv |
| List of Fi | gures | viii |
| List of Ta | ables and Schemes | xvi |
| Glossary | of Symbols and Abbreviations | xviii |
| Abstract | | |
| Résumé | | xxiii |
| CHAPTER 1 | Introduction and Literature Review | |
| 1.1 Overv | view | 2 |
| 1.2 The f | luorescence process | 5 |
| 1.3 Fluor | escence as a detection method | 7 |
| 1.4 Twist | ed intramolecular charge transfer (TICT) excited states | 9 |
| 1.4.1 | The stilbenes and styrylpyridiniums | 12 |
| 1.5 Fluore | escent chemosensors for inorganic ions | 14 |
| | Calcium | 14 |
| 1.5.2 | Other ions (Mg ²⁺ , Na ⁺ , K ⁺ , Cl ⁻ and H ⁺) | 16 |
| 1.6 Fluore | escent chemosensors for detecting and quantitating biological | |
| macr | omolecules | 18 |
| | Proteins | 19 |
| 1.6.2 | Nucleic acids: DNA and RNA | 19 |
| 1.7 Fluore | escent chemosensors for small organic molecules | 22 |
| 1.7.1 | Saccharides | 23 |
| 1.7.2 | Nucleotides | 25 |
| 1.7.3 | Other molecules | 27 |
| 1.8 Molec | cular imprinting | 29 |
| 1.8.1 | The concept of molecular imprinting | 30 |
| 1.8.2 | Potential applications of MIPs | 32 |
| | 1.8.2.1 MIPs as artificial antibodies and receptors in assays | 33 |
| | 1.8.2.2 MIPs as biomimetic recognition elements in biological | |
| | sensors | 35 |
| | MIPs for purine derivatives | 38 |
| 1.9 Fluore | escence measurement of cAMP | 39 |
| 1.9.1 | Aims of the present study | 42 |
| 1.10 Refe | rences | 44 |

| CHAPTER 2 | Effect of Nucleotides on the Charge Transfer Fluorescence of trans-4-(p-N,N-Dimethylamino-styryl)-N-vinylbenzyl-pyridinium Chloride | , |
|------------|---|------------|
| Foreword | | 51 |
| Abstract | | 52 |
| 2.1 Introd | luction | 53 |
| 2.2 Exper | | 56 |
| | ts and Discussion | 58 |
| 2.4 Concl | | 64 |
| | owledgments | 65 |
| 2.6 Endno | | 66 |
| 2.7 Refere | ences | 67 |
| CHAPTER 3 | Nucleotides Enhance the Fluorescence of <i>trans-4-(p-N,N-Dimethylaminostyryl)-N-vinylbenzylpyridinium</i> Chloride | |
| Foreword | | 71 |
| Abstract | | 73 |
| 3.1 Introd | luction | 74 |
| 3.2 Exper | imental | 76 |
| 3.2.1 | Materials | 76 |
| 3.2.2 | Methods | 76 |
| 3.2.3 | Preparation of solutions | 78 |
| 3.2.4 | trans-4-(p-N,N-Dimethylaminostyryl)-N-vinylbenzylpyridinium chloride (1) | 78 |
| 3.3 Result | • • | 80 |
| 3.3.1 | Absorption and fluorescence spectra of 1 | 80 |
| 3.3.2 | Determination of the change in the dipole moment between the | 83 |
| 211 | ground and excited states $(\Delta \mu_{rg})$ of 1 | 0.3 |
| 3.3.3 | Effect of nucleotide and nucleotide-related analytes on the | 97 |
| 3.4 Discu | absorption and fluorescence of 1 | 87 |
| | | 92 102 |
| 3.5 Concl | | |
| 3.7 Refere | owledgments ences | 103 104 |
| CHAPTER 4 | Enhanced Fluorescence of 4-(p-Dimethylaminostyryl)- pyridinium Salts in the Presence of Biological Macromolecules | |
| Foreword | | 108 |
| Abstract | | 109 |
| A 1 Introd | uction | 110 |

| 4.2 Expe | rimental | 111 |
|-----------------|---|-----|
| - | l Materials | 111 |
| 4.2.2 | 2 Fluorescence measurements | 112 |
| | 3 Preparation of solutions | 112 |
| 4.3 Resul | | 113 |
| 4.4 Discu | ission | 120 |
| 4.5 Conc | lusions | 124 |
| | owledgments | 125 |
| 4.7 Refer | • | 126 |
| CHAPTER 5 | Fluorescent Functional Recognition Sites Through Molecular Imprinting. A Polymer-Based Fluorescent Chemosensor for Aqueous cAMP | |
| Foreword | i | 129 |
| Abstract | | 130 |
| 5.1 Introd | duction | 131 |
| 5.2 Expe | rimental | 134 |
| 5.2.1 | Materials | 134 |
| 5.2.2 | 2 Preparation of polymers | 135 |
| 5.2.3 | 3 Fluorescence measurements | 136 |
| 5.3 Resul | Its and Discussion | 137 |
| 5.4 Conc | lusions | 153 |
| 5.5 Ackn | owledgments | 153 |
| 5.6 Refer | rences | 154 |
| CHAPTER 6 | Final Discussion and Conclusions | |
| Final Dis | cussion and Conclusions | 158 |
| Future di | rections | 169 |
| Reference | es | 174 |
| Claims to origi | nal research | 177 |
| APPENDIX 2 | | |
| Section A | L | |
| | Fluorescence spectra of 1 in the presence of cAMP, cGMP and D-ibose-5-phosphate | 180 |
| APPENDIX 3 | | |
| Section A | 1 | |
| F | Synthesis of <i>trans-4-(p-N,N-Dimethylaminostyryl)-N-phenethyl-</i> byridinium Bromide (2) | 183 |
| Section F | l . | |

| B.1 Spectral data for dye 1 and dye 2 | 187 |
|--|-----|
| Section C | |
| C.1 Absorption and fluorescence spectra of 1 in various solvents | 193 |
| Section D | |
| D.1 Fluorescence spectra of 1 in the presence of cAMP, cGMP, ATP | |
| and CMP | 195 |
| Section E | |
| E.1 Fluorescence quantum yield enhancement of 1 and 2 in the | |
| presence of cAMP | 198 |
| E.1.1 Results and Discussion | 199 |
| Section F | |
| F.1 The fluorescence response of A-10 cells loaded with fura-2 to | |
| serotonin in the absence and in the presence of dye 2 | 202 |
| F.1.1 Experimental | 202 |
| F.1.2 Results and Discussion | 203 |
| APPENDIX 4 | |
| Section A | |
| A.1 Fluorescence spectra of dyes 1 and 2 in the presence of biological | |
| macromolecules | 207 |
| Section B | |
| B.1 Fluorescence of dye 2 in the presence of proteins | 210 |
| APPENDIX 5 | |
| Section A | |
| A.1 Control and imprinted polymer I/I values at various cAMP and | |
| cGMP concentrations | 215 |
| Section B | |
| B.1 Preliminary absorption studies with the control and imprinted | 217 |
| DUIVINGIS | Z1/ |

List of Figures

CHAPTER 1

5

10

25

Figure 1.2. Schematic representation of twisted intramolecular charge transfer (TICT) process. The initially planar locally excited (LE) state undergoes a charge transfer from the donor (D) to the acceptor (A) with intramolecular twisting of the D and A groups towards a perpendicular geometry to produce the TICT excited state.

Figure 1.3. Schematic illustration of the LE state, the TICT excited state and the twisted double bond excited state of 4-(dimethylamino)stilbene.

Figure 1.4. Schematic representation of the binding of D-glucose to the boronic-acid-containing diaminomethylanthracene chemosensor designed by James et al., 1994. Adapted from James et al., 1994.

Figure 1.5. Schematic depiction of the binding of ATP to the cyclic multifunctional receptor designed by Dhaenens et al. showing simultaneous electrostatic and aryl stacking interactions. Adapted from Dhaenens et al., 1993.

Figure 1.6. Schematic illustration of the binding of acetylcholine to its fluorescent chemosensor. The fluorescent chemosensor consists of a bowlshaped calixarene-like molecule to which a positively charged pyridinium fluorophore is attached. The binding of acetylcholine displaces the pyridinium dye from the cavity, resulting in an enhancement in its

Figure 1.7. Schematic diagram of the preparation of molecularly imprinted polymers. Functional monomers interact through noncovalent interactions or reversible covalent interactions with the template molecule. The template-functional monomer assembly is then polymerized in the presence of an excess of cross-linking monomer. After polymerization, the template is removed exposing recognition sites with a definite shape and precise orientation of functional groups complementary to the template.

29

Figure 1.8. Schematic illustration of the fiber-optic sensing device for dansyl-L-phenylalanine. The imprinted polymer particles are held in front of the fiber-optic bundle by a nylon net. The excitation light is provided by an optical fiber connected to a light source. The light emitted is measured by a fiber bundle which is connected to a detector. Adapted from Kriz et al., 1995b.

36

Figure 1.9. Schematic illustration of the fluorescence detection of cAMP using Tsien's fluorescein (FI) and rhodamine (Rh) labeled protein kinase cAMP fluorosensor. In the absence of cAMP, the light energy absorbed by fluorescein is transferred to rhodamine, and emission occurs from rhodamine (580 nm). This fluorescence energy transfer is eliminated when cAMP binds to the regulatory (R) subunit of the protein causing the regulatory and catalytic (C) subunits to dissociate. Excitation of fluorescein now results in emission from fluorescein (520 nm) rather than rhodamine. This increase in fluorescein emission and decrease in rhodamine emission in the presence of cAMP allows intracellular cAMP to be measured ratiometrically (520/580 nm). Adapted from Adams et al., 1991.

40

CHAPTER 2

Figure 2.1. Absorption (A) and fluorescence (B) spectra of aqueous solutions of 1 (10-5 M) at 22 ℃ in the absence (1) and presence (2-7) of

| various concentrations of cAMP: (2) 1 mM, (3) 5 mM, (4) 6.67 mM, (5) 10 mM, (6) 20 mM and (7) 50 mM; the excitation wavelength for fluorescence measurements was 469 nm; the emission maxima ranged between 608-612 nm. | 59 |
|--|----|
| Figure 2.2. Fluorescence quantum yield titration curves of 1 as a function of nucleotide concentration. Solutions contained 1 (10 ⁻⁵ M) and various concentrations of D-ribose-5-phosphate (R-5-P, O), cAMP (●), and cGMP (●) in water at 22 °C; the excitation wavelength was 469 nm. The values are means ± standard errors of 3 independent observations. | 61 |
| CHAPTER 3 Figure 3.1. Absorption spectra of 1 (10-5 M) in 0.5 M phosphate buffer (pH 7.2) in the absence and presence of various concentrations of cAMP (6.67, 20 and 50 mM). | 81 |
| Figure 3.2. Fluorescence spectra of 1 (10 ⁻⁵ M) in 0.5 M phosphate buffer (pH 7.2) at excitation wavelengths of 469 nm (A) and 360 nm (B) in the absence and presence of various concentrations of cAMP (1, 5, 6.67, 10, 20, 50 mM). At excitation 469 nm the emission maxima varied between 608 and 613 nm; at excitation 360 nm the emission maximum at 502 nm remained constant, whereas that at 602 nm varied between 602 and 613 nm. | 82 |
| Figure 3.3. Lippert-Mataga plots of the Stokes' shift (in cm ⁻¹), \vec{V}_n , vs. the solvent polarity function, Δf , for 1 in various solvents; slope = 1.04×10^4 cm ⁻¹ / Δf , r = 0.77. The line is a linear least-squares fits through the data. | |
| | 86 |

Figure 3.4. Fluorescence quantum yield titration curves of 1 as a function of analyte concentration. Phosphate buffer solutions (0.5 M, pH 7.2)

| contained 1 (10 ⁻⁵ M) and various concentrations of cGMP (\Diamond), cAMP (∇), | |
|--|-----|
| adenosine (\blacksquare), ATP (∇), ADP (\bullet), AMP (\square), CMP (\triangle) or D-ribose-5- | |
| phosphate (RP, O). The lines through the symbols for cAMP, cGMP, AMP, | |
| ADP and ATP represent curve fits following equation 3. The excitation | |
| wavelength was 469 nm. The values are means ± standard errors of 3 | |
| independent observations. | 88 |
| Time 25 Malandar duratura of the region with and amaintiding | |
| Figure 3.5. Molecular structures of the various purine and pyrimidine | 07 |
| nucleotides. | 97 |
| CHAPTER 4 | |
| Figure 4.1. Fluorescence spectra of 2 (10 μM) in the presence of various | |
| concentrations (0, 0.05, 0.15, 0.3, 0.5, 1.0 mg/mL) of DNA (A) and | |
| denatured BSA (B) in 0.01 M PBS pH 7.2; excitation wavelength, 469 nm; | |
| emission maxima varied between 603 and 595 nm for DNA, and 603 and | |
| 570 nm for denatured BSA. | 114 |
| Figure 4.2. Fluorescence quantum yield titration curves of 1 (a) and 2 (b) | |
| as a function of concentration of DNA (■), RNA (▲), cAMP (□), | |
| nondenatured BSA (•) and denatured BSA (O) in 0.01M PBS pH 7.2. Data | |
| for cAMP was taken from Chapter 3. All standard errors were less than | |
| 10%. | 115 |
| CHAPTER 5 | |
| | |
| Figure 5.1. The fluorescence emission spectra of the imprinted polymer in | |
| the absence of (solid line), and 135 min after the addition of 1.0 mM cAMP | |
| (dashed line). Excitation wavelength, 469 nm; emission wavelength | |
| maximum, ~595 nm. | 140 |

140

| Figure 5.2. Time course for the fluorescence quenching effect of cAMP on | |
|--|-------|
| the cAMP-imprinted polymer at 25 °C. A representative experiment is | |
| illustrated in which 1.0 mM cAMP was added at time 0 min and the | |
| fluorescence emission of the polymer was measured as described in the | |
| Experimental section. Excitation wavelength, 469 nm; emission | |
| wavelength, ~595 nm. | 141 |
| | • • • |
| Figure 5.3. (A) The fluorescence of the control and imprinted polymers in | |
| the presence of various concentrations of cAMP and cGMP. Data were | |
| collected between 90 and 135 min after incubation with ligand. I_a and I | |
| are the fluorescence intensities of the polymers in the absence and presence | |
| of nucleotide, respectively. The data for cAMP are means ± standard error | |
| for concentrations of 1000 (n = 6) and 100 - 1.0 (n = 3) μ M, and means \pm | |
| range for concentrations of 0.1 (n = 2) and 0.01 (n = 2) μ M. The data for | |
| cGMP are means \pm standard error for concentrations of 1000 (n = 7), 10 | |
| (n=4), 100 and 1.0 (n = 3) μ M. For the sake of clarity, the error bars are | |
| only shown one side, however they also exist on the other. Excitation | |
| wavelength, 469 nm; emission wavelength, ~595 nm. | 142 |
| | 142 |
| | |
| Figure 5.3. (B) The fluorescence of the imprinted polymer in the presence | |
| of various concentrations of cAMP. The dashed lines represent the curve | |
| fits following equation 2 through the data for $(I/I_o)_{max}$ values (i.e. k_{np}/k_p | |

values) of 0.81, 0.85 and 0.87, and their average 0.84. See caption to Figure 5.3a for details.

143

CHAPTER 6

Figure 6.1. Schematic representation of a proposed fluorescent chemosensor for cAMP constructed using a cyclodextrin, dye 1 and an imide binding functionality.

171

| | Figure 6.2. Schematic illustration of proposed molecularly imprinted | |
|------|--|-----|
| | recognition site for cAMP containing dye 1 and an imide binding | |
| | functionality. | 173 |
| | | |
| APPE | NDIX 2 | |
| | Figure 2A.1 Fluorescence spectra of 1 (10-5 M) in the absence (water), | |
| | and in the presence of 50 mM D-ribose-5-phosphate (ribose), cAMP and | |
| ı | cGMP; excitation wavelength, 469 nm; emission wavelength, 608 nm for | |
| | D-ribose-5-phosphate, and 612 nm for cAMP and cGMP. Note that the | |
| , | spectra for 1 in water and in the presence of D-ribose-5-phosphate are | |
| | superimposable. | 181 |
| | | 101 |
| APPE | NDIX 3 | |
| | Figure 3A.2. ¹ H NMR spectrum of trans-4-(p-N,N-dimethylaminostyryl)- | |
| | N-phenethylpyridinium bromide (2) in chloroform on a 300 MHz Varian | |
| | XL-300 spectrometer at room temperature. Please see next page. | 185 |
| | Figure 3B.1. Fluorescence spectra of dye 1 and dye 2 (10-5 M) in | |
| | phosphate buffer (0.01 M, pH 7.2); excitation wavelength, 469 nm; | |
| • | emission maxima for 1 and 2, ~603 nm. | 189 |
| 1 | Figure 3B.2. ¹ H NMR spectrum of <i>trans</i> -4-(p-N,N-dimethylaminostyryl)- | |
| 1 | N-vinylbenzylpyridinium chloride (1) in chloroform on a 500 MHz Varian | |
| 1 | Unity-500 spectrometer at room temperature. Please see next page. | 190 |
| 1 | Figure 3B.3. Excitation spectra of 1 (10-5 M) in phosphate buffer (0.01 M, | |
| ! | pH 7.2) at room temperature at emission wavelengths of 510 and 600 nm. | |
| 1 | Uncorrected spectra. | 192 |
| | | |

| | Figure 3C.1 Absorption and fluorescence spectra of 1 (10-5 M) in water | |
|-------------|--|-----|
| | (absorption A; fluorescence B), chloroform (absorption C; fluorescence D), | |
| | and acetonitrile (absorption E; fluorescence F). | 194 |
| | Figure 3D.1 Fluorescence spectra of 1 (10-5 M) in phosphate buffer (0.5 | |
| | M, pH 7.2) in the absence (buffer), and in the presence of 50 mM cAMP, | |
| | cGMP, ATP and CMP; excitation wavelength, 469 nm; emission maximum | |
| | for cAMP, cGMP and ATP, 613 nm; emission maximum for CMP and | |
| | buffer, 608 nm. | 197 |
| | Figure 3E.1. Fluorescence spectra of 10 ⁻⁵ M 1 (A) and 2 (B) in phosphate | |
| | buffer (0.5 M, pH 7.2) in the presence the absence and in the presence of | |
| | various concentrations of cAMP (1, 5, 6.7, 10, 20 and 50 mM); excitation | |
| | wavelength, 469 nm; emission maxima varied between 610 and 617 nm | |
| | for 1; and 605 and 611 nm for 2. | 200 |
| | | |
| | Figure 3E.2. Fluorescence quantum yield titration curves of 1 (●) and 2 | |
| | (a) as a function of cAMP concentration in phosphate buffer (0.5 M pH | |
| | 7.2); excitation wavelength, 469 nm. The lines through the symbols for dye | |
| | 1 and 2 represent curve fits following equation 4. | 201 |
| | Figure 3F.1. Increase in the ratio of the fluorescence emission of fura-2 at | |
| | 510 nm obtained by exciting at 345 nm and 380 nm (Ratio 345/380 nm) | |
| | of fura-2 loaded A-10 cells to serotonin (10-3 M) before (A) and after | |
| | loading with dye 2 (B). | 205 |
| APPEN | NDIX 4 | |
| | Figure 4A.1 Fluorescence spectra of 1 (dotted lines) and 2 (solid lines) | |
| | (10-5 M) in DRS (0.01 M, nH 7.2) in the absence (buffer), and in the | |

(10-5 M) in PBS (0.01 M, pH 7.2) in the absence (buffer), and in the presence of 1 mg/mL denatured BSA, nondenatured BSA (BSA), DNA and RNA; excitation wavelength, 469 nm; emission maximum for dye 1 alone, 603 nm, with nondenatured BSA, 575 nm; and with DNA, 599 nm; emission maximum for dye 2 alone, 603 nm, with denatured and nondenatured BSA, 570 nm; with DNA, 595 nm; and with RNA, 603 nm.

209

Figure 4B.1 Fluorescence spectra of 2 in phosphate buffered saline in the absence (buffer), and in the presence of 1.0 mg/mL of nondenatured BSA, ovalbumin and gelatin; excitation wavelength, 469 nm; emission maxima for 2 in buffer, 603 nm; and for 2 with nondenatured BSA and ovalbumin, 570 nm and with gelatin, 600 nm.

212

Figure 4B.2. Fluorescence intensity titration curves of 2 as a function of nondenatured BSA (♥), ovalbumin (■) and gelatin (●) concentrations between 0 and 33.7 mg/mL in phosphate buffered saline (0.1 M, pH 7.2, 0.1 M NaCl).

213

List of Tables and Schemes

| CHAPIERS | |
|--|-----|
| Table 3.1. Solvent parameters and steady-state spectral data for 1 in various solvents. | 84 |
| Table 3.2. Equilibrium association constants (K_{rq}) for 1 with various analytes | |
| and the fluorescence quantum yields of the dye-analyte complexes (Φ_c) in 0.5 | |
| M phosphate buffer at pH 7.2 and in unbuffered water. | 91 |
| Table 3.3. Equilibrium association constants (K_{eq}) for 1 with various analytes | |
| and the fluorescence quantum yields of the dye-analyte complexes (Φ_c) in 0.5 | |
| M phosphate buffer at pH 6.0 and 8.0. | 91 |
| CHAPTER 4 | |
| Table 4.1. Fluorescence emission intensity ratios (I/I_f) for dyes 1 and 2 with | |
| various compounds. | 119 |
| CHAPTER 5 | |
| Table 5.1. Association (K_a) constants for the imprinted polymer with cAMP | |
| obtained using various k_{np}/k_p values in equation 2. | 145 |
| Table 5.2. Association constants (K_a) for various molecularly imprinted | |
| polymers. | 149 |
| Table 5.3. The fluorescence responses (I/I) of the imprinted polymer to | |
| cAMP and cGMP after the first and second template extractions. The data | |
| are from single experiments unless otherwise indicated. | 152 |

Scheme 5.1. Schematic representation of hypothetical imprint formation. The fluorescent functional monomer (1) and the functional monomer, HEMA (2) are arranged around the template molecule, cAMP (3), as a result of the noncovalent interactions between complementary chemical functionalities. Polymerization captures the topographical relationship present in solution. Extraction of the template molecule exposes recognition sites of complementary shape and functional topography. Arrows represent additional potential hydrogen bonding interactions between HEMA and cAMP.

133

APPENDIX 5

Table 5A.1. I_o/I values for each experiment with the control and imprinted polymers at each concentration of cAMP (0.01 to 1000 μ M) and cGMP (1.0 to 1000 μ M). The averages (*ave*) of the experiments and the standard errors (*se*) for each concentration of cAMP and cGMP are also presented.

216

Table 5B.1. Absorbances (at 259 nm) of the supernatants obtained after incubation of the control and imprinted polymers with cAMP before and after filtration through a Millipore filter. The absorbance of the stock cAMP solution is also given.

218

Table 5B.2. Absorbances (at 259 nm) of the supernatant of the control and imprinted polymers obtained after incubation with various concentrations of cAMP. The samples were incubated with water overnight prior to the addition of cAMP. The supernatants were filtered through a millipore filter. The absorbances of the stock cAMP solutions are also given.

219

Glossary of Symbols and Abbreviations

| $ar{oldsymbol{v}}_a$ | mavimum abaamtian faasuanas | 1 | tuana 4 (n N N dimethylamine |
|--------------------------|---|------------------|------------------------------------|
| | maximum absorption frequency | 1 | trans-4-(p-N,N-dimethylamino- |
| \vec{v}_f | maximum emission frequency | | styryl)-N-vinylbenzylpyridinium |
| \vec{V}_{st} | Stokes' shift | _ | chloride |
| ε | dielectric constant | 2 | trans-4-(p-N,N-dimethylamino- |
| η | refractive index | | styryl)-N-phenethylpyridinium |
| $\Delta\mu_{\epsilon_z}$ | change in the dipole moment | | bromide |
| - | between the ground and excited | 1-AF | 1-aminofluorenone |
| | states | Å | angstrom (1 Å = 10 nm) |
| λ_{a} | absorption maximum | a | spherical solvent cavity radius of |
| λ_{r} | fluorescence maximum | | the solute |
| • | maximum wavelength of the | Α | acceptor |
| λ_{max} | absorption or fluorescence | ADP | adenosine 5'-diphosphate |
| | spectrum | AIBN | 2,2'-azobisisobutyronitrile |
| Φ, | fluorescence quantum yield of 1 | AMP | adenosine 5'-monophosphate |
| • | (or 2) in the absence of analyte, | AT | adenine-thymine |
| | nucleotide or protein | ATP | adenosine 5'-triphosphate |
| • | - | AU | absorbance units |
| Φ, | fluorescence quantum yield of | BAPTA | 1,2-(bis)-2-aminophenoxy- |
| | the dye-analyte, dye-nucleotide | | ethane-N,N,N',N'-tetraacetic acid |
| Φ | or dye-protein complex | BCECF | 2',7'-bis-(2-carboxyethyl)-5- |
| | fluorescence quantum yield of 1 | | carboxyfluorescein |
| | (or 2) in the presence of analyte, | BSA | bovine serum albumin |
| | nucleotide or protein | c | speed of light |
| Δf | solvent polarity function $\Delta f = (\varepsilon - 1/2\varepsilon + 1) - (\eta^2 - 1/2\eta^2 + 1)$ | °C | degrees Celcius |
| | | C | catalytic |
| | | Ca ²⁺ | calcium |
| $\eta_{_{I\!\!P}}$ | specific viscosity | Ca | Cutcituiti |
| X_{dye} | mole fraction of "free" dye 1 or | | |
| | _ | | |

| cAMP | (cyclic AMP) adenosine 3':5'- | g | gram(s); mg, milligram(s); µg |
|-----------------|---|----------------|----------------------------------|
| | cyclic monophosphate | | microgram(s); pg, picogram(s) |
| cGMP | (cyclic GMP) guanosine 3':5' | GMP | guanosine 5'-monophosphate |
| | cyclic monophosphate | GTP | guanosine 5'-triphosphate |
| Cl ⁻ | chloride | h | hour(s) |
| CMP | cytidine 5'-monophosphate | I_{f} | maximum fluorescence |
| concn | concentration (M) | | intensity of free dye 1 or 2 |
| CTP | cytidine 5'-triphosphate | I_c | maximum fluorescence |
| D | Debye units (1 D = 3.33×10^{-30} | | intensity of dye 1 or 2 in the |
| | Cm) | | presence of the various |
| D | donor | | compounds, macromolecules, |
| D-PBS | Dulbecco's phosphate-buffered | | and amino acids |
| | saline | I _o | fluorescence intensity of |
| DAS | trans-4-(p-N,N- | | polymer in the absence of cyclic |
| | dimethylamino)-stilbene | | nucleotide |
| DMAB | p-(dimethylamino)benzoyl | I | fluorescence intensity of |
| DMABN | p-(dimethylamino)benzonitrile | | polymer in the presence of |
| DMASP | 4-(p-dimethylaminostyryl)- | | cyclic nucleotide |
| | pyridine | ICT | intramolecular charge transfer |
| DNA | deoxyribonucleic acid | K* | potassium |
| dsDNA | double-stranded | K_a | association constant |
| | deoxyribonucleic acid | K_{eq} | equilibrium association constant |
| DSMI | trans-4-[4-(dimethylamino)- | K_{d} | dissociation constant |
| | styryl]-1-methylpyridinium | L | liter(s); mL, milliliter(s); µL, |
| | iodide | | microliter(s) |
| EDA | electron-donor acceptor | LE | locally excited |
| EGTA | ethyleneglycolbis(β-amino- | m | meter(s); mm, millimeter(s); |
| | ethylether)-N,N,N',N'-tetra- | | μm, micrometer; nm, nanometer |
| | acetic acid | M | molar; mM, millimolar; μM, |
| Fl | fluorescein | | micromolar; nM, nanomolar |

| Mg^{\star} | magnesium | S_{ι} | relaxed singlet excited |
|--------------|----------------------------------|------------------|--------------------------------|
| MIA | molecular imprinted sorbent | | electronic state |
| | assay | SBFI | sodium-binding benzofuran |
| min | minute(s) | | isophthalate |
| MIP(s) | molecularly imprinted | S _o | ground electronic state |
| | polymer(s) | ssDNA | single-stranded |
| mol | mole(s) | | deoxyribonucleic acid |
| MQAE | N-(6-methoxyquinolyl)- | TFE | trifluoroethanol |
| | acetoethyl ester | THF | tetrahydrofuran |
| Na⁺ | sodium | TICT | twisted intramolecular charge |
| NaCl | sodium chloride | | transfer |
| NMR | nuclear magnetic resonance | TLC | thin layer chromatography |
| | spectroscopy | TMP | thymidine 5'-monophosphate |
| NR | nonradiative | TOTO | thiazole orange homodimer; |
| PBFI | potassium-binding benzofuran | | 1,1'-(4,4,7,7-tetramethyl-4,7- |
| | isophthalate | | diazaundecamethylene)-bis-4- |
| PBS | phosphate-buffered saline | | [3-methyl-2,3-dihydro-(benzo- |
| PTI | Photon Technology | | 1,3-thiazole)-2-methylidene]- |
| | International | | quinolinium tetraiodide |
| r | regression coefficient | TRIM | trimethylolpropane |
| R | regulatory | | trimethacrylate |
| Rh | rhodamine | UMP | uridine 5'-monophosphate |
| RNA | ribonucleic acid | UV | ultraviolet |
| s | second | X _{dye} | is the mole fraction of "free" |
| S,' | singlet excited electronic state | | dye 1 or 2 |

Abstract

The overall objective of this study was to develop a fluorescent chemosensor for cAMP by creating recognition sites for cAMP, that contain a fluorescent molecule, in a polymer matrix by molecular imprinting. Such a fluorescent molecularly imprinted polymer may, therefore, serve as both the recognition element and the measuring element for the fluorescent detection of cAMP in aqueous media.

Two new fluorescent molecules, known as 4-(p-dimethylaminostyryl)pyridinium salts or dyes, were synthesized as possible fluorescent components of a chemosensor. Upon excitation at 469 nm, dye 1, trans-4-(p-N,N-dimethylaminostyryl)-N-vinylbenzylpyridinium chloride, displays a dramatic quantum yield enhancement in an emission band centered at ~ 600 nm, with concomitant slight red shift of the emission maximum, in the presence of the cyclic nucleotides, cAMP and cGMP, in aqueous solution. Other purine nucleotides (AMP, ADP and ATP) and adenosine induce fluorescence quantum yield enhancements of lesser magnitude than those observed for cyclic nucleotides. The pyrimidine nucleotides, CMP and UMP, have almost no effect on the fluorescence of 1, suggesting a specificity of 1 for purine over pyrimidine analytes. Equilibrium association constants for 1 with the purine analytes in aqueous solution (pH 7.2) range from 13.8 M¹ for cAMP to 0.15 M⁻¹ for adenine. We conclude that the interaction of 1 with these analytes requires the presence of a purine base, and is enhanced by the presence of ribose and phosphate moieties. Dye 1 and a structurally-similar dye 2, trans-4-(p-N,Ndimethylaminostyryl)-N-phenethylpyridinium bromide, also display dramatic fluorescence enhancements in the presence of DNA and proteins, suggesting that they also interact with these biomolecules. The environmentally-sensitive fluorescence of dyes

1 and 2 suggests that such compounds may be useful for developing fluorescent chemosensors for purine nucleotides, especially cAMP, and for the fluorescence detection or staining of DNA and proteins.

To increase the recognition ability of 1 for cAMP, we prepared recognition sites for cAMP that contain fluorescent dye 1 in a polymer matrix by molecular imprinting. This is a novel design for such template-selective sites, since dye 1 forms an integral part of the recognition cavity, thereby serving as both the recognition element and the measuring element for the fluorescence detection of cAMP in aqueous media. The polymer displays a concentration-dependent decrease in fluorescence in the presence of aqueous cAMP, whereas almost no effect is observed in the presence of the structurally-similar molecule, cGMP. An association constant of ~ 10⁵ M⁻¹ was calculated for cAMP binding. Such fluorescent molecularly imprinted polymers could serve as a starting point in the development of highly effective synthetic fluorescent sensors for cAMP as well as other important biological molecules.

Résumé

L'objectif global de cette étude était de développer un senseur chimique fluorescent pour le cAMP, en créant un polymère imprimé au cAMP qui contient une molécule fluorescente faisant partie du site de reconnaissance. Un tel polymère fluorescent imprimé pourrait servir à la fois comme unité reconnaissante et unité mesurante pour la détection fluorescente du cAMP en milieu aqueux.

Deux nouvelles teintures 4-(p-diméthylaminostyryl)pyridinium fluorescentes furent synthétisées, à titre de composantes possibles d'un senseur chimique. Suite à l'excitation à 469 nm, la teinture 1, le chlorure de trans-4-(p-N,N-diméthylaminostyryl)-N-vinylbenzyl-pyridinium, démontra une augmentation dramatique en rendement quantique de sa bande d'émission centrée autour de 600 nm en présence des nucléotides cycliques, le cAMP et le cGMP, en solution aqueuse. D'autres nucléotides purines (l'AMP, l'ADP et l'ATP) et l'adénosine induisirent moins d'augmentation en rendement quantique de fluorescence que furent observées pour les nucléotides cycliques. Les nucléotides pyrimidines, le CMP et l'UMP, n'ont eu presqu'aucun effet sur la fluorescence de 1, ce qui suggère une spécificité de 1 pour les analytes purines vis-à-vis les pyrimidines. Les constantes d'équilibre d'association pour 1 avec les analytes purines en solution aqueuse (pH 7.2) variaient de 13.8 M⁻¹ pour le cAMP à 0.15 M⁻¹ pour l'adénine. Nous concluons que l'interaction de 1 avec ces analytes a besoin de la présence d'une base purine, et est augmentée par la présence des groupes ribose et phosphate. La teinture 1 et une autre teinture 2 de structure similaire, le bromure de trans-4-(p-N,Ndiméthylaminostyryl)-N-phénéthylpyridinium, montraient aussi des augmentations dramatiques de fluorescence en présence d'ADN et de protéines, suggérant leurs

interactions aussi avec ces molécules. La fluorescence envirosensible des teintures 1 et 2 suggère que de tels composés pourront être utiles pour développer des senseurs chimiques pour les nucléotides purines, surtout le cAMP, et pour la détection fluorescente ou la teinture de l'ADN et des protéines.

Pour augmenter la capacité de reconnaissance de 1 pour le cAMP, nous avons préparé des sites de reconnaissance pour le cAMP contenant la teinture fluorescente 1 dans une matrice de polymère par impression moléculaire. Ceci est une nouvelle préparation de tels sites étant sélectifs pour la structure, où la teinture 1 forme une partie intégrale de la cavité de reconnaissance, servant donc à la fois d'élément de reconnaissance et d'élément de mesure pour la détection fluorescente du cAMP en milieu aqueux. Le polymère démontre une diminution en fluorescence selon la concentration de cAMP aqueux, tandis que presqu'aucun effet n'est observé en présence de la molécule semblable en structure, le cGMP. Une constante d'association d'environ 10⁵ M⁻¹ fut calculée pour le cAMP. De tels polymères imprimés fluorescents à impression moléculaire pourront servir de point de départ pour le développement de senseurs chimiques très efficace pour le cAMP ainsi que pour d'autres molécules biologiques importantes.

CHAPTER 1

Introduction and Literature Review

1.1 Overview

The physiological responses to many biologically important molecules which act via cell surface receptors are mediated by intracellular second messengers, such as cyclic AMP (cAMP), cyclic GMP (cGMP), calcium, and inositol triphosphate (Darnell et al., 1994). During the transfer of extracellular messages across the cell membrane (signal transduction), the cytoplasmic levels of the messenger molecules rise, initiating a sequence of intracellular biochemical events that produce a cellular response. Elevated intracellular cAMP exerts its effect by activating a specific cAMP-dependent protein kinase enzyme located in that cell which phosphorylates various other enzymes, ultimately producing such responses as hormone secretion, smooth muscle relaxation, and ion regulation. The pivotal role of second messengers has stimulated the development of methods to quantify their levels in solution and in cells, with the hope that this knowledge may contribute to our understanding of the physiology and pathology of many diseases.

Ligand-binding assays are widely used for the determination of analytes in solution, including cAMP and cGMP, and consist of two essential steps—recognition and detection (Price and Newman, 1997; Brooker et al., 1979). Typically, recognition is achieved using a protein, such as an antibody or receptor, that binds the analyte with high affinity and specificity, and such recognition is detected using a radioactive (eg. radioimmunoassay, radioreceptor assay) or nonradioactive enzyme (eg. enzyme immunoassay) tracer. The assay is based on the competition between unlabeled analyte (standard or sample) and a fixed quantity of labeled analyte for a limited number of binding sites on a specific antibody or receptor. An analyte may be measured in

biological media, cell supernatant or cell lysates by ligand-binding assays. However, this method does not permit the measurement of analyte levels in real-time or analysis of its localization within cells undergoing physiological responses. In addition, antibodies and enzymes often require special handling and may suffer from a complicated costly production procedure. Alternative methods for measuring the concentration of an analyte are, therefore, being actively pursued.

One approach is to design and chemically synthesize a molecule, known as a "fluorescent chemosensor" (also fluorescent indicator or fluorescent probe), that selectively and efficiently binds the analyte, and is capable of converting this recognition into a quantifiable fluorescent signal (Czarnik, 1993). Fluorescence is an attractive detection method because of its high sensitivity and nondestructive nature (Czarnik, 1993; Jameson, 1984). In fact, fluorescent chemosensors were reported as early as 1956 (Diehl and Ellingboe, 1956), when Diehl and Ellingboe introduced calcein for measuring calcium. However, it was not until Tsien designed cell membrane-permeant fluorescent chemosensors, which were capable of entering a cell by passively diffusing across the cell membrane, that the field of fluorescent chemosensors began to blossom (Tsien, 1981; Grynkiewicz et al., 1985). Such membrane-permeant analogues were prepared by masking the polar binding groups of a chemosensor with nonpolar ester groups. Once inside the cell, they were deprotected by cytoplasmic esterases, rendering them membrane-impermeant, and therefore trapped inside the cell. Fluorescent chemosensors now provide popular and powerful tools for the measurement of intracellular concentrations of calcium and other ions, especially in single cells where the localization of these changes may be monitored in real-time. They also have been developed to bind

to biological macromolecules, such as proteins and nucleic acids, providing a convenient and sensitive method for their detection and quantitation in solution and in electrophoretic gels (Haugland, 1996; Singer et al., 1997).

In contrast, relatively little progress has been made in the design and synthesis of fluorescent chemosensors for small organic molecules. Recognition of an analyte with high affinity and selectivity requires a cleft or cavity that has a size and shape to match the analyte, as well as the correct spatial arrangement of functional groups complementary to the analyte (Lehn, 1995). Because of their complexity, it is more difficult to obtain such a recognition site for small organic molecules than for simple spherical ions, and often involves elaborate organic syntheses. An appealing alternative approach, is to create recognition sites for an analyte in a polymer matrix by preparing the polymer in the presence of the analyte (molecular imprinting) (Ansell et al., 1996; Kriz et al., 1997; Mosbach and Ramström, 1996; Wulff, 1997). Such molecularly imprinted polymers may also be useful as substitutes for the biological recognition elements (antibodies or receptors) in bioassays, since they combine the advantages of easy tailor design with physical and chemical stability and durability.

Given the above, the general objective of this study is to prepare a fluorescent molecularly imprinted polymer that can serve as both the recognition element and the measuring element for the fluorescent detection of cAMP in aqueous media.

1.2 The fluorescence process

Fluorescence is the emission of photons from the electronically excited states of certain molecules, generally polyaromatic hydrocarbons or heterocycles, called fluorophores or fluorescent dyes (Lakowicz, 1983; Jameson, 1984). The electronic-state diagram (Jablonski diagram) shown in Figure 1.1 illustrates the steps involved in the fluorescence process (Lakowicz, 1983).

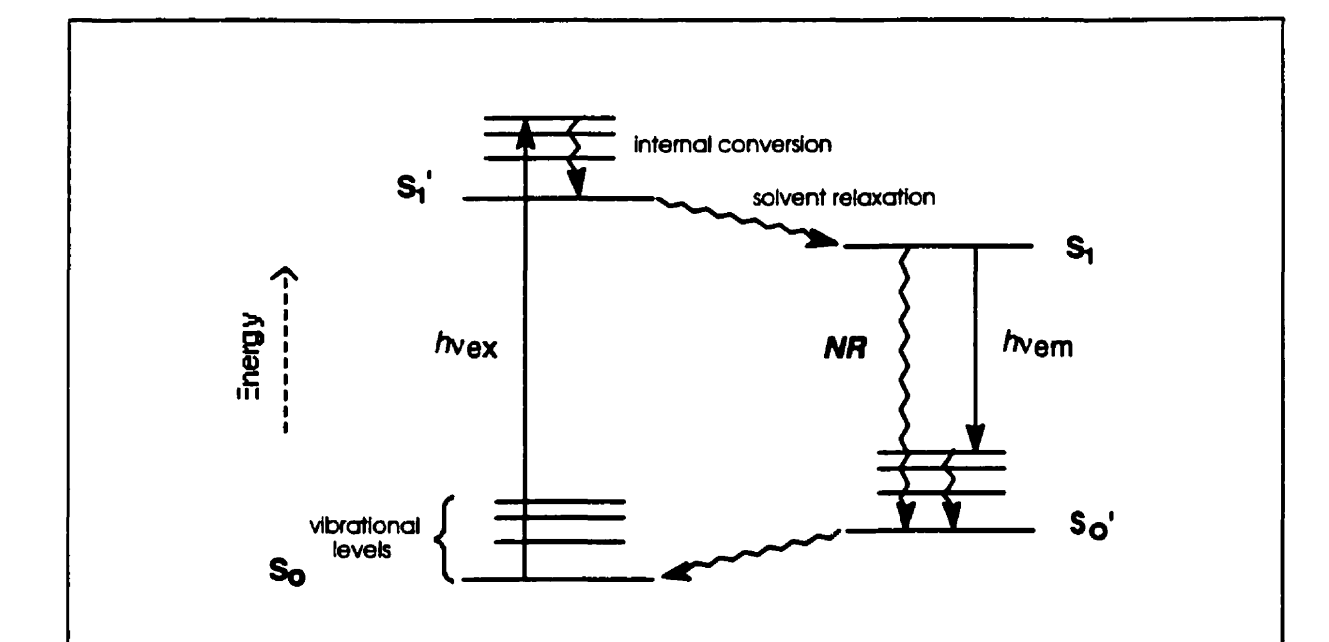


Figure 1.1. Jablonski diagram illustrating the steps involved in the creation of an excited electronic singlet state by optical absorption and subsequent fluorescence emission. NR refers to the nonradiative process of excited state energy dissipation.

A photon of energy hv_{ex} is absorbed by the fluorophore resulting in the elevation of an electron from the molecule's ground electronic state (S_o) to a excited electronic singlet state (S_1') . For most molecules at room temperature this transition usually occurs from the lowest vibrational level of the ground state to some higher vibrational level of the first excited state (S_1') . This absorption of light occurs in a time $(\sim 10^{-15} \text{ s})$ too short for significant displacement of the nuclei, but that allows the redistribution of electrons in both the fluorophore and surrounding solvent (Frank-Condon Principle). In most instances, the molecule then rapidly relaxes $(\sim 10^{-12} \text{ s})$ to the lowest vibrational level of S_1' in a process called internal conversion.

The excited state exists for a finite time (typically 10° - 10° s), during which the energy of S_1 is further dissipated through solvent relaxation (i.e. the reorientation of solvent molecules around the excited state dipole moment, stablizing the excited state), yielding a relaxed electronic singlet state (S_1). This process requires $\sim 10^{\circ 11}$ s. The fluorophore spends the remainder of the time in this relaxed excited state, where it is subject to a multitude of possible interactions with its molecular environment, and may also undergo conformational changes and redistribution of charge (see section 1.4 dealing with twisted intramolecular charge transfer)

A photon of energy hv_{cm} is emitted, returning the fluorophore to any one of the vibrational levels of the ground state S_o . Upon returning to the lowest vibrational level of S_o , the energy of the fluorophore is again further dissipated through solvent relaxation to the relaxed ground state, S_o . Thus, fluorescence is a radiative process. The energy of this photon is lower than the excitation photon hv_{cx} , and therefore of longer wavelength, due to energy dissipation during the excited-state lifetime. This difference in wavelength or

energy between excitation and emission is called the Stokes' shift. The fluorescence quantum yield is the ratio of the number of fluorescence photons emitted to the number of photons absorbed.

Molecules initially excited by absorption may also return to the ground state by some other process without emission of a photon. This is referred to as a nonradiative process (represented as *NR* in Fig. 1.1). The dissipation of the excited state energy of a molecule by transferring it to another molecule, by colliding with another molecule or through *trans-cis* photoisomerization is nonradiative (Bhattacharyya and Chowdhury, 1993).

In general, the fluorescence process is cyclical, since the same fluorophore may be repeatedly excited and emit a photon. Fluorescence intensity data are recorded on a fluorescence instrument, such as a spectrofluorometer or fluorescence microscope (Lakowicz, 1983; Jameson, 1984). The fluorescence emission intensity of a fluorophore may be monitored at a fixed excitation wavelength as a function of wavelength (referred to as an emission spectrum), or at a fixed emission wavelength as a function of excitation wavelength (referred to as an excitation spectrum). Fluorescence lifetimes are recorded on a fluorescence lifetime spectrometer.

1.3 Fluorescence as a detection method

There are several reasons why fluorescence is an attractive detection method for chemosensors (Czarnik, 1993; Jameson, 1984). Fluorescence emission appears at longer wavelengths than excitation (Stokes' shift) which allows it to be detected against a low background, resulting in sensitivities higher than those seen using absorption

spectroscopy, where small differences between two large signals, the high intensity incident and transmitted light, are measured. Furthermore, since fluorescence intensity is directly proportional to the intensity of exciting light, low concentrations of fluorescent substances may be detected by increasing the intensity of exciting light. A diverse selection of fluorophores is available commercially (Molecular Probes Inc.) allowing one to choose a fluorophore especially suited for a particular application. For instance, interferences caused by autofluorescence of biological samples (occurring around 460 nm) may be readily minimized by using long wavelength fluorophores. The virtue of fluorescence is that it is noninvasive and fast, allowing it to be applied in intact cells with high spatial and temporal resolution while cells are undergoing physiological responses.

Fluorescent molecules absorb and emit light at characteristic wavelengths, therefore a particular fluorophore may be selectively excited and detected in a complex mixture of molecules. Fluorescence emission intensity may be monitored at both excitation and emission wavelengths. Intensity-ratio measurements may be performed if there is a shift of wavelength in the emission or excitation spectrum in the presence of an analyte, or if two bands exist in either the emission or excitation spectrum whose intensity responds differently to the presence of an analyte. Such measurements provide an internal calibration, allowing the analyte concentration to be determined independent of dye concentration, cell thickness, photobleaching, instrumental factors and other artifacts. The possibility also exists for the measurement of fluorescence lifetimes.

However, while there exist many reasons for which fluorescence might be regarded as an ideal detection method for sensing, it is not without disadvantages (Czarnik, 1993). Although background signals originating from the autofluorescence of

biological samples, may be reduced by selecting fluorophores that absorb and emit at longer wavelengths, such fluorophores may not always be available. The use of fluorescence signalling may also be limited by irreversible destruction or photobleaching of excited fluorophores, which may occur under high-intensity or long-term illumination conditions. Effective countermeasures are those which allow the excitation intensity to be reduced, such as the use of low-light detection devices with enhanced detection sensitivity. Alternatively, the fluorophore may be substituted for a less photolabile one.

1.4 Twisted intramolecular charge transfer (TICT) excited states

Certain fluorophores that contain both electron donor (D) and electron acceptor (A) moieties linked by a single bond, may undergo an intramolecular charge transfer (ICT) in the excited state. For most of these molecules, complete charge transfer in the excited state is favored by a twisted conformation, where the p orbitals of the D and A groups are perpendicular, producing a twisted intramolecular charge transfer (TICT) excited state (Figure 1.2) (Grabowski et al., 1979; Rettig, 1986; Rettig and Lapouyade, 1994). Molecules exhibiting TICT excited states may show a characteristic dual fluorescence where excitation at one wavelength produces two distinct emission bands: one arising from the initially planar locally excited (LE) state, and the other from the TICT excited state.

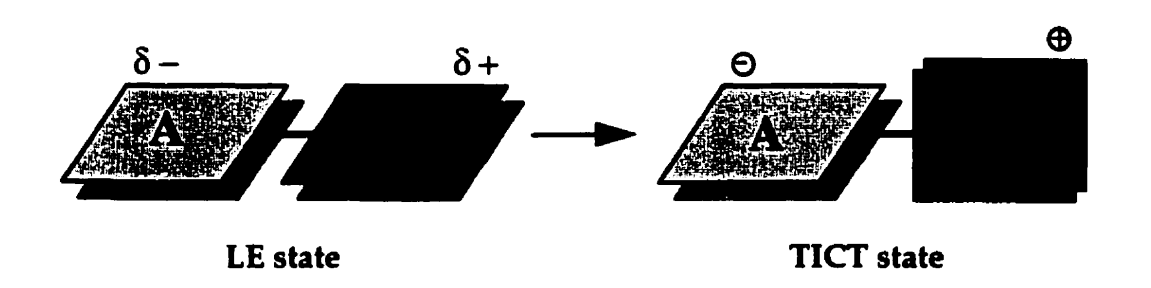


Figure 1.2. Schematic representation of twisted intramolecular charge transfer (TICT) process. The initially planar locally excited (LE) state undergoes a charge transfer from the donor (D) to the acceptor (A) with intramolecular twisting of the D and A groups towards a perpendicular geometry to produce the TICT excited state.

The best known of these molecules, and the one through which the concept of TICT was born, is p-(dimethylamino)benzonitrile (DMABN) (Grabowski et al., 1979; Rettig, 1986). It was postulated that its dual fluorescence arose from two configurations

DMABN

of the same molecule: an initially planar LE state, and a rotational isomer in which a charge transfer from the dimethylamino (donor) group to the benzonitrile (acceptor) moiety has taken place with a twisting of the dimethylamino group towards a plane perpendicular to that of the phenyl ring (TICT state). As a result of the high degree of charge separation between the D and A moieties, TICT excited states possess extremely

large dipole moments. These large electronic and structural changes make the photophysical processes of TICT molecules remarkably sensitive to the microenvironment (Rettig and Lapouyade, 1994). In view of the highly environmentally-sensitive fluorescence of molecules exhibiting TICT excited states, they may be very useful in developing fluorescent chemosensors (Rettig, 1986; Rettig and Lapouyade, 1994).

The large electronic changes associated with the formation of TICT excited states make the fluorescence properties of molecules exhibiting these excited states sensitive to changes in the polarity of the microenvironment (Bhattacharyya and Chowdhury, 1993; Létard et al., 1993; Rettig, 1986; Rettig and Majenz, 1989). As a result of the extremely large change in the dipole moments between the ground and TICT excited states, the fluorescence emission of the TICT excited state shifts to longer wavelengths (red shifts) as the polarity of the local environment increases. This displacement of the fluorescence spectrum (solvatochromism) results from a stabilization of the TICT excited state by the surrounding polar environment, and hence a lowering of its energy. Methods employing the solvatochromic shifts of molecules in various solvents of different polarity, like the Lippert-Mataga method (Lakowicz, 1983), have been used to estimate the dipole moment change between the ground and excited states of molecules. Increases in polarity can also induce changes in the fluorescence quantum yield of the TICT emission. However, these changes vary from molecule to molecule because they are dependent on the photophysical and photochemical processes occurring within the molecule. Molecules exhibiting TICT excited states, have, therefore, been useful for investigating the polarity of organized assemblies, such as micelles (Bhattacharyya and Chowdhury, 1993) and

cyclodextrins (Nag and Bhattacharyya, 1988). The well-known anilinonapthalene sulfonates have been extremely valuable in the study of membrane surfaces, as well as protein structure and function (Slavik, 1982).

The special photophysical properties of TICT molecules also appear to be useful for the design of ion- and molecule-responsive fluorescent chemosensors by coupling them with crown ethers or cyclodextrins whose cavities are capable of incorporating ions or molecules (Fery-Forgues et al., 1988; Hamasaki et al., 1993), for monitoring the degree of polymerization during the course of a polymerization reaction (Loutfy, 1986), for detecting changes in membrane potential (Montana et al., 1989), and for investigating the microviscosity of micelles (Abdel-Mottaleb et al., 1988; Law, 1981; Shin and Whitten, 1988).

1.4.1 The stilbenes and styrylpyridiniums

Among the family of compounds capable of forming TICT excited states, the electron-donor acceptor (EDA) stilbene and styrylpyridinium molecules possess multidimensional photochemical pathways. For the 4-(dimethylamino)stilbenes a TICT excited state formed by a twisting of the single bond linking the dimethylanilino (donor) group and the central ethylenic double bond, with simultaneous charge transfer from the donor to the acceptor was found to be the main fluorescent species (Figure 1.3) (Létard et al., 1993). The main path of nonradiative deactivation competing with fluorescence was shown to be via rotation around the central double bond in the excited state producing a nonemissive twisted double bond excited state, associated with *trans-cis* photoisomerization (Létard et al., 1993).

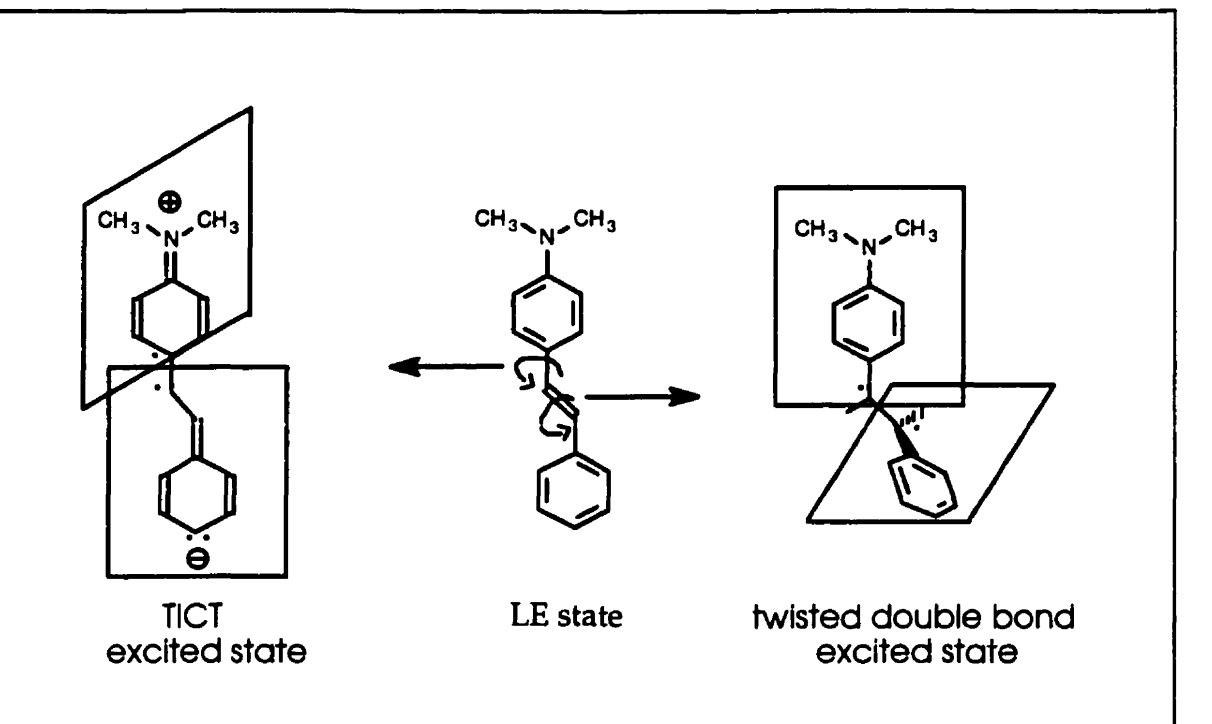


Figure 1.3. Schematic illustration of the LE state, the TICT excited state and the twisted double bond excited state of 4-(dimethylamino)stilbene.

The internal molecular rotation of stilbenes and styrylpyridiniums associated with trans-cis photoisomerization around the ethylenic double bond in the excited state is known to be inhibited by restrictive environments, such as viscous solvents (Abdel-Mottaleb, 1984; Abdel-Mottaleb et al., 1989), microheterogeneous media (eg. micelles) (Abdel-Mottaleb et al., 1988) and cyclodextrin structures (Duveneck et al., 1989), leading to a decrease in the nonradiative decay rate and consequently an increase in their fluorescence quantum yield. Similarly, "chemically" or "physically freezing" this torsional motion also results in fluorescence quantum yield increases (Létard et al., 1993;

Abdel-Mottaleb, 1984; Abdel-Mottaleb et al., 1989). The interaction of stilbene and styrylpyridinium molecules with components of their environment, may also restrict the motion around the double bond in the excited state, causing fluorescence enhancement (Samankumara Sandanayake et al., 1994; Kumar et al., 1993). These styryl dyes have, therefore, been used to explore the structural and dynamic features of microheterogeneous and biological systems. The large fluorescence enhancements observed upon the binding of such compounds to DNA or disaccharides, suggests that they may also be useful for detecting and quantitating various biomolecules (Samankumara Sandanayake et al., 1994; Kumar et al., 1993).

1.5 Fluorescent chemosensors for inorganic ions

Inorganic ions have been the primary targets for the design of fluorescent chemosensors, in particular those involved in important biological processes, such as calcium, magnesium, sodium, potassium and chloride. As a result, fluorescent chemosensors for these ions that are capable of detecting ions inside living cells have emerged. Effective fluorescent chemosensors for measuring intracellular pH have also been developed.

1.5.1 Calcium

The design and synthesis of fluorescent chemosensors for Ca²⁺ measurement have attracted considerable attention, due to the ubiquitous biological importance of intracellular Ca²⁺ signalling (Tsien, 1993). Ca²⁺ represents the first analyte for which fluorescent chemosensors aimed at intracellular applications were specifically designed

(Tsien, 1980). Indeed, the most popular application of fluorescent chemosensors is still for Ca²⁺ measurement.

The most widely used chemosensors today are fluorescent derivatives of Ca²⁺ chelating compound, BAPTA (1,2-(bis)-2-aminophenoxyethane-N,N,N',N'-tetraacetic acid), initially desiged by Tsien (Grynkiewicz et al., 1985). BAPTA is essentially an aromatic version of the Ca²⁺ chelator EGTA (ethyleneglycolbis(β-aminoethylether)-N,N,N',N'-tetraacetic acid) (Tsien, 1993). Incorporation of the aromatic BAPTA ring into conjugated heterocyclic systems has spawned a family of dyes that are currently used for the intracellular measurement of Ca²⁺, of which fura-2 is the most popular (Grynkiewicz et al., 1985). Since fura-2 exhibits a shift in excitation wavelength on Ca²⁺ binding, the ratio of fluorescence at these two excitation wavelengths (340 and 380 nm) can be used to determine Ca²⁺ concentration independent of dye concentration, cell thickness, photobleaching, instrumental effects and other artifacts.

The appeal of these fluorescent chemosensors is further enhanced by an elegant method for smuggling them into living cells using esterified membrane-permeant derivatives (Tsien, 1981). Masking the polar chelating carboxylic acid groups with acetoxymethyl esters allows them to passively diffuse across the plasma membrane into the cytosol, where they are deprotected by cytoplasmic esterases. This renders a

membrane-impermeant form of the dye, resulting in their accumulation in cells. Such membrane-permeant fluorescent chemosensors are extremely useful for intracellular applications since large populations of cells can be loaded by simple incubation with the indicator, avoiding damage or puncture of the plasma membrane that may accompany microinjection or liposome fusion.

Although this class of dyes, represented by fura-2, presents an elegant system for the determination of Ca²⁺ levels inside cells, they require high energy UV light (<400 nm) for excitation which may have harmful effects on the cell. To overcome this, and other problems, a series of dyes, including Calcium Green, Calcium Orange, and Calcium Crimson, which are excited at longer wavelengths have been prepared by conjugating high quantum yield fluorophores such as fluorescein and rhodamine to BAPTA (Eberhard and Erne, 1991; Kuhn, 1993; Haugland, 1996). Further developments include dextran conjugates of Ca²⁺ indicators which reduce the degree of localization of the dyes in intracellular compartments and lipophilic Ca²⁺ indicators which can be used to measure Ca²⁺ levels close to the inside membrane of a cell (Kuhn, 1993). However, even with the many advances made in the area of Ca²⁺ indicators, improvements may still be made, and thus the search for new and improved chemosensors continues with fervor.

1.5.2 Other lons (Mg⁺⁺, Na⁺, K⁺, Cl⁻ and H⁺)

Cousins of the fluorescent calcium indicators have been developed to measure intracellular magnesium (Mg²⁺). An example is mag-fura-2, which, like fura-2, can be used to measure Mg²⁺ on the basis of changes in the ratio of its fluorescence at two different excitation wavelengths (London, 1991). The fluorescent indicator, SBFI

(sodium-binding benzofuran isophthalate), developed for the measurement of intracellular sodium (Na⁺), consists of two fluorophores linked to the nitrogens of a crown ether with a cavity size that confers selectivity for Na⁺ over K⁺ (18-fold) (Minta and Tsien, 1989). Upon Na⁺ binding, SBFI's quantum yield increases and its excitation maximum shifts to shorter wavelengths permitting excitation ratio measurements. Fluorescence measurement of potassium (K⁺) has been achieved with PBFI (potassium-binding benzofuran isophthalate), a fluorescent sensor that is very similar to Na's SBFI (Minta and Tsien, 1989). This potassium-sensitive dye is also capable of K⁺ determination by excitation ratio measurements.

The discovery that altered membrane transport of chloride (Cl') in epithelial cells is a central defect in cystic fibrosis has spurred the development of fluorescent Cl indicators for the measurement of intracellular Cl concentrations (Higgins, 1992). The most popular fluorescent indicator for measuring intracellular Cl is the N-substituted

methoxy quinolinium compound, MQAE [N-(6-methoxyquinolyl)acetoethyl ester]

(Verkman et al., 1989). The presence of Cl causes a quenching of the fluorescence of MQAE, resulting in an ion concentration-dependent fluorescence decrease without a shift in wavelength. Although the fluorescence of MQAE is quenched by other halides, such as Br and I, physiological concentrations of these ions do not significantly affect its fluorescence. In addition, it is also unaffected by pH, bicarbonate, borate, nitrate and sulfate anions.

The most widely used fluorescent indicator for estimating intracellular pH (between ~ 6.8 and 7.4) is the UV-excitable polar fluorescein derivative BCECF [2',7'-bis-(2-carboxyethyl)-5-carboxyfluorescein], which also exists in the cell-permeant acetoxymethyl ester form (Rink et al., 1982). pH measurements are typically performed with dual-excitation ratiometry.

1.6 Fluorescent chemosensors for betecting and quantitating biological macromolecules

The precise quantitation of nucleic acids and proteins in solution is required in many areas of biomedical science. Fluorescent chemosensors that bind to these biological macromolecules noncovalently, with a concomitant change in fluorescence, provide a convenient and sensitive method for their detection in solution, as well as in electrophoretic gels and blots.

1.6.1 Proteins

The detection of proteins in solution using fluorescent probes offers enhanced sensitivity over the widely used Bradford (Bradford, 1976) and Lowry (Lowry et al., 1951) colorimetric methods. A NanoOrange assay, recently introduced by Molecular Probes Inc., is capable of accurate detection of protein concentrations between 10 ng/mL and 10 µg/mL in solution, compared to an effective range of 1µg/mL to 1.5 mg/mL for the colorimetric methods (Haugland, 1996). The unbound NanoOrange reagent is nonfluorescent in aqueous solution, but exhibits a dramatic fluorescence enhancement upon interaction with proteins, with less protein-to-protein variability than the Bradford assay. Reagents are also available for the detection and quantitation of specific proteins in solution; for instance, trace quantities of albumin in biological fluids may be quantitated using Albumin Blue 580 (Kessler et al., 1997).

1.6.2 Nucleic actos: DNA and RNA

Small molecules bind to the DNA double helix noncovalently by two dominant modes: groove binding and intercalation (Suh and Chaires, 1995). Groove binding involves docking of thin ribbon-like molecules, usually positively charged extended heterocycles, in the minor groove of double-stranded DNA (dsDNA) in close proximity to the sugar-phosphate backbone where electrostatic, hydrogen bonding and hydrophobic interactions contribute to the stability of the complex. In contrast, intercalation involves the insertion of planar molecules, usually aromatic cations, into the DNA helix between adjacent base pairs where aryl stacking interactions predominate, with hydrophobic and electrostatic interactions providing additional stabilization.

Over three decades ago, ethidium bromide was shown to be useful for the fluorescence quantitation of dsDNA in solution (LePecq and Paoletti, 1966). This heteroaromatic cationic dye interacts noncovalently with nucleic acids by intercalating

Ethidium Bromide

between adjacent base pairs (LePecq and Paoletti, 1967). Although the fluorescence of this dye is enhanced 20- to 30-fold in the presence of dsDNA, its fluorescence in the absence of dsDNA is also very high, limiting its sensitivity. Moreover, ethidium bromide also binds both RNA and single-stranded DNA (ssDNA) with concomitant fluorescence enhancement. Currently, ethidium bromide is mostly used as a general nucleic acid gel stain (Haugland, 1996).

The Hoechst (bisbenzimide) dyes preferentially bind to the minor groove of dsDNA at AT sequences with fluorescence enhancement, and are thus capable of

Hoechst 33258

selectively detecting and quantitating concentrations of dsDNA as low as 10 ng/mL salt, must be used to achieve selectivity for dsDNA when analyzing samples containing (Labarca and Paigen, 1980). However two different assay solutions, high salt and low

RNA and ssDNA contaminants, respectively. Their use for quantitating dsDNA in solution is further limited by their strong AT-selective binding and fluorescence. These dyes are popular nuclear stains in live cells, since they are cell-permeant and relatively nontoxic (Crissman and Hirons, 1994; Haugland, 1996).

The observation that dimers of nucleic acid-binding dyes have affinities several orders of magnitude greater than those of their monomeric counterparts has spawned the development of a set of dimeric cyanine dyes, the TOTO series (Glazer and Rye, 1992; Rye et al., 1993). TOTO (thiazole orange homodimer) itself is composed of two thiazole orange units connected with a bis-cationic linker that binds to DNA primarily by bisintercalation. These dyes have a higher binding affinity for dsDNA than ethidium bromide or the Hoechst dyes, and exhibit dramatic fluorescence enhancements (over 1000-fold) upon binding to dsDNA that is independent of base sequence. A unique quality of the TOTO series of dyes is their low fluorescence in the absence of dsDNA which increases the sensitivity of detection of dsDNA to concentrations as low as 0.5 ng/mL. However, these dyes show significant fluorescence enhancement in the presence of RNA and ssDNA, making quantitation of dsDNA in the presence of either or both of these nucleic acids difficult. Unlike the Hoechst dyes, the TOTO series are a family of cell-impermeant stains that cover a wide range of excitation and emission wavelengths (Haugland, 1996).

Recently, picogram sensitivity (25 pg/mL) for quantitating dsDNA in solution has been reported for a dye related to the TOTO series, the PicoGreen reagent (Singer et al., 1997). An assay for quantitating picogram quantities of ssDNA or oligonucleotides in solution, the OliGreen assay, has also been also reported (Singer et al., 1995).

The development of fluorescent dyes for the specific detection of RNA in solution has advanced much more slowly than for DNA. This is largely because there are no dyes available that exhibit fluorescence changes specifically induced by RNA. The dyes presented above for the quantitation of DNA in solution may also be used for RNA quantitation if the samples are first treated with DNase to remove the contribution of DNA to the fluorescence signal. Recently, detection of ng/mL quantities of RNA in solution has been reported with the RiboGreen reagent (Landon, 1997), as well as with the SYBR Green II dye (Schmidt and Ernst, 1995).

1.7 Fluorescent chemosensors for small organic molecules

The design and synthesis of fluorescent chemosensors for small organic molecules is often more difficult than for spherical ions (metal cations or halide anions) because of their complexity, and thus has advanced more slowly. Efficient recognition (i.e. high affinity and selectivity) of such molecules requires a chemosensor with a rigid cavity or cleft (pocket) into which the substrate may fit, since this ensures a steric complementarity between the chemosensor and the ligand, as well as a large contact area between them within which properly positioned functional groups may form multiple complementary binding interactions (Lehn, 1995). The shaping of a well-defined pocket requires more or less rigid connections between combinations of suitable binding groups positioned in a three-dimensional array. Macrocyclic structures, such as crown ethers and cyclodextrins, may be used to construct such a pocket, since they provide a rigid framework with numerous branches, bridges, and connections onto which functional groups may be

arranged (Lehn, 1995). They also provide cavities of varying size and shape which may be profitably exploited.

In spite of their complexity, progress is being made in the development of fluorescent chemosensors for small organic molecules. An effort has been made to detect and quantitate molecules that are major players in the metabolic pathways of living organisms, such as saccharides and nucleotides. However, the application of these chemosensors to biological systems has yet to be demonstrated.

1.7.1 Saccharides

The selective detection of D-glucose, a neutral organic molecule, using a fluorescent chemosensor containing boronic acid binding groups was recently reported (James et al., 1994, 1996a and 1996b). A pocket for D-glucose was created by orienting two boronic acid binding groups on a diaminomethylanthracene skeleton, such that the 1,2- and 4,6-hydroxyl groups of glucose form a cyclic complex with the boronic acid groups through reversible covalent interactions (Figure 1.4) (James et al., 1994). A physiological concentration of glucose (~ 1 mM) caused a 5-fold enhancement in anthracene fluorescence in methanol-water buffer, whereas D-fructose and D-galactose, the other main monosaccharides present in the blood, induced fluorescence enhancements about half that observed for glucose. Furthermore, the fluorescence of this chemosensor in the presence of D-glucose, as well as its affinity for D-glucose (log $K_a = 3.6$), were unaffected by physiological concentrations of D-fructose and D-galactose (≤ 0.1 mM), suggesting that it may be suitable for the detection of physiological blood glucose levels (0.3 -1.0 mM). The discrimination between enantiomers of monosaccharides using a

Figure 1.4. Schematic representation of the binding of D-glucose to the boronic-acid-containing diaminomethylanthracene chemosensor designed by James et al., 1994. Adapted from James et al., 1994.

fluorescent chemosensor with boronic acid groups attached to a chiral binapthyl platform was also achieved by the same group (James et al., 1995).

The recognition of disaccharides was also targeted using fluorescent chemosensors with boronic acid binding groups (Samankumara Sandanayake et al., 1994). *trans*-3,3'-Stilbenediboronic acid, which consists of two boronic acid groups attached to a stilbene skeleton, displayed large fluorescence enhancements in the presence of D-melibiose, whereas smaller fluorescence increases were observed for D-isomaltose and D-gentiobiose. The fluorescence enhancements of this chemosensor were attributed to a decrease in nonradiative decay caused by inhibited rotation around the ethylenic double bond in the excited state upon forming a cyclic complex with the disacchardes.

1.7.2 Nucleotibes

A fluorescent chemosensor containing two flat aromatic napthalene groups held apart at a specific distance by two flexible positively charged diethylenetriamine arms displayed a decrease in fluorescence intensity upon nucleotide binding in pyridine-trifluoroacetic acid buffer (Figure 1.5) (Dhaenens et al., 1993). The insertion of the nucleotides between the flat walls of this cyclic artificial receptor resulted from a combination of aryl stacking interactions between the aromatic bases of the nucleotides and the napthalene units, and electrostatic interactions between the negatively charged phosphate groups and the positively charged spacer arms. Association constants for the

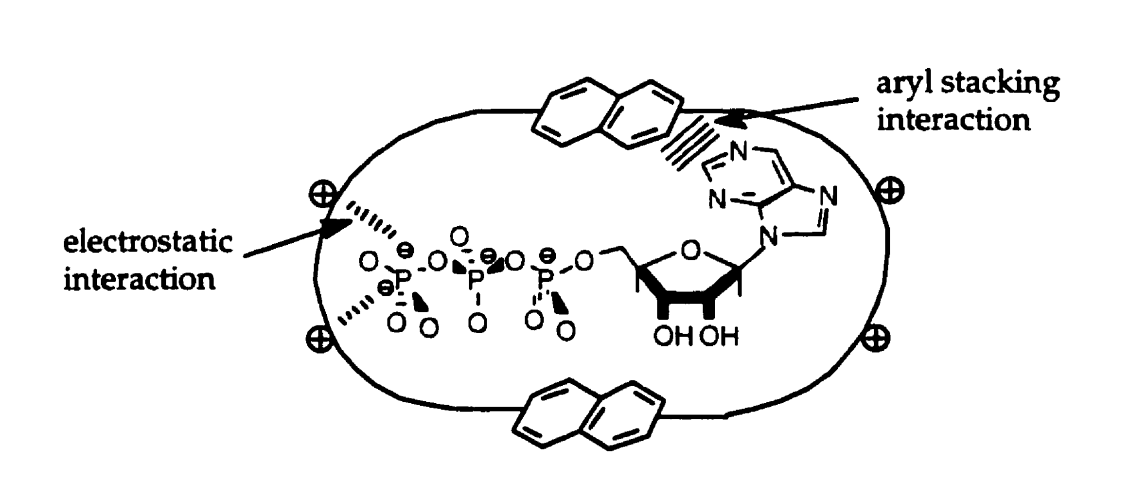


Figure 1.5. Schematic depiction of the binding of ATP to the cyclic multifunctional receptor designed by Dhaenens et al. showing simultaneous electrostatic and aryl stacking interactions. Adapted from Dhaenens et al., 1993.

monophosphate nucleotides revealed that purine nucleotides (AMP $\log K_a = 4.1$, GMP $\log K_a = 4.6$) bind more strongly than pyrimidine nucleotides (UMP $\log K_a = 3.6$, CMP $\log K_a = 3.8$), possibly because of the larger aromatic surface of the purine bases. The affinity of this fluorescent chemosensor for adenine nucleotides increased with the number of negative charges in the ligand; AMP ($\log K_a = 4.1$) < ADP ($\log K_a = 5.0$) < ATP ($\log K_a = 5.1$).

The fluorescence intensity of a fluorescent chemosensor consisting of two positively charged diazapyrenium units linked by a xylene spacer also decreased with nucleotide binding in neutral aqueous solution (Coudret and Harriman, 1992). This artificial receptor enfolded to incorporate the nucleotides, sandwiching it between the two diazapyrenium units by aryl stacking and electrostatic interactions. Again, a selectivity for purine over pyrimidine nucleotides was observed. AMP and GMP displayed association constants of 740 and 945 M⁻¹, respectively, whereas CMP and TMP had affinities of 55 and 210 M⁻¹, respectively. Among the adenine nucleotides, the association constants also increased as the charge on the nucleotide increased. ATP ($K_a = 1220 \text{ M}^{-1}$) was bound more strongly than ADP ($K_a = 1005 \text{ M}^{-1}$); AMP displayed the lowest association constants.

Hosseini et al. (Hosseini et al., 1990) designed a fluorescent chemosensor for ATP that combined a positively charged macrocyclic polyammonium moiety as the anion binding site with a fluorescent acridine group as the purine base binding site. Attractive electrostatic interactions between the polyphosphate chain of ATP and the positively charged macrocyclic moiety of the artificial receptor together with aryl stacking interactions between the acridine group of the latter and the purine base of the nucleotide

contributed to the binding of ATP. The fluorescence of this chemosensor was enhanced slightly upon complexation of ATP and CTP in aqueous buffer (pH 4.0), whereas GTP and AMP caused a slight quenching.

The specific recognition of cAMP in aqueous media was recently reported by Kato et al. (Kato et al., 1994). However, this artificial receptor is nonfluorescent. A water-soluble version of Kemp's triacid imide was combined with a diaminocarbazole unit to create a pocket for adenine binding through simultaneous Watson-Crick and Hoogsteen hydrogen bonding and aryl stacking interactions. A positively charged guanidinium moiety was added to this module for electrostatic interaction with the negatively charged phosphate group of cAMP. Equilibrium constants of association, determined by 'H NMR titration, of 600 and 320 M⁻¹ in 10 mM cacodylate buffer at ionic strengths of 51 mM and 501 mM NaCl, respectively were reported for this synthetic receptor with 3':5'-cAMP.

1.7.3 Other Molecules

β-Cyclodextrin attached to a *p*-(dimethylamino)benzoyl (DMAB) fluorophore is capable of distinguishing between the biologically important bile salts, cholic acid and chenodeoxycholic acid, by TICT fluorescence (Hamasaki et al., 1993). Chenodeoxycholic acid, which lacks a hydroxyl group at the C12 position, caused a greater decrease in the TICT emission intensity of DMAB than cholic acid, translating into an association constant of 51 000 M⁻¹ in aqueous solution, about twice that of cholic acid. The DMAB fluorophore is normally situated within the apolar β-cyclodextrin cavity where it exhibits

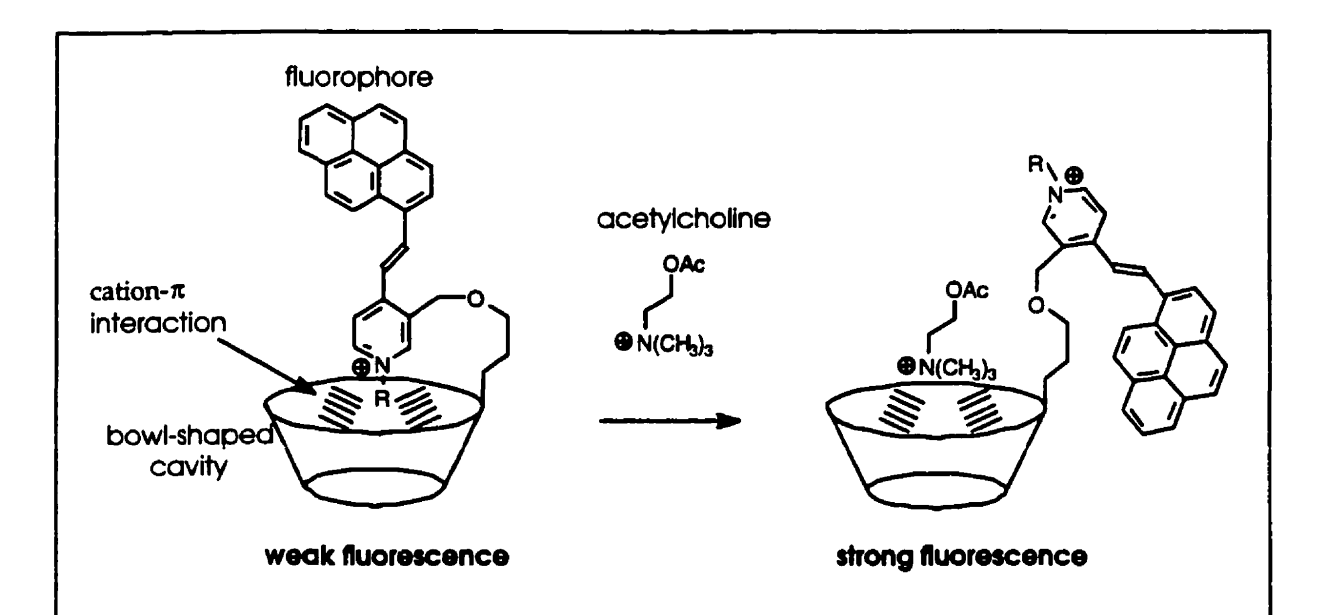


Figure 1.6. Schematic illustration of the binding of acetylcholine to its fluorescent chemosensor. The fluorescent chemosensor consists of a bowl-shaped calixarene-like molecule to which a positively charged pyridinium fluorophore is attached. The binding of acetylcholine displaces the pyridinium dye from the cavity, resulting in an enhancement in its fluorescence. Adapted from Inouye et al., 1994.

a large TICT emission. Displacement of the fluorophore into the polar aqueous environment by the ligand causes a reduction in the TICT emission of the fluorophore.

A fluorescent chemosensor for acetylcholine, prepared by attaching a fluorophore, a pyrene-modified N-alkylpyridinium cation, to the wall of a bowl-shaped calixarene-like molecule, displayed a two-fold fluorescence enhancement in ethanol in the presence of acetylcholine (Figure 1.6) (Inouye et al., 1994). In the absence of acetylcholine, the pyridinium dye is partially incorporated in the cavity of the artificial receptor where cation- π interactions quench its fluorescence. The binding of acetylcholine to the cavity displaces the pyridinium dye from the cavity, resulting in a fluorescence enhancement.

1.8 Molecular imprinting

The emerging technology of molecular imprinting could provide an alternative, and in some cases simpler, approach for preparing synthetic recognition sites for small organic molecules (Wulff, 1995). The highly stable synthetic polymers prepared by this method possess selective molecular recognition properties because of recognition sites within the polymer matrix that possess a three-dimensional structure complementary to the analyte in both shape and chemical functionality.

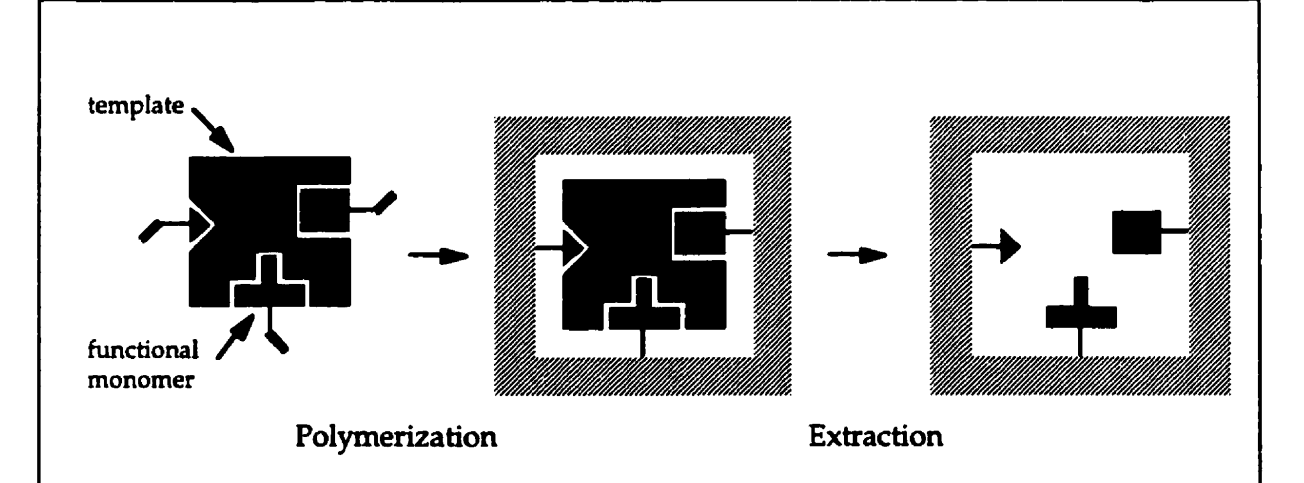


Figure 1.7. Schematic diagram of the preparation of molecularly imprinted polymers. Functional monomers interact through noncovalent interactions or reversible covalent interactions with the template molecule. The template-functional monomer assembly is then polymerized in the presence of an excess of cross-linking monomer. After polymerization, the template is removed exposing recognition sites with a definite shape and precise orientation of functional groups complementary to the template.

1.5.1 The concept of molecular imprinting

Molecular imprinting entails the copolymerization of functional monomers in the presence of a template (print) molecule to produce microcavities in the polymer that are selective for, and have an affinity for, the print molecule (Ansell et al., 1996; Kriz et al., 1997; Mosbach and Ramström, 1996; Muldoon and Stanker, 1996; Steinke et al., 1995; Wulff, 1995; Wulff, 1997). The molecularly imprinted polymers (MIPs) are prepared by first allowing complementary functionalities in the template molecule and functional monomers to interact (Figure 1.7). These interactions may be either of noncovalent or reversible covalent nature. This template-functional monomer assembly is then polymerized in the presence of an excess of cross-linking monomer and a porogenic solvent to form a rigid, insoluble macroporous polymer block. In most cases, the polymer is ground into fine particles for use, thereby increasing the surface area available for interaction. Subsequent removal of the template by extraction or hydrolysis exposes "imprints" with a definite shape and precise orientation of functional groups complementary to the template conserved through the rigidity of the three-dimensional cross-linked polymer network. These microcavities enable the polymer to later selectively bind the print molecule.

The first MIPs were obtained by Wulff and coworkers (Wulff et al., 1973; Wulff et al., 1977). The polymers were prepared by covalently attaching a polymerizable functional monomer, vinylphenylboronate, to a specific enantiomer of a sugar or amino acid derivative through a reversible boronic ester linkage. After removal of the template molecule by hydrolysis, the MIPs preferentially bound the enantiomer used as the template from a mixture containing both enantiomers. These MIPs were also capable of

chromatographically separating the racemates. Molecular imprinting advanced considerably when Mosbach and coworkers (Andersson et al., 1984; Arshady and Mosbach, 1981; Moradian and Mosbach, 1989) prepared an imprinted polymer using exclusively noncovalent interactions between the template and functional monomers, largely because this noncovalent approach simplified the imprinting procedure, and extended the list of molecules amenable to imprinting. They prepared these MIPs by simply mixing the functional monomer with the template in an organic solvent to allow complementary interactions to form between them. In these initial studies, molecular imprints against D- or L-amino acid derivatives, such as L-phenylalanine anilide, were prepared using methacrylic acid as the functional monomer. When such MIPs were investigated chromatographically they efficiently resolved the enantiomers of the template molecule.

Of the two molecular imprinting approaches, covalent and noncovalent, the noncovalent strategy is more easily employed because complementary interactions between the print molecule and functional monomers are formed by simply mixing them together in a suitable solvent prior to polymerization (Andersson et al., 1994). The covalent approach requires the synthesis of a polymerizable derivative of the template. Molecular imprinting systems based on the noncovalent approach are more versatile because a greater variety of possible interactions between the print molecule and functional monomers are available, such as electrostatic, hydrogen-bonding, hydrophobic and aryl stacking interactions, allowing a much greater variety of molecules to be imprinted (Mosbach and Ramström, 1996). In addition, a judiciously chosen "cocktail" of several different functional monomers which interact simultaneously with the template

may be used. In contrast, the use of covalent interactions is limited by the small number of reversible covalent interactions available, thus reducing the flexibility of this approach. On the other hand, less variability among the recognition sites would be expected with the covalent approach, since a more stable interaction of definite stoichiometry exists between the template and functional monomer(s) (Andersson et al., 1994). During the preorganization process, prior to the formation of the polymer, different noncovalent interaction patterns between the template and functional monomer(s) may exist, which may result in a variety of different recognition sites in the polymer (Mosbach and Ramström, 1996). After polymer formation, the noncovalently bound print molecule is removed from the polymer by mild extraction, as opposed to the harsh chemical treatment usually required to release a print molecule that is covalently attached to the polymer matrix (Mosbach and Ramström, 1996). In the future, combinations of these two approaches may be an extremely powerful strategy (method) for producing MIPs (Mosbach and Ramström, 1996).

1.5.2 Potential applications of MIPs

MIPs have been prepared for a wide variety of compounds (Steinke et al., 1995; Wulff, 1995; Mosbach and Ramström, 1996), such as amino acid and carbohydrate derivitives (Moradian and Mosbach, 1989; Wulff et al., 1977; Mayes et al., 1994) therapeutic drugs (theophylline, diazepam, morphine) (Andersson, et al., 1995; Vlatakis et al. 1993), pesticides (Muldoon and Stanker, 1997), purine derivatives (Mathew and Buchardt, 1995; Mathew-Krotz and Shea, 1996; Piletsky et al., 1994; Shea et al., 1993) and peptides (Ramström et al., 1994). The selective binding properties of these polymers

are being investigated for a number of potential applications ranging from tailor-made separation materials, to antibody and receptor mimics in assay systems, biomimetic recognition elements in biological sensors, and artificial enzyme systems for catalytic applications (Kriz et al., 1997; Mosbach and Ramström, 1996; Wulff, 1995). Although the development of MIPs for chromatographic applications has received the most attention, there is currently a surge of interest in the use of MIPs as biomimetic recognition elements for assays or sensors. This attention is largely because MIPs combine the advantages of easy tailor design with physical and chemical stability and durability (Kriz et al., 1997; Mosbach and Ramström, 1996). Molecular imprints may also be made against compounds for which it is difficult to prepare natural antibodies, or when a natural receptor is difficult to obtain. Furthermore, MIPs are often less costly to produce than natural antibodies or receptors, and avoid the use of animals or any material of biological origin.

1.5.2.1 MIPs as artificial antibodies and receptors in assays

MIPs provide an attractive complement or alternative to antibodies and receptors used in bioassays (Andersson et al., 1995; Vlakatis et al., 1993). Molecular imprints against the therapeutic drugs, theophylline (bronchodilator) and diazepam (tranquilizer), were successfully used as substitutes for antibodies in a competitive radioligand binding assay, the Molecular Imprinted sorbent Assay (MIA), for determining their levels in human serum (Vlakatis et al., 1993). The drugs were first extracted from the blood samples into organic solvents, and then allowed to compete with radiolabeled drugs for the binding sites in the MIPs. Calibration curves were generated using blood samples

spiked with known amounts of theophylline or diazepam, from which the concentrations of unknown samples were determined. Drug concentrations in blood samples determined by the MIA compared well to those determined using a commercial immunoassay. In addition, the cross-reactivities of structurally related compounds using the antitheophylline and antidiazepam imprints were comparable to those found with natural antibodies. The use of such an MIP, demonstrating high substrate affinity and specificity, instead of an antibody as the recognition element in a competitive binding assay, was unprecedented.

The noncovalent interactions, mainly electrostatic and hydrogen-bonding, employed for the imprinting of theophylline and diazepam, as well as their subsequent recognition, are most effective in organic media (Vlakatis et al., 1993). Obtaining binding and selectivity in aqueous media is a major requirement for MIPs designed for biological systems, because the binding event occurs under conditions compatible with biological molecules (Andersson et al., 1995; Ansell et al., 1996; Mathew and Buchardt, 1995). It is much more difficult to demonstrate specific binding of ligands in aqueous media compared to organic solvents since substitution of water for organic solvents dramatically alters the relative importance of polar and hydrophobic interactions between MIPs and analytes. Water molecules strongly interfere with polar interactions, such as hydrogen bonding, whereas hydrophobic effects are enhanced in water. Thus, until recently, organic solvents have been used exclusively as the media for studies on the binding of ligands to MIPs.

Recently, an MIP prepared against morphine demonstrated high affinity binding of morphine in aqueous media, suggesting that such an MIP could mimic opioid receptors

and thus provide a useful screening tool in drug development (Andersson et al., 1995). Even though the cross-reactivity of structurally related compounds was higher in aqueous buffer than in organic solvent, the selectivity of this MIP in aqueous media was similar to that reported for antibodies.

1.8.2.2 MIPs as biomimetic recognition elements in biological sensors

A biological sensor is a device that consists of a recognition element, such as an antibody or enzyme, that selectively binds an analyte, and a transducer that senses the bound analyte and emits a quantifiable output signal (Kriz et al., 1997). The remarkable affinities and selectivities demonstrated by some MIPs, together with their physical and chemical stability, make them especially suitable as recognition elements in sensor systems (Kriz et al., 1997).

A fiber-optic sensing device for the fluorescence detection of a fluorescent amino acid derivative, dansyl-L-phenylalanine, was constructed by placing an MIP prepared against the amino acid on the tip of a fiber-optic bundle (Figure 1.8) (Kriz et al., 1995b). The fluorescence signal measured by the device increased to a greater extent with increasing concentrations of the L-amino acid (in acetonitrile) than the D-amino acid, thereby distinguishing the enantiomers. Conversely, when an MIP against dansyl-D-phenylalanine was used in the device, a higher fluorescence signal was observed in the presence of the D-enantiomer. This arrangement places the recognition element and transducer in close proximity, a requirement for a true sensor, and is, thus, one of the most successful biomimetic sensors reported.

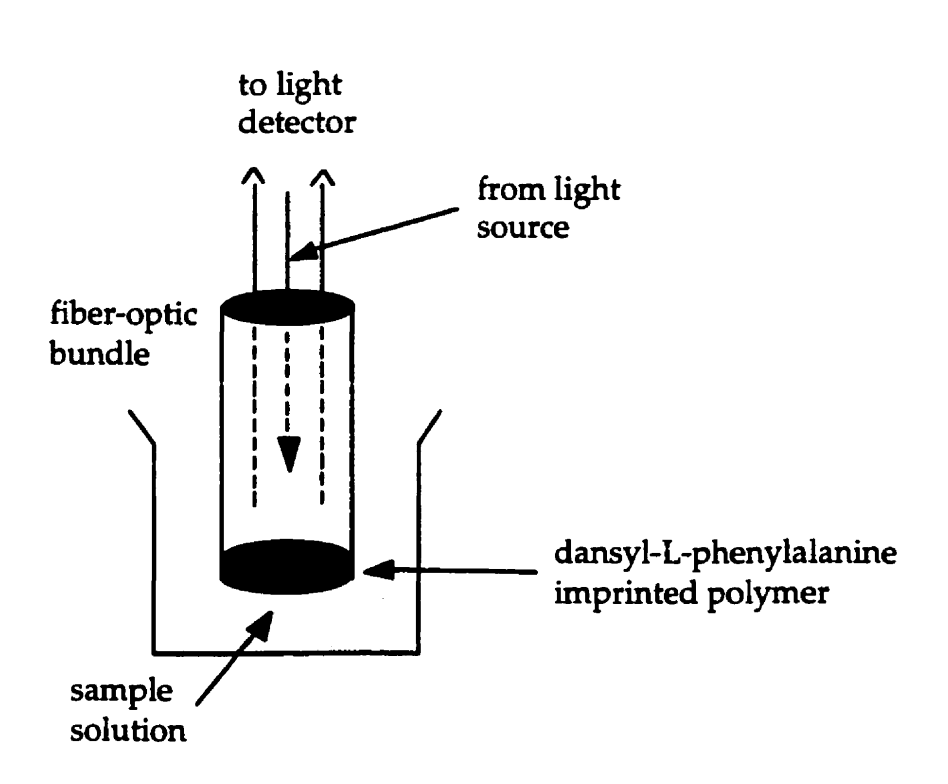


Figure 1.8. Schematic illustration of the fiber-optic sensing device for dansyl-L-phenylalanine. The imprinted polymer particles are held in front of the fiber-optic bundle by a nylon net. The excitation light is provided by an optical fiber connected to a light source. The light emitted is measured by a fiber bundle which is connected to a detector. Adapted from Kriz et al., 1995b.

A biosensor-like device for the detection of morphine was constructed by immobilizing polymer particles imprinted against morphine in an agarose gel at the surface to a platinum electrode (Kriz and Mosbach, 1995a). Morphine was allowed to bind to the imprinted polymer particles, and then codeine, an electroinactive competitor, was added in excess, displacing the bound morphine. The released morphine caused an

increase in the current measured by the device. This current response was dependent on morphine concentration, enabling its detection between 0.1 and 10 µg/mL.

Several MIP systems have used fluorescence detection methods based either on the use of fluorescent-labeled analytes (Piletsky, 1997) or on the formation of fluorescent complexes between added reagents and residual functional groups on the polymer (Piletsky, 1996). In another strategy, fluorescent MIPs against cholesterol were prepared using fluorescent functional monomers, but no change in fluorescence resulted upon the addition of cholesterol (Cooper, 1997).

Recently, Sherrington's group reported a novel way of preparing MIPs which may be used as the recognition element for optical sensors (Steinke et al., 1996). They proposed a route for the synthesis of a transparent MIP containing template-selective sites of a particular orientation. Such a polymer may be created by allowing photoreactive analogues of the template to bind to an MIP prepared against the template molecule. Irradiating the polymer with linearly polarized light would cause all the photoreactive molecules oriented parallel to the polarization plane to become covalently bound to the polymer backbone, whereas those molecules oriented perpendicular to the polarization plane would not become incorporated into the polymer. Subsequent extraction of all the nonactivated photoreactive molecules would expose only those cavities oriented perpendicular to the polarization plane, and thus would create a polymer with sites oriented in the perpendicular direction (i.e. a molecularly imprinted anisotropic polymer). The binding of the template molecules to such imprinted sites may then be detected by measuring the difference in the UV absorption of the polymer (at the absorption maximum of the template) parallel and perpendicular to an axis [i.e. ΔA (anisotropy) =

 A_1 - A_{11} , since only the bound template molecules would cause a change in anisotropy. Thus, it may be possible to selectively detect template molecules in the presence of similar molecules by simply measuring ΔA . They succeeded in synthesizing a transparent MIP against a template that itself was photoreactive, eliminating the need to remove the template from the imprinted polymer and replace it with a photoreactive analogue. Irradiating the polymer with polarized light caused a decrease in the absorbance of the template parallel to the polarization plane as a result of their incorporation into the polymer, and hence an increase in anisotropy. After extracting the polymer, the anisotropy decreased.

1.5.3 MIPs for purine derivatives

Several groups have reported MIPs that can selectively recognize and bind purine derivatives in organic, as well as aqueous media. An MIP prepared against the nucleotide base, 9-ethyladenine, displayed an association constant of 79,000 M⁻¹ in chloroform from binding studies carried out by a batch procedure (Shea et al., 1993). Chromatographic data obtained in chloroform and aqueous solution revealed that polymers imprinted with 9-ethyladenine retained adenine bases in preference to other purine or pyrimidine bases, making them attractive for use as selective separation matrices. In aqueous solution, an association constant of 4,300 M⁻¹ was determined by a batch procedure for the binding of adenine to its MIP (Mathew and Buchardt, 1995). Chromatographic separation of ATP

¹ Batch binding studies are performed by incubating a suspension of the polymer with various concentrations of ligand in a given solvent. Thereafter, the polymer is allowed to settle and the concentration of free ligand in the supernatant is determined (eg. by absorption spectroscopy).

from AMP and ADP in aqueous buffer was reported using an ATP-imprinted polymer (Piletskii et al., 1990)

The selective transport of purine derivatives through molecularly imprinted polymer membranes has also been reported. By measuring the concentration of adenine in the receiving side of a two-compartment cell separated by a 9-ethyladenine-imprinted membrane as a function of time, adenine was found to be transported at a higher rate than thymine from an equimolar methanol solution of adenine and thymine (Mathew-Krotz and Shea, 1996). This selective transport reportedly resulted from a process that involved reversible complexation and exchange between adenine and the adenine-selective binding sites in the polymer membrane, creating a pathway for transport. The selective permeability of AMP in aqueous solution through a polymeric membrane prepared against AMP was demonstrated by measuring the ion current across the membrane (Piletsky et al., 1994).

1.9 Fluorescence measurement of cAMP

A clever method, and the only one currently available, for the nondestructive measurement of cAMP in living cells using fluorescence was recently introduced by Tsien and coworkers (Adams et al., 1991). This "cAMP fluorosensor" consists of a natural cAMP-sensing protein, cAMP-dependent protein kinase, in which the catalytic (C) and regulatory (R) subunits are labeled with fluorescein and rhodamine tags, respectively (Figure 1.9). Due to the proximity of the fluorescein and rhodamine labels in the holoenzyme configuration (C_2R_2), the light energy absorbed by fluorescein is readily transferred to rhodamine. The binding of cAMP to the regulatory subunit of the protein

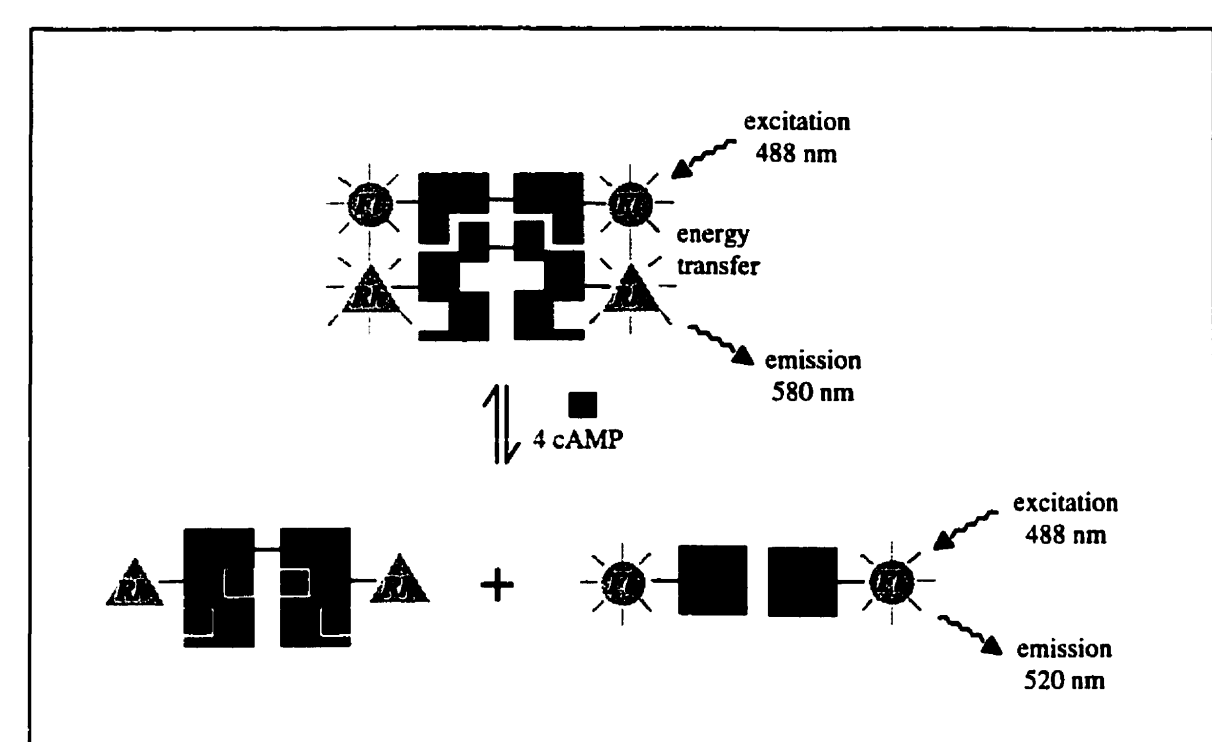


Figure 1.9. Schematic illustration of the fluorescence detection of cAMP using Tsien's fluorescein (FI) and rhodamine (Rh) labeled protein kinase cAMP fluorosensor. In the absence of cAMP, the light energy absorbed by fluorescein is transferred to rhodamine, and emission occurs from rhodamine (580 nm). This fluorescence energy transfer is eliminated when cAMP binds to the regulatory (R) subunit of the protein causing the regulatory and catalytic (C) subunits to dissociate. Excitation of fluorescein now results in emission from fluorescein (520 nm) rather than rhodamine. This increase in fluorescein emission and decrease in rhodamine emission in the presence of cAMP allows intracellular cAMP to be measured ratiometrically (520/580 nm). Adapted from Adams et al., 1991.

causes the two subunits to reversibly dissociate, separating the fluorophores and thereby eliminating this fluorescence energy transfer. The resulting increase of the fluorescein (520 nm) emission and decrease of the rhodamine (580 nm) emission allows intracellular

cAMP to be measured ratiometrically (520/580 nm) upon exciting at 488 nm. Since this fluorosensor is a protein, it must be microinjected into the cytoplasm of individual cells, risking the disruption of their outer membrane, and allowing only single cell experiments to be performed. It must also be handled with care so as not to destroy its enzymatic action.

An alternative approach for measuring the concentration of cAMP by fluorescence would be to use a fluorescent chemosensor that is capable of binding cAMP with high affinity and selectivity, and converting this recognition into a detectable fluorescent signal. This fluorescent chemosensor may be prepared using the technique of molecular imprinting, in which cAMP-selective binding sites are created in a polymer matrix. Such a fluorescent chemosensor may serve as an alternative to the immunoassay for quantitating cAMP in solution, and since it does not involve the use of a biological recognition element, it may also provide enhanced stability. The possibility ultimately exists for preparing such cAMP binding sites in tiny (~ 10 nm in diameter) spherical polymer particles (nanoparticles) which may be inserted into cells (for example by microinjection), thereby providing a means to measure cAMP inside cells.

For measurements of an analyte in solution (eg. cell lysates or supernatants), the higher the affinity of the fluorescent chemosensor for the analyte, the better (Tsien, 1993). Since the concentration of cAMP measured in solution is typically between 10^{-11} and 10^{-8} M, a fluorescent chemosensor for solution measurements of cAMP would require an affinity of at least 10^{9} M⁻¹ [i.e. a dissociation constant (K_d) = 10^{-9} M] (Brooker et al., 1979). On the other hand, a fluorescent chemosensor designed for intracellular applications requires a dissociation constant that is in the range of the intracellular free

concentration of the analyte to be measured (Tsien, 1993). An affinity that is too high is just as undesirable as an affinity that is too low, since the chemosensor would start out already being saturated with the analyte and insensitive to further changes. Intracellular concentrations of cAMP typically vary from 10^{-9} M in resting cells to 10^{-6} M in stimulated cells (Tsien, 1993). A fluorescent chemosensor aimed at measuring the intracellular concentration of cAMP would, therefore, require an affinity of $\sim 10^{7}$ M⁻¹ ($K_d = 10^{-7}$ M).

1.9.1 Aims of the present study

The molecular imprinting of cAMP has not been reported. Furthermore, the preparation of a fluorescent molecularly imprinted polymer against cAMP, or any other template, that is capable of changing its fluorescence in the presence of the template in aqueous media has also not been demonstrated. Therefore, the aim of the present study was to test the feasibility of preparing a fluorescent molecularly imprinted polymer against cAMP. To achieve this goal our objectives were:

- to synthesize a fluorescent molecule (fluorophore) that is capable of changing fluorescence in response to interaction with cAMP;
- to explore the interaction of this fluorophore with cAMP in aqueous solution,and to determine the affinity and specificity of the interaction;
- to investigate the effects of related biomolecules on the fluorescence of the fluorophore in aqueous solution;
- 4. to synthesize a fluorescent cAMP-imprinted polymer as a polymer block, that would subsequently be ground into fine polymer particles for analysis;

5. to examine the binding of cAMP by measuring changes in the polymer fluorescence, and to determine the affinity and specificity of binding.

The fluorophore chosen for this purpose was a vinylbenzyl quaternary ammonium salt of 4-(p-N,N-dimethylamino)styrylpyridine. The cationic charge of this dye allows it to interact with negatively charged cAMP, while the presence of the vinyl group allows it to be incorporated into a polymer matrix. The fluorescence of 4-(p-N,N-dimethylamino)-styrylpyridines is also known to be sensitive to the polarity of the local microenvironment (Abdel-Mottaleb et al., 1988; Abdel-Mottaleb et al., 1989). At the onset of this work, one of the objectives was to synthesize a cAMP-imprinted nanoparticle, such as described above, using microemulsion polymerization. This polymerization technique requires surfactant molecules to stabilize the hydrophobic monomer droplets in an aqueous phase. Since 4-(p-N,N-dimethylamino)styrylpyridine quaternary ammonium salts may be transformed into surfactants through the addition of long alkyl chains, this fluorophore may then serve two purposes—it may act as a surfactant, and as a fluorophore able to interact with cAMP.

1.10 References

Abdel-Mottaleb, M.S.A. Laser Chem. 1984, 4, 305-310.

Abdel-Mottaleb, M.S.A.; Sherief, A.M.K.; Abdel-Azim, A.A.; Habashy, M.M.; Ismail, L.F.M. J. Photochem. Photobiol. 1988, 44, 161-169.

Abdel-Mottaleb, M.S.A.; Sherief, A.M.K.; Ismail, L.F.M.; De Schryver, F.C.; Vanderauweraer, M.A. J. Chem. Soc., Faraday Trans. 2 1989, 85, 1779-1788.

Adams, R. S.; Harootunian, A. T.; Buechier, Y. J.; Taylor, S. S; Tsien, R. Y. *Nature*. 1991, 349, 694-697.

Andersson, L.; Sellergren, B.; Mosbach, K. Tetrahedron Lett. 1984, 25, 5211-5214.

Andersson, L.I.; Müller, R.; Vlatakis, G.; Mosbach, K. *Proc. Natl. Acad. Sci. USA* 1995, 92, 4788-4792.

Andersson, L.I.; Nicholls, I.A.; Mosbach, K.H. In *Highly Selective Separations in Biotechnology*; Street, G., Ed.; Blackie: New York, 1994; pp 206-224.

Ansell, R.J.; Ramström, O.; Mosbach, K. Clin. Chem. 1996, 42, 1506-1512.

Bhattacharyya, K.; Chowdhury, M. Chem. Rev. 1993, 93, 507-535.

Bradford, M.M. Anal. Biochem. 1976, 72, 248-254.

Brooker, G., Harper, J.F., Terasaki, W.L., Moylan, R.D. In Advances in Cyclic

Nucleotide Research, Vol 10; Brooker, G., Greengard, T., Robison, G.A., Eds.; Raven

Press: New York, 1979; p 1-33.

Cooper, M.E.; Hoag, G.P.; Gin, D.L. Polymer Preprints. 1997, 38, 209-210.

Coudret, C.; Harriman, A. J. Chem. Soc., Chem. Commun. 1992, 1755-1757.

Crissman, H.A.; Hirons, G.T. Methods Cell Biol. 1994, 41, 195-209.

- Czarnik, A.W. In *Fluorescent Chemosensors for Ion and Molecule Recognition*; Czarnik, A.W., Ed.; ACS Symposium Series 538; American Chemical Society: Washington, DC, 1993; pp 1-9.
- Darnell, J.G.; Lodish, H.; Baltimore, D. Molecular Cell Biology, 3rd ed; Scientific American Books: New York, 1994.
- Dhaenens, M.; Lehn, J-M.; Vigneron, J-P. J. Chem. Soc., Perkin Trans. 2 1993, 1379-1381.
- Diehl, H.; Ellingboe, J.L. Anal. Chem. 1956, 28, 882-884.
- Duveneck, G.L.; Sitzmann, E.V.; Eisenthal, K.B.; Turro, N.J. J. Phys. Chem. 1989, 93, 7166-7170.
- Eberhard, M.; Erne, P. Biochem. Biophys. Res. Comm. 1991, 180, 209-215.
- Fery-Forgues, S.; Le Bris, M-T.; Guette, J-P.; Valeur, B. J. Phys. Chem. 1988, 92, 6233-6237.
- Glazer, A.N.; Rye, H.S. Nature, 1992, 359, 859-861.
- Grabowski, Z.R.; Rotkiewicz, K.; Siemiarczuk, A.; Cowley, D.J.; Baumann, W. Nouv. J. Chim. 1979, 3, 443-454.
- Grynkiewicz, G.; Poenie, M.; Tsien, R.Y. J. Biol. Chem. 1985, 260, 3440-3450.
- Hamasaki, K.; Ikeda, H.; Nakamura, A.; Ueno, A.; Toda, F.; Suzukia, I.; Osa, T. J. Am. Chem. Soc. 1993, 115, 5035-5040.
- Haugland, R.P. Handbook of fluorescent probes and Research Chemicals, 6th ed.; Spence, M.T.Z., Ed.; Molecular Probes, Inc.: Eugene, Oregon, 1996.
- Higgins, C. Nature, 1992, 358, 536.
- Hosseini, M.W.; Blacker, A.J.; and Lehn, J-M. J. Am. Chem. Soc. 1990, 112, 3896-3904.

- Inouye, M.; Hashimoto, K.; Isagawa, K. J. Am. Chem. Soc. 1994, 116, 5517-5518.
- James, T.D.; Linnane, P.; Shinkai, S. J. Chem. Soc., Chem. Comm. 1996a, 281-288.
- James, T.D.; Samankumara Sandanayake, K.R.A.; Shinkai, S. Angew. Chem. Int. Ed. Engl. 1996b, 35, 1910-1922.
- James, T.D.; Samankumara Sandanayake, K.R.A.; Shinkai, S. *Nature*. 1995, 374, 345-347.
- James, T.D.; Samankumara Sandanayake, K.R.A.; Shinkai, S. *Angew. Chem. Int. Ed. Engl.* 1994, 33, 2207-2209.
- Jameson, D.M. In Fluorescein Hapten: An Immunological Probe; Voss, E. Jr., Ed.; CRC Press (Uniscience series), Boca Raton, Florida, 1984.
- Kato, Y.; Morgan Conn, M.; Rebek, J. Jr. J. Am. Chem. Soc. 1994, 116, 3279-3284.
- Kessler, M.A.; Meinitzer, A.; Woflbeis, O.S. Anal. Biochem. 1997, 248, 180-182.
- Kriz, D.; Ramström, O.; Mosbach, K. Anal. Chem. 1997, 69, 345A-349A.
- Kriz, D.; Mosbach, K. Anal. Chim. Acta. 1995a, 300, 71-75.
- Kriz, D.; Ramström, O.; Svensson, A.; Mosbach, K. Anal. Chem. 1995b, 67, 2142-2144.
- Kuhn, M.A. In Fluorescent Chemosensors for Ion and Molecule Recognition; Czarnik, A.W., Ed.; ACS Symposium Series 538; American Chemical Society: Washington, DC, 1993, p147.
- Kumar, C.V.; Turner, R.S.; Asuncion, E.H. J. Photochem. Photobiol. A: Chem. 1993, 74, 231-238.
- Labarca, C.; Paigen, K. Anal. Biochem. 1980, 102, 344-352.
- Lakowicz, J.R. Principles of Fluorescence Spectroscopy; Plenum: New York, 1983.
- Landon, T.M. BioProbes 26; Molecular Probes, Inc.: Eugene, OR, 1997; p 12-13.

Law, K.Y. Photochem. Photobiol. 1981, 33, 799-806.

Lehn, J-M. Supramolecular Chemistry; VCH: New York, 1995.

LePecq, J-B.; Paoletti, C. Anal. Biochem. 1966, 17, 100-107.

LePecq, J-B.; Paoletti, C. J. Mol. Biol. 1967, 27, 87-106.

Létard, J-F.; Lapouyade R.; Rettig, W. J. Am. Chem. Soc. 1993, 115, 2441-2447

London, R.E. Annu. Rev. Physiol. 1991, 53, 241-258.

Loutfy, R.O. Pure Appl. Chem. 1986, 58, 1239-1248.

Lowry, O.H.; Rosebrough, N.J.; Farr, A.L., Randall, R.J. J. Biol. Chem. 1951, 193, 265-275.

Mathew, J.; Buchardt, O. Bioconjugate Chem. 1995, 6, 524-528.

Mathew-Krotz, J.; Shea, K.J. J. Am. Chem. Soc. 1996, 118, 8154-8155.

Mayes, A.G.; Andersson, L.I.; Mosbach, K. Anal. Biochem. 1994, 222, 483-488.

Minta, A.; Tsien, R.Y. J. Biol. Chem. 1989, 264, 19449-19457.

Montana, V.; Farkas, D.L.; Loew, L.M. Biochemistry 1989, 28, 4536-4539.

Moradian, A.; Mosbach, K. J. Mol. Recogn. 1989, 2, 167-169.

Mosbach, K.; Ramström, O. Biotechnology 1996, 14, 163-170.

Muldoon, M.T.; Stanker, L.H. Anal. Chem. 1997, 69, 803-808.

Muldoon, M.T.; Stanker, L.H. Chem. Ind. 1996, 6, 204-207.

Nag, A.; Bhattacharyya, K. Chem. Phys. Lett. 1988, 151, 474.

Piletskii, S.A.; Fedoryak, D.M.; Kukhar, V.P. Dokl. Akad. Nauk Ukr. SSR Ser. B 1990, 4, 53-54 [Chem. Abstr. 1991, 114, 165457q].

Piletsky, S.A.; Parhometz, Yu.P.; Lavryk, N.V.; Panasyuk, T.L.; El'skaya, A.V. Sens. Actuators B 1994, 18-19, 629-631.

- Piletsky, S.A.; Piletskaya, E.V.; El'skaya, A. V.; Levi, R.; Yano, K.; Karube, I. Anal. Lett. 1997, 30, 445-455.
- Piletsky, S.A.; Piletskaya, E.V.; Yano, K.; Kugimiya, A.; Elgersma, A.V.; Levi, R.; Kahlow, U.; Takeuchi, T.; Karube, I.; Panasyuk, T.I.; El'skaya, A. V. Anal. Lett. 1996, 29, 157-170.
- Price, C.P.; Newman, D.J. *Principles and Practice of Immunoassay, 2nd ed.*; Stockton Press: New York, 1997.
- Ramström, O.; Nicholls, I.A.; Mosbach, K. Tetrahedron: Assymetry 1994, 5, 649-656.
- Rettig, W. Angew. Chem., Int. Ed. Engl. 1986, 25, 971-988.
- Rettig, W.; Lapouyade, R. In *Topics in Fluorescence Spectroscopy, Volume 4: Probe Design and Chemical Sensing*; Lakowicz, J.R., Ed.; Plenum Press, New York, 1994; pp 109-149.
- Rettig, W.; Majenz, W. Chem. Phys. Lett. 1989, 154, 335-341.
- Rink, T.J.; Tsien, R.Y.; Pozzan, T. J. Cell. Biol. 1982, 95, 189-196.
- Rye, H.S.; Dabora, J.M.; Quesada, M.A.; Mathies, R.A.; Glazer, A.N. Anal. Biochem. 1993, 208, 144-150.
- Samankumara Sandanayake, K.R.A.; Nakashima, K.; Shinkai, S. J. Chem. Soc., Chem. Commun. 1994, 1621-1622.
- Schmidt, D.M.; Ernst, J.D. Anal. Biochem. 1995, 232, 144-146.
- Shea, K. J.; Spivak, D.A.; Sellergren, B. J. Am. Chem. Soc. 1993, 115, 3368-3369.
- Shin, M.D.; Whitten, D.G. J. Phys. Chem. 1988, 92, 2945-2956.
- Singer, V.L.; Jones, L.J.; Yue, S. FASEB J. 1995, A1422.
- Singer, V.L.; Jones, L.J.; Yue, S.T.; Haugland, R.P. Anal. Biochem. 1997, 249, 228-238.

Slavik, J. Biochim. Biophys. Acta 1982, 694, 1-25.

Steinke, J. H. G.; Dunkin, I.R.; Sherrington, D.C. Macromolecules 1996, 29, 407-415.

Steinke, J.; Sherrington, D.C.; Dunkin, I.R. Adv. Polym. Sci. 1995, 123, 81-125.

Suh, D.; Chaires, J.B. Bioorg. & Med. Chem. 1995, 3, 723-728.

Tsien, R. Y. Biochemistry 1980, 19, 2396-2404.

Tsien, R. Y. in Fluorescent Chemosensors for Ion and Molecule Recognition; Czarnik, A.W., Ed.; ACS Symposium Series 538; American Chemical Society: Washington, DC, 1993.

Tsien, R.Y. Nature 1981, 290, 527-528.

Verkman, A.S.; Sellers, M.C.; Chao, A.C.; Leung, T.; Ketcham, R. Anal. Biochem. 1989, 178, 355-361.

Vlatakis, G.; Andersson, L.I.; Müller, R.; Mosbach, K. Nature. 1993, 361, 645-647.

Wulff, G. Angew. Chem. Int. Ed. Engl. 1995, 34, 1812-1832.

Wulff, G. EXS 1997, 80 (Frontiers in Biosensorics 1 Fundamental Aspects), 13-26.

Wulff, G.; Sarhan, A.; Zabrocki, K. Tetrahedron Lett. 1973, 44, 4329-4332.

Wulff, G.; Vesper, W.; Grobe-Einsler, R.; Sarhan, A. Makromol. Chem. 1977, 178, 2799-2816.

CHAPTER 2

Effect of Nucleotides on the Charge Transfer Fluorescence of *trans*-4-(*p*- N, N-Dimethylamino-styryl) N-vinylbenzylpyridinium Chloride

Petra Turkewitsch, Barbara Wandelt, Rik R. Ganju, Graham D. Darling,
William S. Powell

"Reprinted from *Chemical Physics Letters*, **1996**, 260, 142-146 with kind permission of Elsevier Science - NL, Sara Burgerhartstraat 25, 1055 KV Amsterdam, The Netherlands".

Foreword

This chapter describes effects of the cyclic purine nucleotides, cAMP and cGMP, on the absorbance and fluorescence of a newly synthesized fluorescent molecule, *trans*-4-(*p-N,N*-dimethylaminostyryl)-*N*-vinylbenzylpyridinium chloride (1), in unbuffered water. Dye 1 is a member of a family of 4-(*p*-dimethylaminostyryl)pyridinium salts prepared by us, which also includes *trans*-4-(*p-N,N*-dimethylaminostyryl)-*N*-phenethylpyridinium bromide (2) (Wandelt et al., 1995a). The synthesis of dye 1 is presented in Chapter 3, and the synthesis of 2 is presented in Appendix 3, Section A. Our previous studies of dye 2 in aqueous solution have suggested that it exhibits TICT behavior (Wandelt et al., 1995a).

Appendix 2, Section A presents a figure (Figure 2A.1) comparing the effects of the highest concentration (50 mM) of D-ribose-5-phosphate, cAMP and cGMP tested on the fluorescence 1 in unbuffered water.

In this chapter and throughout this thesis *trans*-4-(*p*-*N*,*N*-dimethylaminostyryl)-*N*-vinylbenzylpyridinium chloride (1 or dye 1) refers to a 70:30 mixture of *trans*-4-(*p*-*N*,*N*-dimethylaminostyryl)-*N*-*m*-vinylbenzylpyridinium chloride and *trans*-4-(*p*-*N*,*N*-dimethylaminostyryl)-*N*-*p*-vinylbenzylpyridinium chloride.

2.1 Abstract

The addition of the cyclic nucleotides, cAMP and cGMP, to aqueous solutions of trans-4-(p-N,N-dimethylaminostyryl)-N-vinylbenzylpyridinium chloride (1) dramatically enhanced the fluorescence quantum yield of 1 with concomitant slight red shifts of the λ_{max} , and had slight hyperchromic and bathochromic effects on the absorbance of 1. In contrast, D-ribose-5-phosphate had no such effects. These results suggest that 1 preferentially associates with nucleotides in aqueous solution, with equilibrium constants for cAMP and cGMP of 14.0 ± 1.08 and 9.31 ± 0.97 M⁻¹, respectively. Thus, dye 1 may serve as a starting point for the development of more sensitive and specific probes for cyclic nucleotides.

2.1 Introduction

There is considerable interest in sensor molecules that communicate their association with substrates fluorometrically (Czarnik, 1993; James et al., 1995). One possible sensing mechanism utilizes the fluorescence from an intramolecular charge transfer (ICT) excited state since its dynamic processes are known to be remarkably sensitive to the microenvironment (Bhattacharyya and Chowdhury, 1993; Sato et al., 1995; Nag and Bhattacharyya, 1988; Hamasaki et al., 1993; Wang and Eisenthal, 1982; Herbich et al., 1989; Shin and Whitten, 1988; Wandelt et al., 1995a; Ephardt and Fromherz, 1989; Abdel-Mottaleb et al., 1988; Létard et al., 1993; Rettig, 1986). Electron donor-acceptor (EDA) molecules capable of photoinduced ICT have been employed as ion indicators (Lohr and Vogtle, 1985; Fery-Forgues et al., 1988) and fluorescent probes in micelles (Shin and Whitten, 1988; Abdel-Mottaleb et al., 1988), polymeric matrices (Abdel-Mottaleb et al., 1988), and biological membranes (Ephardt and Fromherz, 1989).

Recently, photophysical studies of trans-4-(p-N,N-dimethylamino)stilbene (DAS) by Létard et al. (Létard et al., 1993) have pinpointed the occurrence of a twisted intramolecular charge-transfer (TICT) excited state, which is responsible for the main part of its emission. With bridged derivatives of DAS they have concluded that this emitting TICT state is formed by a twisting of the single bond linking the dimethylanilino (donor) group and the styrene (acceptor) group, with simultaneous charge transfer from the donor to the acceptor. The TICT concept was proposed to explain the dual fluorescence coupled with ICT of p-(dimethylamino)benzonitrile (DMABN)

(Bhattacharyya and Chowdhury, 1993; Rettig, 1986). It was postulated that its dual fluorescence arose from two configurations of the same molecule: an initially planar locally excited (LE) state, and a rotational isomer in which a charge transfer from the dimethylamino (donor) group to the benzonitrile (acceptor) moiety has taken place with a twisting of the dimethylamino group towards a plane perpendicular to that of the phenyl ring (TICT state) (Bhattacharyya and Chowdhury, 1993; Rettig, 1986).

Currently, the TICT model is favored in cases of dual fluorescence (Bhattacharyya and Chowdhury, 1993; Rettig, 1986), although its acceptance in not universal. Several other models have been proposed (Leinhos et al., 1991; Zachariasse et al., 1994; Zachariasse et al., 1993; Gruen and Gorner, 1989). Zachariasse and coworkers (Leinhos et al., 1991) concluded that an ICT reaction in the excited state occurs in the classic DMABN system in toluene, and argued (Zachariasse et al., 1994; Zachariasse et al., 1993) that N-inversion (pyrimidallization) of the amino group acts as the ICT promoting mode. In a study of trans-4-nitro-4'-(dialkylamino)stilbene derivatives, Gruen and Gorner (Gruen and Gorner, 1989) suggested the formation of a TICT state in polar solvents where the nitro group could be orthogonal to the remainder of the molecule. Nontheless, formation of a TICT excited state involves a large structural change, making its photophysical properties remarkably sensitive to the microenvironment. Modification of the TICT photophysical properties of a molecule through changes in its microenvironment is a phenomenon reported for many EDA molecules (Bhattacharyya and Chowdhury, 1993; Sato et al., 1995; Nag and Bhattacharyya, 1988; Hamasaki et al.,

1993; Wang and Eisenthal, 1982; Herbich et al., 1989; Shin and Whitten, 1988; Wandelt et al., 1995a; Ephardt and Fromherz, 1989).

A polar solute molecule may surround itself preferentially with a component of its solvent mixture (i.e. its environment), leading to an inhomogeneity in the solution (Ghoneim and Suppan, 1993; Suppan, 1987; Moog et al., 1991; Hoffman et al., 1995). This preferential solvation results from both nonspecific associations, arising from a general electrostatic effect known as dielectric enrichment, and specific interactions (e.g. aryl stacking, hydrogen bonding) which occur between the solute and its environment. Thus, the solvent shell of a solute molecule may become markedly enriched with a particular component of a solution (i.e. the analyte), resulting in a composition different from that of the bulk solution. If the solute is fluorescent, this preferential solvation may change its fluorescent properties, permitting quantitation of the analyte. This solute selectivity may be very desirable in terms of the ability of a fluorescent molecule to act as a chemical sensor (Hoffman et al., 1995).

The sensitivity of fluorescent DAS (Létard et al., 1993) and other fluorescent stilbene-like molecules (Shin and Whitten, 1988; Wandelt et al., 1995a; Ephardt and Fromherz, 1989; Abdel-Mottaleb et al., 1988; Abdel-Mottaleb, 1984; Abdel-Mottaleb et al., 1989) to their environment, prompted us to synthesize 1 which combined the special photophysical properties of this stilbene moiety with a positive charge which could promote an association with negatively charged cyclic nucleotides. cAMP and cGMP were chosen for our investigation because of their vital role in biological information-

transfer processes (Zubay, 1988). Herein, we report the effects of these cyclic nucleotides on the fluorescent properties of dye 1 in aqueous solution. We found them to dramatically increase the fluorescence quantum yield of 1, suggesting that molecules of this type could act as chemosensors for cyclic nucleotides. This new dye belongs to a family of 4-(p-dimethylaminostyryl)pyridinium salts, some of which appear to be useful for the measurement of intracellular and solution viscosity (Wandelt et al., 1995a; Wandelt et al., 1995b). In addition, the presence of the vinyl group permits the use of dye 1 for the preparation of fluorescent molecular imprinted polymer chemosensors (Turkewitsch et al., 1995; Turkewitsch et al., 1998).

2.2 Experimental

Dye 1 was prepared from 4-(p-dimethylaminostyryl)pyridine (Kost et al., 1964) by simple N-alkylation with 3-vinylbenzyl chloride (70:30 mixture of meta-vinylbenzyl chloride:para-vinylbenzyl chloride) in acetonitrile. The details will be published separately (Please refer to Chapter 3).

Aqueous solutions were prepared using double distilled deionized water (Millipore). Solutions containing various concentrations of adenosine 3':5'-cyclic monophosphate (cAMP, Sigma), guanosine 3':5'-cyclic monophosphate (cGMP, Sigma), and D-ribose-5-phosphate (Aldrich), with a constant concentration (10' M) of dye 1 were prepared. This low concentration of 1 was used to minimize self-absorption and self-aggregation contributions. Spectroscopic measurements were performed the following day on thoroughly mixed nondegassed solutions.

The visible absorption spectra were recorded on a Beckmann DU-64 spectrophotometer. The fluorescence spectra were measured on a Photon Technology International Deltascan 4000 spectrofluorometer with 8 nm emission slits on solutions in 1-cm cubic cuvettes maintained at 22 ± 0.1 °C. An excitation wavelength of 469 nm was used to obtain the fluorescence emission spectra of 1 in all solutions. The fluorescence spectra are not corrected. The fluorescence quantum yield of dye 1 in all solutions was determined by the method of Parker and Rees (Parker and Rees, 1960) from the emission spectrum obtained with excitation at 469 nm relative to the quantum yield of rhodamine B in ethanol ($\Phi = 0.69$; excitation = 366 nm; 22 °C) as a standard. The integrated areas under the emission bands gave the relative intensities of the solutions. The quantum yields were calculated with corrections for the absorbances of all solutions as described by Parker and Rees (Parker and Rees, 1960). In addition, the absorbances of all solutions were approximately < 0.3 in absorbance units at the exciting wavelength, ensuring no complications due to the inner filter effects.

2.3 Results and Discussion

The NMR spectra of dye 1 (see Appendix 3, Section B, Figure 3B.2) suggested that there were no major contaminants in the product. However, it revealed that *trans*-4-(*p-N,N*-dimethylaminostyryl)-*N*-vinylbenzylpyridinium chloride (1 or dye 1) was a 70:30 mixture of *trans*-4-(*p-N,N*-dimethylaminostyryl)-*N-m*-vinylbenzylpyridinium chloride and *trans*-4-(*p-N,N*-dimethylaminostyryl)-*N-p*-vinylbenzylpyridinium chloride. This mixture may make the interpretation of the absorption and fluorescence results in this chapter, and throughout the remainder of the thesis, difficult. However, because dyes 1 and 2 have very similar fluorescence spectra (Figure 3B.1 in Appendix 3, Section B), and behave similarly in the presence of cAMP (Appendix 3, Section E) and biological macromolecules (Figure 4.2 in Chapter 4), it would appear that the substituent on the pyridinium nitrogen (vinylbenzyl in the case of 1, and phenethyl in the case of 2) does not affect the fluorescence properties of these dyes appreciably. Please refer to the Discussion section of Chapter 3 for more detail.)

Figure 2.1 shows the visible absorption and fluorescence spectra of 1 in water. The single broad absorption band of 1 in water exhibited a λ_{max} at 469 nm with a molar extinction coefficient of 18 900 L mol⁻¹ cm⁻¹ (Fig. 2.1a). The fluorescence emission spectrum of 1 in water excited at 469 nm has a maximum at 608 nm, and a quantum yield of 1.20×10⁻³ (Fig. 2.1b). This band closely resembles the ICT spectrum obtained by us for the very similar *trans*-4-(p-N,N-dimethylaminostyryl)-N-phenethylpyridinium bromide (Wandelt et al., 1995a). In addition, similarities exist between dye 1 and related

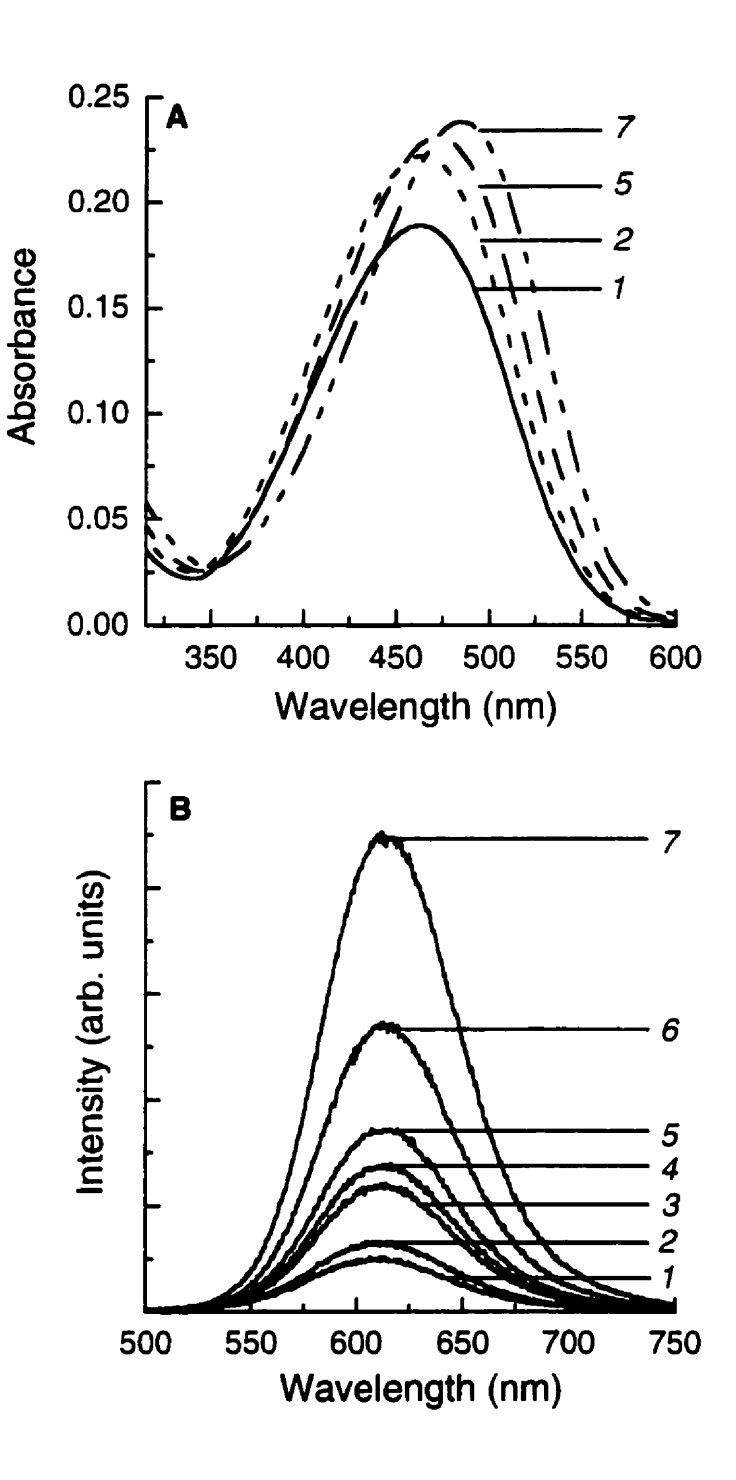


Figure 2.1. Absorption (A) and fluorescence (B) spectra of aqueous solutions of 1 (10⁻⁵ M) at 22 °C in the absence (1) and presence (2-7) of various concentrations of cAMP: (2) 1 mM, (3) 5 mM, (4) 6.67 mM, (5) 10 mM, (6) 20 mM and (7) 50 mM; the excitation wavelength for fluorescence measurements was 469 nm; the emission maxima ranged between 608-612 nm.

styrylcyanine dyes investigated by Abdel-Mottaleb and coworkers (Abdel-Mottaleb et al., 1988; Abdel-Mottaleb, 1984; Abdel-Mottaleb et al., 1989), charge-transfer polyenes reported by Shin and Whitten (Shin and Whitten, 1988), a (dialkylamino)stilbazolium dye examined by Ephardt and Fromherz (Ephardt and Fromherz, 1989), as well as DMABN (Rettig, 1986) and DAS (Létard et al., 1993). On this basis, we have attributed this emission band of 1 in water to a TICT-type state.

The effects of various concentrations of cAMP on the absorption and fluorescence spectra of 1 in water are also shown in Figure 2.1a and 2.1b. Concentrations of nucleotide above 50 mM were not examined due to solubility limitations. Increasing concentrations of cAMP caused a red shift in the absorption maximum accompanied by a hyperchromic effect (Fig. 2.1a). cAMP also induced a dramatic enhancement in the fluorescence quantum yield with a concomitant slight red shift (from 608 nm in water to 612 nm in solutions containing cAMP) (Fig. 2.1b and Fig. 2.2). Similar absorption and fluorescence patterns were observed for 1 upon addition of cGMP, whereas D-ribose-5-phosphate did not induce any changes (Fig. 2.2) (The fluorescence spectra of 1 in the presence of 50 mM D-ribose-5-phosphate, cAMP and cGMP are shown in Figure 2A.1 in Appendix 2, Section A.) The effects of cAMP and cGMP on the absorption and emission spectra of 1 are consistent with the process of preferential solvation (Suppan, 1987).

Hoffmann et al. (Hoffmann et al., 1995) demonstrated strong preferential solvation of the dansyl chromophore, also capable of ICT, in binary solvent mixtures and swollen polymer networks. In addition, the EDA molecule, dimethylaminonitrostilbene,

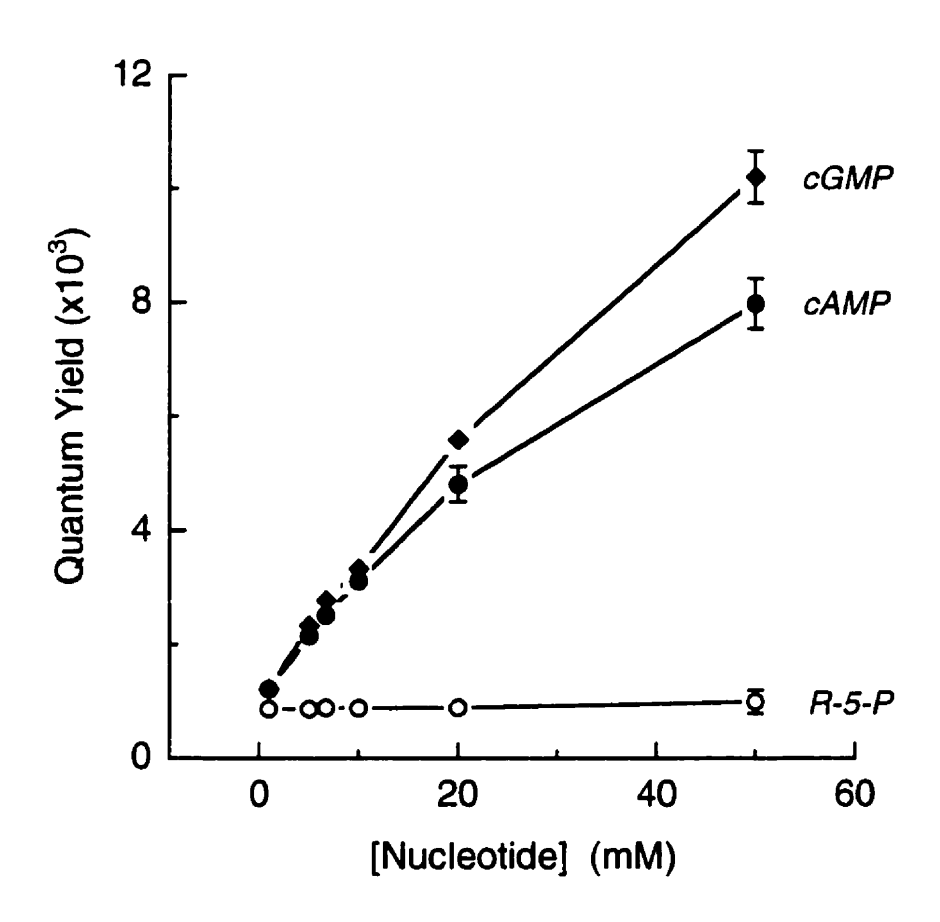


Figure 2.2. Fluorescence quantum yield titration curves of 1 as a function of nucleotide concentration. Solutions contained 1 (10⁻⁵ M) and various concentrations of D-ribose-5-phosphate (R-5-P, O), cAMP (●), and cGMP (♦) in water at 22 °C; the excitation wavelength was 469 nm. The values are means ± standard errors of 3 independent observations.

demonstrated preferential solvation in a tetrahydrofuran (THF)-cyclohexane solvent mixture, where the solvation shell was found to be nearly pure THF in a mixture containing a very low THF mole fraction (0.03) (Suppan, 1987). Preferential solvation effects on the TICT fluorescence of DMABN in several solvent mixtures have also been reported (Ghoneim and Suppan, 1993).

Moog et al. (Moog et al., 1991) observed similar effects in the absorption and fluorescence of 1-aminofluorenone (1-AF) in heptane when they added small amounts of 2,2,2-trifluoroethanol (TFE). They reported a hydrogen-bonded complex between 1-AF and the alcohol, resulting from dielectric enrichment by TFE, which decreased the nonradiative rate constant of 1-AF relative to that in pure heptane. In analogous experiments by Wang and Eisenthal (Wang and Eisenthal, 1982), stabilization of the TICT state of DMABN by interactions with butanol in butanol/hexadecane mixtures was reported to produce very similar effects on the absorption and emission spectra. In addition, Sato et al. (Sato et al., 1995) reported a large increase of fluorescence quantum yield and a lowering of the nonradiative rate constant for the CT emission of an EDA β -diketone upon complexation with Mg²⁺ in acetone and acetonitrile.

The very large dipole moments of TICT states, including DMABN

(Bhattacharyya and Chowdhury, 1993; Rettig, 1986) and the similar DAS molecule

(Létard et al., 1993), have been established, and correspond to a charge separation

between the donor and acceptor moieties. Thus, it would be expected that the dipole

moment of the TICT-type excited state of dye 1 would be larger than that of the ground

state. Since TICT states have extremely large dipole moments, they may be stabilized by an increase in the polarity of the environment, reducing the energy barrier between the Franck-Condon excited state and the TICT state as discussed by Nag and Bhattacharyya (Nag and Bhattacharyya, 1988). As a result, their TICT emission should exhibit a shift of the emission maximum to the red, and an increase in quantum yield (Bhattacharyya and Chowdhury, 1993; Nag and Bhattacharyya, 1988).

The cyclic nucleotides and ribose-5-phosphate are negatively charged species and could therefore affect the polarity surrounding the positively charged dye 1. We observed a red shift, and an increase in the quantum yield of 1 with cAMP and cGMP, but not with ribose-5-phosphate (Fig. 2.2). This suggests that the cyclic nucleotide-induced changes are not solely due to an increase in the polarity of the environment resulting from dielectric enrichment, since they are not induced by ribose-5-phosphate which also has a negatively charged phosphate group (Fig. 2.2). Other factors, such as aryl stacking interactions between the aromatic rings of 1 and the base of the nucleotides may also be involved in the preferential association of 1 with nucleotides.

Figure 2.2 shows the fluorescence titration curves for 10° M 1 as a function of nucleotide concentration. In the concentration range studied, the fluorescence quantum yield is closely correlated with the concentrations of nucleotides. The equilibrium,

dye + nucleotide \iff dye-nucleotide, is controlled by the equilibrium association constant,

$$K_{eq} = [dye-nucleotide] / [dye] [nucleotide]$$
 (1).

The fluorescence quantum yield Φ of 1 in the presence of nucleotide represents the quantum yield of a mixture of fluorescing species, which may be described by the equation:

$$\Phi = x_{\text{Au}}\Phi_{\text{a}} + (1 - x_{\text{Au}})\Phi_{\text{c}} \tag{2}$$

where x_{dre} is the mole fraction of "free" dye 1, and Φ_c and Φ_c are the fluorescence quantum yields of 1 in the absence of nucleotide, and of the dye-nucleotide complex, respectively. Since $x_{dre} = [dye] / ([dye] + [dye-nucleotide])$, it is readily shown from equations 1 and 2 that

$$\Phi = \Phi_o + \left(\Phi_c - \Phi_o\right) \frac{K_{eq}[nucleotide]}{1 + K_{eq}[nucleotide]}$$
(3).

SigmaPlot curve fitter was used to fit the fluorescence titration data in Fig. 2.2 to equation 3 directly to estimate the K_{eq} and Φ_c values. K_{eq} values of 14.0 ± 1.08 and 9.31 ± 0.097 M¹, and Φ_c values of 0.018 ± 0.0003 and 0.031 ± 0.004 were determined for cAMP and cGMP, respectively. Assuming that poorly selective electrostatic and aryl stacking interactions are governing the association process, it is not surprising that these values are similar in solution.

2.4 Conclusions

Dye 1 preferentially associates with the cyclic nucleotides, cAMP and cGMP, in aqueous solution resulting in dramatic increases in its quantum yield. Thus, 1 is capable of detecting cAMP and cGMP by TICT-type fluorescence, although calculation of the

equilibrium constants for their interactions indicate that it has limited capability to discriminate between them in solution. Nonetheless, in combination with other molecular structures providing more specific recognition, this fluorescent dye might form the basis of a chemosensor for either of these nucleotides. This will provide a challenge for future research.

2.5 Acknowledgments

The authors thank the Respiratory Health Network of Centers of Excellence and the Medical Research Council of Canada for financial support of this work, and the Canadian Cystic Fibrosis Foundation for studentship support for P. Turkewitsch. We also wish to acknowledge the contributions of the late Dr. Seymour Heisler.

2.6 Endnotes

¹ Equilibrium association constants of 212 ± 46 and 285 ± 18 M⁻¹ were reported for cAMP and cGMP, respectively, in the published manuscript. However, these values were calculated using an incorrect equation. The correct values are presented in the text.

² The data were analyzed using an incorrect equation in the published manuscript. The correct analysis now appears in the text. The following analysis appeared in the original manuscript

"The data were analyzed according to Suppan's [22] equation (1) for preferential solvation, assuming the fraction of associated species described in terms of fluorescence quantum yield to be given by

$$\Phi_o / (\Phi - \Phi_o) = 1 + 1 / K_{eo}[N]$$
 (1).

The fluorescence quantum yields of 1 in the absence and presence of nucleotide are given by Φ_a and Φ , respectively. The equilibrium:

dye (D) + nucleotide (N)
$$\rightleftharpoons$$
 dye-nucleotide (D-N) (2) is controlled by the equilibrium constant, $K_{sq} = [dye-nucleotide] / [dye]$ [nucleotide]. Linear least-squares analysis of plots of Φ_o/Φ_o vs. [N]⁻¹ led to good correlation coefficients for cAMP (0.9996) and cGMP (0.9978) (data not shown). The K_{sq} values, given by the inverses of the slopes, were 212 ± 46 and 285 ± 18 M⁻¹ for cAMP and cGMP, respectively."

2.7 References

Abdel-Mottaleb, M.S.A. Laser Chem. 1984, 4, 305-310.

Abdel-Mottaleb, M.S.A.; Sherief, A.M.K.; Abdel-Azim, A.A.; Habashy, M.M.; Ismail, L.F.M. J. Photochem. Photobiol. 1988, 44, 161-169.

Abdel-Mottaleb, M.S.A.; Sherief, A.M.K.; Ismail, L.F.M.; De Schryver, F.C.; Vanderauweraer, M.A. J. Chem. Soc., Faraday Trans. 2 1989, 85, 1779-1788.

Bhattacharyya, K.; Chowdhury, M. Chem. Rev. 1993, 93, 507-535.

Czarnik, A.W. Fluorescent Chemosensors for Ion and Molecule Recognition; ACS

Symposium Series 538; American Chemical Society: Washington, DC, 1993.

Ephardt, H.; Fromherz, P. J. Phys. Chem. 1989, 93, 7717.

Fery-Forgues, S.; Le Bris, M-T.; Guette, J-P.; Valeur, B. J. Phys. Chem. 1988, 92, 6233-6237.

Ghoneim, N.; Suppan, P. Pure Appl. Chem. 1993, 65, 1739.

Gruen, H.; Gorner, H. J. Phys. Chem. 1989, 93, 7144.

Hamasaki, K.; Ikeda, H.; Nakamura, A.; Ueno, A.; Toda, F.; Suzukia I.; Osa, T. J. Am. Chem. Soc. 1993, 115, 5035.

Herbich, J.; Grabowski, Z.R.; Wojtowicz H.; Golankiewicz, K. J. Phys. Chem. 1989, 93, 3439.

Hoffmann, D.A.; Anderson, J.E.; Frank, C.W. J. Mater. Chem. 1995, 5, 13.

James, T.D.; Samankumara Sandanayake, K.R.A.; Shinkai, S. Nature 1995, 374-345.

Kost, A.N.; Sheinkman, A.K.; Rozenberg, A.N. J. Gen. Chem. USSR (Eng. Transl.) 1964, 84, 4106-4112.

Leinhos, U.; Kuhnle W.; Zachariasse, K.A. J. Phys. Chem. 1991, 95, 2013.

Létard, J-F.; Lapouyade R.; Rettig, W. J. Am. Chem. Soc. 1993, 115, 2441-2447.

Lohr, H-G.; Vogtle, F. Acc. Chem. Res. 1985, 18, 65.

Moog, R.S.; Burozski, N.A.; Desai, M.M.; Good, W.R.; Silvers, C.D.; Thompson, P.A.; Simon, J.D. J. Phys. Chem. 1991, 95, 8466-8473.

Nag, A.; Bhattacharyya, K. Chem. Phys. Lett. 1988, 151, 474.

Parker, C.A.; Rees, W.T.; Analyst 1960, 85, 587-600.

Rettig, W. Angew. Chem., Int. Ed. Engl. 1986, 25, 971-988.

Sato, Y.; Morimoto, M.; Segewa, H.; Shimidzu, T. J. Phys. Chem. 1995, 99, 35-39.

Shin, M.D.; Whitten, D.G. J. Phys. Chem. 1988, 92, 2945-2956.

Suppan, P. J. Chem. Soc., Faraday Trans. 1 1987, 83, 495.

Turkewitsch P.; Wandelt, B.; Darling, G.D.; Powell, W.S. Functional recognition sites through molecular imprinting. A polymer-based fluorescent indicator for aqueous cAMP. 78th Canadian Society for Chemistry (CSC) Conference, Guelph, ON, Canada, May 28-June 1, 1995; abstract 547.

Turkewitsch P.; Wandelt, B.; Darling, G.D.; Powell, W.S. Anal. Chem. 1998, 70, 2025-2030.

Wandelt, B.; Turkewitsch, P.; Stranix, B.R.; Darling, G.D. J. Chem. Soc., Faraday Trans. 1995a, 91, 4199-4205.

Wandelt, B.; Turkewitsch P.; Stranix, B.R.; Darling, G.D. "Molecular Viscometer"™ for fluorescence imaging of intracellular viscosity. Third International Symposium on Functional Dyes, Santa Cruz, CA, USA, July 16-21, 1995b.

Wang Y.; Eisenthal, K.B. J. Chem. Phys. 1982, 77, 6076.

Zachariasse, K.A.; Von Der Haar, Th.; Hebecker, A.; Leinhos, U.; Kuhnle, W. Pure Appl. Chem. 1993, 65, 1745.

Zachariasse, K.A.; Von Der Haar, Th.; Leinhos, U.; Kuhnle, W. J. Inf. Rec. Mats. 1994, 21, 501.

Zubay, G. Biochemistry, 2nd ed.; Macmillan Publishing Co.: New York, 1988.

CHAPTER 3

Nucleotides Enhance the Fluorescence of *trans*-4-(*p*-N,N-Dimethylaminostyryl)-N-vinylbenzylpyridinium Chloride

Petra Turkewitsch, Barbara Wandelt, Graham D. Darling,

William S. Powell

"Reprinted from the *Journal of Photochemistry and Photobiology A: Chemistry*, in press, Petra Turkewitsch, Barbara Wandelt, Graham D. Darling, William S. Powell, Nucleotides Enhance the Fluorescence of *trans-4-(p-N,N-Dimethylaminostyryl)-N-vinylbenzyl-* pyridinium Chloride, copyright (1998), with permission from Elsevier Science"

Foreword

In this chapter we examine the specificity of the interaction between *trans-4-(p-N,N-dimethylaminostyryl)-N-vinylbenzylpyridinium* chloride (1) and nucleotides by investigating the fluorescence of 1 in the presence of various purine and pyrimidine analytes. The effect of pH on the interaction was also examined. In the previous chapter, we suggested that a TICT-type excited state was responsible for the emission of 1 at 608 nm (excitation 469 nm). Herein, we examine the fluorescence properties of 1 in various solvents to determine the extent of charge transfer in the excited state, thereby providing further evidence of a TICT process in 1.

In chapter 2, we explained the fluorescence quantum yield increase of dye 1 in the presence of cAMP and cGMP using a TICT mechanism. Briefly, we suggested that an increase in polarity of the environment in the presence of these analytes stabilized the large dipole moment of the TICT-type excited state of 1, lowering its energy, and causing an increase in quantum yield of the TICT-type emission of 1, and a shift of it emission maximum to the red. However, upon examining the literature describing closely related molecules more throughly, we now believe that the increase in fluorescence quantum yield of 1 in the presence of cAMP, cGMP and other purine analytes is probably due to a decrease in the nonradiative decay rate of 1. This decrease in the nonradiative decay rate of 1 is most likely caused by a restriction of the rotation around the ethylenic double bond of 1 in the excited state (a motion associated with *trans-cis* photoisomerization) upon binding to the analytes.

¹ trans-4-(p-N,N-Dimethylaminostyryl)-N-vinylbenzylpyridinium chloride (1 or dye 1) refers to a 70:30 mixture of trans-4-(p-N,N-dimethylaminostyryl)-N-m-vinylbenzylpyridinium chloride and trans-4-(p-N,N-dimethylaminostyryl)-N-p-vinylbenzylpyridinium chloride.

The Appendix to this chapter (Appendix 3) contains some additional data and experiments for 1 and 2. Section A presents the synthesis and the 'H NMR spectrum of dye 2 (trans-4-(p-N,N-dimethylaminostyryl)-N-phenethylpyridinium bromide). The fluorescence spectra of 1 and 2 in phosphate buffer obtained by exciting at 360 nm is presented in Section B, together with the 'H NMR spectrum of dye 1 and its excitation spectrum obtained at emission maxima of 510 and 600 nm. Section C presents the absorption and fluorescence spectra of 1 in three solvents (water, chloroform and acetonitrile) chosen from Table 3.1. The fluorescence spectra of 1 in phosphate buffer in the presence of the highest concentration (50 mM) of cAMP, cGMP, ATP and CMP are compared in Section D. In Section E, the fluorescence responses of dyes 1 and 2 in the presence of cAMP concentrations between 1 and 50 mM are presented. The enhancements in the fluorescence quantum yields of 1 and 2 induced by cAMP, and the association constants for 1 and 2 with cAMP were similar, suggesting that the substituent on the pyridinium nitrogen of these dyes has relatively little effect on their fluorescence. This raises the possibility then that the mixture meta and para-vinylbenzyl isomers in 1 also do not appreciably affect the fluorescence of 1. An experiment in which cells were loaded with the calcium responsive dye, fura-2, and their ability to respond to serotonin stimulation in the absence and in the presence of dye 2 is presented in Section F. The magnitude of the response of the cells to serotonin was similar in the absence and in the presence of dye 2. These results suggest that dye 2 is capable of passively diffusing across the plasma membrane, and does not affect the physiological functioning of cells.

Abstract

The newly synthesized trans-4-(p-N,N-dimethylaminostyryl)-Nvinylbenzylpyridinium chloride (1) displays strong solvatochromic behavior resulting from a large increase of ~ 13 D in its dipole moment upon excitation. This indicates that its excited state has considerable charge transfer character, suggesting that it may be subject to solute-induced fluorescence changes. The fluorescence quantum yield of 1 is enhanced dramatically (12-fold) in the presence of a buffered aqueous solution of cAMP, a purine nucleotide. In contrast, the pyrimidine nucleotides, CMP and UMP, have virtually no effect on the fluorescence of 1. cGMP induced an increase in the quantum yield of 1 similar to that induced by cAMP, whereas other purine nucleotides (AMP, ADP and ATP) and adenosine induced changes of somewhat lesser magnitude. Equilibrium association constants for 1 with these analytes ranged from 13.8 M¹ for cAMP to 0.15 M⁻¹ for adenine. We conclude that the interaction of 1 with the purine analytes requires the presence of a purine base, and is enhanced by ribose and phosphate moieties. The environmentally sensitive fluorescence of 1 suggests that such compounds may be useful as chemosensors for purine nucleotides.

3.1 Introduction

Fluorescent indicators are perhaps the most popular and powerful tools for the measurement of intracellular concentrations of various ions and other messengers involved in the transduction of biological signals (Tsien, 1993). The virtue of fluorescence is that it can be applied to intact cells with high spatial and temporal resolution while the cells undergo physiological responses. To this end, sensor molecules that communicate their association with analytes fluorometrically are attracting considerable attention. In particular, electron donor-acceptor (EDA) molecules have been employed as chemosensors for ions (Fery-Forgues et al., 1988), miceiles (Abdel-Mottaleb et al., 1988; Law, 1981; Shin and Whitten, 1988), polymeric matrices (Abdel-Mottaleb et al., 1988; Loutfy, 1986) and biological systems (Kumar et al., 1993; Chan et al., 1996; Montana et al., 1989), since they display fluorescence from intramolecular charge transfer (ICT) excited states, which are known to be remarkably sensitive to the microenvironment (Rettig, 1986; Bhattacharyya and Chowdhury, 1993).

The environmental sensitivity of fluorescent EDA stilbene (Shin and Whitten, 1988; Létard et al., 1993) and styrylpyridinium (Abdel-Mottaleb et al., 1988; Montana et al., 1989; Wandelt et al., 1995; Abdel-Mottaleb, 1984; Abdel-Mottaleb et al., 1989) molecules, prompted us to synthesize 1, which combines the special photophysical properties of these EDA molecules with a positive charge capable of promoting an association with negatively charged nucleotides. We are particularly interested in the cyclic nucleotide, adenosine 3':5'-cyclic monophosphate (cAMP), because of its vital role as an intracellular second messenger, mediating the actions of many hormones, drugs and

neurotransmitters which act via cell surface receptors (Darnell et al., 1994). The presence of the vinyl group permits the use of dye 1 for the preparation of fluorescent molecularly imprinted polymer chemosensors (Turkewitsch et al., 1998).

Recently, we reported (Turkewitsch et al., 1996) a marked fluorescence quantum yield enhancement of 1 in the presence of unbuffered aqueous solutions of cAMP and cGMP, suggesting that dye 1 preferentially associates with these cyclic nucleotides. The objectives of the present study were to further explore the environmentally sensitive fluorescence of 1 under more relevant biological conditions, which would allow investigation into the nature of the association between dye 1 and nucleotides in the physiological pH range, and examination of the structural requirements for the effects of the nucleotides on the quantum yield of 1. We found that dye 1 shows dramatic fluorescence enhancements in the presence of purine nucleotides, but almost no fluorescence enhancement with pyrimidine nucleotides. Thus, dye 1 could be a prototype for fluorescent chemosensors for purine nucleotides such as cAMP.

3.2 Experimental

3.2.1 Materials

4-(p-Dimethylaminostyryl)pyridine (DMASP) was prepared by a published procedure (Kost et al., 1964). 3-Vinylbenzyl chloride (70:30 mixture of metavinylbenzyl chloride: para-vinylbenzyl chloride) was purchased from the Aldrich Chemical Co. and used without further purification. The nucleotides: adenosine 3':5'cyclic monophosphate sodium salt (cAMP), guanosine 3':5'-cyclic monophosphate sodium salt (cGMP), adenosine 5'-monophosphate sodium salt (AMP), adenosine 5'diphosphate sodium salt (ADP), adenosine 5'-triphosphate disodium salt (ATP), cytidine 5'-monophosphate disodium salt (CMP), and uridine 5'-monophosphate (UMP), as well as adenosine were used as received from the Sigma Chemical Co.. D-ribose-5-phosphate disodium salt dihydrate 95%, and adenine hydrochloride hemihydrate (99%, "adenine") were used as received from the Aldrich Chemical Co.. Aqueous solutions were prepared using double distilled deionized water (Millipore). Buffer solutions were prepared from monobasic sodium phosphate, anhydrous dibasic sodium phosphate, and fused-anhydrous sodium acetate, all purchased from Fisher Scientific. Organic solvents used in synthesis were reagent grade or better. Solvents employed in spectroscopic measurements were "Spectrograde".

3.2.2 Methods

The ¹H NMR and ¹³C NMR spectra were recorded on Varian Unity-500 and Varian XL-300 spectrometers, respectively. Elemental analysis was performed by

Robertson Microlit Laboratories, Inc., Madison, N.J. Visible absorption spectra were recorded on a Beckmann DU-64 spectrophotometer. Fluorescence spectra were measured on a Photon Technology International (PTI) Deltascan 4000 spectrofluorometer with 8 nm emission slits on solutions in 1-cm rectangular cuvettes maintained at 22 ± 0.1 °C. Excitation wavelengths of 469 and 360 nm were used to obtain the fluorescence emission spectra of 1 in solutions. The fluorescence spectra are not corrected. The fluorescence quantum yield of dye 1 in all solutions was determined by the method of Parker and Rees (Parker and Rees, 1960) from the emission spectrum obtained with excitation at 469 or 360 nm relative to the quantum yield of rhodamine B in ethanol ($\Phi = 0.69$; excitation = 366 nm; 22 °C) as a standard. The integrated areas under the emission bands gave the relative intensities of the solutions. The quantum yields were calculated with corrections for the absorbances of all solutions (Parker and Rees, 1960). A low concentration of dye (10³ M), which gave absorbances of less than 0.3 absorbance units at the exciting wavelength, was used to minimize the contributions of self-absorption and selfaggregation. To quantify the components in the fluorescence spectra of 1 obtained at 360 nm excitation, curve-fitting was performed, assuming a Gaussian distribution and using a non-linear least squares method based on the Marquardt-Levenberg algorithm, with goodness of fit checked using standard deviation, residuals intensity and the coefficient of determination r², by means of Jandel Scientific's Peakfit software.

3.2.3 Preparation of solutions

The concentration of dye 1 in solvents used for the determination of the change in its dipole moment between the ground and excited states was 10⁻³ M, except in tetrahydrofuran where the concentration was lower due to solubility limitations.

Solutions containing various concentrations of cAMP, cGMP, AMP, ADP, ATP, CMP, UMP, adenosine, adenine, and D-ribose-5-phosphate, with a constant concentration (10⁻⁵ M) of dye 1 were prepared in 0.5 M phosphate or acetate buffer. Spectroscopic measurements were performed the following day on thoroughly mixed nondegassed solutions.

3.2.4 trans-4-(p-N,N-Dimethylaminostyryl)-N-vinylbenzyl-pyridinium chloride (1)

Acetonitrile (10 mL) was added to a round bottom flask equipped with a magnetic stirrer, reflux condenser topped with a nitrogen inlet, and heating mantle, and containing DMASP (0.246 g, 1.10 mmol). While flushing with nitrogen and stirring, the temperature was slowly raised to 60 °C. 3-Vinylbenzyl chloride (0.251 g, 1.68 mmol) was then added dropwise over ~ 15 min to give an orange reaction mixture. After gentle refluxing for ~ 48 h under nitrogen, any remaining undissolved starting material was filtered off, leaving a clear deep red mother liquor which was rotoevaporated to dryness. The product was recrystallized from methylene chloride and carbon tetrachloride and dried under vacuum (20 mm Hg) at 35°C overnight, yielding 0.280 g (68%) of dark red crystals which were stored in a desiccator in the dark. mp = 225-227 °C; one spot by TLC (ethanol:toluene

3:7 / SiO₂). Anal. Calcd for C₂,H₂N₂Cl•0.75 H₂O; C, 73.83; H, 6.84; N, 7.18. Found: C, 73.62; H, 6.57; N, 6.86. H NMR (500 MHz, CDCl₂) and ¹³C NMR (75.43 MHz, CDCl₂) revealed a 70:30 mixture of trans-4-(p-N,N-dimethylaminostyryl)-N-mvinvlbenzylpyridinium chloride and trans-4-(p-N.N-dimethylaminostyryl)-N-pvinylbenzylpyridinium chloride in the product. Meta isomer: 'H NMR (500 MHz, CDCl₁) δ 3.04 ppm (s, 6H, CH₁), 5.24 ppm (d, 1H, H₁^{8'}), 5.78 ppm (d, 1H, H₂^{8'}), 6.01 ppm (s, 2H, CH₂), 6.62 ppm (m, 1H, H^{7}), 6.67 ppm (d, 2H, $H^{11.13}$), 6.77 ppm (d, 1H, H^{7}), 7.28 ppm (t, 1H, $H^{5'}$), 7.34 ppm (d, 1H, $H^{4'}$), 7.47 ppm (d, 2H, $H^{10,14}$), 7.49 ppm (d, 1H, $H^{6'}$), 7.52 ppm (d, 1H, H⁸), 7.63 ppm (s, 1H, meta H^{2'}), 7.73 ppm (d, 2H, H^{3.5}), 9.19 ppm (d, 2H, H^{2.6}); ¹³C NMR (75.43 MHz, CDCl.) 40.2 (CH.), 62.5 (CH.), 112.2 (C^{11.13}), 115.5 (C^{8'}). $116.6 (C^7), 122.6 (C^{3.5}), 127.1 (C^{2',4'}), 128.6 (C^{6'}), 129.6 (C^{5'}), 130.6 (C^{10,14}), 135.7 (C^{7'}),$ 133.1, 134.1, 138.7 (C1'3', and C9), 142.8 (C6), 143.6 (C2.6), 152 (C12), 154 (C4). Para isomer: ¹H NMR (500 MHz, CDCl₂) δ 3.04 ppm (s, 6H, CH₂), 5.24 ppm (d, 1H, H₈), 5.69 ppm (d, 1H, para $H_s^{s'}$), 6.01 ppm (s, 2H, CH_s), 6.62 ppm (m, 1H, $H_s^{r'}$), 6.67 ppm (d, 2H, $H^{11,13}$), 6.77 ppm (d, 1H, H^7), 7.34 ppm (d, 2H, $H^{3',5'}$), 7.47 ppm (d, 2H, $H^{10,14}$), 7.52 ppm (d, 1H, H⁸), 7.58 ppm (d, 2H, H^{2',6'}), 7.73 ppm (d, 2H, H^{3.5}), 9.19 ppm (d, 2H, H^{2.6}); ¹³C NMR (75.43 MHz, CDCl₁) 40.2 (CH₂), 62.5 (CH₂), 112.2 (C^{11,13}), 115.3 (C^{8'}), 116.6 (C^7) , 122.6 $(C^{3.5})$, 127.1 $(C^{3'.5'})$, 129.6 $(C^{2'.6'})$, 130.6 $(C^{10.14})$, 135.7 $(C^{7'})$, 133.1, 134.1, 138.7 $(C^{1',4'} \text{ and } C^9)$, 142.8 (C^8) , 143.6 $(C^{2.6})$, 152 (C^{12}) , 154 (C^4) .

3.3 Results

The NMR spectra of dye 1 suggested that there were no major contaminants in the product (Figure 3B.2 in Appendix 3, Section B). However, the spectra revealed that trans-4-(p-N,N-dimethylaminostyryl)-N-vinylbenzylpyridinium chloride (1 or dye 1) was a 70:30 mixture of trans-4-(p-N,N-dimethylaminostyryl)-N-m-vinylbenzylpyridinium chloride and trans-4-(p-N,N-dimethylaminostyryl)-N-p-vinylbenzylpyridinium chloride. The TLC of this product in ethanol:toluene (3:7) displayed one spot close to the baseline. However this result must be interpreted with caution, because the ionic nature of 1 would not allow it to migrate an appreciable distance on the TLC, and therefore it may not been separated from contaminants. The product 1 may, therefore, contain a small amount of impurity which cannot be detected by NMR or TLC. Precautions were taken to avoid contamination from other ions, such as iodide, but this was not verified. The possibility, therefore, remains that small amounts of iodide were present which may be capable of forming an intermolecular charge-transfer complex with 1. Kosower reported that the absorption spectrum of 1-ethyl-4-methoxycarbonylpyridinium iodide contained a new absorption band distinct from, and at a longer wavelength than, the pyridinium ion itself, which corresponded to a charge-transfer complex between the pyridinium cation and the iodide anion (Kosower, 1958).

3.3.1 Absorption and fluorescence spectra of 1

Fig. 3.1 shows the visible absorption spectra of 1 in phosphate buffer (pH 7.2). The single broad absorption band of 1 exhibited a λ_{max} at 469 nm with a molar extinction

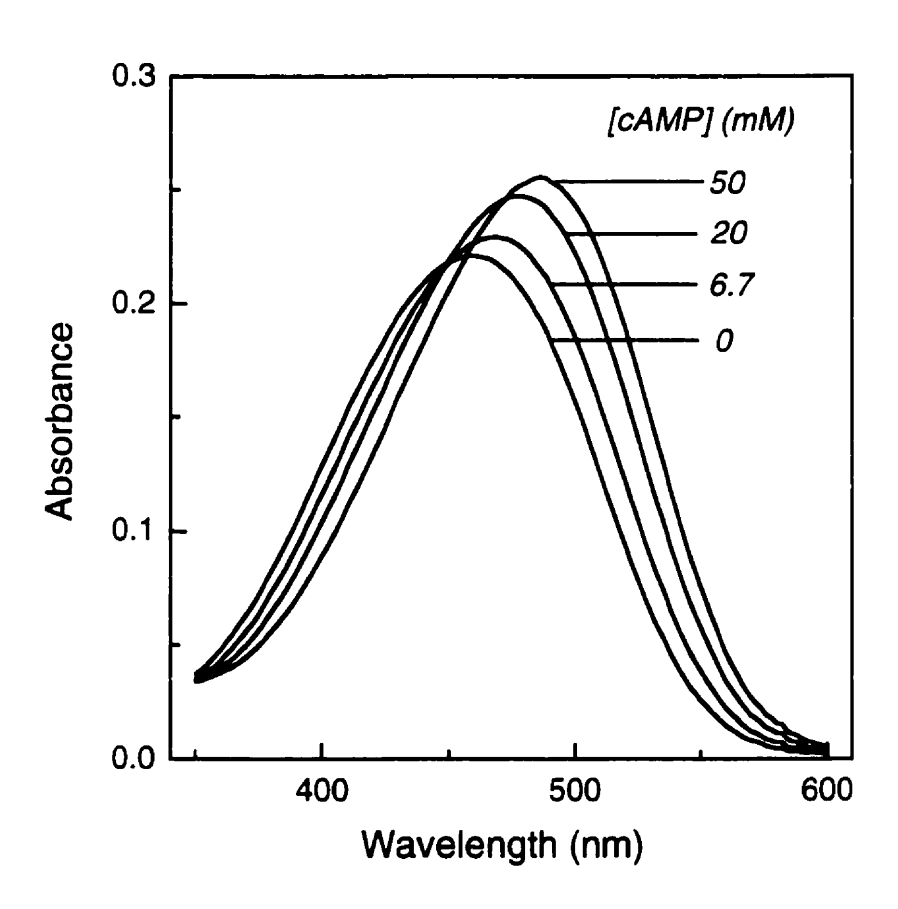


Figure 3.1. Absorption spectra of 1 (10⁻⁵ M) in 0.5 M phosphate buffer (pH 7.2) in the absence and presence of various concentrations of cAMP (6.67, 20 and 50 mM).

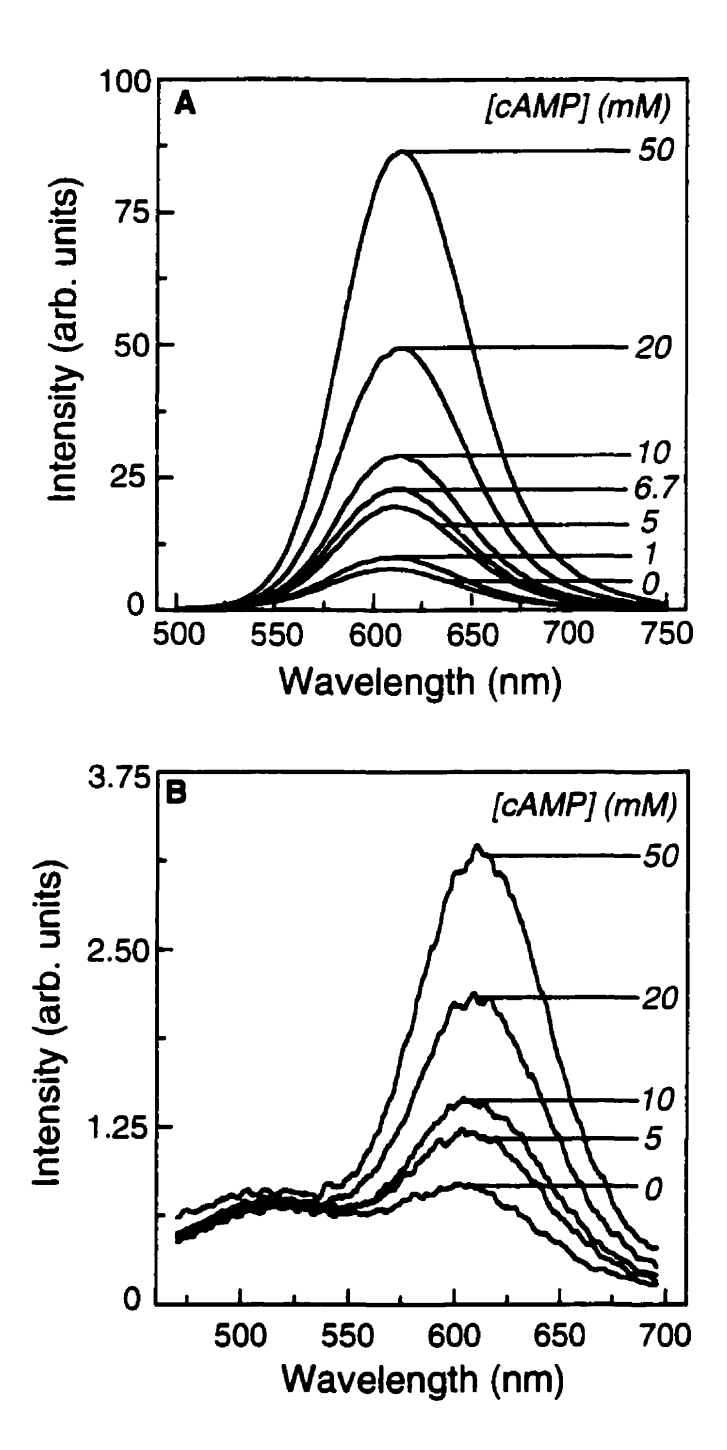


Figure 3.2. Fluorescence spectra of 1 (10-5 M) in 0.5 M phosphate buffer (pH 7.2) at excitation wavelengths of 469 nm (A) and 360 nm (B) in the absence and presence of various concentrations of cAMP (1, 5, 6.67, 10, 20, 50 mM). At excitation 469 nm the emission maxima varied between 608 and 613 nm; at excitation 360 nm the emission maximum at 502 nm remained constant, whereas that at 602 nm varied between 602 and 613 nm.

coefficient of 22 000 L mol⁻¹ cm⁻¹, very similar to that obtained in water (Turkewitsch et al., 1996). The fluorescence spectra of 1 in phosphate buffer (pH 7.2) at excitation 469 nm and 360 nm are presented in Fig. 3.2 (Also see Appendix 3, Section B, Figure 3B.1). Irradiation of 1 at 469 nm generated a single emission band with a maximum at 608 nm, and a quantum yield of 1.18×10⁻³ (Fig. 3.2a). This band is very similar to that obtained inunbuffered water at excitation 469 nm (Turkewitsch et al., 1996). Excitation of 1 at 360 nm resulted in a broad structured emission spectrum (Fig. 3.2b) that could be decomposed by curve-fitting analysis (r² > 0.995, standard error ± 10%) into two Gaussian emission peaks with local maxima at 502 and 602 nm, and quantum yields of 3.66×10⁻⁴ and 6.93×10⁻⁴, respectively. The intensity of this dual emission was about an order of magnitude lower than that obtained by exciting at 469 nm. A similar emission spectrum was obtained in unbuffered water by exciting at 360 nm (unpublished results). The deconvoluted peak with a maximum at 602 nm appeared to be similar to the single emission band obtained at excitation 469 nm.

3.3.2 Determination of the change in the dipole moment between the ground and excited states ($\Delta\mu_{\rm A}$) of 1

The main characteristics of the visible and fluorescence spectra of 1 in various solvents together with some solvent polarity parameters are reported in Table 3.1. (The absorption and fluorescence spectra of 1 in water, chloroform and acetonitrile are presented in Figure 3C.1 in Appendix 3, Section C.) Dye 1 exhibits a large Stokes' shift (\vec{v}_{st}) which is solvent dependent, suggesting that the excited state reached upon excitation

Table 3.1. Solvent parameters and steady-state spectral data for 1 in various solvents.

| number | solvent | ε, | η' | Δf^{d} | λ' nm | λ'nm | \vec{v}_{s} cm ⁻¹ |
|--------|-----------------------|-------|--------|----------------|-------|------|--------------------------------|
| | | | | | | | |
| 1 | chloroform | 4.81 | 1.4429 | 0.1492 | 500 | 571 | 2487 |
| 2 | tetrahydrofuran | 7.58 | 1.4072 | 0.2096 | 480 | 582 | 3651 |
| 3 | N,N-dimethylformamide | 12.47 | 1.3877 | 0.2514 | 482 | 618 | 4566 |
| 4 | dimethyl sulfoxide | 46.68 | 1.4783 | 0.2634 | 484 | 621 | 4558 |
| 5 | acetone | 20.70 | 1.3587 | 0.2843 | 484 | 613 | 4348 |
| 6 | acetonitrile | 37.50 | 1.3441 | 0.3054 | 482 | 613 | 4434 |
| 7 | 2-propanol | 19.92 | 1.3772 | 0.2762 | 495 | 600 | 3535 |
| 8 | ethanol | 24.55 | 1.3614 | 0.2887 | 491 | 606 | 3865 |
| 9 | methanol | 32.70 | 1.3284 | 0.3086 | 488 | 606 | 3990 |
| 10 | water | 78.39 | 1.3330 | 0.3199 | 469 | 610 | 4929 |

^a concentration 10⁻⁵ M, except in tetrahydrofuran where solubility was lower.

b dielectric constant, ε , obtained from Reichardt, 1979.

 $^{^{\}circ}$ refractive index, η , obtained from Reichardt, 1979.

d solvent polarity function, $\Delta f = (\varepsilon - 1/2\varepsilon + 1) - (\eta^2 - 1/2\eta^2 + 1)$ (defined in eq 1).

^e absorption maximum, λ_a ; maximum uncertainty ± 2 nm.

fluorescence maximum, λ_i ; maximum uncertainty ± 2 nm; excitation wavelength 469 nm.

⁵ Stokes' shift calculated from difference in absorption and fluorescence maxima; maximum uncertainty ± 300 cm⁻¹.

at 469 nm has substantial charge transfer character, analogous to related derivatives (Létard et al., 1993; Abdel-Mottaleb et al., 1989; Lapouyade et al., 1992).

Within the dielectric continuum approximation of the solvent, the steady-state Stokes' shift, \vec{v}_{st} (in cm⁻¹), may be related to the change in the dipole moment between the ground and the excited states, $\Delta\mu_{es}$, of 1 according to the Lippert-Mataga equation 1 (Lakowicz, 1983).

$$\vec{v}_{st}\left(cm^{-1}\right) = \vec{v}_a - v_f = 2\frac{\left(\Delta\mu_{eg}\right)^2}{hca^3} \left[\frac{\varepsilon - 1}{2\varepsilon + 1} - \frac{\eta^2 - 1}{2\eta^2 + 1}\right] + A = 2\frac{\left(\Delta\mu_{eg}\right)^2}{hca^3} \times \Delta f + A \qquad (1).$$

In the above equation, \vec{v}_a and \vec{v}_f , refer to the maximum frequencies of the absorption and emission spectra, respectively; h is Planck's constant; c is the speed of light; a is the spherical solvent cavity radius of the solute; ε and η are the dielectric constant and refractive index of the solvent, respectively, and A is a constant. The Lippert-Mataga analysis of the steady-state spectroscopic data for 1 is shown in Fig. 3.3. The magnitude of $\Delta\mu_{e_t}$ may be obtained from the slope of the \vec{v}_n vs. Δf plot in Fig. 3.3 by estimating the value of the solute radius, a (5.40 Å), from the molecular volume as calculated from the molecular weight and the density of N,N-dimethylaniline (0.95 g cm⁻³) (Létard et al., 1993). A Least-squares fit of the plot gave a slope of 1.04×10^4 cm⁻¹/ Δf (r = 0.77), yielding a dipole moment change of 13 Debye units (D) (1 D = 3.33 × 10^{-30} Cm). Considering the large $\Delta\mu_{e_t}$, it is reasonable to conclude that the excited state of 1 has considerable charge transfer character.

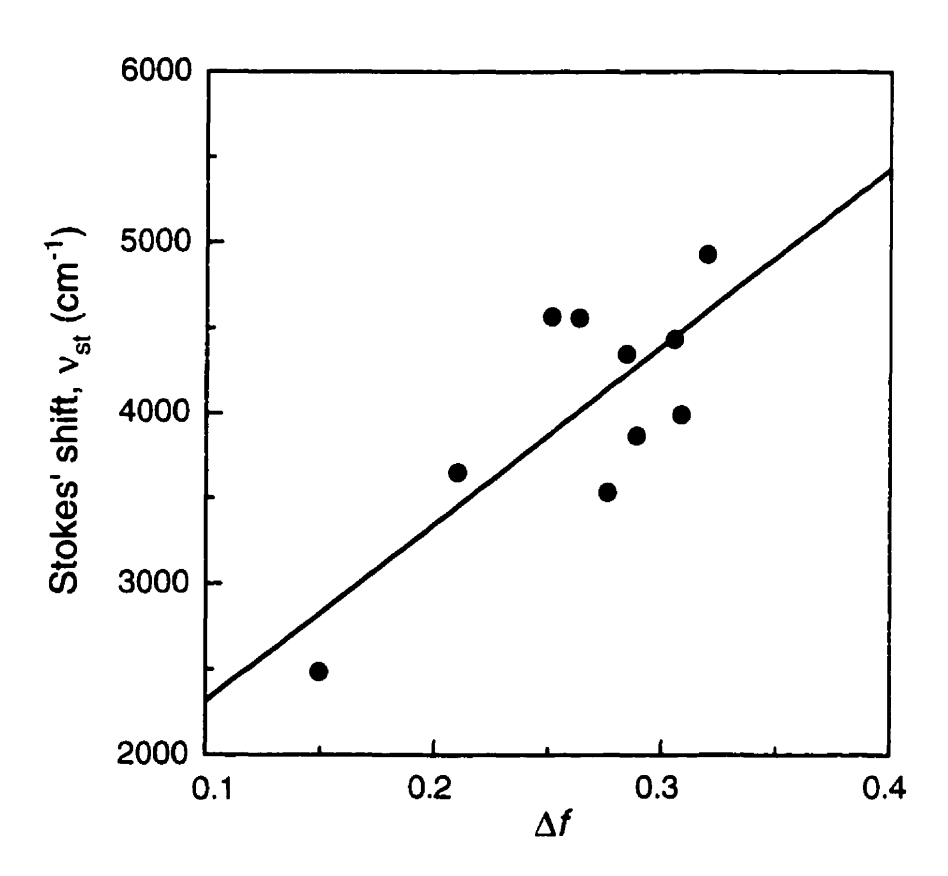


Figure 3.3. Lippert-Mataga plot of the Stokes' shift (in cm⁻¹), \vec{v}_{st} , vs. the solvent polarity function, Δf , for 1 in various solvents; slope = 1.04×10^4 cm⁻¹/ Δf , r = 0.77. The line is a linear least-squares fit through the data.

3.3.3 Effect of nucleotibe and nucleotibe-related analytes on the absorption and fluorescence of 1

Figure 3.1 also shows the visible absorption spectra of 1 in phosphate buffer (pH 7.2) in the presence of various concentrations of cAMP. The addition of increasing concentrations of cAMP caused a red shift of ~17 nm in the absorption maximum accompanied by a hyperchromic effect, which could be observed visually as a change from orange to red-orange. All other nucleotide and nucleotide-related analytes induced similar changes in the absorbance of 1, whereas D-ribose-5-phosphate had no effect (data not shown). Concentrations of analyte above 50 mM were not examined due to solubility limitations. These changes were also observed for 1 in unbuffered water upon addition of cAMP, cGMP and D-ribose-5-phosphate (Turkewitsch et al., 1996).

The addition of cAMP induced a dramatic concentration-dependent enhancement in the fluorescence quantum yield of 1 at excitation 469 nm with a concomitant slight red shift of the λ_{max} from 608 nm in buffer alone to 613 nm at 50 mM cAMP (Fig. 3.2a). The quantum yield of the emission band of 1 with maximum at 602 nm obtained by exciting at 360 nm also increased as the concentration of cAMP increased (Fig. 3.2b). This increase in fluorescence was accompanied by a slight red shift of the λ_{max} from 602 nm in buffer alone to 613 nm in the presence of 50 mM cAMP, reminiscent of the emission band produced upon excitation at 469 nm. However, it was less sensitive to the presence of cAMP than the similar peak arising from the 469 nm excitation. In contrast, the emission band of 1 with a maximum at 502 nm obtained by exciting at 360 nm remained relatively constant as the concentration of cAMP was increased.

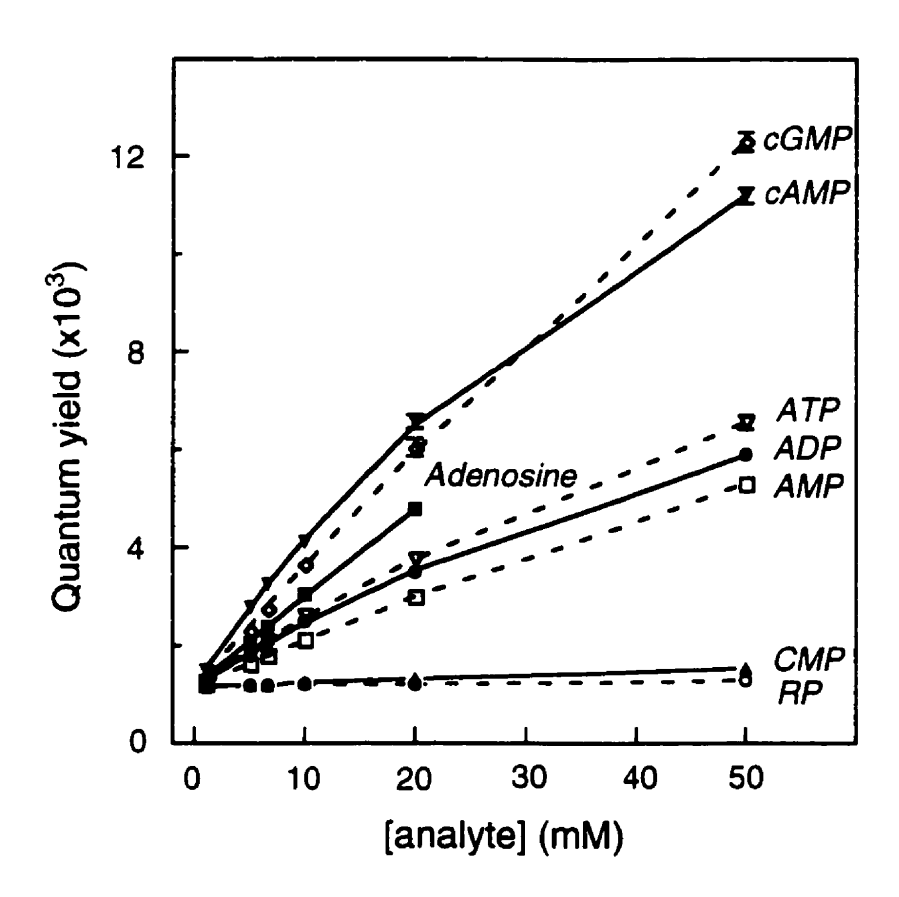


Figure 3.4. Fluorescence quantum yield titration curves of 1 as a function of analyte concentration. Phosphate buffer solutions (0.5 M, pH 7.2) contained 1 (10⁻⁵ M) and various concentrations of cGMP (\Diamond), cAMP (\blacktriangledown), adenosine (\blacksquare), ATP (∇), ADP (\blacksquare), CMP (\blacktriangle) or D-ribose-5-phosphate (RP, O). The lines through the symbols for cAMP, cGMP, AMP, ADP and ATP represent curve fits following equation 3. The excitation wavelength was 469 nm. The values are means \pm standard errors of 3 independent observations.

Fig. 3.4 shows the fluorescence quantum yield titration curves obtained at excitation 469 nm when various concentrations of nucleotide and nucleotide-related analytes were added to 1 (10⁻⁵ M) in phosphate buffer (pH 7.2). (The effects of cAMP. cGMP, ATP and CMP on the fluorescence of 1 in buffer are compared in Figure 3D.1 in Appendix 3, Section D. The increases in the emission of 1 induced by these analytes correlate with the fluorescence quantum yield enhancements observed in Figure 3.4). These concentration-response curves show that the purine nucleotides (cAMP, cGMP, AMP, ADP, and ATP) and adenosine all induce a fluorescence quantum yield enhancement of 1. In contrast, the pyrimidine nucleotide, CMP, has virtually no effect on quantum yield. UMP, another pyrimidine nucleotide, behaved almost identically to CMP (data not shown). D-ribose-5-phosphate has no effect on the fluorescence of 1. Of the purine nucleotides, the cyclic nucleotides, cAMP and cGMP have the greatest effects on the fluorescence quantum yield of 1 whereas the noncyclic nucleotides, AMP, ADP and ATP have somewhat smaller effects. Adenosine has an effect intermediate between those of the cyclic and noncyclic nucleotides. However, it was not possible to examine concentrations of adenosine above 20 mM due to solubility limitations.

The data in Fig. 3.4 can be used to calculate the equilibrium association constant (K_{eq}) for the interaction of dye 1 with analyte, as well as the fluorescence quantum yield (Φ_c) of the dye-analyte complex. The association of dye with analyte, $dye + analyte \iff dye-analyte$, is controlled by the equilibrium association constant,

 $K_{ca} = [dye-analyte] / [dye] [analyte]$ (2).

In the concentration range studied, the fluorescence quantum yield is closely correlated with the concentrations of the analytes. The fluorescence quantum yield Φ of 1 in the presence of nucleotide represents the quantum yield of a mixture of fluorescing species, which may be described by the equation:

$$\Phi = x_{bc}\Phi_a + (1 - x_{bc})\Phi_c \tag{3}$$

where x_{dye} is the mole fraction of "free" dye 1, and Φ_o and Φ_c are the fluorescence quantum yields of 1 in the absence of analyte, and of the dye-analyte complex, respectively. Since $x_{dye} = [dye] / ([dye] + [dye-analyte])$, it is readily shown from equations 2 and 3 that

$$\Phi = \Phi_o + \left(\Phi_c - \Phi_o \left\{ \frac{K_{eq}[analyte]}{1 + K_{eq}[analyte]} \right\}$$
 (4).

SigmaPlot curve fitter was used to fit the fluorescence titration data in Fig. 3.4 to equation 4 directly to estimate the K_{rq} and Φ_c values. Table 3.2 presents these values obtained in phosphate buffer at 7.2 and in unbuffered water (The equilibrium association constants for cAMP and cGMP in water were calculated incorrectly in Turkewitsch et al., 1996. The corrected values are presented in Table 3.2.) (Turkewitsch et al., 1996).

The association constants obtained in phosphate buffer at pH 7.2 (Table 3.2) range from 13.8 M^{-1} for cAMP to 0.15 M^{-1} for adenine. To compare the effects of the adenine base alone to those of the nucleotides, the pH had to be lowered to 4.0 to dissolve the adenine. Under these conditions, cAMP exhibited a K_{eq} value (13.0 M^{-1}) similar to the

Table 3.2. Equilibrium association constants $(K_{eq})^a$ for 1 with various analytes and the fluorescence quantum yields of the dye-analyte complexes (Φ_c) in 0.5 M phosphate buffer at pH 7.2 and in unbuffered water.^b

| | phosph | phosphate buffer ^c | | water | | |
|----------------------|-----------------|-------------------------------|------------------|--------------------|--|--|
| analyte | K | Φ, | $K_{\epsilon a}$ | Φ, | | |
| cAMP | 13.8 ± 0.80 | 0.026 ± 0.001 | 14.0 ± 1.08 | 0.018 ± 0.0003 | | |
| cGMP | 2.67 ± 0.35 | 0.099 ± 0.009 | 9.31 ± 0.97 | 0.031 ± 0.004 | | |
| AMP | 3.81 ± 1.12 | 0.031 ± 0.007 | | | | |
| ADP | 10.1 ± 0.79 | 0.015 ± 0.001 | | 744 | | |
| ATP | 8.08 ± 0.73 | 0.020 ± 0.001 | 400 | | | |
| adenosine | 0.54 ± 0.10 | 0.373 ± 0.067 | | *** | | |
| adenine ^d | 0.15 ± 0.01 | 0.331 ± 0.005 | | | | |

units, M'.

Table 3.3. Equilibrium association constants $(K_{eq})^4$ for 1 with various analytes and the fluorescence quantum yields of the dye-analyte complexes (Φ_c) in 0.5 M phosphate buffer at pH 6.0 and 8.0.

| | pH 6.0 | | pH 8.0 | | |
|---------|----------|-------|--------|-------|--|
| analyte | K_{ca} | Φ | K | Φ | |
| cAMP | 14.1 | 0.022 | 16.7 | 0.020 | |
| cGMP | 2.57 | 0.092 | 1.62 | 0.130 | |
| AMP | 6.67 | 0.028 | 4.87 | 0.019 | |
| ADP | 6.64 | 0.021 | 8.56 | 0.016 | |
| ATP | 7.27 | 0.021 | 11.8 | 0.014 | |

units, M'.

Turkewitsch et al., 1996, see footnote "i" in text.

^c values are means ± standard error of 3 independent observations.

^d in 0.5 M acetate buffer at pH 4.0. The K_{eq} and Φ_c for cAMP under these conditions were 13.0 M⁻¹ and 0.023, respectively.

b values are the result of a single observation.

those in phosphate buffer and unbuffered water, whereas adenine exhibited an association constant of $0.15 \,\mathrm{M}^{-1}$, much less than that of cAMP. The equilibrium constant for cAMP in unbuffered water resembles that in phosphate buffer, whereas the K_{eq} for cGMP in water is somewhat greater than that in phosphate buffer.

In contrast to the relatively low apparent affinities of adenine and adenosine for 1, the quantum yield for their dye-analyte complex ($\Phi_c \sim 0.35$) was higher than that for any of the purine nucleotides tested. However, this result must be interpreted with caution since we could not use concentrations of adenine or adenosine in excess of 20 mM due to their limited solubilities. Similarly, cGMP, although it has a lower K_{eq} than cAMP, induces a greater change in the quantum yield of 1 at the highest concentration tested. The value of Φ_c for cGMP is nearly 4 times that for cAMP. The values of Φ_c for AMP, ADP and ATP were similar to that for cAMP at pH 7.2 (Table 3.2) as well as at pH values of 6.0 and 8.0 (Table 3.3). Similarly, the K_{eq} values for these nucleotides were not influenced to a large extent by pH (Table 3.3).

3.4 Discussion

1 is a mixture of meta and para isomers, and therefore it is possible that each isomer could contribute differently to the absorption and emission spectra, making interpretation of the results difficult. Thus, the data and the interpretation of the results presented in this chapter, and throughout the remainder of this thesis, have a level of uncertainty. However, because the vinylbenzyl group in 1 is not in conjugation with the remainder of the molecule (i.e. the *trans-4-(p-N,N-dimethylaminostyryl)*pyridinium

portion), and is therefore separated from the part of the molecule giving rise to the fluorescence, it probably does not contribute to a large degree to the fluorescence of 1. This argument is supported by the fact that the fluorescence spectra of dye 1 and dye 2, which differs from 1 only in the substituent on the pyridinium nitrogen (vinylbenzyl in the case of 1, and phenethyl in the case of 2), are similar (Figure 3B.1 in Appendix 3, Section B). Further, the magnitude of the fluorescence enhancements of the dyes (and the red shifts of their emission maxima) to increasing concentrations of cAMP between 1 and 50 mM (Appendix 3, Section E) are also similar. Biological macromolecules also induce similar fluorescence quantum yield increases in dyes 1 and 2 (Figure 4.2 in Chapter 4). The association constants for dyes 1 and 2 with cAMP $(K_{eq} \sim 16 \text{ M}^{-1})$, and with nondenatured BSA ($K_a \sim 10^4 \,\mathrm{M}^4$), are, as well, almost identical. These results suggest that the substituent of the pyridinium nitrogen has relatively little effect on the fluorescence of the dyes, and on their ability to respond to the presence of analytes. Furthermore, since the association constants for 1 and 2 with cAMP, as well as with nondenatured BSA, are almost identical, the involvement of vinylbenzyl and phenethyl substituents in the interaction of 1 and 2 with these analytes is probably minor. These results also raise the possibility that the meta and para-vinylbenzyl isomers in 1 have relatively little effect on the fluorescence properties and the fluorescence response of this dye.

The similarity of the molecular structure of 1 with those of closely related EDA stilbene (Létard et al., 1993; Lapouyade et al., 1992) and styrylpyridinium (Ephardt and Fromherz, 1989) dyes, suggests that 1 may form a twisted intramolecular charge transfer

(TICT) excited state. As with most molecules exhibiting TICT behavior, dye 1 contains several possible rotatable moieties with excellent donor properties, linked to acceptor groups. TICT excited states may form in flexible EDA molecules where the possibility of rotation of the donor and acceptor groups around certain bonds exists (Rettig, 1986). In some of these cases, upon excitation at a single wavelength dual fluorescence may be observed from two configurations of the same molecule: an initially planar locally excited (LE) state, and a TICT excited state in which a charge transfer from the donor group to the acceptor group has taken place with a twisting of the donor towards a plane perpendicular to that of the acceptor. The high degree of charge separation between the donor and acceptor moieties in the excited molecule leads to an abrupt increase in the dipole moment with respect to the ground state (Rettig, 1986).

Recent studies on a fluorescent EDA molecule, *trans*-4-(*p*-N,N-dimethylamino)-stilbene (DAS) (Létard et al., 1993), similar to dye 1, revealed the occurrence of a TICT excited state. Moreover, we (Wandelt et al., 1995) reported that *trans*-4-(*p*-N,N-dimethylaminostyryl)-N-phenethylpyridinium bromide, which differs from dye 1 only in the substituent on the pyridinium nitrogen, displayed two charge transfer fluorescence bands (close to 600 nm) associated with different excitations, 360 and 469 nm. Our studies suggested that the emission band obtained by exciting at 360 nm, which is part of a broad structured emission spectrum, may arise by a TICT process. The single emission band observed upon excitation at 469 nm may arise from direct excitation of an already twisted ground state, providing an alternative route to a TICT-type emission similar to that obtained by 360 nm excitation.

The identification of the TICT process in flexible donor-acceptor compounds is made difficult because two distinct emission bands (dual fluorescence) are not always observed in steady-state fluorescence experiments (Rettig, 1986). Here, however, we observe dual emission of dye 1 with maxima at 502 nm and 602 nm upon exciting at 360 nm (Fig. 3.2b) which suggests a TICT process in this compound. This excitation wavelength (360 nm) was employed even when the absorption of 1 is almost at a minimum at this wavelength, because the excitation spectrum of 1 in buffer at room temperature taken at an emission wavelength of 510 nm displays a maximum at ~360 nm (Figure 3B.3, Appendix 3, Section B). However, the possibility that the emission band of 1 at 502 nm is the result of an artifact or impurity cannot be ruled out, since this excitation spectrum has a much lower intensity than that obtained at an emission maximum of 600 nm, and since the quantum yield of the 502 emission band is small. The spectra presented in this work are also not corrected. Furthermore, dye 1 contains a mixture of meta- and para-vinylbenzyl isomers. It must be pointed out, however, that none of the major conclusions presented in this work are based on the 502 nm emission band.

The sensitivity of the emission band with a maximum at 602 nm to cAMP (albeit much less than that obtained upon exciting at 469 nm) also implies its origin from a TICT excited state. On the other hand, the insensitivity of the 502 nm emission band to the environment, especially to an environment which possesses highly polar species, suggests that it may be due to a planar locally excited state. Furthermore, the environmental

sensitivity of the emission band of 1 with a maximum at ~ 600 nm obtained by exciting at 469 nm would also support the idea that it originates from some kind of ICT state.

The Stokes'shift for 1 (~5000 cm⁻¹) is similar to that reported by Létard for the DAS TICT molecule (Létard et al., 1993). The average change in the dipole moment (ie. $\Delta\mu_{rt}$) of 1 of 13 D is also consistent with those reported for other molecules which exhibit TICT excited states, including DAS (10 D) (Létard et al., 1993), 4-(N,N-dimethylamino)-4'-cyanostilbene (15 D) (Lapouyade et al., 1992), and a donor-acceptor-type stilbene laser dye (20 D) (Meyer et al., 1990), suggesting a TICT nature to dye 1. Based on the studies of DAS, the large change in the dipole moment of 1 is probably due to a charge transfer from the dimethylanilino donor group to the vinylpyridinium acceptor moiety in the excited state (Létard et al., 1993).

The large change in the dipole moment of 1 upon excitation, along with the considerations discussed above would all be consistent with a TICT-type excited state being responsible for the emission of 1 at ~600 nm. This environmentally sensitive fluorescence suggests that 1 may be useful as a chemosensor.

The structures of the analytes investigated are presented in Fig. 3.5. The nucleotides (cAMP, cGMP, AMP, ADP, ATP, CMP and UMP) consist of a purine or pyrimidine base, a ribose sugar and a phosphate group. However, the nature of the phosphate group differs among them: cAMP and cGMP possess cyclized phosphate groups whereas the other nucleotides have uncyclized phosphates. Adenosine consists of an adenine base linked to a ribose sugar, and D-ribose-5-phosphate consists of a ribose sugar and a phosphate group.

$$Y - O - CH_2$$
 $Y - O - CH_2$
 $Y -$

Figure 3.5. Molecular structures of the various purine and pyrimidine nucleotides.

The data in Fig. 3.4 indicate that dye 1 displays a specificity for purine over pyrimidine analytes in the concentration range studied (1-50 mM), since all of the purine analytes induce a fluorescence quantum yield enhancement of 1, whereas the pyrimidine analytes have almost no effect. We (Wandelt et al., 1995) have previously shown that high solution viscosities can enhance the fluorescence of dyes structurally related to 1. However, this could not explain the effects of purine nucleotides, since equivalent concentrations of pyrimidine nucleotides did not effect the fluorescence of 1 significantly. It is clear that neither the ribose nor the phosphate groups alone are responsible for the change in fluorescence quantum yield of 1, since the quantum yield of 1 is unaffected by D-ribose-5-phosphate and phosphate. The results in Table 3.2 further indicate that the adenine base alone is not capable of interacting strongly with 1, since adenine displays a K_{a} of only 0.15 M¹. The addition of a ribose to give adenosine results in an increase in the K_a to 0.54 M⁻¹; and the further addition of a noncyclic phosphate group (AMP) dramatically increases the K_{eq} to 3.81 M^{-1} . Cyclization of the phosphate group further increases the affinity of the nucleotide for 1, resulting in a higher K_{a} value for cAMP (13.8 M¹) than for AMP, ADP and ATP. It is possible that the cyclic phosphate group is in a more favorable conformation to interact with the positively charged dye 1. Thus, the adenine base, the ribose and the phosphate groups appear to act synergistically to increase the affinity of the ligand for the dye. The association of 1 with the purine analytes probably involves concurrent aryl stacking interactions and electrostatic interactions. Aryl stacking interactions could occur between the aromatic rings of 1 and the purine base of the analytes, whereas electrostatic interactions could occur between charged 1 and the phosphate and/or ribose sugar moieties of the analytes, in a multiple-point binding to 1.

Although the magnitude of the fluorescence changes induced in dye 1 by cAMP and cGMP were similar within the concentration range investigated, curve fitting of the data in Fig. 3.4 suggested that the K_{eq} and Φ_{c} for these two nucleotides were substantially different from one another. The K_{aa} calculated for cAMP (13.8 M¹) was about 5 times higher than that for cGMP (2.67 M^{-1}), but this was offset by the higher value of Φ_c calculated for cGMP (0.099 vs 0.026 for cAMP). The concentrations of nucleotides required to induce maximal fluorescence changes in dye 1 would be far in excess of those used in our studies, since it was not feasible to use concentrations of cAMP or cGMP greater than 50 mM. Therefore the values calculated for K_{eq} and Φ_{e} for the interactions of these compounds with dye 1 must be interpreted with some caution. However, in support of the calculated values, the reproducibility of the measurements was very high, as seen from the error bars in Fig. 3.4. It might be argued that the calculated values for K_{ra} and Φ_{c} are overly influenced by the data from the highest concentration (50 mM) of cAMP and cGMP, which was the only concentration at which the fluorescence of dye 1 was greater in the presence of cGMP than cAMP. However, similar results were obtained even when the data for this concentration were excluded. This would suggest that although cGMP appears to have a lower affinity than cAMP for dye 1, it can induce a greater maximal increase in fluorescence. To confirm this, further studies would be required to measure lifetimes.

A water-soluble nonfluorescent chemosensor with multiple recognition sites for cAMP was reported by Kato et al. (Kato et al., 1994). Two Kemp's triacid imide (This molecule is prepared from Kemp's triacid, a molecule with a triaxial conformation of three acid groups on a cyclohexane skeleton, by dehydrating two of the acid groups to an anhydride, and then converting this anhydride to an imide acid (i.e. Kemp's triacid imide) by ammonolysis. This imide presents a hydrogen bonding surface similar to that of thymine, and thus provides an ideal microenvironment for adenine derivatives. Combining two Kemp's triacid imide molecules with a spacer, such as diaminocarbazole, provides a cleft or claw-like structure into which adenine may fit.) molecules were combined with a diaminocarbazole unit to create a pocket for adenine-binding through simultaneous Watson-Crick and Hoogsteen hydrogen bonding and aryl stacking interactions. A positively charged guanidinium mojety was added to this module for electrostatic interaction with the negatively charged phosphate group of cAMP. Equilibrium constants of association, determined by 'H NMR titration, of 600 and 320 M⁻¹ in 10 mM cacodylate buffer at ionic strengths of 51 mM and 501 mM NaCl, respectively were reported for this synthetic receptor with 3':5'-cAMP. Hosseini et al. (Hosseini et al., 1990) designed an artificial receptor capable of binding ATP in aqueous solution that combined a positively charged macrocyclic polyammonium moiety as the anion binding site with a fluorescent acridine group as the purine base binding site. Attractive electrostatic interactions between the polyphosphate chain of ATP and the positively charged macrocyclic mojety of the artificial receptor together with aryl stacking interactions between the acridine group of the latter and the purine base of the

nucleotide contributed to the binding of ATP. The fluorescence of this receptor was enhanced by a factor of ~1.9 upon complexation of ATP and CTP in aqueous buffer (pH 4.0), whereas GTP and AMP caused a slight quenching. Furthermore, Kawai et al. (Kawai and Nagamuar, 1995) state that a strong tendency of association through arylstacking interactions, reportedly dominated by electrostatics, can be expected from similar long and planar structures such as nitrostyrylpyridinium molecules which possess extensive charge delocalization favoring electronic interactions.

The main path of nonradiative deactivation of stilbene derivatives, including DAS, is known to be via rotation around the ethylenic double bond in the excited state, associated with trans-cis photoisomerization (Létard et al., 1993; Samankumara Sandanayake et al., 1994). Environments that restrict this internal molecular rotation of these molecules in the excited state, such as viscous solvents (Abdel-Mottaleb, 1984; Abdel-Mottaleb et al., 1989), microheterogeneous micelle (Abdel-Mottaleb et al., 1988) and cyclodextrin structures (Duveneck et al., 1989), lead to a decrease in the nonradiative decay rate and consequently an increase in the fluorescence quantum yield. In addition, increases in fluorescence quantum yield and lifetime have been reported for dimethylaminostilbene (Létard et al., 1993) and (dimethylaminostyryl)pyridinium (Abdel-Mottaleb, 1984; Abdel-Mottaleb et al., 1989) molecules by "chemical" or "physical freezing" of torsional motion around the ethylenic double bond in the excited state. The presence of environmental components capable of associating with these stilbene sensors, may also rigidify their molecular structure, causing fluorescence enhancement (Samankumara Sandanayake et al., 1994; Kumar et al., 1993). Such

enhanced fluorescence emission was reported for *trans*-3,3'-stilbenediboronic acid upon forming of a cyclic complex with disaccharides and subsequent freezing of the rotation around the ethylenic bond (Samankumara Sandanayake et al., 1994). Given this, we propose that dye 1 associates with purine analytes in such a way that the rotation about the double bond in the excited state is restricted, inhibiting nonradiative decay and increasing the fluorescence quantum yield.

3.5 Conclusions

Purine nucleotide and nucleotide-related analytes dramatically enhance the TICT-type fluorescence of dye 1, whereas pyrimidine nucleotides have virtually no effect on the fluorescence of 1 suggesting a specificity of 1 for purine over pyrimidine analytes.

However, relatively high concentrations of purine analytes are required to induce these changes, because of the modest association constants for 1 with these analytes. Although the fluorescence enhancements induced by cAMP and cGMP are greater than those induced by other purine analytes, the ability of 1 to distinguish between different purine analytes is somewhat limited. Nonetheless, in combination with other molecular structures designed to provide more specific recognition, this fluorescent dye might form the basis of a fluorescent chemosensor for purine nucleotides.

Fluorescent dye 1 possesses several features that make it attractive for potential use in laboratory practice, especially for biological applications. Dye 1 exhibits an intense absorption band in the visible region (Fig. 3.1) which should have significant excitation using standard argon, argon/krypton, or conventional lamp sources. The long

wavelength fluorescence of 1 (608-613 nm, Fig. 3.2a), generated by exciting at 469 nm, reduces interference from cell or tissue autofluorescence (occurring around 460 nm), and provides a large Stokes' shift, separating excitation from emission wavelengths. The fluorescence quantum yield responses to the nucleotide and nucleotide-related analytes show insignificant fluctuations in the physiological pH range of 6-8 (Table 3.2 and 3.3). In addition, an experiment with a very similar family member, *trans*-4-(*p*-N,N-dimethylaminostyryl)-N-phenethylpyridinium bromide (2), revealed that it is capable of passively diffusing across the cell membrane, and that it does not interfere with the physiological functioning of cells (Appendix 3F). Finally, it has also been demonstrated that this family of dyes is amenable to the synthesis of esterified membrane-permeant derivatives, and that such derivatives are capable of staining live microorganisms without affecting viability (Chan et al., 1996).

3.6 Acknowledgments

The authors thank the Respiratory Health Network of Centers of Excellence for financial support of this work, and the Canadian Cystic Fibrosis Foundation for studentship support for P. Turkewitsch. We would like to acknowledge the contributions of the late Dr. Seymour Heisler. We thank Dr. F. Sauriol for assistance with NMR measurements, and Dr. J. Silvius for assistance with equations. We are grateful to Dr. P. Hurst and R. Ganju for stimulating and helpful discussions.

3.7 References

Abdel-Mottaleb, M.S.A. Laser Chem. 1984, 4, 305-310.

Abdel-Mottaleb, M.S.A.; Sherief, A.M.K.; Abdel-Azim, A.A.; Habashy, M.M.; Ismail, L.F.M. J. Photochem. Photobiol. 1988, 44, 161-169.

Abdel-Mottaleb, M.S.A.; Sherief, A.M.K.; Ismail, L.F.M.; De Schryver, F.C.; Vanderauweraer, M.A. J. Chem. Soc., Faraday Trans. 2 1989, 85, 1779-1788.

Bhattacharyya, K.; Chowdhury, M. Chem. Rev. 1993, 93, 507-535.

Chan, E.C.S.; Stranix, B.R.; Darling, G.D.; Noble, P.B. Can. J. Microbiol. 1996, 42, 875-879.

Darnell, J.G.; Lodish, H.; Baltimore, D. Molecular Cell Biology, 3rd ed; Scientific American Books: New York, 1994.

Duveneck, G.L.; Sitzmann, E.V.; Eisenthal, K.B.; Turro, N.J. J. Phys. Chem. 1989, 93, 7166-7170.

Ephardt, H.; Fromherz, P. J. Phys. Chem. 1989, 93, 7717.

Fery-Forgues, S.; Le Bris, M-T.; Guette, J-P.; Valeur, B. J. Phys. Chem. 1988, 92, 6233-6237.

Hosseini, M.W.; Blacker, A.J.; and Lehn, J-M. J. Am. Chem. Soc. 1990, 112, 3896-3904.

Kato, Y.; Morgan Conn, M.; Rebek, J. Jr. J. Am. Chem. Soc. 1994, 116, 3279-3284.

Kawai, H.; Nagamuar, T. Mol. Cryst. Liq. Cryst. 1995, 267, 235-240.

Kost, A.N.; Sheinkman, A.K.; Rozenberg, A.N. J. Gen. Chem. USSR (Eng. Transl.) 1964, 84, 4106-4112.

Kosower, E.M. J. Am. Chem. Soc. 1958, 80, 3253-3260.

Kumar, C.V.; Turner, R.S.; Asuncion, E.H. J. Photochem. Photobiol. A: Chem. 1993, 74, 231-238.

Lakowicz, J.R. *Principles of Fluorescence Spectroscopy*; Plenum: New York, 1983; pp 187-215.

Lapouyade, R.; Czeschka, K.; Majenz, W.; Rettig, W.; Gilabert, E.; Rullière, C. J. Phys. Chem. 1992, 96, 9643-9650.

Law, K.Y. Photochem. Photobiol. 1981, 33, 799-806.

Létard, J-F.; Lapouyade R.; Rettig, W. J. Am. Chem. Soc. 1993, 115, 2441-2447.

Loutfy, R.O. Pure & Appl. Chem. 1986, 58, 1239-1248.

Meyer, M.; Mialocq, J-C.; Perly, B.; J. Phys. Chem. 1990, 94, 98-104.

Montana, V.; Farkas, D.L.; Loew, L.M. Biochemistry 1989, 28, 4536-4539.

Moog, R.S.; Burozski, N.A.; Desai, M.M.; Good, W.R.; Silvers, C.D.; Thompson, P.A.; Simon, J.D. J. Phys. Chem. 1991, 95, 8466-8473.

Parker, C.A.; Rees, W.T.; Analyst 1960, 85, 587-600.

Reichardt, C. Solvent Effects in Organic Chemistry; Verlag Chemie: New York, 1979; pp 270-272.

Rettig, W. Angew. Chem., Int. Ed. Engl. 1986, 25, 971-988.

Samankumara Sandanayake, K.R.A.; Nakashima, K.; Shinkai, S. J. Chem. Soc., Chem. Commun. 1994, 1621-1622.

Shin, M.D.; Whitten, D.G. J. Phys. Chem. 1988, 92, 2945-2956.

- Tsien, R. Y. in Fluorescent Chemosensors for Ion and Molecule Recognition; Czarnik, A.W., Ed.; ACS Symposium Series 538; American Chemical Society: Washington, DC, 1993.
- Turkewitsch, P.; Wandelt, B.; Darling, G.D.; Powell, W.S. Anal. Chem. 1998, 70, 2025-2030.
- Turkewitsch, P.; Wandelt, B.; Ganju, R.R.; Darling, G.D.; Powell, W.S. Chem. Phys. Lett. 1996, 260, 142-146.
- Wandelt, B.; Turkewitsch, P.; Stranix, B.R.; Darling, G.D. J. Chem. Soc., Faraday Trans. 1995, 91, 4199-4205.

CHAPTER 4

Enhanced Fluorescence of 4-(p-Dimethylaminostyryl)pyridinium Salts in the Presence of Biological Macromolecules

Petra Turkewitsch, Graham D. Darling,
William S. Powell

"Reprinted from the *Journal of the Chemical Society, Faraday Transactions*, in press, Petra Turkewitsch, Graham D. Darling, William S. Powell, with permission from the Royal Society of Chemistry"

Foreword

We reported in a recent publication (Wandelt et al., 1995) that dye 2 displayed increases in the fluorescence of a similar TICT-type emission band with increasing solution viscosity. This raised the possibility that 2 may be useful as a fluorescent probe (a patent has been filed 1994/08/11) for viscosity measurements in small biological samples, in particular small mucus samples from cystic fibrosis patients who are known to have thick mucus secretions (Davis et al., 1996). These highly viscous secretions have been shown to contain large amounts of DNA, which is thought to contribute to the viscosity. It was, therefore, necessary to investigate whether dye 2 bound to DNA and RNA, and changed fluorescence upon doing so. In addition, in the previous chapter we found that purine nucleotides (analytes), including cAMP, dramatically enhanced the TICT-type fluorescence of trans-4-(p-N,N-dimethyl-aminostyryl)-N-vinylbenzylpyridinium chloride (1) centered at 600 nm, whereas pyrimidine nucleotides had almost no effect on its emission. These results raised the possibility that polynucleotides, such as DNA, which contain purine nucleotides may also induce fluorescence changes in 1 and 2. Thus, since DNA also forms viscous solutions, changes in the fluorescence of 1 or 2 may also be due to changes in solution viscosity. Herein, we examine the effects of various biomolecules, including DNA and proteins, on the fluorescence of these dyes.

¹ trans-4-(p-N,N-Dimethylaminostyryl)-N-vinylbenzylpyridinium chloride (1 or dye 1) refers to a 70:30 mixture of trans-4-(p-N,N-dimethylaminostyryl)-N-m-vinylbenzylpyridinium chloride and trans-4-(p-N,N-dimethylaminostyryl)-N-p-vinylbenzylpyridinium chloride.

Abstract

The fluorescence quantum yields of two cationic styrylpyridinium dyes, *trans-4*-(*p*-N,N-dimethylaminostyryl)-N-vinylbenzylpyridinium chloride (1) and *trans-4*-(*p*-N,N-dimethylaminostyryl)-N-phenethylpyridinium bromide (2), increase dramatically in the presence of low concentrations of DNA with slight blue shifts (4 and 8 nm, respectively) of the emission maxima. These spectral changes suggest that the dyes are interacting with double helical DNA. Dyes 1 and 2 display similar enhancements in fluorescence in the presence of proteins, such as bovine serum albumin, with blue shifts in the emission maxima of 28 and 33 nm, respectively, suggesting that they also interact with proteins. Equilibrium association constants in the order of 10⁴ M⁻¹ were determined for the binding of 1 and 2 to bovine serum albumin. This family of dyes may be useful for the fluorescence detection of very low concentrations of DNA and proteins, and for the fluorescence staining of DNA and proteins in electrophoresis gels.

4.1 Introduction

Fluorescent styrylpyridinium chemosensors possessing electron donor and acceptor groups have been employed to explore the structural and dynamic features of microheterogeneous (Abdel-Mottaleb et al., 1988; Montana et al., 1989), polymeric (Abdel-Mottaleb et al., 1988) and biological systems (Montana et al., 1989; Chan et al., 1996; Kumar et al., 1993). The usefulness of these dyes lies in their environmentally sensitive fluorescence from an intramolecular charge transfer (ICT) excited state.

Recently, we have developed a family of 4-(p-dimethylaminostyryl)pyridinium salts for use as fluorescent chemosensors. Upon exciting at 469 nm, trans-4-(p-N,N-dimethyl-aminostyryl)-N-vinylbenzylpyridinium chloride (1), displayed dramatic quantum yield enhancements in a TICT-type emission band centered at 608 nm in the presence of purine nucleotides (Turkewitsch et al., 1996; Turkewitsch et al., 1998). In contrast, pyrimidine nucleotides had almost no effect on the fluorescence of 1. These fluorescence responses are presumably due to an association of dye 1 with the purine nucleotides. Studies (Wandelt et al., 1995; Darling et al., 1993) in aqueous solution on another member of this family, trans-4-(p-N,N-dimethylaminostyryl)-N-phenethyl-pyridinium bromide (2), revealed that the fluorescence quantum yield of a similar TICT-type emission band, also produced by exciting at 469 nm, increased with increasing solvent viscosity. These results raised the possibility that changes in the fluorescence of 1 or 2 may also be induced by polynucleotides, such as DNA which contains purine nucleotides and forms viscous solutions.

Given the above, our aim was to further explore the environmentally sensitive fluorescence of dyes 1 and 2 in the presence of DNA, and to determine whether an effect

of DNA on the fluorescence of the dyes was related to the solution viscosity, or due to a direct interaction between them. The results indicate that DNA induced dramatic enhancements in the fluorescence of 1 and 2 which were much greater than would have been predicted from the solution viscosity or from interactions with individual nucleotides. Furthermore, fluorescence enhancements of a similar magnitude could be induced by proteins, such as bovine serum albumin.

4.2 Experimental

4.2.1 Materials

trans-4-(p-N,N-Dimethylaminostyryl)-N-vinylbenzylpyridinium chloride (1) (Turkewitsch et al., 1998) and trans-4-(p-N,N-dimethylaminostyryl)-N-phenethylpyridinium bromide (2) (Wandelt et al., 1995; Darling et al., 1993) were prepared as previously described. Deoxyribonucleic acid sodium salt type lll from salmon testes (DNA), ribonucleic acid type Xl from yeast (RNA), adenosine 3':5'-cyclic monophosphate sodium salt (cAMP), bovine serum albumin (BSA, essentially fatty-acid free), ovalbumin grade V from chicken egg, and gelatin type ll from porcine skin were used as received from Sigma Chemical Co.. The amino acids, L-glutamic acid (Fisher Scientific Co.), L-leucine (Sigma Chemical Co.), and L-lysine monohydrochloride, L-threonine, and L-tryptophan (Nutritional Biochemicals Corporation, Cleveland, Ohio) were all used without further purification.

Aqueous solutions were prepared using double distilled deionized water

(Millipore). Phosphate-buffered saline (PBS, 0.01M) was prepared from Dulbecco's phosphate-buffered saline (D-PBS) powder (Gibco BRL) which consisted of anhydrous

monobasic sodium phosphate (0.2 g/L), anhydrous dibasic sodium phosphate (1.15 g/L), potassium chloride (0.2 g/L), and sodium chloride (8 g/L) unless otherwise stated.

4.2.2 Fluorescence measurements

Fluorescence spectra were measured on a Photon Technology International (PTI) Deltascan 4000 spectrofluorometer with 4 nm emission slits on solutions in 1-cm rectangular cuvettes maintained at 22 ± 0.1 °C. Excitation wavelengths of 469 nm were used to obtain the fluorescence emission spectra of 1 and 2 in solutions. The fluorescence spectra are not corrected. The fluorescence quantum yields of dyes 1 and 2 in all solutions were determined by the method of Parker and Rees (Parker and Rees, 1960) from the emission spectra obtained with excitation at 469 nm relative to the quantum yield of rhodamine B in ethanol ($\Phi = 0.69$; excitation = 366 nm; 22 °C) as a standard. The integrated areas under the emission bands gave the relative fluorescence intensities of the solutions. The quantum yields were calculated with corrections for the absorbances of all solutions (Parker and Rees, 1960). A low concentration of dye (10^{-5} M), which gave absorbances of less than 0.3 absorbance units at the exciting wavelength, was used to minimize the contributions of self-absorption and self-aggregation.

4.2.3 Preparation of solutions

Solutions containing various concentrations of DNA, RNA, cAMP, BSA, ovalbumin, gelatin, and amino acids with a constant concentration (10⁻⁵ M) of dye 1 or dye 2 were prepared in PBS. Spectroscopic measurements were performed on thoroughly mixed nondegassed solutions. Solutions containing DNA and gelatin were heated and

vortexed gently to aid dissolution, then thoroughly cooled to room temperature prior to measurement. Denatured BSA solutions were prepared by placing the previously measured BSA solutions in a 95 °C water bath for 30 min. Their fluorescence emissions were measured after cooling the mixtures to room temperature.

4.3 Results

The fluorescence spectra of 2 in PBS (0.01M, pH 7.2) in the presence of various concentrations of DNA (a) and denatured BSA (b) are presented in Fig. 4.1. Upon exciting at 469 nm, DNA induced a dramatic concentration-dependent enhancement in the fluorescence of 2 with a blue shift of the λ_{max} of approximately 8 nm, from 603 nm in buffer alone to 595 nm at 1.0 mg/mL DNA (Fig. 4.1a). Slightly greater fluorescence enhancements were observed for dye 2 in the presence of denatured BSA, with a blue shift of the λ_{max} of about 33 nm, from 603 nm in buffer alone to 570 nm at 1.0 mg/mL protein (Fig. 4.1b). A similar fluorescence enhancement and blue shift was observed in the fluorescence of 2 in the presence of nondenatured BSA (see Fig. 4.2b) (A comparison the the fluorescence spectra of 2 in the presence of 1 mg/mL denatured and nondenatured BSA, DNA and RNA is presented in Figure 4A.1 in Appendix 4, Section A). The absorbance of 2 alone at 469 nm was 0.18 absorbance units. Slight increases in the absorbance of 2 at 469 nm were observed in the presence of 1.0 mg/mL concentrations of DNA (0.03 AU), RNA (0.01 AU) and nondenatured (0.01 AU) and denatured (0.02 AU) BSA. DNA and nondenatured BSA induced similar enhancements in the fluorescence of the related dye 1, upon exciting at 469 nm (see Fig. 4.2a), with blue shifts of approximately 4 and 28 nm, respectively (Figure 4A.1 in appendix 4, Section A also

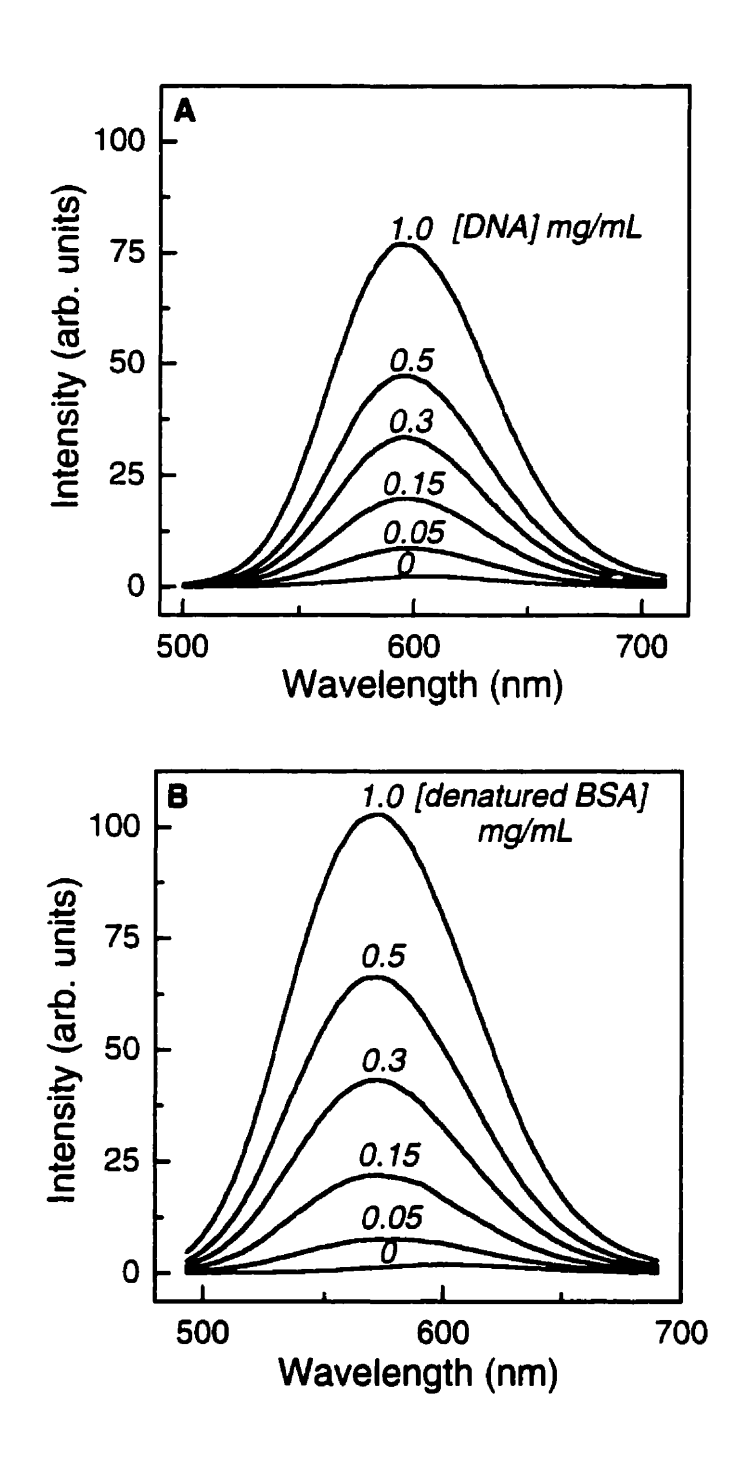


Figure 4.1. Fluorescence spectra of 2 (10 μ M) in the presence of various concentrations (0, 0.05, 0.15, 0.3, 0.5, 1.0 mg/mL) of DNA (A) and denatured BSA (B) in 0.01 M PBS pH 7.2; excitation wavelength, 469 nm; emission maxima varied between 603 and 595 nm for DNA, and 603 and 570 nm for denatured BSA.

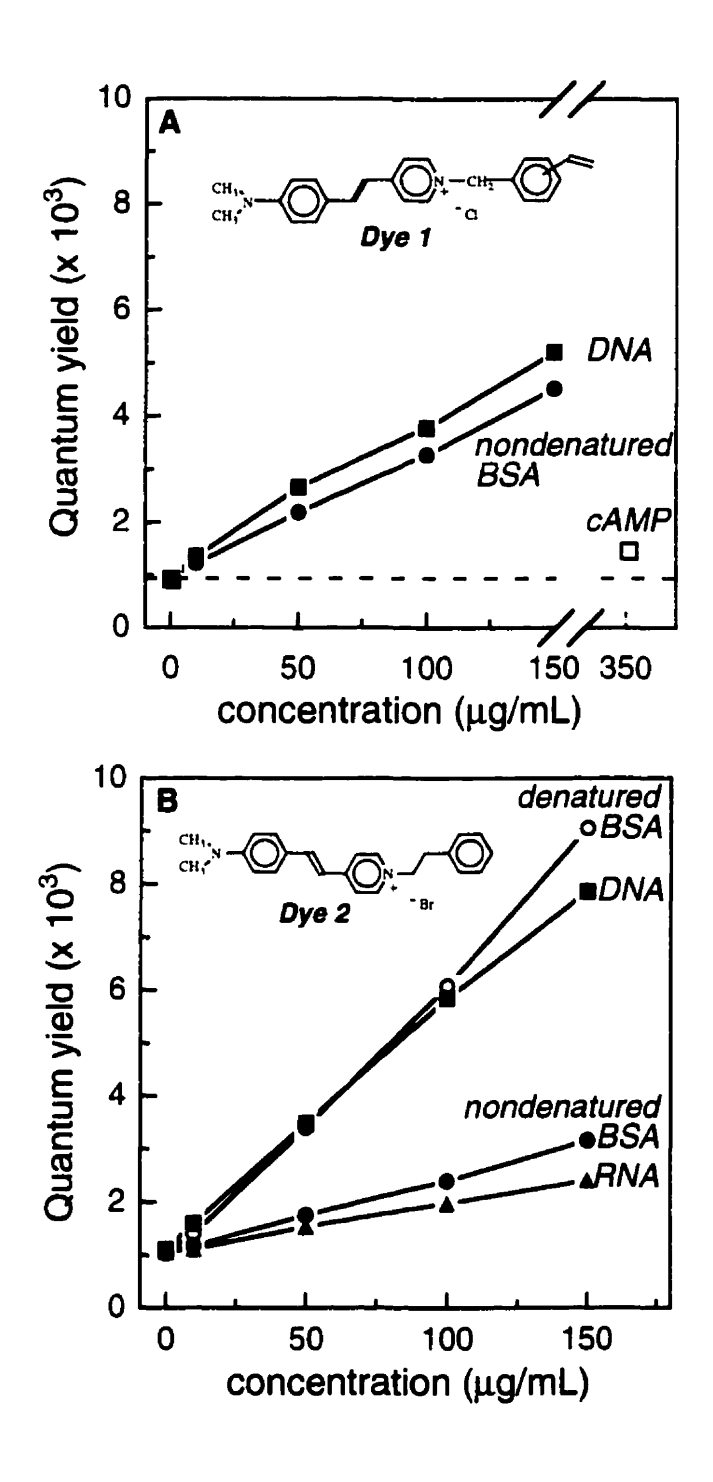


Figure 4.2. Fluorescence quantum yield titration curves of 1 (A) and 2 (B) as a function of concentration of DNA (■), RNA (△), cAMP (□), nondenatured BSA (●) and denatured BSA (O) in 0.01M PBS pH 7.2. Data for cAMP was taken from Chapter 3. All standard errors were less than 10%.

presents the fluorescence spectra of 1 in the presence of 1mg/mL nondenatured BSA and DNA). Concentrations of 1.0 mg/mL of both DNA and nondenatured BSA increased the absorbance of 1 at 469 nm by 0.02 units from an initial absorbance of 0.15 units for 1 alone.

These enhancements in the fluorescence of dyes 1 and 2 induced by DNA, RNA, and denatured and nondenatured BSA are plotted as a function of concentration (0 to 150 μg/mL) in Figure 4.2. For comparison, the effect of cAMP (350 μg/mL) on the fluorescence of 1 is also shown (Fig. 4.2a). The increases (~5-fold) in the fluorescence of 1 induced by DNA and nondenatured BSA at concentrations of 150 µg/mL were of similar magnitude (Fig. 4.2a). In contrast, a higher concentration of cAMP (350 µg/mL) had only a very slight effect on the fluorescence of 1 (1.5-fold enhancement) (Turkewitsch et al., 1996; Turkewitsch et al., 1998). Similar changes in the quantum yield of dye 2 were induced by polynucleotides and proteins (Fig. 4.2b). Denatured BSA induced the greatest fluorescence quantum yield enhancement of 2, exhibiting an approximate 9-fold increase at a concentration of 150 µg/mL. Smaller effects were observed for DNA, nondenatured BSA and RNA with 8, 3, and 2-fold increases in fluorescence, respectively, at this concentration. The changes in the fluorescence of 2 induced by nondenatured BSA were slightly lower than those observed for dye 1, whereas those induced by DNA were somewhat higher. The fluorescence enhancements of 1 and 2 induced by DNA, RNA, denatured and nondenatured BSA were linear over the concentration range examined (0 to 150 µg/mL), whereas at higher concentrations there was evidence of saturation in the response (see Fig. 4.1).

The concentration-dependent fluorescence quantum yield enhancements in dyes 1 and 2 may be used to calculate equilibrium association constants (K_{eq}) for their interaction with nondenatured and denatured BSA (molecular weight, 66 400). The association of dye with protein, $dye + protein \iff dye-protein$, is controlled by the equilibrium association constant.

$$K_{ca} = [dye-protein] / [dye] [protein]$$
 (1).

The fluorescence quantum yield Φ of dye 1 or dye 2 in the presence of protein represents the quantum yield of a mixture of fluorescing species, which may be described by the equation:

$$\Phi = x_{dw}\Phi_a + (1 - x_{dw})\Phi_c \tag{2}$$

where x_{dye} is the mole fraction of "free" dye 1 or 2, and Φ_c and Φ_c are the fluorescence quantum yields of 1 or 2 in the absence of protein, and of the dye-protein complex, respectively. Since $x_{dye} = [dye] / ([dye] + [dye-protein])$, it is readily shown from equations 1 and 2 that

$$\Phi = \Phi_o + \left(\Phi_c - \Phi_o\right) \left(\frac{K_{eq}[protein]}{1 + K_{eq}[protein]}\right)$$
(3).

SigmaPlot curve fitter was used to fit the fluorescence quantum yield enhancements in dyes 1 and 2 in the presence of nondenatured and denatured BSA concentrations between 10 and 1000 µg/mL to equation 3 directly to determine the K_{eq} and Φ_c values. Equilibrium association constants were obtained for 1 in the presence of nondenatured BSA (2.7 × 10⁴ M⁻¹; $\Phi_c = 0.06$) and for 2 in the presence of nondenatured (0.7 × 10⁴ M⁻¹; $\Phi_c = 0.12$) and denatured BSA (1.7 × 10⁴ M⁻¹; $\Phi_c = 0.22$).

To determine whether individual amino acids could induce fluorescence enhancements of 2 similar to those induced by BSA, we investigated the effects of several representative amino acids. Table 4.1 presents fluorescence emission intensity ratio values $(I_{c}I_{f})$ for dye 2 in the presence of L-threonine and L-leucine (neutral amino acids), L-lysine (a basic amino acid), L-glutamic acid (an acidic amino acid), and L-tryptophan (an aromatic amino acid) at concentrations of 1.7 mg/mL. I_{f} is the maximum fluorescence intensity of free dye, and I_{c} is the maximum fluorescence intensity of dye in the presence of the various compounds, macromolecules, and amino acids. None of the amino acids tested affected the fluorescence of 2 significantly. For comparison, the $I_{c}I_{f}$ values for 2 in the presence of high concentrations (1.0 mg/mL) of nondenatured and denatured BSA, DNA and RNA, as well as the $I_{c}I_{f}$ values for 1 with nondenatured BSA, DNA and cAMP are also shown in Table 4.1.

We also investigated the effects of other proteins on the fluorescence of dye 2.

Ovalbumin had virtually the same effect as nondenatured BSA, with an I/I_f value of 11.7 at a concentration of 1.0 mg/mL, compared to a value of 12.4 for nondenatured BSA (Table 4.1). On the other hand, gelatin, at this same concentration, had a considerably smaller effect than nondenatured BSA, resulting in an I/I_f value of only 1.49. (Appendix 4, Section B presents the fluorescence spectra of 2 in the presence of ovalbumin, nondenatured BSA and gelatin concentrations of 1 mg/mL (Fig. 4B.1). Ovalbumin induced a fluorescence increase and a blue shift in the emission maximum (from 603 nm in buffer alone to 570 nm at 1 mg/mL ovalbumin) of 2 similar to nondenatured BSA, whereas a much smaller fluorescence increase and blue shift (from 603 nm in buffer alone to 600 nm at 1 mg/mL gelatin) of 2 was observed for gelatin.) Furthermore, it is of

Table 4.1. Fluorescence emission intensity ratios $(I/I)^b$ for dyes 1 and 2 with various compounds.

| compound | dye | concn° | I_{ℓ}/I_{f} | η _{sp} ⁴ |
|-------------------------------|-----|--------|------------------|------------------------------|
| DNA° | 1 | 1.0 | 26.4 | 5.00 ^h |
| | 2 | 1.0 | 31.4 | 5.00 |
| RNA° | 2 | 1.0 | 6.03 | |
| cAMP | 1 | 1.8 | 2.50 | |
| nondenatured BSA ^c | 1 | 1.0 | 22.9 | 0.004 ^h |
| | 2 | 1.0 | 12.4 | 0.004 |
| denatured BSA ^e | 2 | 1.0 | 49.2 | $0.\dot{0}1_{\mu}$ |
| ovalbumin ^t | 2 | 1.7 | 11.7 | |
| gelatin ['] | 2 | 1.7 | 1.49 | 0.18 |
| L-glutamic acid ⁽ | 2 | 1.7 | 1.02 | |
| L-lysine ⁽ | 2 | 1.7 | 1.01 | |
| L-threonine ¹ | 2 | 1.7 | 1.03 | |
| L-leucine ^f | 2 | 1.7 | 1.01 | |
| L-tryptophan' | 2 | 1.7 | 1.07 | |
| sucrose | 2 | 280 | 2.98 | 0.79 |
| poly(ethylene glycol)* | 2 | 100 | 6.49 | 5.05 |

^a excitation 469 nm.

b I_f is the maximum fluorescence intensity of free dye, and I_c is maximum fluorescence intensity of dye in the presence of various compounds.

⁴ specific viscosity [(viscosity of solution/viscosity of solvent) - 1].

in 0.01M PBS pH 7.2.
in 0.1M phosphate buffer pH 7.2, 0.1M NaCl.
in water, data calculated from Wandelt et al., 1995.
calculated from intrinsic viscosity and concentration (Richards, 1993; Tanford, 1961).

in 0.15 M NaCl, pH 5.1 at 17.8°C (Boedtker and Doty, 1954).

interest to note that at a very high concentration (33.7 mg/mL), nondenatured BSA and ovalbumin induced a 5-fold greater increase in the fluorescence intensity of 2 than did gelatin, which produced a gel state under these conditions. (The fluorescence intensities of 2 at concentrations of ovalbumin, nondenatured BSA and gelatin between 0 and 33.7 mg/mL are presented in Figure 4B.2 in Appendix 4, Section B.) In addition, at this high concentration there was evidence of saturation in the responses induced by BSA and ovalbumin, whereas the response induced by gelatin remained linear.

4.4 Discussion

Dyes 1 and 2 display dramatic fluorescence quantum yield enhancements in the presence of DNA and both nondenatured and denatured BSA. For DNA, these changes could theoretically be due to increases in viscosity since we have previously shown that the TICT-type fluorescence of 2 displays enhancements with increasing solvent viscosity (Wandelt et al., 1995; Darling et al., 1993). However, very low concentrations of DNA, 10 - 150 μg/mL, which would be expected to exhibit very small changes in viscosity, dramatically enhance the fluorescence of 2 from 1.5-fold at 10 μg/mL to 8-fold at 150 μg/mL (Fig. 4.2b). In addition, we (Wandelt et al., 1995) recently reported that a very high concentration of poly(ethylene glycol) (100 mg/mL), with a specific viscosity of 5.05, gave a 6.5-fold increase in the fluorescence quantum yield of 2, whereas DNA which has a similar specific viscosity (5.00) at a concentration of only 1.0 mg/mL induced a 31-fold fluorescence enhancement in 2 (Table 4.1). Likewise, 1.0 mg/mL solutions of nondenatured and denatured BSA with specific viscosities of 0.004 and 0.01, respectively, induced much greater fluorescence enhancements in 2 (12 and 49-fold,

respectively) than did poly(ethylene glycol). A sucrose solution (280 g/L) with a specific viscosity of 0.789 induced an increase in fluorescence of only 3-fold (Wandelt et al., 1995). Furthermore, at 1.0 mg/mL concentrations, DNA with a higher specific viscosity (5.00), induced a smaller fluorescence enhancement (31-fold) in 2 than denatured BSA (49-fold) which has a much lower viscosity (0.01). Thus, the enhancements in the fluorescence of dyes 1 and 2 induced by DNA and BSA do not correlate with the solution viscosities since the changes are much greater than would have been predicted from the solution viscosity. This suggests that the dyes may be specifically interacting with DNA and BSA.

Small molecules which bind to the DNA double helix noncovalently may do so by two dominant modes: groove binding and intercalation (Kumar et al., 1993). Groove binding involves docking of thin ribbon-like molecules, usually positively charged extended heterocycles, in the DNA minor groove in close proximity to the sugarphosphate backbone where electrostatic, hydrogen bonding and hydrophobic interactions contribute to the stability of the complex. In contrast, intercalation involves the insertion of planar molecules, usually aromatic cations, into the DNA helix between adjacent base pairs where aryl stacking interactions predominate, with hydrophobic and electrostatic interactions providing additional stabilization. Thus, whereas intercalated molecules are well protected from the aqueous solvent, groove-bound molecules are only partially protected.

Recently, Kumar et al. (Kumar et al., 1993) studied the interaction of a cationic styryl dye, *trans*-4-[4-(dimethylamino)styryl]-1-methylpyridinium iodide (DSMI), to double helical calf thymus DNA by absorption and fluorescence measurements. DSMI

displayed a marked fluorescence enhancement with no shift of the emission maximum in the presence of DNA, together with a small red shift and increase in the absorption. The authors suggested that DSMI was binding to the minor groove of DNA, rather than intercalating, since its long thin flexible structure was favorable for this type of interaction, and since the spectral changes observed were in contrast to the behavior observed for many fluorescent intercalators. The similarities in structure and spectral patterns of dyes 1 and 2 in the presence of DNA to DSMI raise the possibility that 1 and 2 may be binding to the minor groove of the DNA helix. RNA, which consists of only one polynucleotide chain, induces a much smaller effect in 2 than DNA, also supporting this proposition.

The main path of nonradiative deactivation of stilbene derivatives is known to be via rotation around the ethylenic double bond in the excited state associated with *trans-cis* photoisomerization (Létard et al., 1993; Samankumara Sandanayake et al., 1994).

Restrictions imposed by environments such as viscous solvents (Abdel-Mottaleb, 1984; Abdel-Mottaleb et al., 1989), microheterogeneous micelle (Abdel-Mottaleb et al., 1988) and cyclodextrin structures (Duveneck et al., 1989), or by the presence of molecules capable of interacting with these stilbene sensors (Samankumara Sandanayake et al., 1994) inhibit the internal motion around the ethylenic bond of these molecules in the excited state causing decreased nonradiative decay and increased fluorescence yields. In addition, Kumar et al. (Kumar et al., 1993) postulated that minor groove binding of DSMI inhibits its nonradiative deactivation by imposing a restriction on the rotation around the double bond in the excited state, resulting in enhanced fluorescence yields. Thus, the dramatic enhancements in the fluorescence of 1 and 2 may be due to a

restriction of the internal rotation about the ethylenic bond in the excited state on binding to the minor groove of the DNA double helix.

TICT excited states possess extremely large dipole moments, and are thus destabilized by a decrease in the polarity of the environment (Bhattacharyya and Chowdhury, 1993; Rettig, 1986). This leads to an increase in the energy gap between the ground and excited states, and hence a blue shift in the emission. Recently, we (Turkewitsch et al., 1998) have reported a large change in the dipole moment between the ground and TICT-type excited states of 1 of ~18 D upon excitation at 469 nm. It would be expected that dye 2 would behave similarly since its structure is almost identical to that of 1. The minor groove of DNA would also be expected to be less polar than the bulk aqueous phase. Thus, the blue shift in the emission of 1 and 2 in the presence of DNA may be attributed to a reduction in polarity of the environment.

The effects of nondenatured and denatured BSA on the fluorescence of 1 and 2 suggest that they also interact with proteins. Similar spectral patterns have been reported for diethylaminocoumarin laser dyes (Nag and Bhattacharyya, 1990) and anilinonapthalene sulfonates (Slavik, 1982) in the presence of bovine serum albumin, as well as in other fluorescent dyes used for protein detection and quantitation (Haugland, 1996). Equilibrium association constants in the order of 10⁴ M¹ were determined for the binding of dyes 1 and 2 to nondenatured and denatured BSA. These affinities are about 3 orders of magnitude higher than those which we recently found for 1 with purine nucleotides (Turkewitsch et al., 1998).

To determine whether the effects of proteins on the fluorescence of dyes 1 and 2 could be mimicked by individual amino acids, we examined the effects of several

representative amino acids on the fluorescence of 2 (Table 4.1). The lack of response of 2 to the presence of neutral (L-threonine and L-leucine), basic (L-lysine), acidic (L-glutamic acid), and aromatic (L-tryptophan) amino acids suggests that 2 is probably not interacting with individual amino acids. The fact that denatured BSA induces a response about twice that of BSA suggests that 2 may be interacting with sequences of amino acids in the protein exposed by denaturation, and that dye 2 is sensitive to protein conformation. Given the discussion presented above for DNA, the fluorescence enhancements of 1 and 2 induced by proteins may also be due to restricted ethylenic double bond rotation in the excited state on binding to proteins. A reduction in the polarity of the environment could also explain the blue shift of 1 and 2 in the presence of protein.

4.5 Conclusions

Dramatic fluorescence enhancements of dyes 1 and 2 in the presence of double helical DNA and both nondenatured and denatured BSA suggest that there is an interaction between them. For DNA, this interaction may involve binding to the minor groove, whereas the binding of dyes 1 and 2 to the proteins probably involves interactions with sequences of amino acids.

These highly environmentally sensitive dyes are attractive practical chemosensors for biological systems. Their intense absorption band in the visible region should have significant excitation using standard argon, argon/krypton, or conventional lamp sources. Dyes 1 and 2 display long wavelength fluorescence which provides a large Stokes' shift, separating excitation from emission wavelengths, and which is well above the wavelength

of significant biological autofluorescence (~ 460 nm). The fluorescence quantum yield of the dyes varies linearly over a broad range of polynucleotide and protein concentrations indicating that their fluorescence could be used as a sensitive method to determine DNA and protein concentration. Their marked fluorescence enhancements in the presence of DNA and proteins, and the poor fluorescence yield of the dyes in their absence, suggest that 1 and 2 may be useful for the fluorescence staining of DNA and proteins in electrophoresis gels. In addition, their sensitivity to conformation and environment may make them especially useful for investigating protein structure and function. In addition, an experiment with 2 revealed that it is capable of passively diffusing across the cell membrane, and that it does not interfere with the physiological functioning of cells (Appendix 3F). Finally, it has also been demonstrated that this family of dyes is amenable to the synthesis of esterified membrane-permeant derivatives, and that such derivatives are capable of staining live microorganisms without affecting viability (Chan et al., 1996; Darling et al., 1993).

4.6 Acknowledgments

The authors thank the Respiratory Health Network of Centers of Excellence for financial support of this work, as well as the Canadian Cystic Fibrosis Foundation for studentship support for P. Turkewitsch. We would also like to acknowledge the contributions of the late Dr. Seymour Heisler.

4.7 References

Abdel-Mottaleb, M.S.A. Laser Chem. 1984, 4, 305-310.

Abdel-Mottaleb, M.S.A.; Sherief, A.M.K.; Abdel-Azim, A.A.; Habashy, M.M.; Ismail, L.F.M. J. Photochem. Photobiol. 1988, 44, 161-169.

Abdel-Mottaleb, M.S.A.; Sherief, A.M.K.; Ismail, L.F.M.; De Schryver, F.C.; Vanderauweraer, M.A. J. Chem. Soc., Faraday Trans. 2 1989, 85, 1779-1788.

Bhattacharyya, K.; Chowdhury, M. Chem. Rev. 1993, 93, 507-535.

Boedtker, H.; Doty, P. J. Phys. Chem. 1954, 58, 968-983.

Chan, E.C.S.; Stranix, B.R.; Darling, G.D.; Noble, P.B. Can. J. Microbiol. 1996, 42, 875-879.

Davis, P.B.; Drumm, M.; Konstan, M.W. Am. J. Respir. Crit. Care Med. 1996, 154, 1229-1256.

Duveneck, G.L.; Sitzmann, E.V.; Eisenthal, K.B.; Turro, N.J. J. Phys. Chem. 1989, 93, 7166-7170.

Haugland, R.P. Handbook of fluorescent probes and Research Chemicals, 6th ed.; Spence, M.T.Z., Ed.; Molecular Probes, Inc.: Eugene, Oregon, 1996.

Kumar, C.V.; Turner, R.S.; Asuncion, E.H. J. Photochem. Photobiol. A: Chem. 1993, 74, 231-238.

Létard, J-F.; Lapouyade R.; Rettig, W. J. Am. Chem. Soc. 1993, 115, 2441-2447.

Montana, V.; Farkas, D.L.; Loew, L.M. Biochemistry 1989, 28, 4536-4539.

Nag, A.; Bhattacharyya, K. Chem. Phys. Lett. 1990, 169, 12-16.

Rettig, W. Angew. Chem., Int. Ed. Engl. 1986, 25, 971-988.

Richards, J.L. J. Chem. Educ. 1993, 70, 685-689.

- Samankumara Sandanayake, K.R.A.; Nakashima, K.; Shinkai, S. J. Chem. Soc., Chem. Commun. 1994, 1621-1622.
- Slavik, J. Biochim. Biophys. Acta., 1982, 694, 1-25.
- Tanford, C. Physical Chemistry of Macromolecules; Wiley: New York, 1961.
- Turkewitsch, P.; Wandelt, B.; Darling, G.D.; Powell, W.S. J. Photochem. Photobiol. A: Chem. 1998, in press.
- Turkewitsch, P.; Wandelt, B.; Ganju, R.R.; Darling, G.D.; Powell, W.S. Chem. Phys. Lett. 1996, 260, 142-146.
- Wandelt, B.; Turkewitsch, P.; Stranix, B.R.; Darling, G.D. J. Chem. Soc., Faraday Trans. 1995, 91, 4199-4205.

CHAPTER 5

Fluorescent Functional Recognition Sites Through Molecular Imprinting. A Polymer-Based Fluorescent Chemosensor for Aqueous cAMP

Petra Turkewitsch, Barbara Wandelt, Graham D. Darling,
William S. Powell

"Reprinted in part with permission from *Analytical Chemistry* **1998**, *70*, 2025-2030, Copyright, 1998, American Chemical Society".

Foreword

trans-4-(p-N,N-Dimethylaminostyryl)-N-vinylbenzylpyridinium chloride (1)¹ displayed large fluorescence enhancements in the presence of cAMP and other purine analytes. However, the ability of 1 to act as a fluorescent chemosensor for cAMP is limited due to its low affinity and selectivity for this nucleotide. Nonetheless, the large fluorescence enhancement induced by cAMP suggests that dye 1 may be useful as the fluorescent component of a structure that provided more efficient recognition of cAMP. In an attempt to increase the recognition ability of dye 1 for cAMP we chose to prepare recognition sites for cAMP that contain dye 1 in a polymer matrix using the technique of molecular imprinting.

Appendix 5, Section A contains a table (Table 5A) of the I_0/I values for each experiment with the control and imprinted polymers at each concentration of cAMP (0.01 to 1000 μ M) and cGMP (1 to 1000 μ M) tested, as well as the averages and standard errors of these experiments. These averages and errors are plotted in Figure 5.3.

The affinity and specificity of the MIP for cAMP was examined using fluorescence spectroscopy in this chapter. Appendix 5, Section B describes some preliminary studies using absorption spectroscopy to evaluate the binding of cAMP to the polymers.

¹ trans-4-(p-N,N-Dimethylaminostyryl)-N-vinylbenzylpyridinium chloride (1 or dye 1) refers to a 70:30 mixture of trans-4-(p-N,N-dimethylaminostyryl)-N-m-vinylbenzylpyridinium chloride and trans-4-(p-N,N-dimethylaminostyryl)-N-p-vinylbenzylpyridinium chloride.

Abstract

A novel design for template-selective recognition sites in polymers prepared by molecular imprinting is reported. Molecular imprints were prepared against cAMP that contain a fluorescent dye, *trans-4-(p-N,N-dimethylaminostyryl)-N-vinylbenzyl-* pyridinium chloride, as an integral part of the recognition cavity, thus serving as both the recognition element and the measuring element for the fluorescence detection of cAMP in aqueous media. This fluorescent molecularly imprinted polymer displays a quenching of fluorescence in the presence of aqueous cAMP, whereas almost no effect is observed in the presence of the structurally-similar molecule, cGMP. The association constant for the binding of cAMP to the imprinted polymer was determined to be in the order of 10⁵ M⁻¹. Such fluorescent molecularly imprinted polymers containing selective sites for cAMP may find applications as fluorescent chemosensors for the aqueous detection of this molecule.

5.1 Introduction

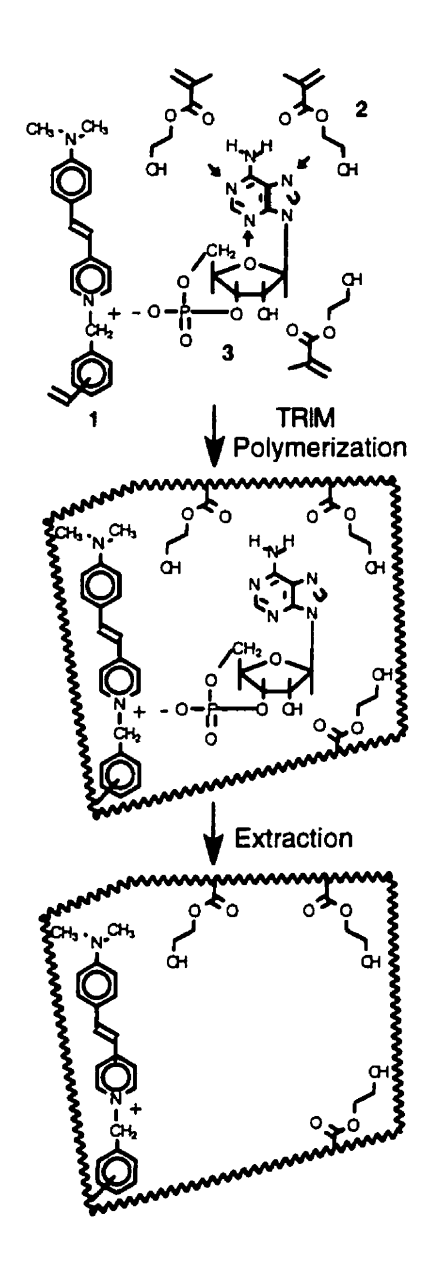
Adenosine 3':5'-cyclic monophosphate (cAMP) is an important second messenger in cells, mediating the actions of many hormones, drugs and neurotransmitters which act via cell surface receptors (Darnell et al., 1994). Methods aimed at measuring the levels of cAMP, as well as other intracellular second messengers, are therefore highly desirable (Tsien, 1993). Biological recognition elements, such as antibodies, are typically used in ligand-binding assays to specifically bind cAMP, but they often require special handling, and may suffer from poor stability and a complicated costly production procedure (Brooker et al., 1979). An appealing alternative approach is the use of molecularly imprinted polymers (MIPs), synthetic polymers with substrate-selective recognition properties, as the recognition element, since they combine the advantages of easy tailor design with physical and chemical stability and durability (Ansell et al., 1996; Kriz et al., 1997; Mosbach and Ramström, 1996; Muldoon and Stanker, 1996; Steinke et al., 1995; Steinke et al., 1995; Wulff, 1997; Vlatakis et al., 1993).

Molecular imprinting entails copolymerization of functional monomers in the presence of a template (print molecule) (Ansell et al., 1996; Kriz et al., 1997; Mosbach and Ramström, 1996; Muldoon and Stanker, 1996; Steinke et al., 1995; Wulff, 1995). Imprinting is achieved by interactions, either non-covalent or covalent, which occur between complementary functionalities in the template molecule and functional monomer units. Non-covalent interactions are formed simply by mixing the template molecule with a suitable mixture of monomers prior to polymerization. Following polymerization, removal of the template by extraction leaves microcavities with a three-dimensional structure complementary to the template in both shape and chemical functionality, thus

enabling subsequent recognition of the template. Such MIPs have been used as tailor-made separation materials, antibody and receptor mimics in assay systems, biomimetic recognition elements in biological sensors, and artificial enzyme systems for catalytic applications (Kriz et al., 1997; Mosbach and Ramström, 1996; Wulff, 1995).

We report here a novel approach towards the design of biomimetic sensors in which a fluorescent MIP serves as both the recognition element and the measuring element for the fluorescent detection of cAMP in aqueous media. Fluorescence is an attractive detection method for sensors due to its high sensitivity and nondestructive nature (Czarnik, 1993). Several other MIP systems have used fluorescence detection methods based either on the use of fluorescent-labeled analytes (Kriz et al., 1995; Piletsky et al., 1997), or on the formation of fluorescent complexes between added reagents and residual functional groups on the polymer (Piletsky et al., 1996). However, we have created template-selective sites in a methacrylate polymer for cAMP which contain a fluorescent reporter group as an integral part of the recognition cavity (Scheme 5.1). Obtaining binding and selectivity in aqueous media is a major requirement for MIP-based sensors designed for biological systems, because the binding event occurs under conditions compatible with biological molecules (Ansell et al., 1996; Andersson et al., 1995; Mathew and Buchardt, 1995; Kugimiya et al., 1996).

The fluorophore chosen, *trans-4-(p-N,N-dimethylaminostyryl)-N-*vinylbenzylpyridinium chloride (1), was especially designed by us for the purpose of preparing MIPs. This functional monomer combines microenvironmental sensitive fluorescence, due to its intramolecular charge transfer behavior, with a positive charge



Scheme 5.1. Schematic representation of hypothetical imprint formation. The fluorescent functional monomer (1) and the functional monomer, HEMA (2) are arranged around the template molecule, cAMP (3), as a result of the noncovalent interactions between complementary chemical functionalities. Polymerization captures the topographical relationship present in solution. Extraction of the template molecule exposes recognition sites of complementary shape and functional topography. Arrows represent additional potential hydrogen bonding interactions between HEMA and cAMP.

that is capable of promoting an association with negatively charged nucleotides, together with a vinyl group, necessary for covalent attachment to a polymer matrix. Recently, we (Turkewitsch et al., 1996; Turkewitsch et al., 1998) found that 1 displays a dramatic fluorescence quantum yield enhancement in the presence of purine nucleotides, including cAMP and cGMP, but almost no fluorescence enhancement with pyrimidine nucleotides. These results suggested that dye 1 associates with the purine nucleotides in aqueous solution presumably through electrostatic and aryl stacking interactions. Polymerization of 1 in the presence of other monomers created a fluorescent molecularly imprinted polymer chemosensor capable of specifically detecting cAMP in aqueous media.

5.2 Experimental

5.2.1 Materials

trans-4-(p-N,N-Dimethylaminostyryl)-N-vinylbenzylpyridinium chloride (1) was prepared as described previously (Turkewitsch et al., 1998). Trimethylolpropane trimethacrylate (TRIM, alternatively known as 2-ethyl-2-(hydroxymethyl)-1,3-propanediol trimethacrylate), and 2-hydroxyethyl methacrylate (HEMA) were purchased from Aldrich Chemical Co. and were used without further purification. Inhibitor was removed from the monomers by passing them through a column of aluminum oxide (activated basic, Brockmann 1, Aldrich) immediately before use. 2,2'-Azobisisobutyronitrile (AIBN) was used as purchased from Kodak. The cyclic nucleotides, adenosine 3':5'-cyclic monophosphate sodium salt (cAMP) and guanosine 3':5'-cyclic monophosphate sodium salt (cGMP), were used as received from the Sigma Chemical Co.. Aqueous solutions of the nucleotides were prepared and all measurements

were performed using double distilled deionized water (Millipore). Methanol used in synthesis was reagent grade or better.

5.2.2 Preparation of polymers

A cAMP imprinted polymer was prepared by adding a solution of 1 (31.5 mg, 83.6 umol) in 30 ml of methanol to the template molecule, cAMP (41.7 mg, 119 umol) in a glass specimen bottle. The mixture was shaken and sonicated until all the cAMP dissolved. The crosslinking monomer, TRIM (29.0 g, 86.0 mmol), the functional monomer, HEMA (0.675 g, 5.19 mmol), and the initiator, AIBN (0.665 g, 4.05 mmol), were then added and dissolved successively. The bottle was purged with nitrogen for 10 minutes, and polymerized by irradiation (350 nm) in a Rayonet Photochemical UV Reactor (The Southern New England Ultraviolet Co.) at room temperature for 1.5 h. The sample was subsequently placed in an oil bath at 60°C for 24 h. The red-orange transparent starting polymerization mixture was transformed into a pink opaque solid during this time. The solid pink polymer mass was released by breaking the bottle, wiped free of broken glass, then ground by hand with a mortar and pestle and wet-sieved (water). Particles of 45-106 µm were collected, because this fraction was the easiest to obtain when grinding by hand. These polymer particles were placed in a Soxhlet extractor for continuous washing by 300 mL water-methanol (7:3, v:v) for a minimum of 24 h, then by 300 mL methanol for a minimum of 24 h. The polymer particles were dried in vacuo (20 mm Hg) at 35°C overnight, and stored in air tight vials in the dark. A nonimprinted control polymer containing no cAMP was prepared at the same time under identical conditions.

5.2.3 Fluorescence measurements

Fluorescence spectra were measured on a Photon Technology International (PTI) Deltascan 4000 spectrofluorometer by front-face illumination with emission slits at 2 nm, in a 1-cm triangular quartz cuvette (Hellma) placed in a cuvette holder that was maintained at 25 ± 0.1 °C. A polarizer, set at 54.7° from the vertical was placed in the emission beam to reduce the amount of scattered light from the samples (Lakowicz, 1983). An excitation wavelength of 469 nm was used to obtain the fluorescence emission spectra of all polymer suspensions. The fluorescence spectra are not corrected.

The steady-state fluorescence of the control and imprinted polymers was evaluated on 150 mg (polymer powder dry weight) samples that had been shaken in a vial with 4 mL water overnight, separated by centrifugation, then resuspended in 1.25 mL water in a triangular cuvette which was then sealed with parafilm. After vigorous shaking of the cuvette to suspend the polymer particles, the fluorescence emission spectrum was measured by exciting at 469 nm. Preliminary experiments determined that 150 mg of polymer powder was the amount necessary to obtain a constant fluorescence emission intensity reading at the maximum wavelength of emission (~595 nm) for the duration of the measurement (-1.5 min). The fluorescence emission spectrum was acquired in triplicate (shaking vigorously between each measurement to suspend the particles) every 10-15 minutes until a stable reading was attained, whose average maximum intensity near 595 nm was taken to be I_a (the fluorescence intensity in the absence of cyclic nucleotide). The cuvette contents were then transferred back to the vial, the solid particles spun down, the supernatant decanted, and 1.25 mL of cyclic nucleotide solution of known concentration added. After incubating in a shaker bath at 25°C for 1.5 h, the contents of

the vial were transferred back into the same cuvette, and the fluorescence emission spectrum was acquired in triplicate every 10-15 min for 45 min, shaking vigorously between each measurement. The average of the time points was taken to be I (the fluorescence intensity in the presence of cyclic nucleotide).

To evaluate the time course of cAMP binding to the control and imprinted polymers, fluorescence emission measurements began immediately after addition of cyclic nucleotide, as described above.

5.3 Results and Discussion

A fluorescent cAMP-imprinted polymer was prepared by polymerization of TRIM, HEMA, and the fluorescent functional monomer 1 in the presence of cAMP. Photochemical free radical polymerization at room temperature using AIBN was used, since it has been demonstrated that polymers prepared at higher temperatures exhibit reduced recognition capabilities (Steinke et al., 1995; Andersson et al., 1994). TRIM, a trifunctional monomer, has been reported to produce polymers with excellent recognition properties, and thus was chosen to be the main component of the monomer mixture (Kempe and Mosbach, 1995; Steinke et al., 1996). Methanol was used as the solvent porogen because it was the only convenient one capable of dissolving cAMP and all other monomers.

In this system, both electrostatic and aryl stacking interactions between the template, cAMP, and the fluorescent functional monomer, 1, are expected to be present during polymerization and subsequent recognition (Turkewitsch et al., 1996; Turkewitsch et al., 1998). A slight (0.4-fold) molar excess of cAMP over 1 was used to increase the

proportion of dye complexed, ensuring that the majority of 1 was present in imprinted binding cavities. HEMA was added to provide additional hydrogen bonding sites in the polymer to which cAMP could bind (Scheme 5.1). The addition of HEMA to a methacrylate polymer prepared against sialic acid has been shown to increase the amount of sialic acid bound to the imprinted polymer in phosphate buffer (Kugimiya et al., 1996). The authors suggested that the increased hydrophilicity of the polymer, due to the hydroxyl residues of HEMA, facilitated the penetration of sialic acid into the polymer, thereby enhancing the selective binding. Because of this, and the multiple potential hydrogen bonding interactions between HEMA and cAMP, a large molar excess of HEMA over cAMP was employed in imprinting. This could result in the presence of binding sites containing only HEMA functional groups, but these sites would not contain the fluorescent dye 1 and therefore should not affect the fluorescence of 1.

The choice of solvents used to extract the template molecule was also dictated by the template solubility. Accessible cAMP was removed from the polymer by washing exhaustively with methanol and water. The presence of impurities (possibly oligomers or residual monomers, and initiator fragments) in the washes hampered attempts to determine the amount of cAMP recovered. Fluorescence measurements of the washes showed that negligible amounts of fluorescent dye were released from the polymer during the extraction procedure.

The recognition properties of the cAMP-imprinted polymer were examined in aqueous media by fluorescence spectroscopy. First, the effect of the template molecule, cAMP, on the fluorescence of the control and imprinted polymers was evaluated.

Exciting the polymers at 469 nm generated a broad structureless emission band with a

maximum at ~595 nm. Fig. 5.1 shows the fluorescence emission spectra of the imprinted polymer in the absence and 135 min after the addition of 1 mM cAMP. The fluorescence emission of the imprinted polymer was quenched by cAMP. The time course (0-280 min) of the fluorescence quenching effect of cAMP on the cAMP-imprinted polymer is presented in Fig. 5.2. The time required for a steady response was approximately 30 min.

Subsequently, the fluorescence of the control and imprinted polymers was measured at various concentrations of cAMP in the 90-135 min time interval. This time period was chosen to evaluate the effects of various concentrations of cyclic nucleotides on the fluorescence of the polymers to ensure that equilibrium had been reached. (Table 5A.1 in Appendix 5, Section A shows the I/I values for each experiment with the control and imprinted polymers at each concentration of cAMP (0.01 to 1000 µM) and cGMP (1 to 1000 µM) tested. The averages of these experiments, as well as the standard errors, for a particular concentration of cAMP and cGMP are plotted in Figure 5.3.) Fig. 5.3a shows the effects of concentrations of cAMP between 10 nM and 1 mM on the fluorescence of the control and imprinted polymers. Concentrations of cAMP of 100 nM or above resulted in quenching of the fluorescence of the imprinted polymer. The effect of cAMP was concentration dependent, reaching a maximal level by about 10 to 100 μM, probably due to saturation of the accessible sites on the polymer. In contrast, the control polymer exhibited relatively little response to cAMP, its I/I value fluctuating around 1.0. This suggests that cAMP has the ability to induce changes in the fluorescence of 1 only if dye 1 is located in an imprinted cavity. Thus, although cAMP may interact with 1 other than at the imprinted sites (i.e. nonspecifically), it appears that this nonspecific binding does not affect the fluorescence of 1 to a great extent. As both polymers have the same

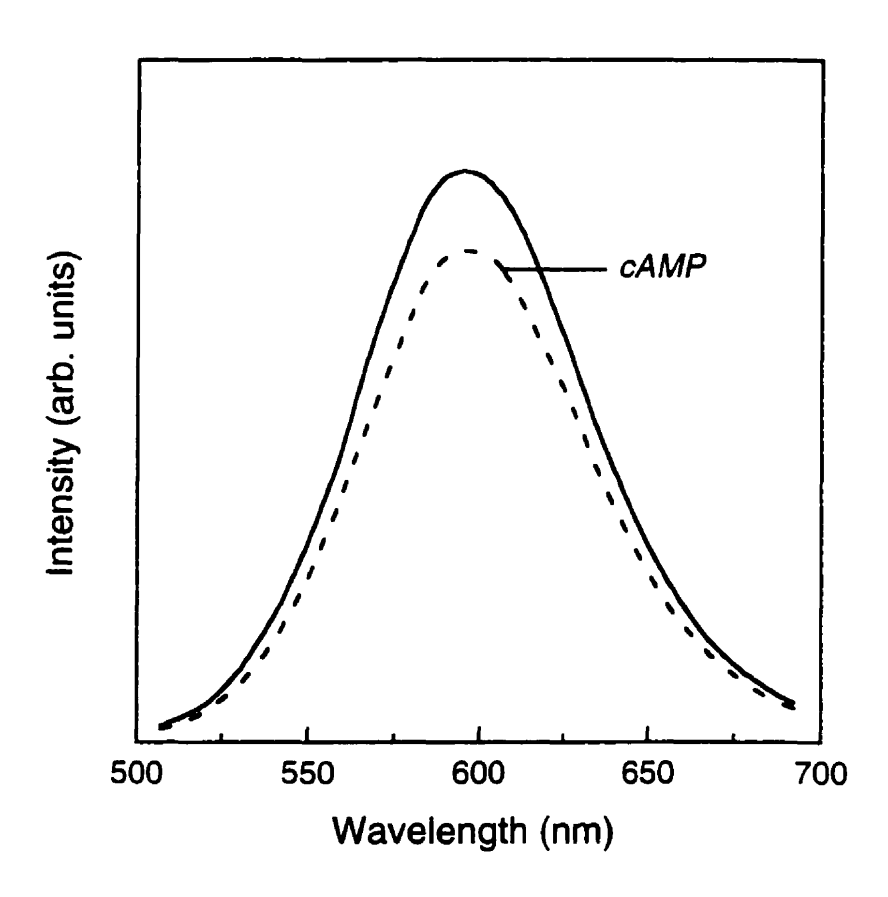


Figure 5.1. The fluorescence emission spectra of the imprinted polymer in the absence of (solid line), and 135 min after the addition of 1.0 mM cAMP (dashed line). Excitation wavelength, 469 nm; emission wavelength maximum, ~595 nm.

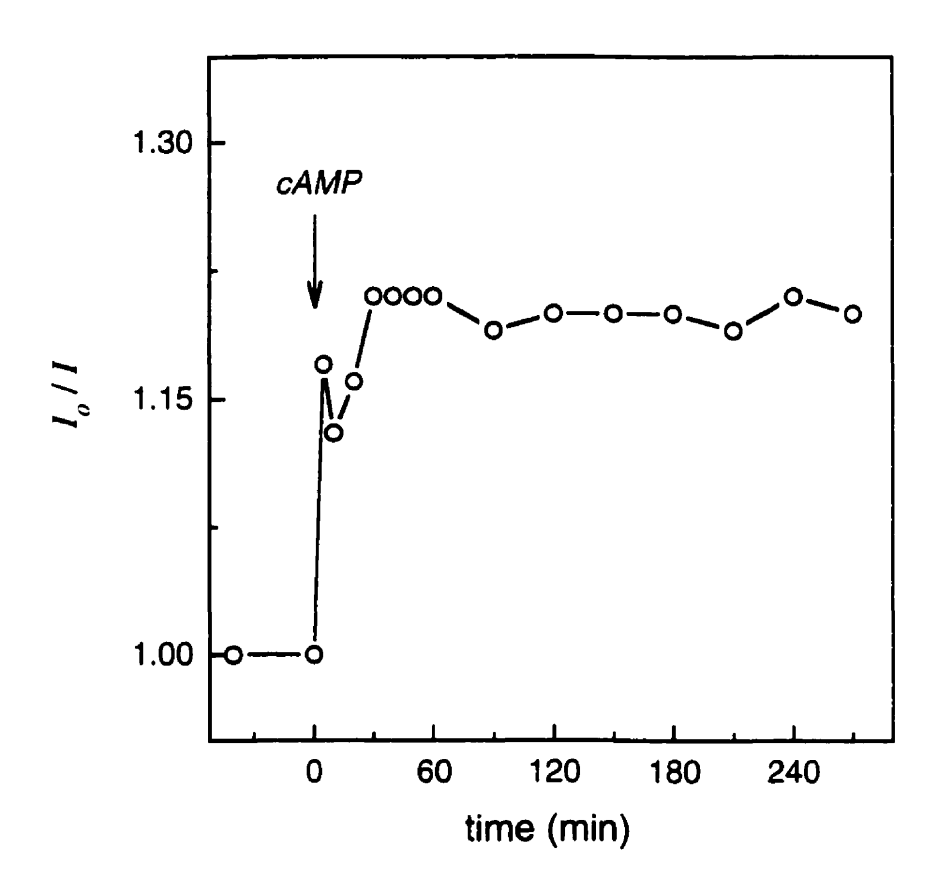


Figure 5.2. Time course for the fluorescence quenching effect of cAMP on the cAMP-imprinted polymer at 25 °C. A representative experiment is illustrated in which 1.0 mM cAMP was added at time 0 min and the fluorescence emission of the polymer was measured as described in the Experimental section. Excitation wavelength, 469 nm; emission wavelength, ~595 nm.

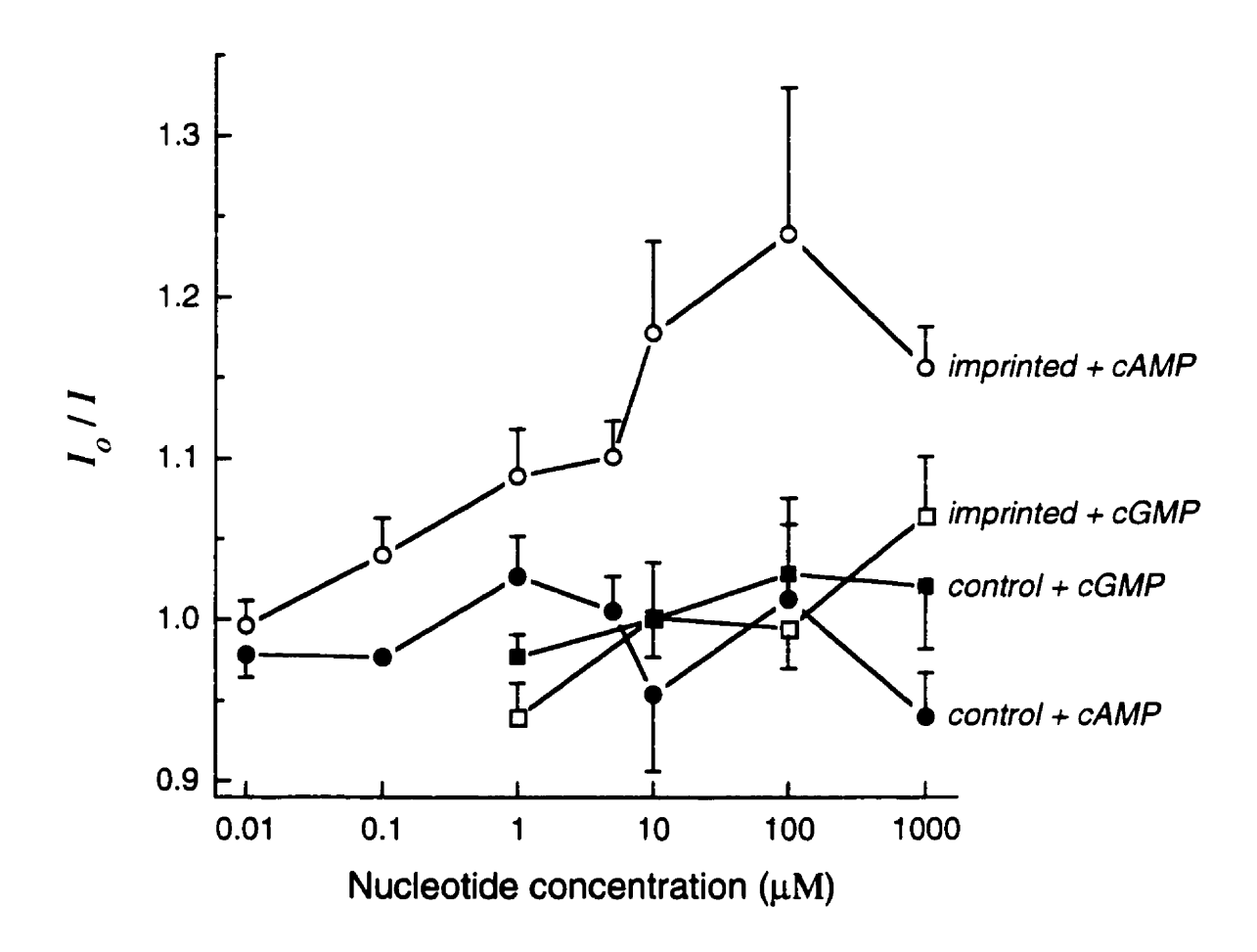


Figure 5.3. (A) The fluorescence of the control and imprinted polymers in the presence of various concentrations of cAMP and cGMP. Data were collected between 90 and 135 min after incubation with ligand. I_o and I are the fluorescence intensities of the polymers in the absence and presence of nucleotide, respectively. The data for cAMP are means \pm standard error for concentrations of 1000 (n = 6) and 100 - 1.0 (n = 3) μ M, and means \pm range for concentrations of 0.1 (n = 2) and 0.01 (n = 2) μ M. The data for cGMP are means \pm standard error for concentrations of 1000 (n = 7), 10 (n=4), 100 and 1.0 (n = 3) μ M. For the sake of clarity, the error bars are only shown one side, however they also exist on the other. Excitation wavelength, 469 nm; emission wavelength, ~595 nm.

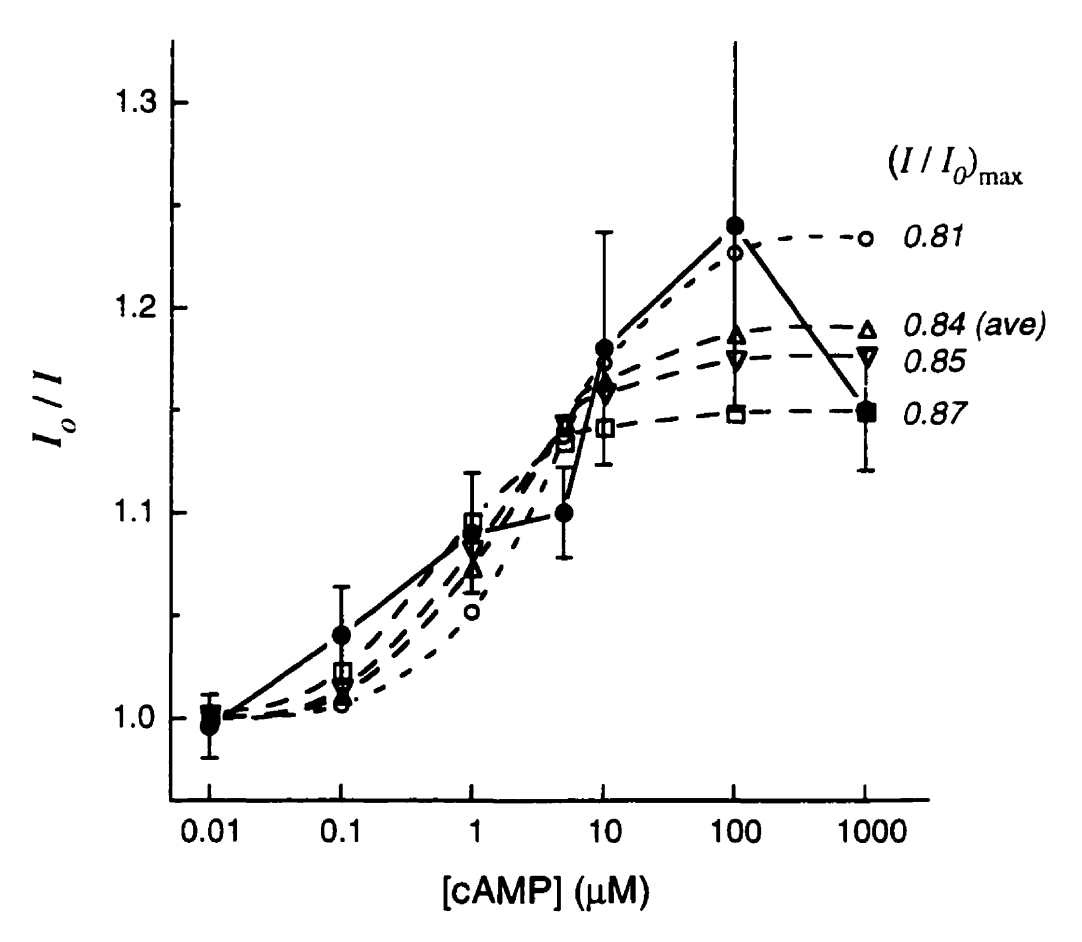


Figure 5.3. (B) The fluorescence of the imprinted polymer in the presence of various concentrations of cAMP. The dashed lines represent the curve fits following equation 2 through the data for $(I/I_o)_{\text{max}}$ values (i.e. k_{np}/k_p values) of 0.81, 0.85 and 0.87, and their average 0.84. See caption to Figure 5.3a for details.

monomer composition, differences in the quenching behavior are likely due to the imprinting effect. The saturation of the response of the imprinted polymer to cAMP suggests that this response is due to the interaction of cAMP with a limited number of specific binding sites rather than to nonspecific sites on the polymer.

To assess the selectivity of the cAMP-imprinted polymer, the effects of the structurally related molecule, cGMP, on polymer fluorescence were examined (Fig. 5.3a). In contrast to cAMP, cGMP concentrations between 1 and 1000 μ M induced relatively little change in the fluorescence of both the imprinted and the control polymer. In all cases, the value for I_0/I did not differ greatly from 1.0, although there was a considerable degree of variability in the results possibly due to the relatively large size and size distribution of the polymer particles. The use of smaller particles would probably have improved the reproducibility of the results. The ability of the imprinted polymer to discriminate between cAMP and cGMP is unlikely to be due to changes in pH, ionic strength or counter ions, since solutions containing equal amounts of cAMP and cGMP had similar pH values, and since both were present as sodium salts.

An estimate of the association constant $(K_a = [NP]/[N][P])$ for the association of cAMP (N) with the imprinted polymer (P)

$$N + P \rightleftharpoons NP$$
 (1)

was obtained from the equation (Connors, 1987)

$$\frac{I_o}{I} = \frac{1 + K_a[N]}{1 + (k_{np}/k_p)K_a[N]}$$
 (2).

Fluorescence intensity, I is proportional to concentration according to $I = 2.3I_o \Phi \varepsilon bc$, where I_o is the intensity of the excitation source, ε is the molar absorptivity at the

excitation wavelength, b is the path length, c is the molar concentration, and Φ is the fluorescence quantum yield. k_{np} and k_p are then proportionality constants which relate the intensities of the cAMP-polymer complex and the polymer, respectively, to their concentrations, and thus include the term $2.3I_o\Phi\epsilon b$. Since the data in Figure 5.3 were collected using exactly the same experimental conditions, the value of k_{np}/k_p may be approximated by Φ_{np}/Φ_p , assuming that the molar extinction coefficients of the polymer and the cAMP-polymer complex are the same. Oster estimated the value of k_{np}/k_p from $(l/l_o)_{max}$ (Oster, 1951). Due to the variability in the results, k_{np}/k_p values of 0.81, 0.85 and 0.87, as well as their average, 0.84, were chosen from the data in Figure 5.3b. Using SigmaPlot curve fitter, the data for the imprinted polymer in the presence of cAMP (Fig. 5.3b) were fit directly to equation 2, and the K_a values obtained using the various k_{np}/k_p are presented in Table 5.1. As the k_{np}/k_p value increases (i.e. the saturation point in Figure

Table 5.1. Association (K_a) constants for the imprinted polymer with cAMP obtained using various k_{np}/k_p values in equation 2.

| k_{np}/k_{p}^{a} | $K_a(M^{-1})$ | | |
|--------------------|-----------------------------|--|--|
| 0.81 | $3.5 \pm 1.7 \times 10^{5}$ | | |
| 0.85 | $10 \pm 6.62 \times 10^{5}$ | | |
| 0.87 | $21\pm21\times10^{5}$ | | |
| 0.84 | $7.4 \pm 4.2 \times 10^{5}$ | | |

[&]quot; estimated from $(I/I_a)_{max}$ in Figure 5.3b.

^b average of 0.81, 0.85 and 0.87.

5.3b decreases) from 0.81 to 0.87, the association constant increases 6 fold. Alternatively, an approximation of the association constant may also be obtained by estimating the concentration of cAMP which induces a half-maximal response [i.e. the dissociation constant $(K_d) = 1/K_a$] from the graph in Fig. 5.3. By this method, a value for the dissociation constant of 6.0×10^{-6} M $(K_a = 1.7 \times 10^5 \text{ M}^{-1})$ was obtained. Due to the large variability in the data between 10 and 1000 μ M for the imprinted polymer with cAMP it is possible that the data is not reliable above 10 μ M.

During the preorganization process, prior to the formation of the polymer, there may be different interaction patterns between the template and the functional monomers (Mosbach and Ramström, 1996; Ansell et al., 1996) because of the relatively low association constant between 1 and cAMP ($K_a = 13.8 \text{ M}^{-1}$) (Turkewitsch et al., 1998) in aqueous solution, and the highly polar solvent used in the imprinting protocol. This may result in the formation of different recognition sites for cAMP in the polymer, and thus the apparent association constant calculated represents an average affinity of the polymer receptor site population.

The ability of the cAMP-imprinted polymer to distinguish between cAMP and the structurally similar cGMP suggests that cAMP is interacting with specific cAMP-imprinted sites in the polymer. cAMP and cGMP differ only in the substituents on their purine base moiety: the adenine base of cAMP contains an NH₂ group at the C6 position, whereas in the guanine base of cGMP the C6 is carboxylated and the C2 is substituted with an NH₂ group.

This suggests that the binding of cAMP to the recognition sites on the polymer is based not only on an electrostatic interaction involving the cyclic phosphate group, but also on interactions with the aromatic base unit of the nucleotide, possibly through aryl stacking (Turkewitsch et al., 1996; Turkewitsch et al., 1998) or hydrogen bonding. This supports the concept that noncovalently imprinted polymers are highly sensitive to the nature and orientation of the functional groups of the ligand binding species, due to the precise localization of complementary functional groups in the polymer binding sites (Kriz et al., 1997; Mayes et al., 1994; Muldoon and Stanker, 1996; Steinke et al., 1995; Wulff, 1995). Studies have suggested that shape-selective cavities also contribute to the binding of template molecules to their imprinted polymers, particularly in the case of aromatic molecules (Dunkin et al., 1993; Kriz et al., 1997; Steinke et al., 1995; Steinke et al., 1996). The much higher affinity of the imprinted polymer for cAMP ($K_a = 3.5 \pm 1.7 \times 10^5$ M¹), compared to that which we (Turkewitsch et al., 1998) recently found for 1 with cAMP ($K_a = 13.8 \text{ M}^{-1}$) in aqueous solution, also suggests that the three-dimensional network of the polymer enabled recognition of the size and shape of the template molecule. Thus, molecular imprint recognition of the template molecule may be attributed to the precise spatial orientation of the functional groups in the cavity complementary to the groups on the ligand, as well as to the size and shape of the binding cavity (Kriz et al., 1997; Mayes et al., 1994; Muldoon and Stanker, 1996; Steinke et al., 1995; Wulff, 1995). Further studies examining the effects of a variety of related purine and pyrimidine nucleotides would be required to further explore the structural requirements of the cAMP binding sites in the polymer.

It has only very recently been demonstrated that MIPs show selective ligand binding in aqueous media under conditions compatible with biological systems (Ansell et al., 1996; Andersson et al., 1995; Mathew and Buchardt, 1995; Kugimiya et al., 1996). It is much more difficult to demonstrate specific binding of ligands in aqueous media compared to organic solvents since substitution of water for organic solvents dramatically alters the relative importance of polar and hydrophobic interactions between MIPs and analytes. Water molecules strongly interfere with polar interactions, such as hydrogen bonding, whereas hydrophobic effects are enhanced in water. Thus, until recently, organic solvents have been used exclusively as the media for studies on the binding of ligands to MIPs.

The affinity of the cAMP-imprinted polymer for its original template molecule is similar to those of other MIPs (Table 5.2), despite differences in the method of estimating K_a and the solvent employed. A polymer complement to the nucleotide base, 9-ethyladenine, displayed an association constant of 79,000 M^{-1} in chloroform from binding studies carried out by a batch procedure (Shea et al., 1993). Chromatographic data obtained in chloroform and aqueous KH_2PO_a /acetonitrile (3:7, pH = 4.5) revealed that polymers imprinted with 9-ethyladenine retained adenine bases in preference to other purine or pyrimidine bases. A competitive radioligand binding assay, termed Molecularly Imprinted sorbent Assay (MIA), has shown binding site populations with

Table 5.2. Association constants (K_a) for various molecularly imprinted polymers.

| template molecule | assay solvent | $K_{a}(\mathbf{M}^{1})$ |
|-----------------------------|--------------------------|-------------------------|
| cAMP | water | 3.5×10^{5} |
| 9-ethyladenine ⁴ | chloroform | 7.9×10^4 |
| adenine' | water | 4.3×10^{3} |
| theophylline | acetonitrile/acetic acid | 2.9×10^{6d} |
| • • | | 1.5×10^4 |
| diazepam ^c | toluene/heptane | 5.6×10^{7} |
| | | 43×10^4 |
| | | 1.7×10^4 |
| morphine ^f | toluene/acetic acid | 1.1×10^{7} |
| | | 1.1×10^{5} |
| | 20mM sodium citrate | 83×10^{4} |
| | (pH 6.0); 10% ethanol | 4.2 × 10 ⁴ |

[&]quot; Shea et al., 1993.

^b Mathew and Buchardt, 1995.

^{&#}x27;Vlatakis et al., 1993.

^d K_a values for the ophylline are associated with site population densities of 0.016 and 1.3 μmol/g of polymer, respectively.

 K_a values for diazepam are associated with site population densities of 0.0062, 0.17 and 1.2 μ mol/g of polymer, respectively.

^{&#}x27;Andersson et al., 1995.

 $^{^{4}}$ K_a values for morphine in organic solvent are associated with site population densities of 1.2 and 39 μ mol/g of polymer, respectively.

 $^{^{}h}$ K_a values for morphine in aqueous solution are associated with site population densities of 0.78 and 6.9 μ mol/g of polymer, respectively.

affinities in the 10⁷ - 10⁴ M¹ range for theophylline and diazepam MIPs in organic solvents (Vlatakis et al., 1993). When these antitheophylline and antidiazepam imprints were tested in competitive assays, recognition of closely related structures was either nonexistent or far below that of the original template molecule. An approach similar to ours was reported by Cooper et al. (Cooper et al., 1997) who investigated the interaction between cholesterol and a fluorescent cholesterol-imprinted polymer in organic media. However, this was not successful, since the fluorescence of the resultant MIP was not responsive to cholesterol. This study differed from ours in that the cholesterol used to imprint the polymer was covalently linked to the fluorescent functional monomer.

Several groups have demonstrated excellent binding affinity and selectivity of MIPs in aqueous systems (Table 5.2). An adenine-imprinted polymer displayed an association constant of 4,300 M⁻¹ for the binding of adenine in aqueous solution determined from a batch binding procedure (Mathew and Buchardt, 1995). Competitive radioligand binding studies revealed high affinity binding of ligands to antimorphine imprints in aqueous media and organic solvents (Andersson et al., 1995). The selectivities of these MIPs were similar to those of antibodies in both solvents. Piletskii et al. (Piletskii et al., 1990) reported that an ATP-imprinted methacrylate polymer was capable of chromatographically separating ATP from AMP and ADP when aqueous buffer was used as an eluent. Selective transport of adenine through a polymeric membrane imprinted with 9-ethyladenine was also demonstrated by measuring the concentration of adenine by HPLC in the receiving side of an two-compartment cell separated by the imprinted membrane as a function of time (Mathew-Krotz and Shea, 1996). Adenine was found to be transported at a higher rate than thymine from an equimolar methanol

solution of adenine and thymine. This selective transport reportedly resulted from a process that involved reversible complexation and exchange between adenine and the adenine-selective binding sites in the polymer membrane, creating a pathway for transport. Similarly, selective permeability of AMP in aqueous solution through a polymeric AMP-imprinted membrane was demonstrated by measuring the ion current across the membrane (Piletsky et al., 1994).

Recently, we (Turkewitsch et al., 1996; Turkewitsch et al., 1998) found that, in contrast to the decrease in fluorescence intensity of the imprinted polymer in the presence of cAMP observed in present results, 1 displays a dramatic enhancement in fluorescence intensity and quantum yield in the presence cAMP and other purine nucleotides. The environment of 1 would be much more restricted in the polymer due to its presence in the polymer matrix, which could affect its conformation and charge distribution. The restricted environment of dye in this state could result in an increase in its quantum yield compared to that in aqueous solution in the absence of nucleotides (Loutfy, 1986). Thus, the state of the dye in the polymer with which cAMP interacts could be quite different from that in aqueous solution, possibly resulting in differences in the effect of cAMP on its quantum yield.

Finally, an interesting feature of the fluorescent MIP is its ability to be reused. This stability has also been reported for a fluorescent imprinted polymer for sialic acid (Piletsky et al., 1996), as well as for other MIPs (Fischer et al., 1991; Kempe and Mosbach, 1994). After synthesizing the imprinted and control polymers, each was washed prior to the first binding experiment. This wash step is referred to as the first template extraction. The polymers were then washed a second time (second template

extraction) following the first binding experiment, prior to use in a second binding experiment. Table 5.3 presents the fluorescence responses (I/I) of the imprinted polymer to cAMP (1000, 1 and 0.01 μ M) and cGMP (1000 μ M) after the first and second template extractions. The results suggest that it is possible to remove nucleotide bound to the polymer as a result the first binding experiment, by washing the polymer a second time, and to obtain similar binding results when used in a second binding experiment.

Table 5.3. The fluorescence responses (I_d/I) of the imprinted polymer to cAMP and cGMP after the first and second template extractions. The data are from single experiments unless otherwise indicated.

| nucleotide | conen (µM) | I/I (1stemplate extraction) | I/I (2 nd template extraction) |
|------------|------------|-----------------------------|---|
| cAMP | 1000 | $1.14 \pm 0.03^{\circ}$ | 1.22 |
| | 1.0 | 1.07 ± 0.04^d | 1.13 |
| | 0.01 | 0.98 | 1.01 |
| cGMP | 1000 | 1.07 ± 0.05^d | 1.12 ± 0.14^d |

^a first template extraction refers to the washing step performed after synthesizing the polymers, prior to the first binding experiment. See Results and Discussion for details. ^b second template extraction refers to the washing step performed after the first binding experiment, prior to the second binding experiment. See Results and Discussion for details.

[°] data are means \pm standard error (n = 6).

^d data are means \pm range (n = 2).

5.4 Conclusions

Fluorescent template-selective sites for cAMP, prepared in methacrylate polymer, display high affinity and selectivity for aqueous cAMP. This affinity and selectivity for cAMP in aqueous solution is comparable to those of other MIPs, despite differences in the method of estimating K_a and the solvent employed. This fluorescent molecularly imprinted polymer chemosensor containing both the recognition element and the measuring element for the fluorescent detection of cAMP may serve as a starting point in the design of highly effective synthetic fluorescent sensors for this important biological molecule.

5.5 Acknowledgments

This work was supported by the Respiratory Health Network of Centers of Excellence and the J. T. Costello Memorial Research Fund. P. Turkewitsch was supported by a studentship award from the Canadian Cystic Fibrosis Foundation. We thank Dr. B. Lennox, Dr. W. Galley, and Dr. P. Hurst for stimulating and helpful discussions. We would also like to acknowledge the contributions of the late Dr. Seymour Heisler.

5.6 References

- Andersson, L.I.; Müller, R.; Vlatakis, G.; Mosbach, K. *Proc. Natl. Acad. Sci. USA* 1995, 92, 4788-4792.
- Andersson, L.I.; Nicholls, I.A.; Mosbach, K.H. In Highly Selective Separations in Biotechnology; Street, G., Ed.; Blackie: New York, 1994; p 206-224.
- Ansell, R.J.; Ramström, O.; Mosbach, K. Clin. Chem. 1996, 42, 1506-1512.
- Brooker, G.; Harper, J.F.; Terasaki, W.L.; Moylan, R.D. In Advances in Cyclic

 Nucleotide Research, Vol 10; Brooker, G., Greengard, T., Robison, G.A., Eds.; Raven

 Press: New York, 1979; p 1-33.
- Connors, K.A. Binding Constants; John Wiley and Sons: Toronto, 1987; p 341.
- Cooper, M.E.; Hoag, B.P.; Gin, D.L. Polymer Prepr. 1997, 38, 209-210.
- Czarnik, A.W. In Fluorescent Chemosensors for Ion and Molecule Recognition; Czarnik, A.W., Ed.; ACS Symposium Series 538; American Chemical Society: Washington, DC, 1993.
- Darnell, J.G.; Lodish, H.; Baltimore, D. *Molecular Cell Biology*, 3rd ed.; Scientific American Books: New York, 1994.
- Dunkin, I.R.; Lenfeld, J.; Sherrington, D. C. Polymer 1993, 34, 77-84.
- Fischer, L.; Müller, R.; Ekberg, B; Mosbach, K. J. Am. Chem. Soc. 1991, 113, 9358-9360.
- Kempe, M.; Mosbach, K. J. Chromatogr., A 1994, 664, 276-279.
- Kempe, M.; Mosbach, K. Tetrahedron Lett. 1995, 36, 3563-3566.
- Kriz, D.; Ramström, O.; Mosbach, K. Anal. Chem. 1997, 69, 345A-349A.
- Kriz, D.; Ramström, O.; Svensson, A.; Mosbach, K. Anal. Chem. 1995, 67, 2142-2144.

Kugimiya, A.; Takeuchi, T.; Matsui, J.; Ikebukuro, K.; Yano, K.; Karube, I. Anal. Lett. 1996, 29, 1099-1107.

Lakowicz, J.R. Principles of Fluorescence Spectroscopy; Plenum: New York, 1983.

Loutfy, R.O. Pure Appl. Chem. 1986, 58, 1239-1248.

Mathew, J.; Buchardt, O. Bioconjugate Chem. 1995, 6, 524-528.

Mathew-Krotz, J.; Shea, K.J. J. Am. Chem. Soc. 1996, 118, 8154-8155.

Mayes, A.G.; Andersson, L.I.; Mosbach, K. Anal. Biochem. 1994, 222, 483-488.

Mosbach, K.; Ramström, O. Biotechnology 1996, 14, 163-170.

Muldoon, M.T.; Stanker, L.H. Chem. Ind. 1996, 6, 204-207.

Oster, G. Trans. Faraday Soc. 1951, 47, 660-666.

Piletskii, S.A.; Fedoryak, D.M.; Kukhar, V.P. Dokl. Akad. Nauk Ukr. SSR Ser. B 1990, 4, 53-54; Chem. Abstr. 1991, 114, 165457q.

Piletsky, S.A.; Parhometz, Yu.P.; Lavryk, N.V.; Panasyuk, T.L.; Elískaya, A.V. Sens. Actuators B 1994, 18-19, 629-631.

Piletsky, S.A.; Piletskaya, E.V.; Yano, K.; Kugimiya, A.; Elgersma, A.V.; Levi, R.; Kahlow, U.; Takeuchi, T.; Karube, I.; Panasyuk, T.I.; Elískaya, A. V. Anal. Lett. 1996, 29, 157-170.

Piletsky, S.A.; Piletskaya, E.V.; Elískaya, A. V.; Levi, R.; Yano, K.; Karube, I. Anal. Lett. 1997, 30, 445-455.

Shea, K.J.; Spivak, D.A.; Sellergren, B. J. Am. Chem. Soc. 1993, 115, 3368-3369.

Steinke, J.; Sherrington, D.C.; Dunkin, I.R. Adv. Polym. Sci. 1995, 123, 81-125.

Steinke, J.H.G.; Dunkin, I.R.; Sherrington, D.C. Macromolecules 1996, 29, 407-415.

- Tsien, R. Y. In Fluorescent Chemosensors for Ion and Molecule Recognition; Czarnik, A.W., Ed.; ACS Symposium Series 538; American Chemical Society: Washington, DC, 1993; p 130-146.
- Turkewitsch, P.; Wandelt, B.; Darling, G.D.; Powell, W.S. J. Photochem. Photobiol., A: Chem. 1998, in press.
- Turkewitsch, P.; Wandelt, B.; Ganju, R.R.; Darling, G.D.; Powell, W.S. Chem. Phys. Lett. 1996, 260, 142-146.
- Vlatakis, G.; Andersson, L.I.; Müller, R.; Mosbach, K. Nature 1993, 361, 645-647.
- Wulff, G. Angew. Chem. Int. Ed. Engl. 1995, 34, 1812-1832.
- Wulff, G. EXS 1997, 80 (Frontiers in Biosensorics 1 Fundamental Aspects), 13-26.

CHAPTER 6

Final Discussion and Conclusions

Final Discussion and Conclusions

Two new cationic fluorescent dyes were synthesized, trans-4-(p-N,N-dimethylaminostyryl)-N-vinylbenzylpyridinium chloride (1) and trans-4-(p-N,N-dimethylaminostyryl)-N-phenethylpyridinium bromide (2). The NMR spectra of trans-4-(p-N,N-dimethylaminostyryl)-N-vinylbenzylpyridinium chloride revealed that it was a 70:30 mixture of trans-4-(p-N,N-dimethylaminostyryl)-N-m-vinylbenzyl-pyridinium chloride and trans-4-(p-N,N-dimethylaminostyryl)-N-p-vinylbenzylpyridinium chloride (Figure 3B.2 in Appendix 3, Section B). It also suggested that there were no major contaminants in product 1. Likewise, the NMR spectrum for dye 2 also suggested that no major impurities were present. However, the presence of a small amount of impurity which could not be detected by NMR or TLC in dye 1 or dye 2 cannot be ruled out. Contamination from other ions, such as iodide, was also not verified, although precautions were taken to avoid this.

Since 1 is a mixture of meta and para isomers, the interpretation of the results is complicated, because it is possible that each isomer could contribute differently to the absorption and emission spectra. This casts a level of uncertainty on the data and interpretation presented in this thesis. However, because the vinylbenzyl group in 1 is not in conjugation with the remainder of the molecule (i.e. the *trans-4-(p-N,N-dimethylaminostyryl)*)pyridinium portion), and is thus separated from the part of the molecule giving rise to the fluorescence, it probably does not contribute to a large degree to the fluorescence of 1. This argument is supported by the fact that the fluorescence spectra of dye 1 and dye 2, which differs from 1 only in the substituent on the pyridinium nitrogen (vinylbenzyl in the case of 1, and phenethyl in the case of 2), are similar (Figure

3B.1 in Appendix 3, Section B). Further, the magnitude of the fluorescence enhancements of the dyes, and the red shifts of their emission maxima, to increasing concentrations of cAMP between 1 and 50 mM (Appendix 3, Section E) are also similar. Biological macromolecules also induce similar fluorescence quantum yield increases in dyes 1 and 2 (Figure 4.2 in Chapter 4). The association constants for dyes 1 and 2 with cAMP ($K_{rq} \sim 16 \text{ M}^{-1}$), and with nondenatured BSA ($K_{rq} \sim 10^4 \text{ M}^{-1}$), are, as well, almost identical. These results suggest that the substituent of the pyridinium nitrogen has relatively little effect on the fluorescence of the dyes, and on their ability to respond to the presence of analytes. Furthermore, since the association constants for 1 and 2 with cAMP, as well as with nondenatured BSA, are almost identical, the involvement of vinylbenzyl and phenethyl substituents in the interaction of 1 and 2 with these analytes is probably minor. These results also raise the possibility that the *meta* and *para*vinylbenzyl isomers in 1 have relatively little effect on the fluorescence properties and the fluorescence response of this dye.

Fluorescence studies of 1 in aqueous solution revealed both dual excitation and dual emission. Dye 1 was also found to exhibit a large change in its dipole moment upon excitation (Turkewitsch et al., 1998c). These results, together with the results of our previous investigation (Wandelt et al., 1995) of dye 2 in aqueous solution which could be explained by a TICT process, raised the possibility that dye 1 may also be of TICT nature. However, as discussed in Chapter 3, the possibility that the emission band of 1 at 502 nm obtained by exciting at 360 nm is the result of an artifact or impurity cannot be ruled out.

The fluorescence behavior of dyes 1 and 2 was investigated in the presence of

various nucleotides and related biomolecules. Upon exciting at 469 nm, dye 1 displayed marked fluorescence enhancements in a TICT-type emission band centered at 608 nm, with slight red-shifts of the λ_{max} in the presence of cAMP and cGMP in unbuffered water (Turkewitsch et al., 1996). Slight hyperchromic and bathochromic effects were also observed in the absorbance of 1. These results suggest that 1 preferentially associates with the cyclic nucleotides. Equilibrium association constants (K_{eq}) of 14.0 and 9.31 M⁻¹ were obtained for cAMP and cGMP, respectively, from their concentration-dependent fluorescence enhancements.

Spectral patterns similar to those in unbuffered water were observed for dye 1 in the presence of cAMP and cGMP in phosphate buffer (pH 7.2) (Turkewitsch et al., 1998c). The enhancements in the fluorescence of 1 induced by cAMP and cGMP were of similar magnitude, and were somewhat greater than those observed in unbuffered water. This more detailed study further revealed that purine nucleotides with uncyclized phosphate groups (AMP, ADP and ATP) and adenosine induced fluorescence quantum yield enhancements in 1 that were of lesser magnitude than those induced by the cyclic nucleotides. In contrast, the pyrimidine nucleotides, CMP and UMP, had almost no effect on the fluorescence of 1. These results indicate that dye 1 displays a specificity for purine over pyrimidine analytes.

Among the purine nucleotides, cAMP ($K_{eq} = 13.8 \text{ M}^{\circ}$) displayed the highest equilibrium association constant in phosphate buffer (pH 7.2), and cGMP the lowest ($K_{eq} = 2.67 \text{ M}^{\circ}$). The affinity of cGMP for 1 in buffer is somewhat smaller than that in unbuffered water, largely because cGMP is capable of inducing a greater maximal increase in the fluorescence quantum yield of 1 in buffer ($\Phi_{c} = 0.099$) than in unbuffered

water ($\Phi_c = 0.031$). The affinity of cAMP remains more or less constant on moving from unbuffered water to phosphate buffer. In phosphate buffer, affinities less than that of cAMP were observed for the nucleotides possessing uncyclized phosphate groups (AMP $K_{eq} = 3.81$, ADP $K_{eq} = 10.1$ and ATP $K_{eq} = 8.08$ M⁻¹), as well as for adenosine (K_{eq} to 0.54 M⁻¹) and adenine ($K_{eq} = 0.15$ M⁻¹). These association constants were not influenced to a large extent by pH.

The results above suggest that the fluorescence enhancements in 1 induced by the purine nucleotides require the presence of a purine base, and are enhanced by ribose and phosphate moieties. However, high concentrations (5 mM) of the purine analytes are required to induce these changes, because of their low association constants for 1 (i.e. in the order of 10 M¹). Thus, although the fluorescence enhancements in 1 induced by the purine analytes differ, the ability of 1 to distinguish between the different purine analytes is somewhat limited since the differences among their low association constants are relatively small.

In chapter 2, we explained the fluorescence quantum yield increase of dye 1 in the presence of cAMP and cGMP using a TICT mechanism. Briefly, we suggested that an increase in polarity of the environment in the presence of these analytes stabilized the large dipole moment of the TICT-type excited state of 1, lowering its energy, and causing an increase in quantum yield of the TICT-type emission of 1, and a shift of it emission maximum to the red. However, upon examining the literature describing closely related molecules more thoroughly, we now believe that the increase in fluorescence quantum yield of 1 in the presence of cAMP, cGMP and other purine analytes is probably due to a decrease in the nonradiative decay rate

of 1 is most likely caused by a restriction of the rotation around the ethylenic double bond of 1 in the excited state (a motion associated with *trans-cis* photoisomerization) upon binding to the analytes.

The association of 1 with the purine analytes probably involves simultaneous aryl stacking and electrostatic interactions. Various other fluorescent chemosensors for nucleotides involving aryl stacking and electrostatic interactions have been reported. They differ from dye 1 in that they all contain combinations of suitable binding groups arranged to form a somewhat inflexible three-dimensional pocket into which the nucleotides fit. Dye 1 does not possess such a pocket. As a result, these fluorescent chemosensors display a stronger binding for their ligands than does dye 1. A fluorescent chemosensor consisting of positively charged diazapyrenium units linked by a spacer displayed association constants of 1220, 1005 and 740 M⁻¹ for ATP, ADP and AMP, respectively, in neutral aqueous solution (Coudret and Harriman, 1992). In another study, association constants of $\log K_a = 5.1, 5.0, \text{ and } 4.1 \text{ were determined for the binding of }$ ATP, ADP, and AMP in organic media (pyridine-deuterated trifluoroacetic acid buffer, pH 6.0) to a fluorescent chemosensor containing two napthalene groups held apart at a specific distance by two spacer arms (Dhaenens et al., 1993). Finally, Kato's nonfluorescent cleft-like molecule designed for cAMP displayed equilibrium association constants of 600 and 320 M⁻¹ for 3':5'-cAMP in 10 mM cacodylate buffer at ionic strengths of 51 mM and 501 mM NaCl, respectively (Kato et al., 1994).

A further study revealed that dyes 1 and 2 displayed much greater fluorescence enhancements in the presence of DNA and RNA than individual nucleotides, suggesting that they interact more strongly with polynucleotides (Turkewitsch et al., 1998a). Based

on similarities in structure and spectral patterns of dyes 1 and 2 in the presence of DNA to the structurally-related minor groove binder, *trans*-4-[4-(dimethylamino)styryl]-1-methylpyridinium iodide (DSMI) (Kumar et al., 1993), we propose that the dyes may be binding to the minor groove of the DNA helix. The fluorescence enhancements of the dyes in the presence of DNA are likely due to a restriction on the rotation around the ethylenic double bond in the excited state, leading to decreased nonradiative decay rates and enhanced fluorescence yields, as suggested for DSMI. Dyes 1 and 2 were capable of detecting as low as 10 µg/mL of DNA by fluorescence. Lower detection limits for dsDNA are observed for the Hoechst dyes (10 ng/mL) (Labarca and Paigen, 1980), the TOTO series (0.5 ng/mL) (Glazer and Rye, 1992; Rye et al., 1993), and the PicoGreen assay (100 pg/mL) (Singer et al., 1997).

Proteins, such as bovine serum albumin and ovalbumin, also induced large fluorescence increases in dyes 1 and 2, whereas individual amino acids did not affect their fluorescence, suggesting that the dyes also associate with proteins (Turkewitsch et al., 1998a). These fluorescence enhancements were similar to those induced by DNA. Since denatured BSA induced a fluorescence increase in 2 about twice that of nondenatured BSA, dye 2 appears to be sensitive to protein conformation, and may be interacting with sequences of amino acids in the protein exposed by denaturation. Dyes 1 and 2 are capable of detecting as little as 10 µg/mL of protein in solution. However, they are considerably less sensitive than NanoOrange, which has a detection limit of 10 ng of protein/mL (Haugland, 1996).

We conclude that dye 1 would not be an effective chemosensor for cAMP as is, since its affinity and selectivity for cAMP is very low, most likely due to the lack of a

well-defined pocket into which cAMP may bind. Since the structure of dye 2 is very similar to dye 1, it is also likely that dye 2 would not be an effective chemosensor. A fluorescent chemosensor for solution measurements of cAMP would require an affinity of at least $10^9 \,\mathrm{M}^{-1}$ [i.e. a dissociation constant $(K_d) = 10^{-9} \,\mathrm{M}$] (Brooker et al., 1979), since the concentration of cAMP measured in solution is typically between 10^{-11} and $10^{-8} \,\mathrm{M}$. On the other hand, intracellular concentrations of cAMP typically vary from $10^{-9} \,\mathrm{M}$ in resting cells to $10^{-6} \,\mathrm{M}$ in stimulated cells (Tsien, 1993). A fluorescent chemosensor aimed at measuring the intracellular concentration of cAMP would, therefore, require an affinity of $\sim 10^7 \,\mathrm{M}^{-1} \,(K_d = 10^{-7} \,\mathrm{M})$.

In spite of the relatively low affinity of dye 1 for cAMP, the results presented are promising because of the large fluorescence enhancement in dye 1 induced by this cyclic nucleotide. This suggests that in combination with other molecular structures designed to provide enhanced affinity and specificity, this dye may be highly effective at detecting cAMP in aqueous solution. The environmentally-sensitive fluorescence of this family of dyes may, however, be useful for the fluorescence detection of low concentrations of DNA or proteins in solution, or for their fluorescence staining in electrophoretic gels. Their sensitivity to protein conformation may also make them useful for investigating protein structure and function.

Dyes 1 and 2 possess several features that make them attractive fluorescent chemosensors for potential biological applications, such as an intense absorption band in the visible region, and a long wavelength fluorescence emission. The single emission of dye 1 upon exciting at 469 nm and the dual fluorescence obtained by exciting at 360 nm, provide an opportunity for internal calibration by the ratioing of signals at two excitation

or two emission wavelengths, canceling out irrelevancies such as cell thickness, dye concentration, excitation intensity variations and detection efficiency (Czarnik, 1993). The fluorescence quantum yield responses of dye 1 to cAMP and other nucleotides show insignificant fluctuations in the physiological pH range of 6-8. In addition, an experiment with 2, revealed that it is capable of passively diffusing across the cell membrane, and that it does not interfere with the physiological functioning of cells (Appendix 3, Section F). Finally, it has also been demonstrated that this family of dyes is amenable to the synthesis of esterified membrane-permeant derivatives, and that such derivatives are capable of staining live microorganisms without affecting viability (Chan et al., 1996).

In an attempt to increase the recognition ability of dye 1 for cAMP we prepared recognition sites for cAMP that contain 1 in a polymer matrix by molecular imprinting (Turkewitsch et al., 1998b). As a integral part of the recognition cavity, dye 1 serves as both a recognition element and a measuring element for the fluorescence detection of cAMP. In aqueous media, cAMP binding caused a concentration-dependent quenching of the polymer fluorescence. In contrast, the structurally-related cGMP induced relatively little change in fluorescence. The limit of detection of the cAMP-imprinted polymer is approximately 0.1 μM. An association constant of ~ 10⁵ M⁻¹ was calculated for cAMP binding. This selectivity for cAMP over cGMP suggests that the binding of cAMP to the imprinted polymer sites involves not only an electrostatic interaction of the phosphate group, but also interactions with the aromatic purine base of the nucleotide, possibly through aryl stacking or hydrogen bonding. The affinity of the imprinted polymer for cAMP is much higher than that of dye 1 for cAMP in buffered aqueous solution, suggesting that the size and shape of cAMP was recognized by the three-dimensional

polymer network. The low affinity and selectivity of dye 1 for cAMP in solution could, therefore, be partially attributed to the lack of a well-defined cavity for cAMP, and partially due to the lack of the correct three-dimensional spatial arrangement of functional binding groups.

The association constant of the cAMP-imprinted polymer for cAMP is similar to those of other MIPs despite differences in the method of estimating K_a and the solvent employed. Binding studies performed by a batch procedure revealed an association constant of 79,000 M^1 for the binding of 9-ethyladenine to its MIP in chloroform (Shea et al., 1993), whereas the binding of adenine to its MIP displayed an association constant of 4,300 M^1 in aqueous solution (Mathew and Buchardt, 1995). A competitive radioligand binding assay in organic solvents was used to estimate affinities in the $10^7 - 10^4 M^1$ range for MIPs prepared against theophylline and diazepam (Vlatakis et al., 1993). Similar assays revealed association constants in the $10^4 M^1$ range for antimorphine imprints in aqueous solution, compared to association constants between 10^5 and $10^7 M^1$ in organic media (Andersson et al., 1995).

We have presented a novel design for recognition sites in imprinted polymers (Turkewitsch et al., 1998b). Molecular imprints containing a fluorescent dye that is able to interact with the template molecule and convert this recognition into a detectable fluorescence signal have not been previously reported. We have demonstrated that such molecular imprints may be prepared against cAMP, a molecule for which an MIP has not previously been prepared, and that cAMP binding to these recognition sites may be detected in aqueous solution by fluorescence. In a similar approach, Cooper et al., (Cooper et al., 1997) prepared a fluorescent cholesterol-imprinted polymer by covalently

linking a fluorescent functional monomer to cholesterol. However, they found that the fluorescence of this MIP was not responsive to cholesterol.

To be useful for measurement of cAMP in solution, or as a substitute for antibodies or enzymes in bioassays, the affinity of the cAMP-imprinted polymer for cAMP would have to be increased by two to three orders of magnitude. Once optimized, our approach could be extended to cover a wide variety of biologically important molecules. We conclude that our approach for preparing recognition sites with a built-in fluorescence detection element is very promising, and serves as a starting point for the development of highly effective biomimetic sensors for biologically important molecules.

We have presented two different approaches for measuring the concentration of an analyte in solution. One approach uses a soluble fluorescent molecule to recognize and detect analytes in solution, whereas the other uses an insoluble recognition site created for the analyte in a polymer matrix. Achieving efficient recognition (i.e. high affinity and selectivity) of an analyte with the soluble fluorescent chemosensor requires the proper positioning of functional groups complementary to the substrate in a well-defined cavity into which the analyte may fit. This often involves substantial effort and elaborate organic synthesis. This work has demonstrated that the affinity of a soluble fluorescent chemosensor for a ligand may be increased by preparing a polymer with the fluorescent chemosensor-ligand complex, such that recognition sites containing the fluorophore are created for the ligand in a polymer matrix. The preparation of an MIP may often offer a simpler synthetic scheme, since functional monomers are merely polymerized around a template molecule, capturing its molecular shape in a cavity.

The possibility of preparing cell membrane-permeant derivatives that enter a cell

by simple passive diffusion across the cell membrane, is a distinct advantage of a soluble fluorescent chemosensor, since this avoids the damage to the cell membrane that often occurs with microinjection. However, the elaborate multimodular structures required to achieve efficient recognition (i.e. high affinity and specificity) of an analyte may not be membrane permeant, or amenable to the synthesis of membrane-permeant derivatives, and may, therefore, have to be introduced into a cell by microinjection or liposome fusion, as would be the case with MIPs.

Even though the design of soluble chemosensors is time-consuming, and often involves substantial effort and long organic synthesis, the tools with which to carry out this work are available and the basic chemical principles are understood. On the other hand, the technology of molecular imprinting is still in its infancy, and a great deal more basic research is required before the optimal fluorescent MIP chemosensor may be obtained. However, by gaining a better understanding of molecular imprinting, we are investing in the future of science, and since there is such a need for good fluorescent chemosensors in many areas of science, each approach, with its particular virtues and foibles, is welcomed.

Future directions

The efficient recognition of small organic molecules requires a more or less rigid cavity or cleft into which the ligand may fit (Lehn, 1995). This cavity should have a size and shape to match the ligand, as well as the correct spatial arrangement of multiple complementary functional groups. Given this, the low affinity and selectivity of dye 1 for cAMP in solution may be augmented by combining 1 with additional molecular structures bearing functional groups complementary to cAMP. Structural and interactional complementarity may then be obtained by arranging these molecular components in a three-dimensional array to create a pocket for cAMP. We envision using the imide functionality, such as found in thymine or uracil, to provide an additional point of interaction with the adenine base of cAMP through hydrogen bonding, akin to the complementary base-pairings found in the DNA double helix. Such an imide moiety was used by Kato et al. (Kato et al., 1994) in the design of a nonfluorescent chemosensor for cAMP.

To achieve a well-defined geometry of molecular components within the supermolecule in which conformational freedom is minimized, macrocyclic cyclodextrins or crown ethers could be used, since they provide rigid building blocks onto which the molecular components may be attached. The steroid nucleus may also serve as a scaffolding, since its inflexible structure also contains functionalities for appending ligand recognition elements. A cyclodextrin with positively charged amino groups attached to its lower rim bound adenine nucleotides (5'-AMP $K_a = 1 \times 10^5 \,\mathrm{M}^{-1}$) inside its hydrophobic cavity more strongly than other purine (5'-GMP $K_a = 4 \times 10^4 \,\mathrm{M}^{-1}$) or pyrimidine (5'-CMP $K_a = 2 \times 10^4 \,\mathrm{M}^{-1}$) nucleotides in water (Eliseev and Schneider, 1993).

The highest affinity was observed for 5'-ATP ($K_a = 3 \times 10^6 \,\mathrm{M}^{-1}$), although ribose-5phosphate was also found to bind strongly $(K_a = 9 \times 10^5 \text{ M}^{-1})$. A fluorescent chemosensor for cAMP may, therefore, be constructed by attaching fluorescent positively charged dye 1 (with or without extra amino groups) to the lower rim of a cyclodextrin cavity to which the negatively charged phosphate group of cAMP may bind, and an imide containing moiety, such as thymine or uracil, to the upper rim of the cavity to which the adenine base of cAMP may bind by hydrogen bonding interactions (Figure 6.1). With the additional point of interaction provided by the imide moiety, and through the proper positioning of the binding groups within the cyclodextrin cavity, it may be possible to achieve selectivity for cAMP over other nucleotides. Alternatively, dye 1 and an imidecontaining moiety may also be arranged on the rigid steroid backbone so as to provide a pocket with high affinity and specificity for cAMP. Due to their elaborate structure, such fluorescent chemosensors may not be amenable to the design of cell membrane-permeant analogues, and therefore would have to be introduced into the cell by microinjection, similar to Tsien's (Adams et al., 1991) labeled protein kinase cAMP fluorosensor.

Future studies with the cAMP-imprinted polymer should first be aimed at reducing the degree of variability in the results. The broad distribution of rather large polymer particles (45-106 μ m) used in the study probably contributed to this variability. The use of smaller particles with a narrower distribution of particle size should improve the reproducibility of the results by decreasing the error in the measurement. It would be useful to investigate the binding of cAMP and cGMP under more relevant biological conditions, for example in phosphate buffer. The effects of other nucleotides and related analytes should also be examined to provide a better understanding of the specificity of

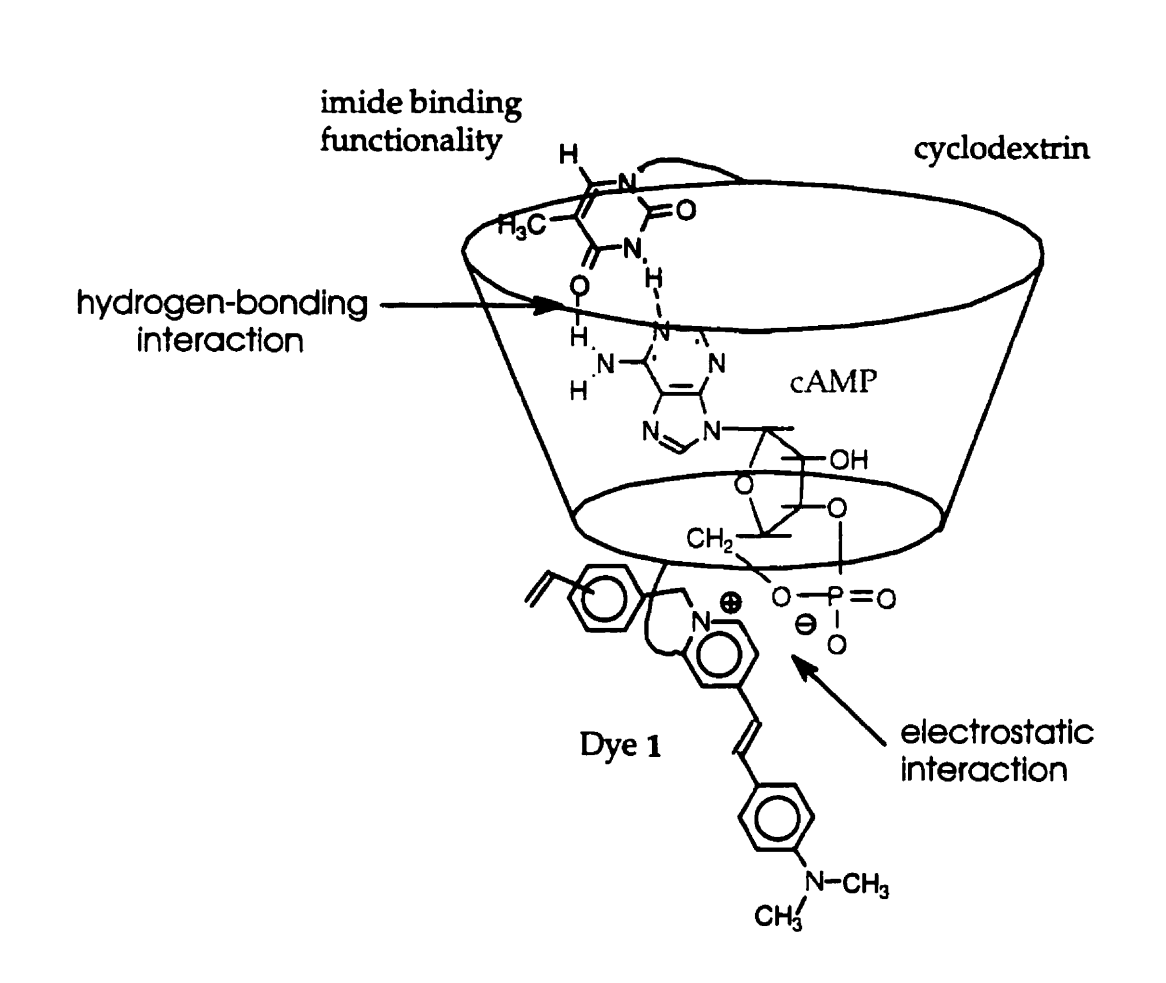


Figure 6.1. Schematic representation of a proposed fluorescent chemosensor for cAMP constructed using a cyclodextrin, dye 1 and an imide binding functionality.

the polymer. For instance, the binding of pyrimidine nucleotides to the control and imprinted polymers should be investigated, because even though they do not enhance the fluorescence of dye 1 in solution, they may bind to the polymers and quench the fluorescence.

Investigations on MIPs have shown that enhanced recognition of the template

molecule may be obtained by increasing the number of interactions between the template and the imprinted site (Steinke et al., 1995; Wulff, 1995). By providing an additional point of interaction with cAMP, the imide functionality may also be used to increase the affinity and specificity of the cAMP-imprinted polymer for cAMP. This functionality may be incorporated into the molecularly imprinted cavities for cAMP by synthesizing a polymerizable analogue. For example, a derivative of thymine or uracil containing a vinyl group could be used. The resultant fluorescent MIP would contain positively charged fluorescent dye 1 to which the negatively charged phosphate group of cAMP may bind by electrostatic interaction, and an imide functionality capable of hydrogen bonding with the adenine base of cAMP (Figure 6.2). Ultimately, such fluorescent MIPs for cAMP may be used to develop a fluorometric assay to quantitate cAMP in solution.

The possibility also exists of preparing fluorescent molecularly imprinted nanoparticles, which would be sufficiently small to permit microinjection inside living cells, and thus allow the fluorescence measurement of cAMP inside living cells.

Although the synthesis of molecularly imprinted nanoparticles has yet to be demonstrated, the synthesis of micron-sized spherical polymer particles has been accomplished by either grafting/coating the imprinted polymer onto preformed silica or trimethylolpropane trimethacrylate particles (Narrlöw, 1984; Glad, 1995), or by preparing beads through suspension or emulsion polymerization techniques (Mayes, 1996; Sellergren, 1994).

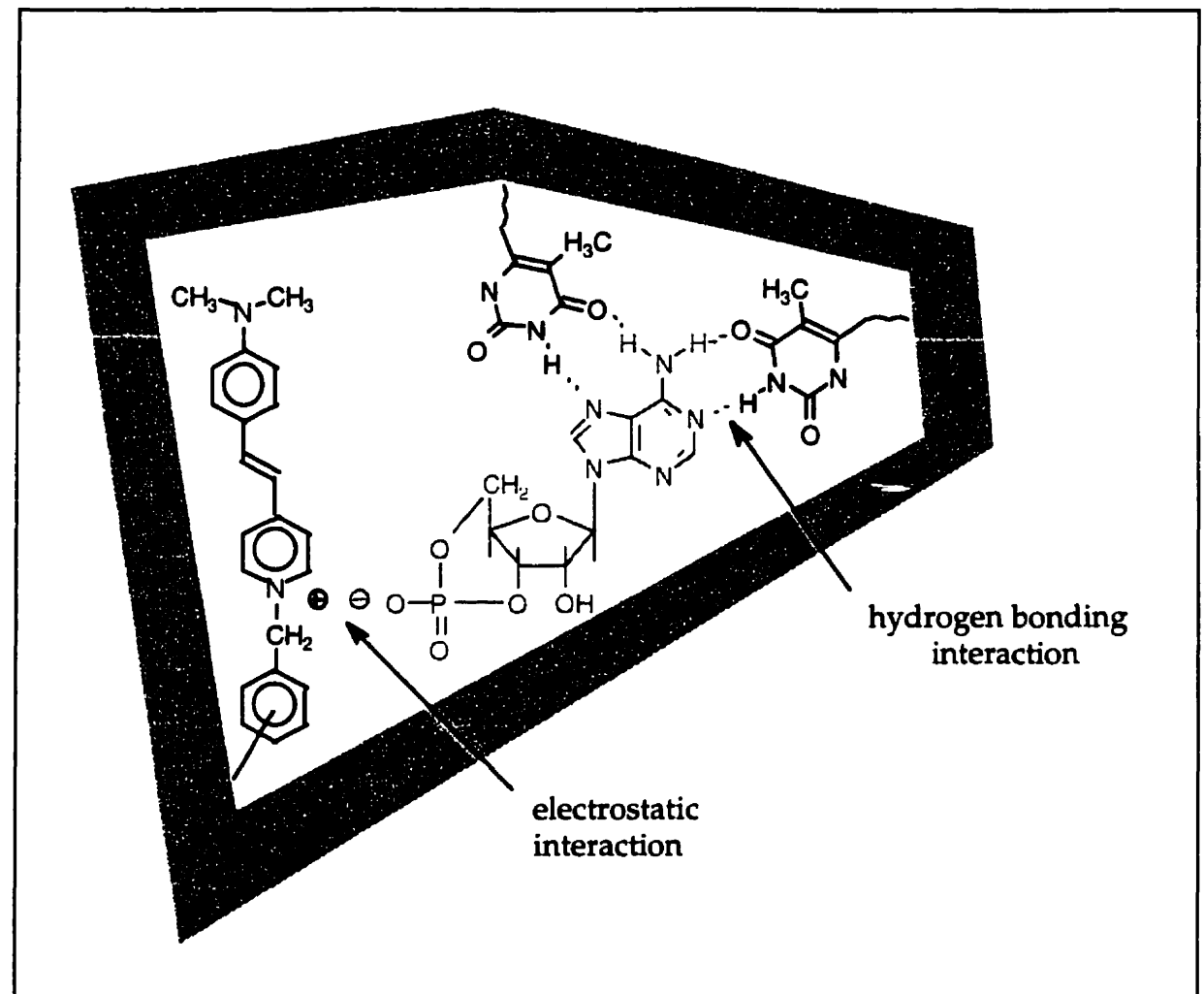


Figure 6.2. Schematic illustration of proposed molecularly imprinted recognition site for cAMP containing dye 1 and an imide binding functionality.

References

- Adams, R. S.; Harootunian, A. T.; Buechier, Y. J.; Taylor, S. S; Tsien, R. Y. *Nature*. 1991, 349, 694-697.
- Andersson, L.I.; Müller, R.; Vlatakis, G.; Mosbach, K. *Proc. Natl. Acad. Sci. USA* 1995, 92, 4788-4792.
- Brooker, G., Harper, J.F., Terasaki, W.L., Moylan, R.D. In Advances in Cyclic

 Nucleotide Research, Vol 10; Brooker, G., Greengard, T., Robison, G.A., Eds.; Raven

 Press: New York, 1979; p 1-33.
- Chan, E.C.S.; Stranix, B.R.; Darling, G.D.; Noble, P.B. Can. J. Microbiol. 1996, 42, 875-879.
- Cooper, M.E.; Hoag, B.P.; Gin, D.L. Polymer Prepr. 1997, 38, 209-210.
- Coudret, C.; Harriman, A. J. Chem. Soc., Chem. Commun. 1992, 1755-1757.
- Czarnik, A.W. In *Fluorescent Chemosensors for Ion and Molecule Recognition*; Czarnik, A.W., Ed.; ACS Symposium Series 538; American Chemical Society: Washington, DC, 1993; pp 1-9.
- Dhaenens, M.; Lehn, J-M.; Vigneron, J-P. J. Chem. Soc., Perkin Trans. 2 1993, 1379-1381.
- Eliseev, A.V.; Schneider, H-J. Angew. Chem. Int. Ed. Engl. 1993, 32, 1331-1333.
- Glad, M.; Reinholdsson, P.; Mosbach, K. Reactive Polymers 1995, 25, 47-54.
- Glazer, A.N.; Rye, H.S. Nature, 1992, 359, 859-861.
- Haugland, R.P. Handbook of fluorescent probes and Research Chemicals, 6th ed.; Spence, M.T.Z., Ed.; Molecular Probes, Inc.: Eugene, Oregon, 1996.
- Kato, Y.; Morgan Conn, M.; Rebek, J. Jr. J. Am. Chem. Soc. 1994, 116, 3279-3284.

Kumar, C.V.; Turner, R.S.; Asuncion, E.H. J. Photochem. Photobiol. A: Chem. 1993, 74, 231-238.

Labarca, C.; Paigen, K. Anal. Biochem. 1980, 102, 344-352.

Lehn, J-M. Supramolecular Chemistry; VCH: New York, 1995.

Mathew, J.; Buchardt, O. Bioconjugate Chem. 1995, 6, 524-528.

Mayes, A.G.; Mosbach, K. Anal. Chem. 1996, 68, 3769-3774.

Norrlöw, O.; Glad, M.; Mosbach, K. J. Chromatogr. 1984, 396, 374-377.

Rye, H.S.; Dabora, J.M.; Quesada, M.A.; Mathies, R.A.; Glazer, A.N. Anal. Biochem. 1993, 208, 144-150.

Sellergren, B. J. Chromatogr. A. 1994, 673, 133-141.

Shea, K. J.; Spivak, D.A.; Sellergren, B. J. Am. Chem. Soc. 1993, 115, 3368-3369.

Singer, V.L.; Jones, L.J.; Yue, S.T.; Haugland, R.P. Anal. Biochem. 1997, 249, 228-238.

Steinke, J.; Sherrington, D.C.; Dunkin, I.R. Adv. Polym. Sci. 1995, 123, 81-125.

Tsien, R. Y. in Fluorescent Chemosensors for Ion and Molecule Recognition; Czarnik, A.W., Ed.; ACS Symposium Series 538; American Chemical Society: Washington, DC, 1993.

Turkewitsch, P.; Darling, G.D.; Powell, W.S. J. Chem. Soc., Faraday Trans. 1998a, in press.

Turkewitsch, P.; Wandelt, B.; Darling, G.D.; Powell, W.S. Anal. Chem. 1998b, 70, 2025-2030.

Turkewitsch, P.; Wandelt, B.; Darling, G.D.; Powell, W.S. J. Photochem. Photobiol. A: Chem. 1998c, in press.

Turkewitsch, P.; Wandelt, B.; Ganju, R.R.; Darling, G.D.; Powell, W.S. Chem. Phys.

Lett. 1996, 260, 142-146.

Vlatakis, G.; Andersson, L.I.; Müller, R.; Mosbach, K. Nature. 1993, 361, 645-647.

Wandelt, B.; Turkewitsch, P.; Stranix, B.R.; Darling, G.D. J. Chem. Soc., Faraday Trans. 1995, 91, 4199-4205.

Wulff, G. Angew. Chem. Int. Ed. Engl. 1995, 34, 1812-1832.

Claims to original research

- 1. This thesis presents the first synthesis of two fluorophores, *trans*-4-(*p*-N,N-dimethylaminostyryl)-N-vinylbenzylpyridinium chloride (1) and *trans*-4-(*p*-N,N-dimethylaminostyryl)-N-phenethylpyridinium bromide (2).
- 2. We also show for the first time that dye 1 exhibits a large increase in dipole moment upon excitation, supporting the concept of a TICT process in this compound.
- 3. We are the first to demonstrate that dye 1 exhibits large fluorescence enhancements in the presence of nucleotides, especially cAMP and cGMP, and that it interacts more strongly with cAMP than other nucleotides. This environmentally-sensitive fluorescence establishes that dye 1 may serve as an excellent fluorescent component of a chemosensor for nucleotides.
- 4. We further demonstrate that biological macromolecules, such as DNA and proteins, induce dramatic fluorescence enhancements dyes 1 and 2, establishing the potential usefulness of 1 and 2 for quantitating these biomolecules in solution.
- 5. We present, for the first time, a novel design for template-selective recognition sites in polymers prepared by molecular imprinting. Recognition sites containing a fluorescent molecule as an integral part of the cavity that can serve as both the recognition element and the measuring element for the fluorescence detection of an analyte (i.e. the template)

have not been previously reported for any ligand. We have demonstrated that such molecular imprints may be prepared against cAMP, and that cAMP binding to these recognition sites may be detected in aqueous solution by fluorescence.

APPENDIX 2

Section A

A.1. Fluorescence Spectra of 1 in the presence of cAMP, cGMP and D-ribose-5-phosphate

In Chapter 2, increasing concentrations of cAMP and cGMP caused dramatic fluorescence quantum yield increases in the 1, whereas D-ribose-5-phosphate did not affect the fluorescence of 1 (Figure 2.2). At a concentration of 50 mM (the highest concentration tested), cGMP induced a larger fluorescence quantum yield increase in 1 (~9-fold), than cAMP (~ 8-fold). In this appendix, the fluorescence spectra of 1 in water and in the presence of 50 mM cAMP, cGMP and D-ribose-5-phosphate are compared (Figure 2A.1).

D-ribose-5-phosphate did not induce an increase in the fluorescence of 1 (the spectra of 1 in water, and in the presence of 50 mM D-ribose-5-phosphate are superimposable in Figure 2A.1), nor a shift of the emission maximum. The fluorescence emission maxima of 1 in water remained at 608 nm upon adding D-ribose-5-phosphate. However, fluorescence increases in 1, as well as slight red shifts of the emission maximum of 1 (from 608 in water to 612 in solutions containing cAMP or cGMP), are observed in the presence of both cAMP and cGMP. cGMP induced the largest change, whereas cAMP induced a smaller increase in the fluorescence of 1. These results are consistent with those presented in Figure 2.2.

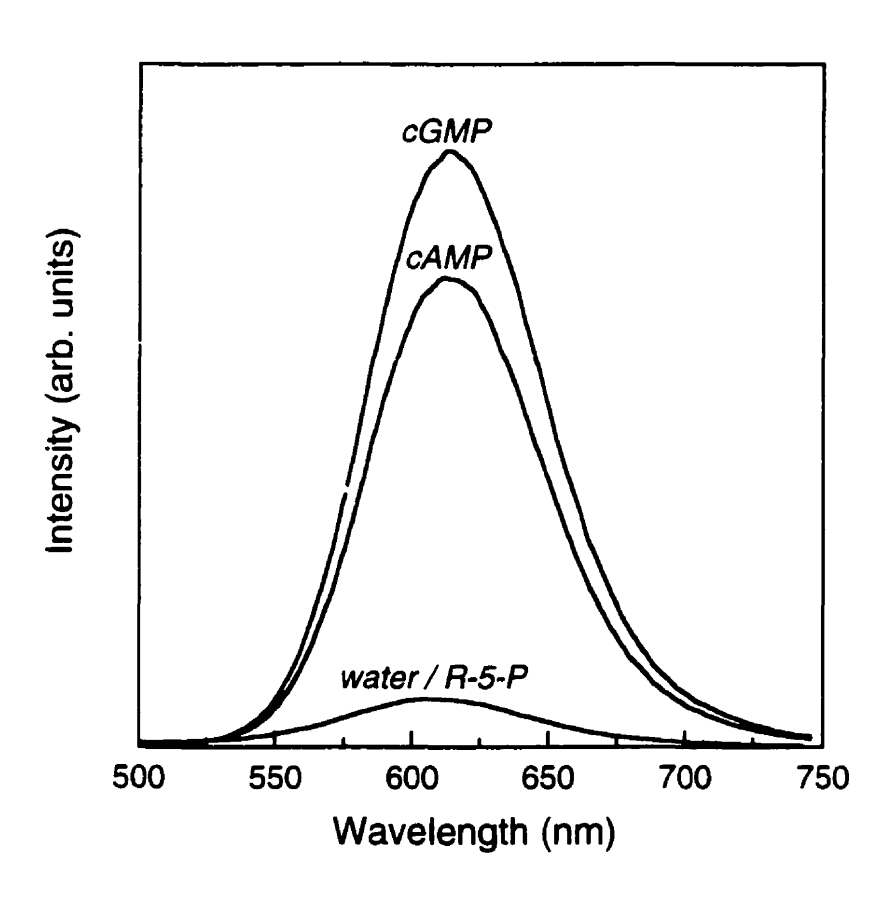


Figure 2A.1 Fluorescence spectra of 1 (10⁻⁵ M) in the absence (water), and in the presence of 50 mM D-ribose-5-phosphate (ribose), cAMP and cGMP; excitation wavelength, 469 nm; emission wavelength, 608 nm for D-ribose-5-phosphate, and 612 nm for cAMP and cGMP. Note that the spectra for 1 in water and in the presence of D-ribose-5-phosphate are superimposable.

APPENDIX 3

Section A

A.1 Synthesis of *trans*-4-(p-N.N-Dimethylaminostyryl)-N-phenethyl-pyribinium Bromibe (2)

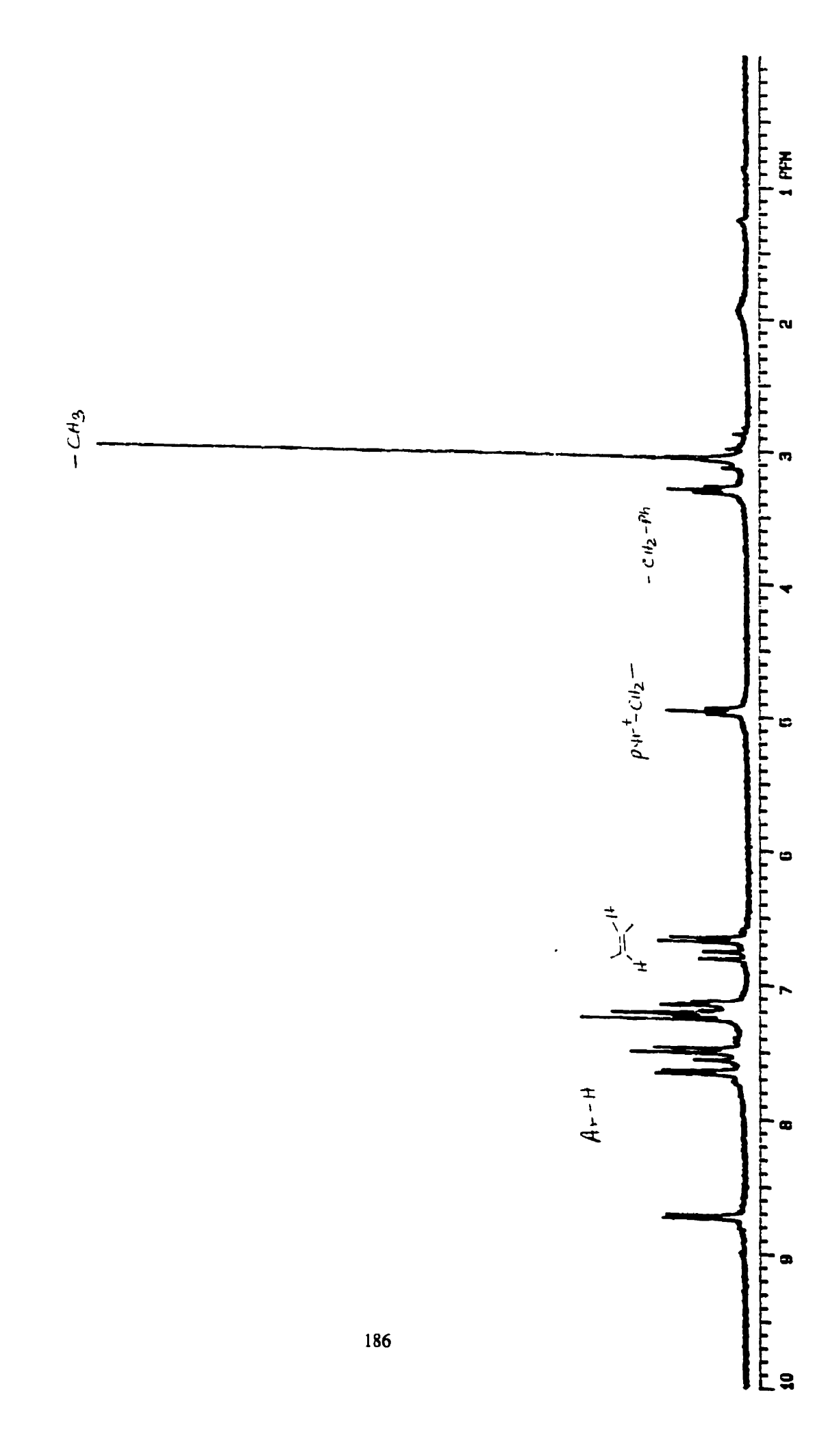
"Reprinted from J. Chem. Soc., Faraday Trans. 1995, 91, 4199-4205 with kind permission of The Royal Society of Chemistry, Cambridge, UK".

Recently, I participated in a collaborative study (*J. Chem. Soc., Faraday Trans.* 1995, 91, 4199-4205) with Barbara Wandelt, Brent R. Stranix and Graham D. Darling in which the fluorescence of *trans*-4-(p-N,N-dimethylaminostyryl)-N-phenethylpyridinium bromide (2) was investigated in solutions of differing viscosity. My contribution to this study was the synthesis of dye 2, which is described in this section of the appendix. The fluorescence behavior of 2 in the presence of biological macromolecules is described in Chapter 4 (Turkewitsch et al., *J. Chem. Soc., Faraday Trans.* 1998, in press). The 'H NMR spectrum of 2 in chloroform is presented in Figure 3A.1

2-Bromoethylbenzene (1.63 g, 8.80 mmol) was added dropwise to a refluxing yellow solution of 4-(zp-dimethylaminostyryl)pyridine (0.500 g, 2.23 mmol) in toluene (35 mL). After refluxing for 5 h, the red-orange precipitate that had formed was collected by filtration of the warm reaction mixture, washed several times with hot toluene, and dried under vacuum at 50 °C, to afford red-orange crystals of 2 which were stored in a desiccator in the dark (0.392 g, 43%): mp 253-255 °C; one spot by TLC (EtOH: toluene

3:7/SiO₂); ¹H NMR (Jeol CPF-270, 270 MHz, CDCl₃) δ 7.23-7.75 (m, 13 H, Ar-H), 6.80-6.94 (dd, 2H, C•CH), 5.1 (t, 2 H, Pyr⁺CH₂CH₂), 3.44 (t, 2H, CH₂CH₂Ph), 3.20 (s, 6H, NCH₃).

Figure 3A.1. ¹H NMR spectrum of *trans*-4-(*p*-N,N-dimethylaminostyryl)-N-phenethylpyridinium bromide (2) in chloroform on a 300 MHz Varian XL-300 spectrometer at room temperature. Please see next page.



Section B

B.1 Spectral data for due 1 and due 2

Additional spectral data for *trans*-4-(*p*-N,N-dimethylaminostyryl)-N-vinylbenzyl-pyridinium chloride (1) and *trans*-4-(*p*-N,N-dimethylaminostyryl)-N-phenethylpyridinium bromide (2) are presented in this section. Figure 3B.1 shows the fluorescence spectra of 1 and 2 in phosphate buffer obtained by exciting at 469 nm. The spectrum for dye 1 has a slightly lower intensity than dye 2, whereas their emission maxima are similar (603 nm). This similarity in the fluorescence spectra of 1 and 2 suggests that the substituent of the pyridinium nitrogen of these dyes does not appreciably affect their fluorescence. This is discussed in more detail in the Discussion section of Chapter 3, and in the Final Discussion and Conclusions (Chapter 6).

The ¹H NMR spectra of dye 1 in chloroform, shown in Figure 3B.2, suggests that there were no major contaminants in this product. However, it did show that *trans-4-(p-N,N-dimethylaminostyryl)-N-vinylbenzylpyridinium* chloride was a 70:30 mixture of *trans-4-(p-N,N-dimethylaminostyryl)-N-m-vinylbenzylpyridinium* chloride and *trans-4-(p-N,N-dimethylaminostyryl)-N-p-vinylbenzylpyridinium* chloride. Please refer the Experimental and Results sections of Chapter 3 for more detail.

The absorption spectrum of dye 1 in water or in buffer exhibits a maximum at 469 nm (Figure 2.1a and 3.1). However, we employed an excitation wavelength of 360 nm in Chapter 3, even when the absorption of 1 is almost at a minimum here, and observed a dual emission with maxima at 502 and 602 nm. This excitation wavelength was chosen,

because the excitation spectrum of 1 in buffer at an emission of 510 nm exhibits a maximum at ~360 nm (Figure 3B.3). This maximum is, however, of much lower intensity than that obtained at an emission maximum of 600 nm (maximum at ~469 nm). This, together with the fact that the quantum yield of the 502 emission band (excitation 360 nm) is small, that the emission spectra presented throughout this work are uncorrected, and that dye 1 is a mixture of *meta* and *para*-vinylbenzyl isomers, raises the possibility that the 502 emission band is due to an artifact or impurity. Please refer to the Discussion section of Chapter 3 for a more detail.

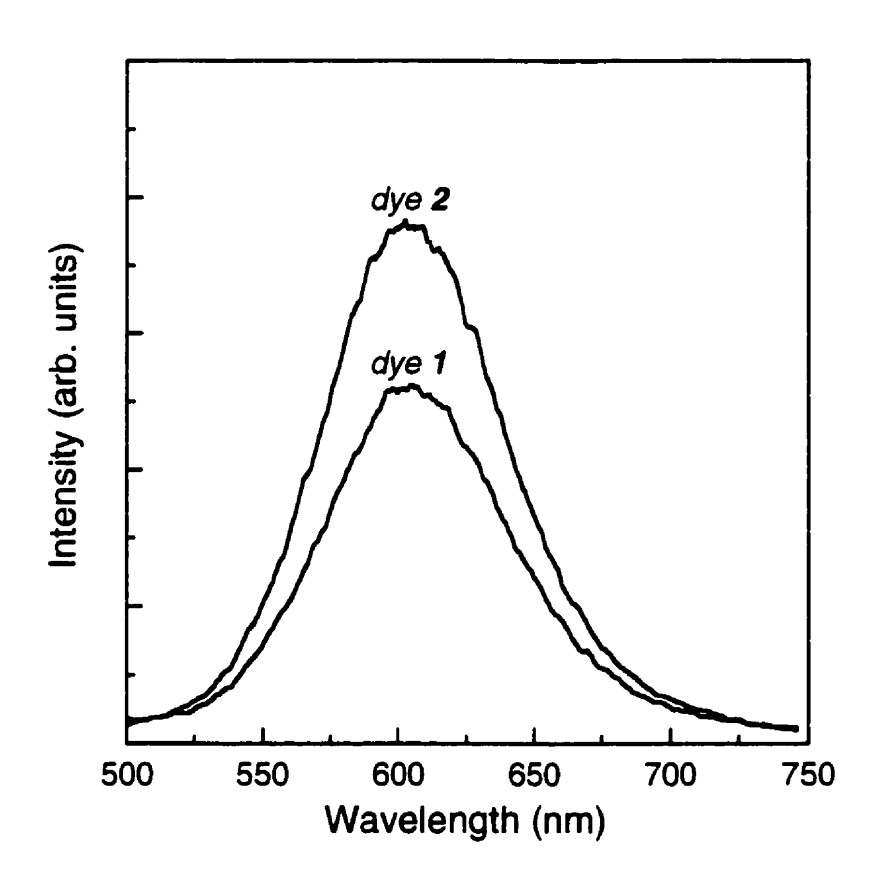
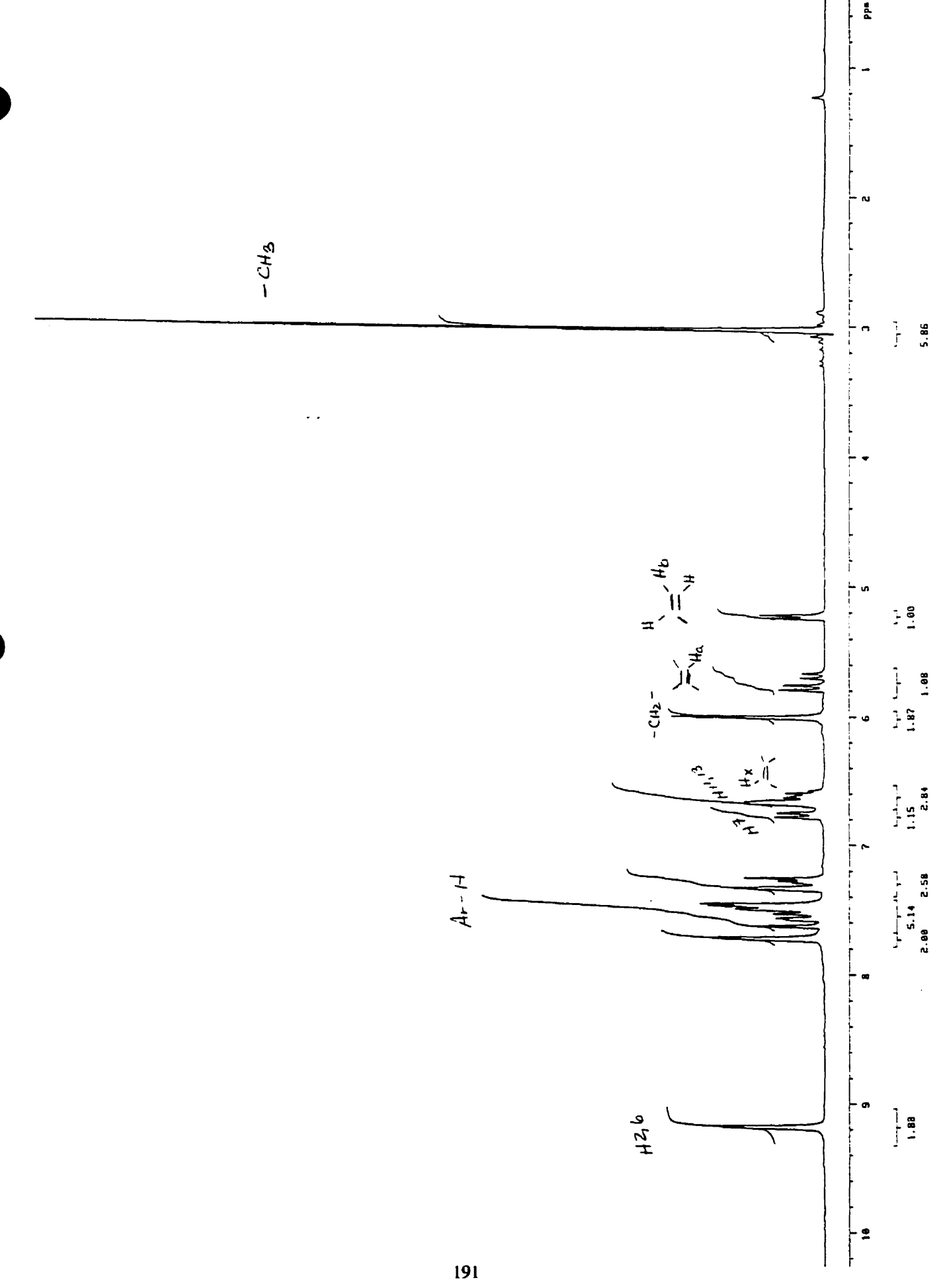


Figure 3B.1. Fluorescence spectra of dye 1 and dye 2 (10^{-5} M) in phosphate buffer (0.01 M, pH 7.2); excitation wavelength, 469 nm; emission maxima for 1 and 2, \sim 603 nm.

Figure 3B.2. ¹H NMR spectrum of *trans*-4-(*p*-N,N-dimethylaminostyryl)-N-vinylbenzylpyridinium chloride (1) in chloroform on a 500 MHz Varian Unity-500 spectrometer at room temperature. Please see next page.



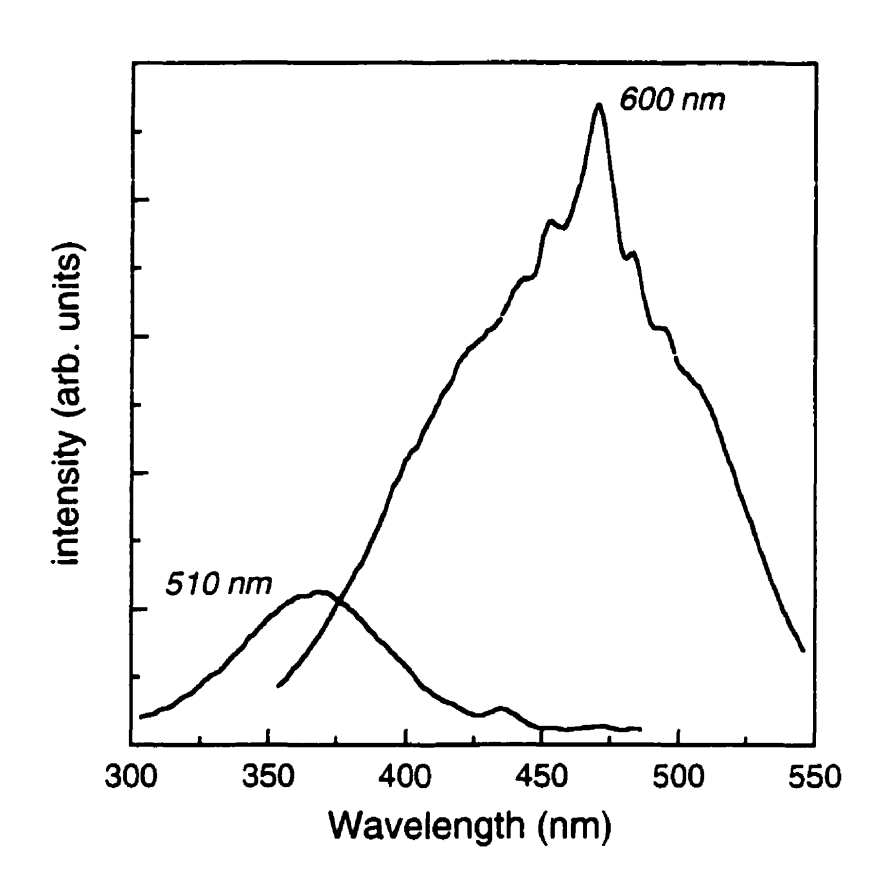


Figure 3B.3. Excitation spectra of 1 (10⁻⁵ M) in phosphate buffer (0.01 M, pH 7.2) at room temperature at emission wavelengths of 510 and 600 nm. The spectra are not corrected.

Section C

C.1 Absorption and fluorescence spectra of 1 in various solvents.

The absorption and fluorescence spectra of 1 in various solvents (water, chloroform and acetonitrile) of different polarity is presented in Figure 3C.1. Table 3.1 presents the solvent parameters and the steady-state spectral data for 1 in these and other solvents. In water, dye 1 shows the largest Stokes' shift (4929 cm⁻¹) with an absorption and emission maximum of 469 and 610 nm, respectively. The smallest Stokes' shift is observed for chloroform (2487 cm⁻¹), which has an absorption and emission maximum of 500 and 571 nm, respectively. The absorption and emission maximum of 1 in acetonitrile are 482 and 613 nm, respectively, giving an intermediate Stokes' shift of 4434 cm⁻¹.

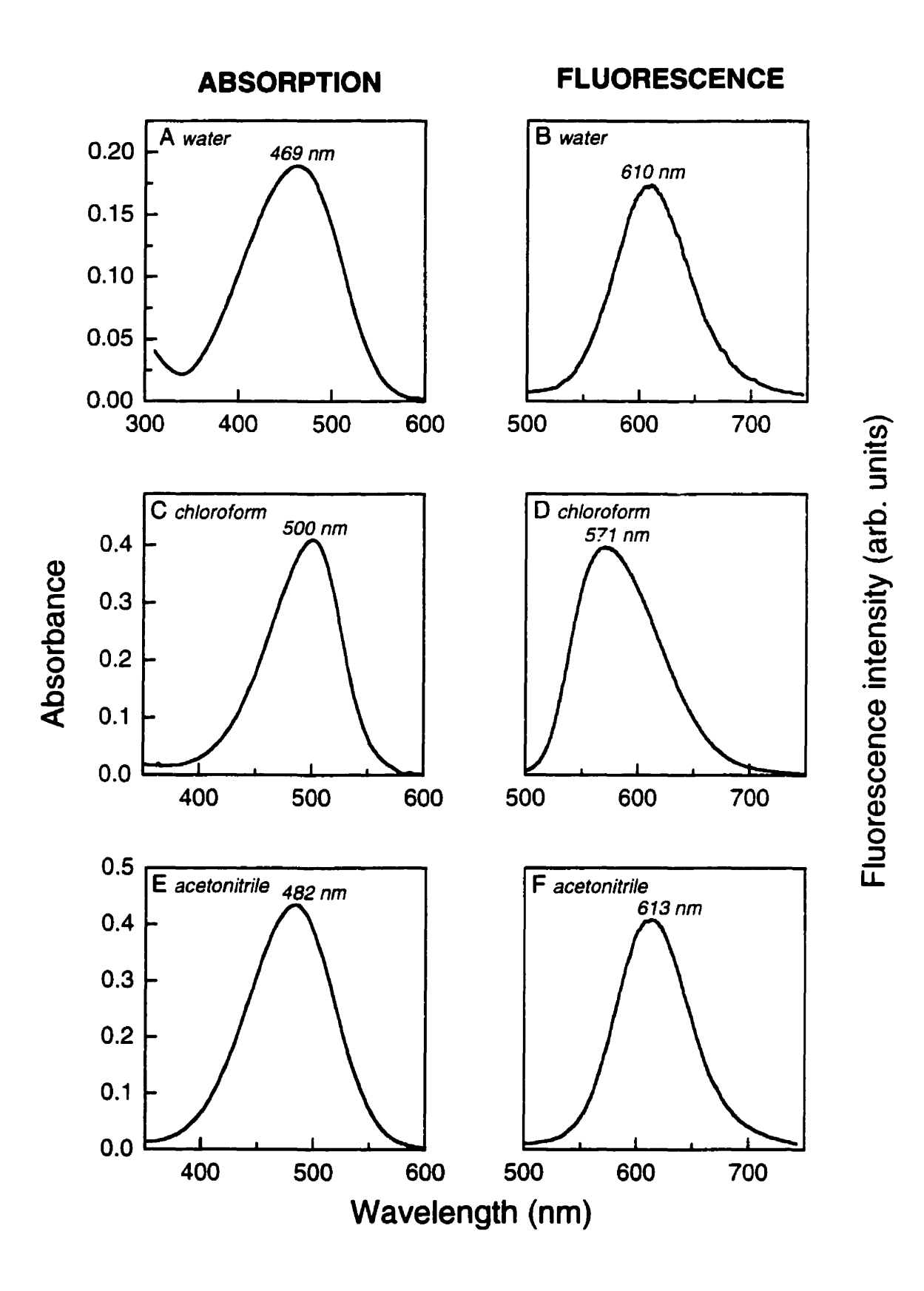


Figure 3C.1 Absorption and fluorescence spectra of 1 (10⁻⁵ M) in water (absorption A; fluorescence B), chloroform (absorption C; fluorescence D), and acetonitrile (absorption E; fluorescence F).

Section D

D.1 Fluorescence spectra of 1 in the presence of cAMP, cGMP, ATP and CMP.

In Chapter 3, the purine nucleotides (cAMP, cGMP, AMP, ADP and ATP) and adenosine all induced fluorescence enhancements in 1 in phosphate buffer, whereas the pyrimidine nucleotides (CMP and UMP) had virtually no effect on fluorescence. Of the purine analytes, the cyclic nucleotides, cAMP and cGMP, had the greatest effects on the fluorescence of 1. At the highest concentration examined (50 mM), cGMP induced a slightly larger fluorescence quantum yield enhancement in 1 (~ 12-fold) than cAMP (~ 11-fold). The smallest changes in fluorescence were observed for the noncyclic nucleotides, AMP, ADP and ATP. Adenosine had an effect intermediate between those of the cyclic and noncyclic nucleotides. Herein, the fluorescence spectra of 1 in phosphate buffer, and in the presence of the highest concentration (50 mM) of cAMP, cGMP, ATP and CMP are compared (Figure 3D.1).

The fluorescence intensity of 1 in the presence of CMP (50 mM) is only slightly larger than 1 in phosphate buffer alone, and the fluorescence emission maximum of 1 in buffer remained at 608 nm upon adding CMP. In contrast, cAMP and cGMP concentrations of 50 mM induce the largest fluorescence increases in 1, with cGMP displaying a slightly higher fluorescence intensity than cAMP. These cyclic nucleotides also shift the fluorescence emission maximum of 1 from 608 nm in buffer alone to 613 nm in solutions of 50 mM cAMP and cGMP. Like the cyclic nucleotides, 50 mM ATP

also causes a shift of the emission maximum of 1 to 613 nm, however it induces a lower fluorescence intensity increase in 1 than the cyclic nucleotides. These fluorescence changes in 1 are consistent with those presented in Figure 3.4. Furthermore, the fluorescence increases in 1 in phosphate buffer induced by cAMP and cGMP are similar to those presented in Appendix 2, Section A, Figure 2A.1. These results suggest that 1 displays a specificity for purine over pyrimidine nucleotides.

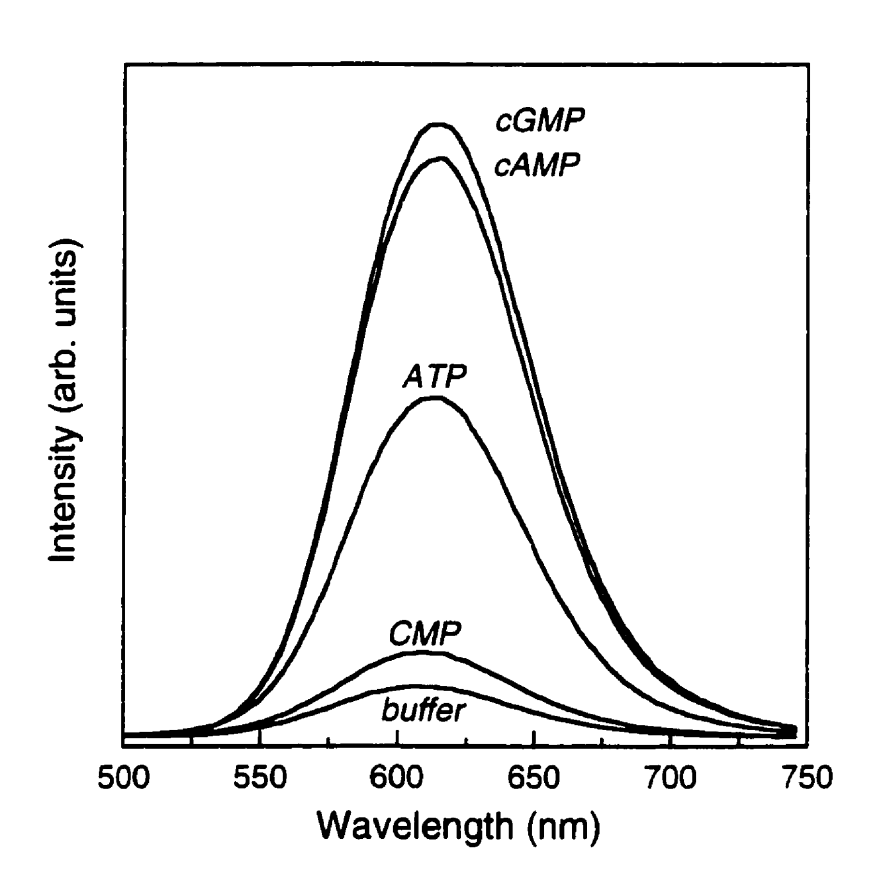


Figure 3D.1 Fluorescence spectra of 1 (10⁻⁵ M) in phosphate buffer (0.5 M, pH 7.2) in the absence (buffer), and in the presence of 50 mM cAMP, cGMP, ATP and CMP; excitation wavelength, 469 nm; emission maximum for cAMP, cGMP and ATP, 613 nm; emission maximum for CMP and buffer, 608 nm.

Section E

E.1 Fluorescence quantum yield enhancement of 1 and 2 in the presence of cAMP

The fluorescence spectra of dye 1 and 2 were found to be similar (Figure 3B.1), suggesting that the substituent on the pyridinium nitrogen of these dyes (i.e. vinylbenzyl in the case of 1 and phenethyl in the case of 2) has relatively little affect on their fluorescence. This also raises the possibility that the mixture of meta and para isomers in dye 1 does not appreciably affect the fluorescence properties of 1. In Chapter 4 we also found that the fluorescence quantum yield enhancements in 1 and 2 in the presence of biological macromolecules (DNA and bovine serum albumin) was similar, further indicating that the vinylbenzyl and phenethyl groups do not significantly affect the ability of the dyes to respond to these macromolecules, and therefore probably plays a small role in the interaction with them. To determine whether the fluorescence responses of dyes 1 and 2 are also similar in the presence of individual nucleotides, the effect of cAMP concentrations between 0 and 50 mM (i.e. the same concentration range examined in Chapters 2 and 3) on the fluorescence of dyes 1 and 2 are examined in this section. The materials and instruments used, and experimental procedure employed are as described in Chapter 3, however the setup of the spectrofluorometer is different and thus the fluorescence quantum yields are not comparable with those presented in Chapter 3.

E.1.1 Results and Discussion

Concentrations of cAMP between 1 and 50 mM induce a similar increase in the fluorescence of 1 and 2, as well as a similar shift in their λ_{max} to longer wavelengths (Figure 3E.1). These concentration-dependent fluorescence increases are presented in the form of fluorescence quantum yield titration curves in Figure 3E.2. The magnitude of the fluorescence quantum yield responses of 1 and 2 in phosphate buffer (0.5 M, pH 7.2) are similar, with 1 displaying a ~13-fold enhancement, and 2 a ~17-fold enhancement.

Association constants (K_{eq}) and Φ_c values for 1 and 2 with cAMP were obtained by fitting the data in Figure 3E.2 to equation 4 as described in Chapter 3. K_{eq} and Φ_c values of 16.1 M^{-1} and 0.028 were obtained for dye 1. Dye 2 displayed a very similar K_{eq} value (K_{eq} 16.5 M^{-1}), whereas it had a higher Φ_c value (0.035). This difference in Φ_c values is largely because dye 2 displays a slightly larger fluorescence quantum yield enhancement than 1 at all concentrations tested.

The similar increases in the fluorescence of 1 and 2 in the presence of increasing concentrations of cAMP suggest that the vinylbenzyl and phenethyl substituents of 1 and 2, respectively, have relatively little effect on the fluorescence responses of the dyes to cAMP. Furthermore, since the association constants for 1 and 2 with cAMP are almost identical, the involvement of these substituents in the interaction of 1 and 2 with cAMP is probably minor. The results also support the argument that the meta and para isomers in 1 have relatively little effect on the fluorescence properties and the fluorescence response of this dye.

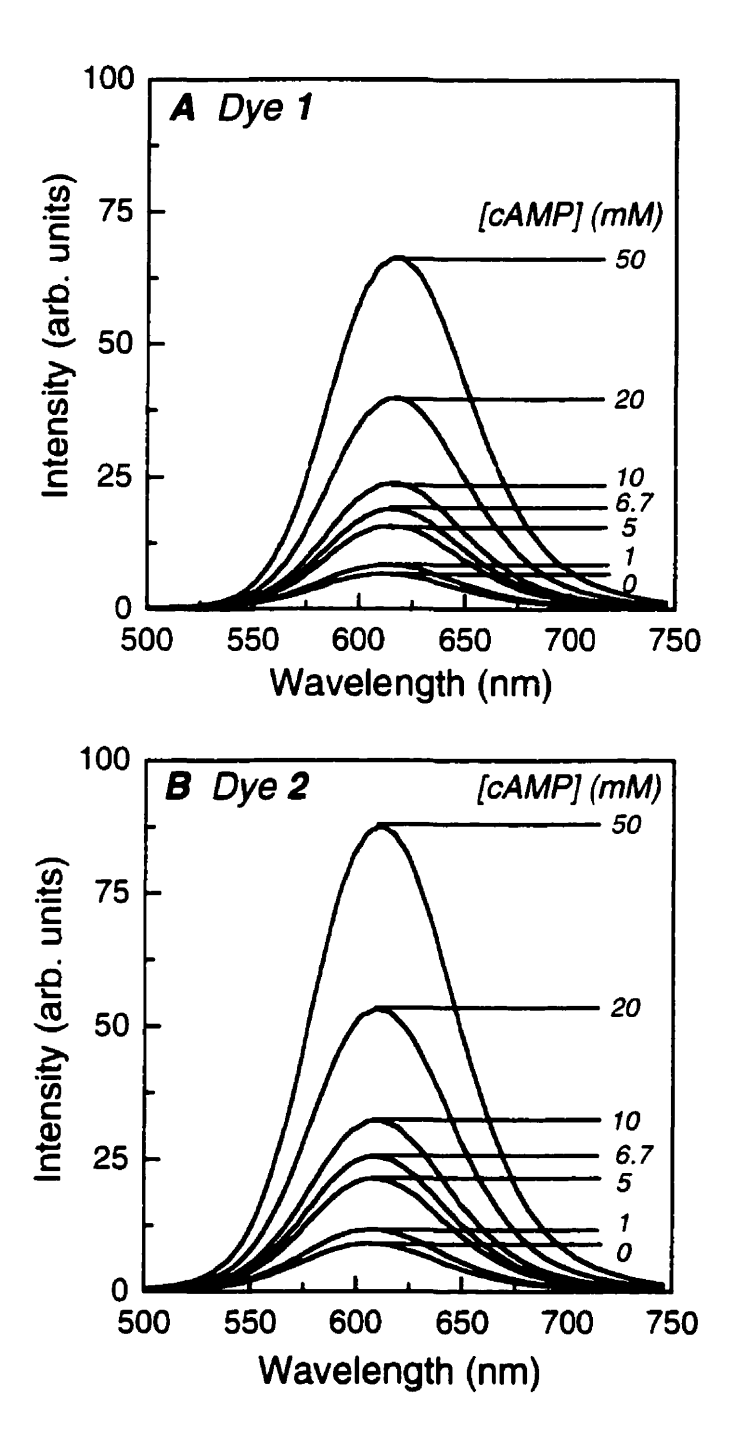


Figure 3E.1. Fluorescence spectra of 10⁻⁵ M 1 (A) and 2 (B) in phosphate buffer (0.5 M, pH 7.2) in the presence the absence and in the presence of various concentrations of cAMP (1, 5, 6.7, 10, 20 and 50 mM); excitation wavelength, 469 nm; emission maxima varied between 610 and 617 nm for 1; and 605 and 611 nm for 2.

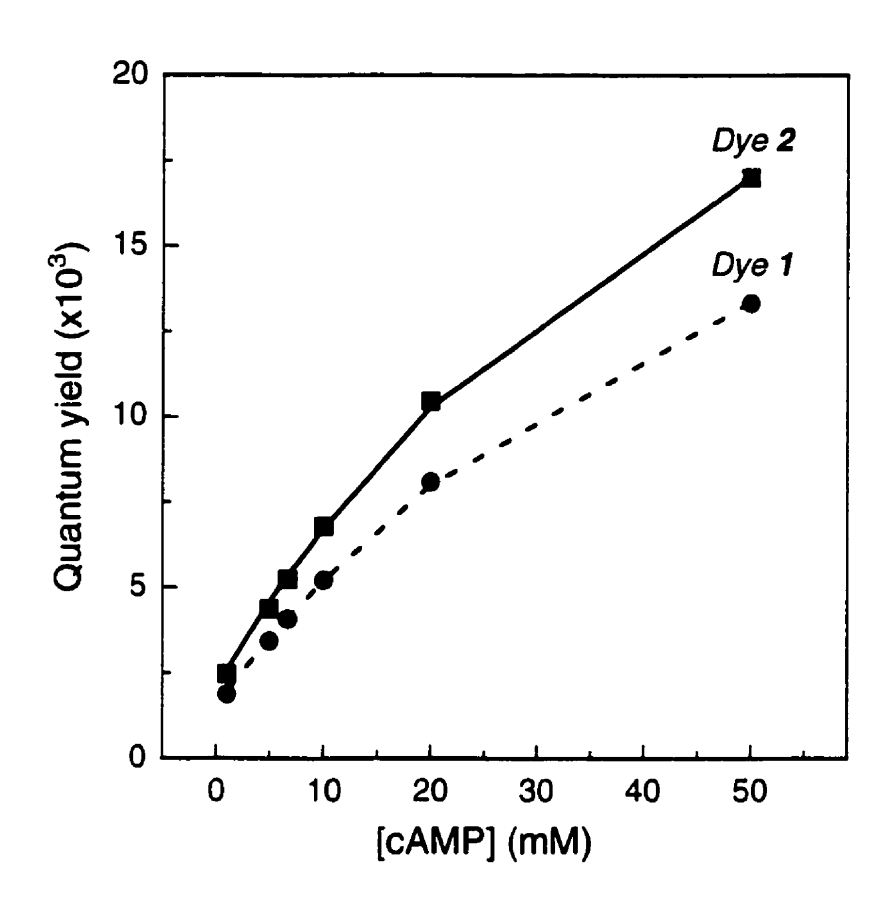


Figure 3E.2. Fluorescence quantum yield titration curves of 1 (●) and 2 (■) as a function of cAMP concentration in phosphate buffer (0.5 M pH 7.2); excitation wavelength, 469 nm. The lines through the symbols for dye 1 and 2 represent curve fits following equation 4.

Section F

F.1 The fluorescence response of A-10 cells loaded with fura-2 to serotonin in the absence and in the presence of due 2

A fluorescent chemosensor used in intracellular applications must be evaluated for short and long-term toxic affects on cells. Furthermore, the physiological functioning to the cells in the presence of the fluorescent chemosensor must be investigated to determine whether it affects normal behavior. To determine whether dye 2 was toxic to cells, the ability of cells to respond to a stimulus was investigated before and after dye 2 had been introduced into the cells.

F.1.1 Experimental

A-10 embryonic thoracic aorta cells were grown on round glass coverslips (25 mm diameter) placed in 6 well culture dishes in 1:1 Dulbecco's modified Eagle medium (DMEM, Gibco):Ham's F-12 medium supplemented with 20 % fetal bovine serum (FBS, Gibco). Cell culture was maintained at 37°C in humidified 5% CO₂ atmosphere. The medium was changed every 3 days.

Cells on a coverslip were loaded with fura-2 by incubating them for 20 min at 37°C in the dark with Hanks' buffer (in mmol/L: 137 NaCl, 4.2 NaHCO₃, 10 glucose, 3 Na₂HPO₄, 5.4 KCl, 0.4 KH₂PO₄, 0.5 MgCl₂, 0.8 MgSO₄, 5 N-2-hydroxyethylpiperazine-N'-2-ethane sulfonic acid) containing 4 µM fura-2 acetoxy methylester (Molecular Probes

4

Inc.). Loaded cells were washed with three changes of Hanks' buffer and the coverslip was placed, along with Hanks' buffer, in a Leiden chamber (Medical Systems, Greenville, NY) on the stage of an inverted microscope equipped for epifluorescence with a ×40 oil-immersion objective (Nikon, Montreal, Quebec, Canada). The ratio of the fluorescence emission of the cells at 510 nm obtained by exciting at 345 nm and 380 nm (Ratio 345/380 nm) was measured at room temperature using a PTI D401 microphotometer (Photon Technology International, Princeton, NJ). Background fluorescence was automatically subtracted. Serotonin (10⁻³ M) was added to the buffer and the fluorescence response of the cells was measured. When the cells had recovered from this stimulation, the buffer was removed and fresh Hanks' buffer containing 10° M dye 2 was added. The cells were incubated for 10 min at 37°C, and then washed with three changes of Hanks' buffer. The cells appeared bright orange when examining their fluorescence emission at 610 nm (excitation wavelength 469 nm), confirming incorporation of dye 2 into the cells. The fluorescence emission of the cells before and after stimulation with serotonin (10⁻³ M) was then measured at room temperature using the fura-2 conditions described above.

F.1.2 Results and Discussion

The fluorescence emission of fura-2 at 510 nm obtained by exciting at 345 nm and 380 nm (Ratio 345/380 nm) in A-10 cells in culture after stimulation with serotonin (10⁻³ M), and after loading with dye 2 and stimulation with serotonin is presented in Figure 3F.1. Cells loaded with fura-2 displayed a rapid increase in the fluorescence ratio upon stimulation with serotonin followed by a gradual decrease back to baseline (Figure

3F.1a). This response profile reflects the increase in intracellular calcium levels in these cells with stimulation and the recovery of these calcium levels back to normal resting levels. After a recovery period, the same cells were loaded with dye 2 and stimulated again with serotonin (Figure 3F.1b). The magnitude of the response of the cells to stimulation by serotonin is similar in the presence of dye 2 is similar that obtained in the absence of dye 2. These results suggest that the physiological functioning of these cells is maintained in the presence of dye 2. Cells subject to this treatment were treated with trypan blue stain 24 hours later, and were found to be viable.

Thus, dye 2 is capable of entering cells by passively diffusing across the cell membrane, and, therefore, does not have to be injected into cells, minimizing disruption to the membrane. Such cells loaded with dye 2, responded to stimulation equally as well as cells that had not been loaded with the dye, suggesting that the dye does not have any adverse affects on the ability of the cells to respond to stimulation. Thus, the normal physiological functioning of the cells appears to be maintained in the presence of dye 2.

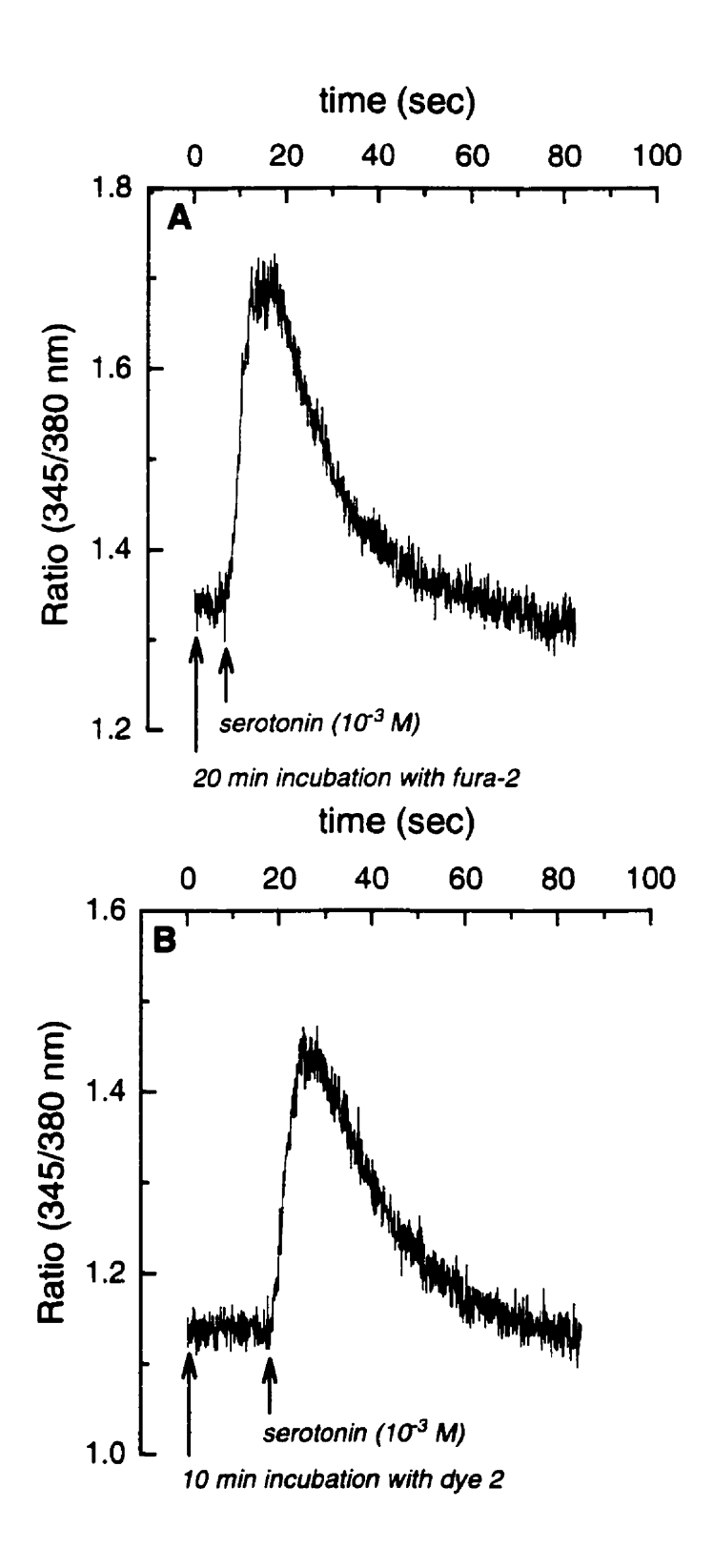


Figure 3F.1. Increase in the ratio of the fluorescence emission of fura-2 at 510 nm obtained by exciting at 345 nm and 380 nm (Ratio 345/380 nm) of fura-2 loaded A-10 cells to serotonin (10-3 M) before (A) and after loading with dye 2 (B).

APPENDIX 4

Section A

A.1 Fluorescence spectra of diges 1 and 2 in the presence of biological macromolecules

In Chapter 4, we found that the fluorescence quantum yields of dyes 1 and 2 increased dramatically in the presence of biological macromolecules, such as BSA and DNA (Figure 4.1, 4.2 and Table 4.1). The increases in the fluorescence of 1 induced by DNA and nondenatured BSA at concentrations of 150 µg/mL were if similar magnitude (~5-fold), and were much greater than those induced by a higher concentration of cAMP (350 µg/mL). Denatured BSA (150 µg/mL) induced the greatest fluorescence quantum yield enhancement in 2 (~9-fold). However, smaller effects were observed for DNA (~8fold), nondenatured BSA (~3-fold) and RNA (~2-fold). These increases in the fluorescence of 2 induced by nondenatured BSA were slightly lower than those observed for 1, whereas those induced by DNA were somewhat higher. The presence of polynucleotides and proteins also caused a shift in fluorescence λ_{max} of these dyes. DNA induced a slight blue shift in the λ_{max} of 1 of approximately 4 nm, from 603 nm in buffer alone to 599 nm at 1 mg/mL DNA, whereas a much larger blue shift of 28 nm was observed in the presence of nondenatured BSA (λ_{max} 575 nm). The λ_{max} of dye 2 shifted from 603 nm in buffer to 595 nm in the presence of 1 mg/mL DNA, a shift to shorter wavelengths of approximately 8 nm. Denatured and nondenatured BSA induced a blue shift of the λ_{max} of dye 2 of about 33 nm, from 603 nm in buffer to 570 nm at 1 mg/mL

protein. In contrast, the λ_{max} of dye 2 did not change in the presence of RNA (1 mg/mL). These fluorescence intensity changes and shifts of the λ_{max} in 1 and 2 are easily identified, and may be better appreciated when their fluorescence spectra are compared. Herein, the fluorescence spectra of 1 and 2 in phosphate buffer in the presence of the 1 mg/mL denatured BSA, nondenatured BSA, DNA and RNA are compared (Figure 4A.1).

The fluorescence intensities of 1 in the presence of DNA and nondenatured BSA are very similar (Figure 4A.1), and consistent with those presented in Figure 4.2. However, the λ_{max} of 1 is shifted to the blue much more in the presence of nondenatured BSA(~ 575 nm) than DNA (~599 nm). Denatured BSA induces the largest fluorescence intensity increase in 2, whereas DNA, nondenatured BSA and RNA induce much smaller fluorescence increases (Figure 4A.1), also consistent with the results presented in Figure 4.1 and 4.2. A greater blue shift of the λ_{max} of 2 is also observed in the presence of nondenatured and denatured BSA shift the λ_{max} of 2 from 603 nm in buffer to 570 nm in solutions of protein. The λ_{max} of dye 2 shifts from 603 in buffer to 595 in the presence of 1 mg/mL DNA. RNA does not induce a shift in the λ_{max} of 2. The fluorescence increases of 1 in the presence of nondenatured BSA are slightly greater than those observed for 2, however the λ_{max} of 1 does not shift to the blue as much as that of 2. On the other hand, DNA induces a lower fluorescence intensity increase in 1 than in 2, as well as a smaller blue shift of the λ_{max} .

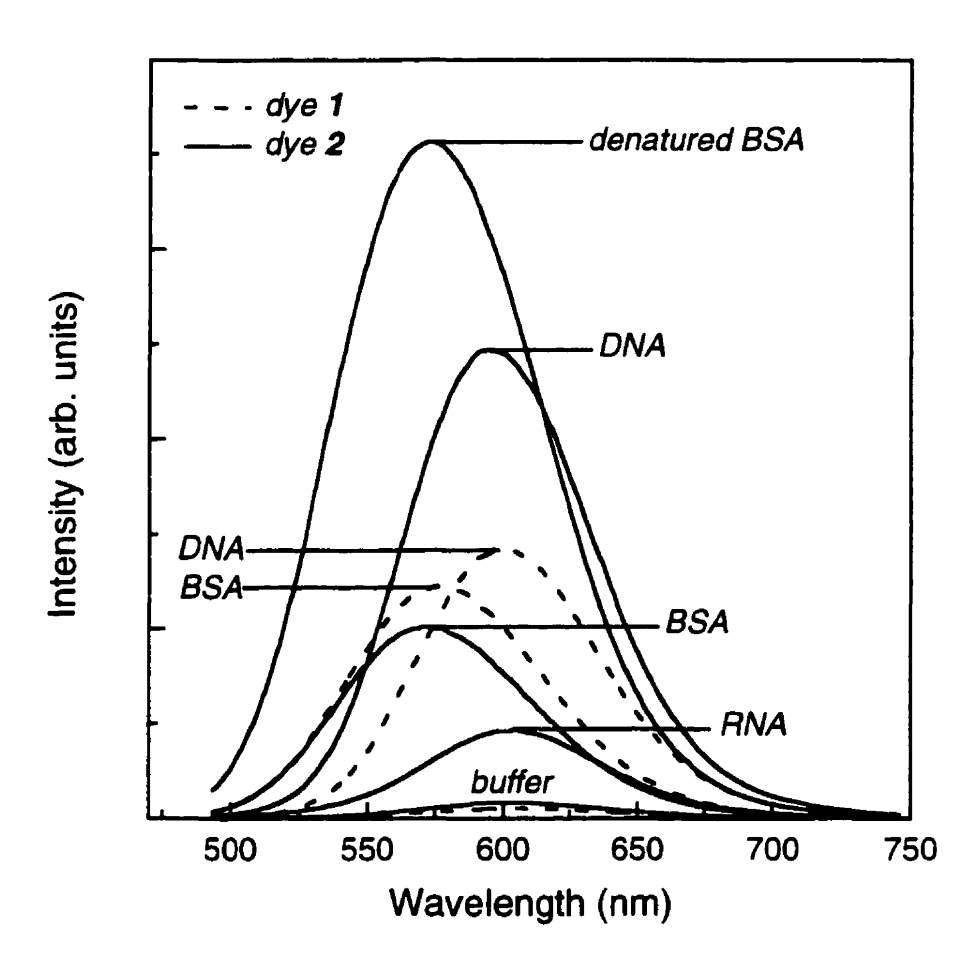


Figure 4A.1 Fluorescence spectra of 1 (dotted lines) and 2 (solid lines) (10⁻⁵ M) in PBS (0.01 M, pH 7.2) in the absence (buffer), and in the presence of 1 mg/mL denatured BSA, nondenatured BSA (BSA), DNA and RNA; excitation wavelength, 469 nm; emission maximum for dye 1 alone, 603 nm, with nondenatured BSA, 575 nm; and with DNA, 599 nm; emission maximum for dye 2 alone, 603 nm, with denatured and nondenatured BSA, 570 nm; with DNA, 595 nm; and with RNA, 603 nm.

Section B

B.1 Fluorescence of dye 2 in the presence of proteins

The effects of ovalbumin and gelatin on the fluorescence of 2 were also investigated in Chapter 4. Ovalbumin induced a fluorescence enhancement in 2 similar to that of nondenatured BSA, with an I/I_f value of 11.7 at a concentration of 1 mg/mL, compared to 12.4 for nondenatured BSA (Table 4.1). In contrast, gelatin, at this same concentration, had a considerably smaller effect than nondenatured BSA, with an I/I_f value of only 1.49. In this section the fluorescence spectra of dye 2 in the presence of 1 mg/mL nondenatured BSA, ovalbumin and gelatin are presented (Figure 4B.1). The fluorescence intensities of 2 as a function of nondenatured BSA, gelatin and ovalbumin concentrations between 1.0 and 33.7 mg/mL concentrations are also shown (Figure 4B.2).

The fluorescence intensity of 2 with 1 mg/mL nondenatured BSA is greater than with ovalbumin, and much greater than with gelatin in Figure 4B.1, consistent with the results in Table 4.1. However, at a much higher concentration of 33.7 mg/mL, ovalbumin induces a larger fluorescence intensity increase in 2 than nondenatured BSA (Figure 4B.2). Furthermore, at this concentration, nondenatured BSA and ovalbumin both induce a greater increase (approximately 5-fold) in the fluorescence of 2 than gelatin, which produces a gel state under these conditions. The fluorescence responses induced by BSA and ovalbumin appear to be saturating at this high concentration (33.7 mg/mL), whereas the response induced by gelatin remained linear (Figure 4B.2). Nondenatured BSA and ovalbumin also induce a much larger blue shifts in the λ_{mx} of 2, from 603 nm in buffer to

570 nm at 1 mg/mL protein, than gelatin which exhibits from 603 nm in buffer to 600 nm at 1 mg/mL gelatin (Figure 4A.1).

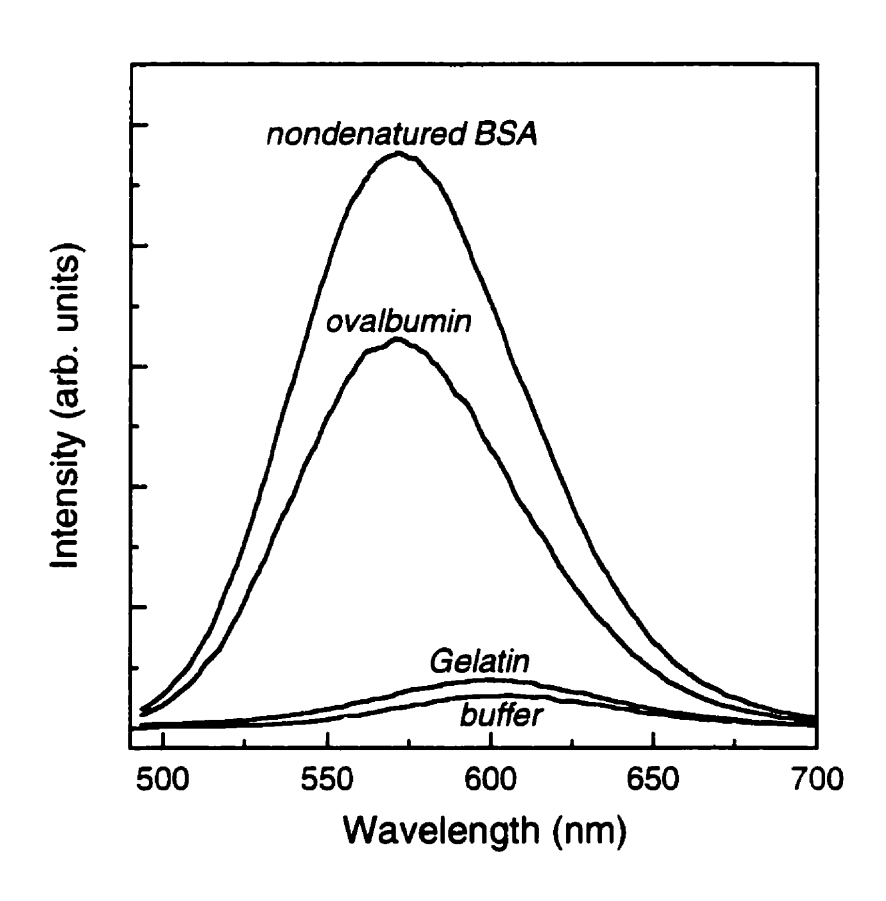


Figure 4B.1 Fluorescence spectra of 2 in phosphate buffered saline in the absence (buffer), and in the presence of 1.0 mg/mL of nondenatured BSA, ovalbumin and gelatin; excitation wavelength, 469 nm; emission maxima for 2 in buffer, 603 nm; and for 2 with nondenatured BSA and ovalbumin, 570 nm and with gelatin, 600 nm.

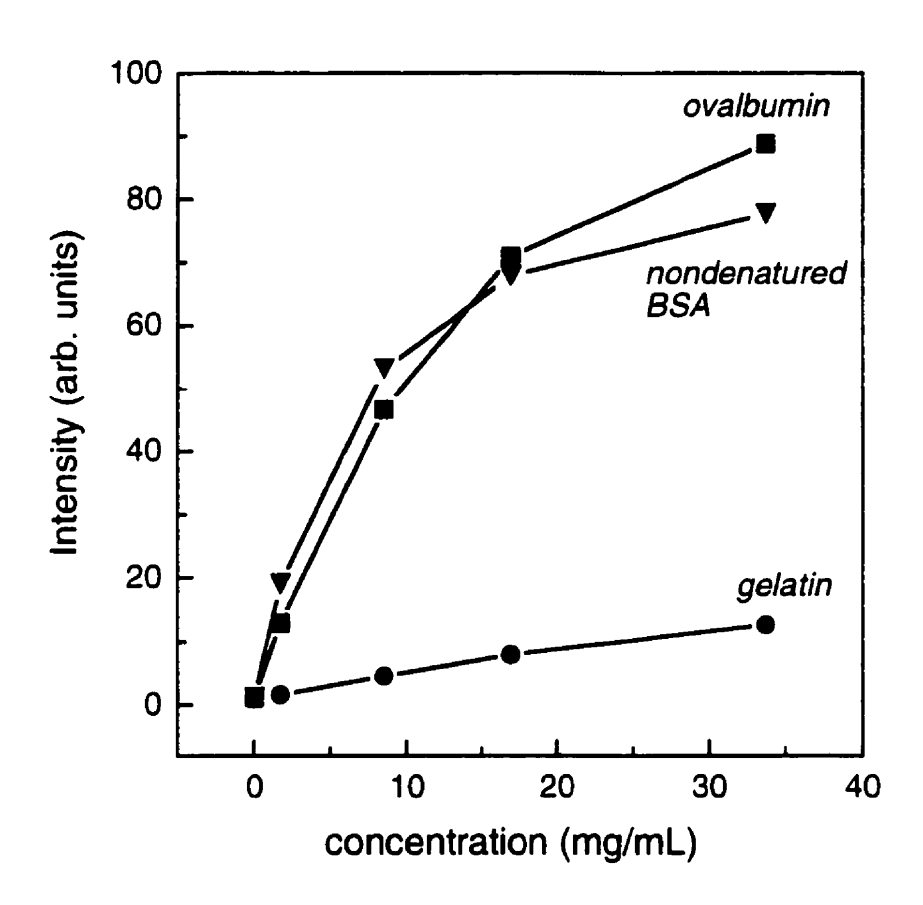


Figure 4B.2. Fluorescence intensity titration curves of 2 as a function of nondenatured BSA (♥), ovalbumin (■) and gelatin (●) concentrations between 0 and 33.7 mg/mL in phosphate buffered saline (0.1 M, pH 7.2, 0.1 M NaCl).

Appendix 5

Section A

A.1 Control and imprinted polymer I//values at various cAMP and cGMP concentrations

Figure 5.3a in Chapter 5 presents the fluorescence (I/I) of the control and imprinted polymers in the presence of cAMP concentrations between 0.01 and 1000 μ M, and cGMP concentration between 1 and 1000 μ M. I_o and I are the fluorescence intensities of the polymers in the absence and in the presence of nucleotide, respectively. Herein, a Table showing the I/I values for each experiment with the control and imprinted polymers at the various concentrations of cAMP and cGMP. The average of the experiments for a particular concentration, as well as the standard errors are also presented.

Table 5A.1. I_dI values for each experiment with the control and imprinted polymers at each concentration of cAMP (0.01 to 1000 μ M) and cGMP (1.0 to 1000 μ M). The averages (ave) of the experiments and the standard errors (se) for each concentration of

cAMP and cGMP are also presented.

| | control | imprinted | | control : | · 3000 / 1000 / |
|-------------|-----------------------|--------------|-----------------|--------------|---|
| | polymer | polymer | IN STATE | polymer 🚁 | polymer. |
| concn mM | , lo/t | lo/I | concn mM | | lo/I |
| 1000 cAMP | 0.863 | 1.130 | 0.01 cAMP | 0.964 | 0.981 |
| 1000 074111 | 0.965 | 1.250 | | 0.993 | 1.012 |
| | 0.922 | 1.130 | ave | 0.978 | 0.996 |
| | 0.863 | 1.056 | range | 0.014 | 0.015 |
| | 0.940 | 1.109 | 3 | | |
| | 0.952 | 1.221 | 1000 cGMP | 1.068 | 1.115 |
| ave | <u>9.932</u> 0.918 | 1.149 | | 1.015 | 1.030 |
| se | 0.018 | 0.030 | | 1.223 | 1.261 |
| | 3.3.3 | | | 0.926 | 0.982 |
| 100 cAMP | 0.992 | 1.177 | | 0.956 | 1.045 |
| | 0.945 | 1.124 | | 0.946 | 0.988 |
| | <u>1.101</u> | <u>1.418</u> | | 1.014 | 1.030 |
| ave | 1.013 | 1.239 | ave | 1.021 | 1.064 |
| se | 0.046 | 0.091 | se | 0.038 | 0.037 |
| | | | | | |
| 10 cAMP | 0.987 | 1.291 | 100 cGMP | 0.952 | 0.947 |
| | 0.860 | 1.116 | | 1.115 | 1.029 |
| | <u>1.015</u> | <u>1.126</u> | | <u>1.018</u> | 1.008 |
| ave | 0.954 | 1.178 | ave | 1.028 | 0.995 |
| se | 0.048 | 0.057 | se | 0.047 | 0.025 |
| | | | | | |
| 5 cAMP | 0.995 | 1.080 | 10 cGMP | 1.039 | 1.029 |
| | 1.046 | 1.145 | | 1.069 | 1.041 |
| | <u>0.974</u> | <u>1.078</u> | | 0.909 | 0.931 |
| ave | 1.005 | 1.101 | | <u>0.984</u> | <u>1.004</u> |
| se | 0.021 | 0.022 | ave | 1.000 | 1.001 |
| | | | se | 0.035 | 0.025 |
| 1 cAMP | 1.009 | 1.099 | | | |
| | 0.995 | 1.034 | 1 cGMP | 0.989 | 0.907 |
| | <u>1.076</u> | <u>1.134</u> | | 0.950 | 0.932 |
| ave | 1.027 | 1.089 | | <u>0.993</u> | <u>0.979</u> |
| se | 0.025 | 0.029 | ave | 0.977 | 0.940 |
| | | | se | 0.014 | 0.021 |
| 0.1 cAMP | 0.981 | 1.063 | | | |
| | <u>0.972</u> | <u>1.016</u> | | | |
| ave | 0.977 | 1.040 | | | |
| range | 0.005 | 0.023 | | | |

Section B

B.1 Preliminary absorption studies with the control and imprinted polymers

Prior to the fluorescence studies presented in Chapter 5, we attempted to observe the binding of cAMP to the control and imprinted polymers by absorption spectroscopy. An aqueous cAMP solution (~ 10⁴ M, 4 mL) was added to a vial containing 20 mg of dried control and imprinted polymer powder. After shaking at room temperature overnight, the polymer was spun down at 3000 rpm for ~ 20 min, and the supernatants were carefully transferred to a clean vial using a glass pipette. They appeared cloudy, possibility due to the presence of very fine particulate matter or impurities that had leached from the polymer samples, and their absorbances at 259 nm (the absorption maximum for cAMP) were higher than the stock cAMP solution (Table 5B.1, column "Absorbance before filtration"). Filtering the samples through a Millipore filter lowered their absorbance values, but they still remained higher than the stock solution (Table 5B.1, column "Absorbance after filtration"). However, the stock solution was not filtered, and thus it would have to have been determined whether filtering changed its absorbance. ***Since the absorbance of supernatant of the control polymer after filtration was close to that of the stock, whereas that of the imprinted polymer was higher, it is possible that cAMP that was trapped inside the imprinted polymer and inaccessible to the

Table 5B.1. Absorbances (at 259 nm) of the supernatants obtained after incubation of the control and imprinted polymers with cAMP before and after filtration through a Millipore filter. The absorbance of the stock cAMP solution is also given.

| | Absorbance before filtration | Absorbance after filtration |
|----------------------------------|------------------------------|-----------------------------|
| Stock cAMP solution ^b | 1.259 | a |
| control polymer | 2.132 | 1.626 |
| imprinted polymer | 1.353 | 1.275 |

^a the stock solution was not filtered.

washing procedure was being released. In fact, Dunkin (Dunkin et al., 1993) found that after drying the polymer, contact with further extraction solvent released additional template, and suggested that drying may cause structural changes in the polymer enabling further template to be released. We, therefore, decided to include an overnight incubation of the polymers with water, prior to the addition of cAMP.

To 75 mg of control and imprinted polymers in glass vials was added 4 mL of double distilled water. The vials were shaken overnight at room temperature, the polymers were spun down, the supernatants were carefully transferred to clean glass vials and filtered. The absorbances (at 259 nm) of these water washes were ~ 0.01 for the control polymer, and ~ 0.05 for the imprinted. However, since the absorption spectra of these washes were not recorded, the presence of cAMP in them would have to had been verified. It is possible that impurities released from the polymer, such as initiator fragments, residual monomers and oligomers, may contribute to the absorbances of the washes.

 $^{^{}b} \varepsilon \text{ cAMP} = 14970 \text{ L mol}^{-1} \text{ cm}^{-1}$

Aqueous cAMP solutions were added to the polymers. The polymers were shaken overnight at room temperature, the polymers were spun down, the supernatants were carefully transferred to clean glass vials, filtered and their absorbances (at 259 nm) measured (Table 5B.2). The absorbances of the control and imprinted supernatants are lower than the stock cAMP solutions for experiment 1 (Table 5B.2). Furthermore, the absorbances of the imprinted supernatants are lower than the control, indicating, as expected, that more cAMP was bound in the presence of the imprinted polymer. However, when the concentration of cAMP was increased (experiment 2), the absorbances of the control supernatants are all slightly above those of the stock (Table 5B.2). The absorbances of the imprinted supernatants are, however, below the stock.

Table 5B.2. Absorbances (at 259 nm) of the supernatant of the control and imprinted polymers obtained after incubation with various concentrations of cAMP. The samples were incubated with water overnight prior to the addition of cAMP. The supernatants were filtered through a millipore filter. The absorbances of the stock cAMP solutions are also given.⁴

| Concentration of stock (M) | Absorbance of stock ^b | Absorbance of control supernatant | Absorbance of imprinted supernatant |
|----------------------------|----------------------------------|-----------------------------------|-------------------------------------|
| experiment 1 | | | |
| 3.8×10^{-5} | 0.569 | 0.264 | 0.232 |
| 3.0×10^{-5} | 0.442 | 0.209 | 0.188 |
| 2.4×10^{-5} | 0.360 | 0.166 | 0.143 |
| 1.9×10^{-5} | 0.279 | 0.125 | 0.123 |
| experiment 2 | | | |
| 1.8×10^{-4} | 2.654 | 2.707 | 2.575 |
| 1.5×10^4 | 2.213 | 2.279 | 2.136 |
| 1.2×10^4 | 1.826 | 1.873 | 1.727 |
| 9.5×10^{-5} | 1.424 | 1.403 | 1.269 |

the stock solution was not filtered.

 $^{^{}b} \epsilon \text{ cAMP} = 14970 \text{ L mol}^{-1} \text{ cm}^{-1}$

These preliminary results suggest that it may be possible to evaluate the binding of cAMP to the imprinted and control polymers using absorption spectroscopy. The trends in the data are promising. Namely, that after a prior water wash and filtration of the supernatant, the imprinted polymer appears to bind more cAMP than the control polymer. Thus, this experiment is worth pursuing, and once optimized may yield very valuable information about the binding of cAMP to the control and imprinted polymers.